
Pedestrian Traffic

Simulation and Experiments

Vom Fachbereich Physik
der Universität Duisburg-Essen
zur Erlangung des akademischen Grades
eines Doktors der Naturwissenschaften
genehmigte Dissertation

von
Tobias Kretz
aus
Mosbach

Referent: Prof. Dr. Michael Schreckenberg
Korreferent: Prof. Dr. Andreas Schadschneider
Tag der mündlichen Prüfung: 23. Februar 2007

Contents

Contents	i
Abstract	v
Zusammenfassung	vii
1 Introduction	1
1.1 The Benefit of Pedestrian Traffic Simulation	1
1.2 Steps on the Way to Reliable and Realistic Simulations	1
1.3 Overview of Existing Models and Approaches	2
1.4 Outline	4
2 Some Remarks on Cellular Automata	5
2.1 From Typical Cellular Automata to General Discrete Models	5
3 A Discrete Model of Pedestrian Motion	11
3.1 Definition of the F.A.S.T.-Model	11
3.1.1 Choosing an Exit	11
3.1.2 Choosing a Destination Cell	13
3.1.3 Moving Toward the Destination Cell	28
3.2 Discussion	33
3.2.1 Higher Speeds	33
3.2.2 The Static Floor Field	37
3.2.3 The Dynamic Floor Field	42
3.2.4 The Effects of Inertia and Repulsive Walls	46
3.2.5 The Effect of Inter-Agent Repulsion	47
3.2.6 The Influence of Friction	49
3.2.7 The Influence of the Blocking Variant on the Fundamental Diagram	57
3.2.8 Comparison to Empirical Data	57
3.2.9 Exit Strategies	60
3.2.10 Correlations in Oscillations at Bottlenecks	64
3.2.11 Counterflow in Corridors	75
3.2.12 Computation Times	76
3.3 Fire and Smoke	79
3.3.1 The Model for the Spreading of Combustion Products: MRFC . . .	79
3.3.2 Biological Impact of Physical Pollutant Concentrations: FED . . .	79
3.3.3 Reaction on Irritant Smoke	80

3.3.4	Intrinsic Errors of the FED Model	81
3.3.5	Caveats	81
3.4	Simulation Output	83
3.4.1	Roundwise Output	83
3.4.2	Summarized Output	84
3.4.3	Statistics	90
3.4.4	Fire and Smoke Simulation Output	92
4	Empirical Results and Validation	97
4.1	Evacuation Exercise in a Primary School	97
4.1.1	Results	97
4.1.2	Comparison to Simulation Results	97
4.2	Upstairs Walking Speed on a Long Stairway	103
4.2.1	Scenario, Methods and Materials	103
4.2.2	Results	105
4.2.3	Discussion	108
4.3	Experiment: Counterflow in a Corridor	110
4.3.1	The Scenario	110
4.3.2	Results	112
4.3.3	Summary and Conclusions	126
4.4	Experiment: Flow Through a Bottleneck	127
4.4.1	Experimental Setting	129
4.4.2	Results	131
4.4.3	Comparison to Similar Studies	145
4.4.4	Summary and Conclusions	147
5	Applications	149
5.1	Example Study on the Optimization of Egress Routes	149
5.2	Example Study on the Optimization of a Floor Plan	153
5.3	Obstacle in a Corridor	154
5.4	Example Study on Organizational Optimization Potential	155
5.5	Example Study with Inclusion of Combustion Product Data	157
5.5.1	A Cabin Fire	157
6	Outlook	161
6.1	Concerning the F.A.S.T.-Model	161
6.2	Concerning Experiments and Observations	162
A	Historical Overview of Crowd Disasters	165
B	Competition, Cooperation, Panic, and Altruism	173
B.1	Panic	173
B.2	Altruism and Cooperation in Evolutionary Biology	177
B.3	Concepts of Altruism and Cooperation with Respect to Crowd Disasters .	181

C	Details of the Experiment “Counterflow in a Corridor”	187
C.1	The Participants	187
C.2	The Script	189
D	Participants’ Details of the Experiment “Flow Through a Bottleneck”	191
	Bibliography	195
	Ausblick	213
	List of Figures	217
	List of Tables	225
	Danksagung (Acknowledgments)	227
	Lebenslauf (Curriculum Vitae)	231
	Teilpublikationen (Pre-Publications)	233
	Erklärung (Declaration)	235

Abstract

In recent years and decades the development of ever more powerful computer hardware has been accompanied by the evolution of simulational or computer physics as a third element of physics next to theory and experiment.

This thesis deals with the simulation of pedestrian traffic with a focus on evacuation processes. While theory and experiment, respectively empiricism, relied on each other since the dawn of modern physics, they do not necessarily rely on simulations, although they have begun to make heavy use of it. Simulations on the contrary can never be carried out meaningfully without theories and experiments backing them and making use of them in the interpretation process of the results. This dependence is reflected in this thesis, which includes elements of all three operation methods. It begins with an overview of elements that are necessary to build reliable simulation models. The interrelation between simulation, theory and experiment is set out in more detail there. Then a survey of existing models of pedestrian evacuation dynamics is given.

The second chapter deals with the semantic - and therefore rather theoretical - problem of how a cellular automaton model can evolve toward a model which is better referred to as “discrete” model when the model is extended. This question is irrelevant for the issue of reliability, yet it is often asked.

In the third chapter a discrete model of pedestrian evacuation dynamics is constructed and tested. The tests of the various elements of the model focus on the elements’ influence on the fundamental diagram, yet there are also some other tests which include some background from theory. The main results of this chapter are the construction of the model itself, the proof that it is very well able to reproduce a widely accepted empirical fundamental diagram up to a density of roughly four persons per square meter, and that - concerning computing times - the model is applicable to scenarios with a few million persons.

The fourth chapter deals with the analysis of two observations and two experiments. The first observation was done during an evacuation exercise in a primary school. The empirical data was partly used to calibrate the parameters of the simulation and partly to compare them with the results of simulations which were done using these parameters. The second observation is a study of upstairs walking speed distributions on a long stair. In the counterflow experiment a rich variety of self-organisational structures showed up, which will be a challenge to model in the future. The finding that the sum of flux and counterflux is always larger than the flux in no counterflow situations may be seen as the most interesting result of this experiment. The main results of the “bottleneck experiment” is that the flux is neither a linear nor especially a step function of the width of a bottleneck and that therefore some legal regulations are based upon wrong assumptions.

Chapter five consists of five examples with diverse focuses for the application of crowd simulations.

The appendix includes a record of crowd disasters as well as - following from that - some considerations on human behavior in dangerous situations.

Zusammenfassung

In den vergangenen Jahren und Jahrzehnten hat sich parallel zur rasanten Entwicklung der Rechnertechnologie die Simulations- bzw. Computer-Physik als drittes Element der Physik neben Theorie und Empirie entwickelt.

Diese Arbeit handelt allgemein von der Simulation des Fußgängerverkehres und hierbei speziell von der Simulation von Evakuierungsprozessen. Während Theorie und Experiment bzw. Empirie während der gesamten Geschichte der modernen Physik wechselseitig aufeinander beruhen, bedürfen beide nicht unbedingt der Simulation, auch wenn in beiden Bereichen Simulationen zu den unterschiedlichsten Fragestellungen durchgeführt werden. Simulationen hingegen kommen weder ohne Theorie noch ohne Empirie aus, sofern ihre Ergebnisse in einem quantitativen Verhältnis zur Wirklichkeit stehen sollen. Diese Abhängigkeit spiegelt sich in dieser Arbeit wieder, die daher Elemente aller drei Arbeitsweisen enthält. Sie beginnt in der Einleitung mit einem Überblick über notwendige Elemente zur Konstruktion eines verlässlichen Personenstrom-Simulationsmodells. Hierbei wird auch der Zusammenhang zwischen Simulation, Theorie und Experiment etwas näher beleuchtet. Es schließt sich ein Überblick über existierende Modelle der Personen-Evakuierungsdynamik an.

Im zweiten Kapitel wird der semantischen - und daher eher theoretischen - Frage nachgegangen, wie sich ein Zellularautomatenmodell durch Erweiterungen zu einem Modell entwickeln kann, das möglicherweise besser schlicht als „diskretes“ Modell bezeichnet werden sollte. Diese Frage ist für die Frage nach der Verlässlichkeit der Simulationsergebnisse ohne Belang, sie wird jedoch häufig gestellt.

Im dritten Kapitel wird ein diskretes Modell zur Personen-Evakuierungsdynamik präsentiert und untersucht. Die Untersuchungen der einzelnen Elemente des Modells konzentrieren sich auf die Frage nach dem Einfluss des Elementes auf das Fundamentaldiagramm. Zu einigen Elementen gibt es jedoch zusätzliche Untersuchungen mit weitergehendem theoretischen Hintergrund. Als Hauptergebnis des dritten Kapitels seien die Konstruktion des Modells selbst, der Nachweis, dass es in der Lage ist, ein weithin anerkanntes empirisches Fundamentaldiagramm bis zu einer Dichte von ca. vier Personen pro Quadratmeter sehr präzise zu reproduzieren, und dass das Modell im Hinblick auf die Rechenzeiten beim derzeitigen Stand der Computertechnik auf Szenarien mit mehreren Millionen Agenten angewandt werden kann, genannt.

Im vierten Kapitel werden zwei Beobachtungen und zwei Experimente analysiert. Bei der ersten Beobachtung handelt es sich um eine Feueralarmübung in einer Grundschule. Die gewonnenen Daten werden zum einen zur Kalibrierung der Simulationsparameter benutzt, zum anderen verwendet, um sie mit Ergebnissen von mit diesen Parametern durchgeführten weiteren Simulationen zu vergleichen. Es folgt die Auswertung von Beobachtungen zur Gehgeschwindigkeit von auf einer langen Treppe aufwärts

gehenden Personen. Das anschließend ausgewertete Gegenstrom-Experiment zeigt eine große Bandbreite von Selbst-Organisationsstrukturen, deren Reproduktion in Simulationen eine Herausforderung darstellt. Dass sich die Summe aus Strom und Gegenstrom immer größer herausstellt als der Strom in Situationen ohne Gegenstrom, ist wohl das interessanteste Ergebnis dieses Experimentes. Das Hauptergebnis des Engstellen-Experimentes ist, dass der Fluss weder eine lineare noch eine Stufenfunktion der Durchgangsbreite ist. Dies bedeutet, dass einige gesetzlichen Regelwerke auf falschen Annahmen beruhen.

Kapitel fünf besteht aus fünf Beispielen der Anwendung von Personenstrom-Simulationen.

Der Anhang enthält eine Auflistung historischer Massenunglücken sowie - darauf aufbauend - einige Überlegungen zum Verhalten in gefährlichen Situationen.

1 Introduction

The simulation of pedestrian evacuation processes and other situations with large numbers of pedestrians has gained growing interest in recent years. There are two main reasons for this: At first it simply has become feasible to simulate large crowds due to the immense technical progress in computational power. The second reason is that the history of accidents involving large numbers of people (see appendix A) makes a need for action apparent. Furthermore there seems to be a tendency toward a culture of mass events: Cruise ships and ferries grow bigger for commercial reasons, high rise buildings still increase by number and height, the success of soccer marketing has generated an industry of regular mass events and carnivals, religious events like world youth days, soccer world championships, rock concerts and love parades successfully use the global media to attract people worldwide and not only from one region anymore.

1.1 The Benefit of Pedestrian Traffic Simulation

Before dealing with the details and problems of the creation of a realistic pedestrian motion simulation this chapter will give some examples of the benefits of such simulations for different groups of users:

1. Simulations are not only cheaper but also less dangerous than real exercises. Probably the best example is the legally prescribed demonstration “by analysis and tests” [1, 2] of the possibility to evacuate an airplane within 90 seconds. During past exercises of this kind repeatedly various kinds of accidents happened [3].
2. Constructors of buildings, ships and aircraft can use simulations to gain insight into possible problems concerning evacuation issues early in the planning phase, when the costs of re-planning are still limited.
3. Operators of large public constructions can use simulations to optimize evacuation plans.
4. Rescue forces at large events can gain a better understanding of different kinds of situations using simulations in advance.

1.2 Steps on the Way to Reliable and Realistic Simulations

There are quite a few steps that lead to realistic simulations which authorities as well as constructors then can rely on.

1. Qualitative observation of phenomenons in pedestrian (crowd) motion.
2. Identification of “crucial elements” that are the major influences for the behavior and therefore for the final results.
3. A model of pedestrian (crowd) motion that reproduces the typical phenomenons and the behavior at critical elements.
4. A software implementation of the model.
5. Quantitative observations and experiments to gage the model parameters.
6. Standardized test cases.
7. Legal regulations.
8. Certification authorities.

Observation, experiments, model building, implementation, testing and certifying are an ever-continuing circle of improvement. The role of legal regulations and certification authorities must not be underestimated. Without these, there is always a payoff for the strategy to build good animators instead of good and realistic simulations, which in the end will lead to decreased instead of increased public safety, as it is a fairly easy task to impress non-experts with good animations and convince them of the evacuability of a construction [4]. Without legal certainty the persons in charge deciding about approval of plans or events will not be willing to accept simulation results as arguments.

1.3 Overview of Existing Models and Approaches

Up to now there do exist a whole lot of simulation models and software packages for simulating pedestrian motion. Without claiming the list’s completeness, some of these are (if a model has not been given a name by its author(s), it is named after its author.): AENEAS [5], ALLSAFE [6], ASERI [7], BFires [8], BGRAF [9], Blue and Adler [10], Brogan et al. [11, 12], Continuum Crowds [13], Cost Function Model [14], CRISP [15], Dijkstra [16], EARM, EESCAPE [17], Egress [18], ENTROPY [19], E-Scape [20], EVACNET [21], EvacSim [22], Evi [23], Exit89 [24], EXITT [25], Exodus [26], Firescap [27], Floor Field Model [28–30], FPETool [31], Fridman and Kaminka [32], Funge et al. [33], GridFlow [34], Group Psychology Model [35], Lamarche and Donikian [36], Legion [37], Magnetic Model [38], MASCM [39], Massive [40], Micro-PedSim [41, 42], Musse and Thalmann [43], Myriad [44], Ohi et al. [45], PathFinder [46], PEDFLOW [47], Pedroute/Paxport [48], PedGo [49], Pelechano et al. [50], Schultz et al. [51], SGEM [52], Shao and Terzopoulos [53], Simulex [54], SimWalk [55], Social Force Model [56], STEPS [57], Sugiyama et al. [58], Sung et al. [59], Swarm Information Model [60], Takahashi et al. [61], TIMTEX [62], VEgAS/Myriad [44], WayOut [63], Waş et al. [64], and Yamamoto et al. [65]. A review of some of these models can be found in [66, 67] and a categorization in [68, 69].

Some of the categories by which these models and software packages can be distinguished are

- **Space representation:** continuous vs. fine grain (grid-based) vs. coarse grain (network-structure)
- **Population representation:** microscopic (individual) vs. macroscopic (reduction to variables of averages as in hydro- or thermodynamics)
- **Population behavior generation:** artificial-intelligence-based vs. functional vs. implicit vs. rule-based (cellular automaton)
- **Stochastic vs. deterministic behavior**
- **Purpose:** Specific purpose vs. general model of pedestrian motion
- **Availability:** open source vs. commercially available vs. not yet implemented or released

While the large number of models exhibit the big effort that has been put into creating models and implementations especially during the last two decades, the number of standardized test cases needed to compare these models is small. In principle a user would have to test a bunch of models on his own to find out if it suits his needs. Even more, he can hardly be sure about the quality of the simulation results. The situation is worsened by the fact that typically commercial software providers do not grant much insight into neither the model nor the source code. So even experts with long experience in the field have no other chance to judge the quality of the model than to experiment with the software. One element to improve the situation are comparative feature description lists [66, 67, 70]. A feature description list (e.g. “The model is able to handle multiple floors.”, “The model is able to include the effects of fire and smoke.” or “The program enables the user to set the cultural background of the pedestrians.”) is given by most authors of a model, especially commercial ones. See [71, 72] for a compilation of such lists for some of the mentioned models. Yet the important question that typically remains unanswered is “How realistic are the results these features produce?”. A second element are very basic tests that compare a model with elementary facts of reality (“Persons cannot walk through walls.”, “Velocity is density dependent.” or “The flow through a door cannot exceed 1.33 persons per second and meter width.”) [73–77]. These tests answer the question if a model is basically capable to simulate pedestrian motion or if it is not. In an extreme case they can demonstrate that a model with a long feature list, is not even able to reproduce the empirically observed flow reduction for high densities for example. The third stage are tests that report which set of parameters leads to which (quantitative) results if they are applied to standardized test scenarios. The results may include far more observables than just the evacuation time. Such tests are absolutely essential for certification authorities to fix set(s) of parameters that have to be applied in certain cases such that simulations can be used to demonstrate that a construction agrees with the terms of regulation.

1.4 Outline

After a short prologue in chapter 2 that shows how models may evolve from typical cellular automata to models that are better described as “discrete models”, one such discrete model is presented and tested in chapter 3. The tests of section 3.2 are tests where simulation results are compared to existing data from the literature or to each other to demonstrate the effects the individual elements of the model have. These tests are not only considered to merely test this specific model, but they are meant as examples of what should at minimum be published together with any simulation model of which the authors claim that it generates realistic results in whatever framework. Contrary to these tests, which compare the model elements toward each other and results of existing literature, in chapter 4 simulation results are compared to own measurements. The larger part of chapter 4, however, consists of the results of observations and two experiments. The details of these results are too fine to be reproduced by a simulation at present. Chapter 5 concludes this work with specific and general examples from application. The first part of the appendix includes a record of the history of crowd disasters, the second part consists of some considerations on the term “panic”, the differences between the ideas of disaster researchers and the public of how people react in dangerous situations and possible origins and implications of this difference.

2 Some Remarks on Cellular Automata

In discrete models space gets discretized into cells of a finite size. While coarse grain discrete models discretize space according to the semantics of the floor plan (room, corridor etc.), fine grain models discretize space using a periodic - mostly regular - lattice. A pedestrian - or an “*agent*” [78] as a pedestrian’s counterpart in the model and the simulation shall generally be called - then occupies one or more of these cells. Time gets discretized as well, such that the evolution of the system progresses in rounds. If the model fulfills certain conditions one has a (probabilistic) *cellular automaton* (CA, pl. “cellular automata”). There is no generally acknowledged definition of CA. However, typically the following properties are mentioned to define CA:

1. CA are discrete dynamical systems.
2. CA are discrete in space, time and their state variables. The discreteness in space is a regular, uniform lattice.
3. CA are local in their update rules. That is, a cell’s next state does only depend on a finite number of neighboring cells.
4. All cells of a CA get updated synchronously.
5. The update rules are identical for all cells. This implies that a CA has to be either cyclic or infinite in space, as boundary cells would require different update rules.

The last restriction can in a sense always be fulfilled by introducing additional states which may stay constant throughout the whole evolution of the process. The second to last restriction is not part of all definitions of CA. One of the most popular CA is the “Game of Life” [79]. For an overview on CA see for example [80, 81].

2.1 From Typical Cellular Automata to General Discrete Models

It has been proven [80, 82–84] that there are CA that are computationally universal which implies that they - just like a Turing machine - can do any kind of computation one can think of. Probably the simplest CA of this type is Wolfram’s CA-110. Therefore any type of simulation implemented into a computer program - at least at a classical computer - can be thought of as being a CA. However this section will not deal with these more theoretical issues but with the way how a very typical CA - namely Wolfram’s CA-184

[81] (see figure 2.1) - can evolve into a system - namely the Nagel-Schreckenberg model [85] - that without doubt still is a (probabilistic) CA but which for reasons of simplicity and descriptiveness is better formulated in a way that it is sometimes more generally referred to as a “discrete model”. Note: This section deals with different formulations, interpretations and relations of those closely related or partly even identical models. For a detailed analytical comparison of CA-184 with the Nagel-Schreckenberg model see [86].

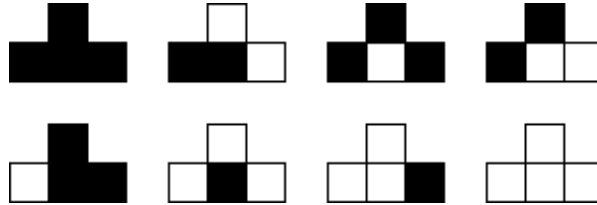


Figure 2.1: Rule table for CA-184 - The state of three cells determines the state of the center cell for the next round in the given way.

Calling the left, central and right cell (l, c, r) and (b, w) as possible states black and white CA-184 (figure 2.1) can be formulated in logical form:

$$\begin{aligned} &\text{if } (((l^t = b) \wedge (c^t = w)) \vee ((c^t = b) \wedge (r^t = b))) \\ &\text{then } (c^{t+1} := b) \text{ else } (c^{t+1} := w) \end{aligned}$$

This shows that the rule table for CA-184 can be formulated in a more compact way,



Figure 2.2: Compacted rule table for CA-184. Cells where the state does not matter (logical OR) are split diagonally.

as shown in figure 2.2. The compact representation immediately gives rise to two more interpretations of the rule, of which one is sufficient to determine the behavior of the system:

- For a black cell: “If there is no black cell to the right, move one cell to the right, otherwise stay.”
- For a white cell: “If there is no white cell to the left, move one cell to the left, otherwise stay.”

What happens in this interpretation step - without any change in the dynamics of the system - is that the cell-oriented view of a continuously existing static cell that can take

one of two states changes to a particle-oriented view of a continued existence from one round to the other of either white or black particles. (This of course is only possible for CA rules where the number of cells taking a certain state is conserved. This is the case for CA-184.) With this particle- or car-oriented formulation of CA-184 the most simplified version of the Nagel-Schreckenberg model lies right ahead.

The Nagel-Schreckenberg model in its original formulation:

1. **Acceleration:** If the speed of a vehicle is lower than v_{max} , then the speed is advanced by one. [$v \rightarrow v + 1$]
2. **Slowing down** (due to other cars): If a vehicle at site i sees the next vehicle at site $i + j$ (with $j \leq v$), then it reduces its speed to $j - 1$. [$v \rightarrow j - 1$]
3. **Randomization:** With probability p , the speed of each vehicle (if greater than zero) is reduced by one. [$v \rightarrow v - 1$]
4. **Car motion:** Each vehicle is advanced v sites.

For the simplest version of this model with $v_{max} = 1$ and $p = 0$ these rules can be simplified to

1. **Acceleration:** Set the speed of all cars to 1. [$v = 1$]
2. **Slowing down** (due to other cars): If a vehicle at site i sees the next vehicle at site $i + 1$, then it reduces its speed to zero [$v = 0$]
3. **Car motion:** Each vehicle is advanced v sites.

The only difference between this simplest version of the Nagel-Schreckenberg model and the first alternative formulation of CA-184 is that a car in the Nagel-Schreckenberg model can have two states ($v = 0$ and $v = 1$). This implies that a cell can have three states. However this does not influence the dynamics as the memory on the speed of a car is erased in the acceleration step where the speed of all cars is set to one. Therefore CA-184 and the deterministic $v_{max} = 1$ version of the Nagel-Schreckenberg model are identical.

It is possible to formulate any deterministic v_{max} version of the Nagel-Schreckenberg model in just the same way as the original formulation of CA-184. The only thing one needs is a larger area of influence to the left and more colors to represent the different speeds. If one wants to distinguish between cars with $v_{max} - 1$ and v_{max} between the rounds (which is not necessary due to the acceleration step) the rule table contains $(v_{max} + 2)^{(v_{max} + 2)}$ elements. Already for $v_{max} = 2$ there are 256 elements. However just like in figure 2.2 quite a few reductions are possible. These lead to figure 2.3, which shows the compact rule table for the deterministic $v_{max} = 2$ version of the Nagel-Schreckenberg model.

The considerations so far show that even for $p = 0$ the cell-oriented formulation appears to be more complicated than the car-oriented formulation - not for a computer but for the human mind. This holds maybe even for $v_{max} = 1$ but in any case for

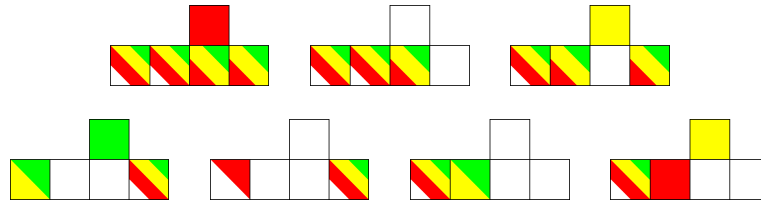


Figure 2.3: Cell-oriented formulation of the deterministic $v_{max} = 2$ version of the Nagel-Schreckenberg model. A white cell does not contain a car. The different speeds are represented by red ($v = 0$), yellow ($v = 1$) and green ($v = 2$)

Red Yellow Green

Figure 2.4: Color table for black and white copies of this work.

$v_{max} = 2$ and other higher speeds. One also quickly realizes that the cell-oriented formulation becomes ever more complicated for increasing v_{max} as the number of possible elements in the rule table increases due to the increase of states and area of influence. For $v_{max} = 5$ one would have $7^7 = 823543$ elements. This could surely be reduced significantly as it was done for $v_{max} = 2$ but the reduction process as well includes ever more computation steps. The car-oriented formulation however can be handled as easily for any v_{max} as it can be handled for $v_{max} = 2$.

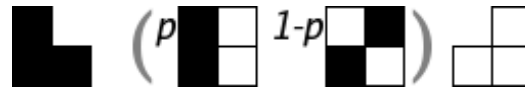


Figure 2.5: Cell-oriented formulation of the $v_{max} = 1$ version of the Nagel-Schreckenberg model. The brackets enclose alternatives of which one is chosen probabilistically. In cases where dawdling is possible, the state of two cells is fixed for the next round.

The rule table of the Nagel-Schreckenberg model for $v_{max} > 1$ can be gained out of the rule table in the deterministic case by the following algorithm:

1. Increase the area of influence by one to the right. (Since via overreaction the speed of a car can drop to zero due to cars two cells in front.)
2. Identify all situations where dawdling/overreaction is possible.
3. Write down the two elements of the rule (if possible) with and without dawdling. (Remember that if dawdling is possible the state of two cells is determined for the next round.)

4. Erase all cells at the border of elements where the state of the cell does not matter.
5. Erase all elements which occur more than once.

The last two steps are not necessary, but they reduce the number of elements. On the negative side they make the application of the rules appear more complicated. For $v_{max} = 2$ the result is shown in figure 2.6. In the context of complexity the crucial point is that the generation algorithm for the rule table becomes ever more complex in actual execution as well as it has an ever larger amount of input data (the deterministic rules) to be processed for increasing v_{max} .

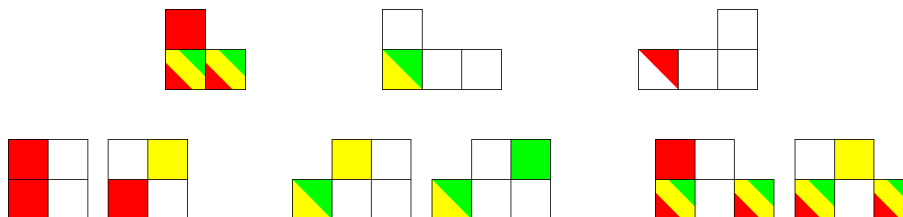


Figure 2.6: Cell-oriented formulation of the probabilistic $v_{max} = 2$ version of the Nagel-Schreckenberg model. Of the elements in the lower line, the left version is chosen with probability p and the right with $1 - p$.

The examples so far show a tendency that cell-oriented formulations become ever more complex while particle-oriented models do not when a model is extended e.g. to larger velocities. This continues if one has an arbitrary model that includes forward and backward motion with some v_{max} and even more if the model has two or more dimensions. It becomes evident that a particle-oriented formulation of a model is the natural choice if one has to deal with particles, that is, if the number of certain states is globally conserved in number at least for a certain number of rounds. On the way of modeling some phenomenon of reality one then often ends up with models that are better described as “being discrete in space and time” than as “CA with certain extensions”. Especially the expansion of the neighborhood to more than cells that share an edge or at least a corner with the center cell, is in principle in agreement with the CA definitions, as long as the neighborhood remains finite. But to some extent this violates the intention of most of the original CA, where the idea of strict locality prevailed. All this does not exclude the possibility that a proof is possible that some reformulation into a CA model is possible, at least with respect to some variants of CA definitions. It should be stated that from a point of algorithmic parallelizability and therefore calculation time for the simulation of very large systems a classical CA ansatz with common-edge neighborhoods is favorable (this was part of the original idea). Yet an implementation of this idea is - at least in the field of human transport systems - obstructed by the need of a dynamical space requirement. Therefore the constraint to reproduce a realistic fundamental diagram and a decision for a model with strict locality for parallelizability does hold great difficulties for the creation of the model and excludes a variety of model

types. Compare subsection 3.1.3 of this work, section 3.2 of [87], section 3.7 of [88] and [75, 89, 90]. Very recently the idea has been expressed [91] that the synchronous update per se is unsuitable to produce realistic results. While this statement can be doubted in this generality it is probably be enlightening to compare the fundamental criticism in [91] of what can be called a CA and how powerful CA might be with the way the F.A.S.T.-model is constructed and where the F.A.S.T.-model deviates from the very narrow definition of a CA and for what reasons this deviation was chosen.

3 A Discrete Model of Pedestrian Motion

3.1 Definition of the F.A.S.T.-Model

The F.A.S.T.-model (*“Floor field- and Agentbased Simulation Tool model”*) of pedestrian traffic that is now going to be presented is discrete in space and time, the spatial lattice is orthogonal. There is a hard-core repulsion between the agents, of which at maximum one can occupy a cell at a certain point in time. An agent - as the representation of a person in the model shall be called - requires the space of one cell. This implies a cell size of roughly $40 \cdot 40 \text{ cm}^2$ [92], the minimum space a pedestrian occupies. From this follows a maximum density of 6.25 persons per square meter. So far the model follows earlier models [87, 93]. In fact this model is in many aspects an extension of the model presented in [29] which itself had predecessors [28, 94, 95]. Other extensions of this model can be found in [30, 90, 96].

For the agents there are three levels of decision making, which will be explained in detail in the following subsections:

1. The choice of an exit,
2. The choice of a destination cell,
3. The path between the current and the destination cell.

The first two are modeled as probabilistic processes. The third one for simplicity as a deterministic one, except for the order in which the agents carry out their steps to reach the destination cell in some model variants.

Contrary to some model variants presented in [90], the actual motion process (see figure 3.1) of the F.A.S.T.-model does not contain a planning or optimization phase for the path between current and destination cell. Each agent on whom it is the turn to advance one cell toward the destination cell actually does so. He only considers the (partial) paths of agents that advanced before him and his own motion forward only influences the steps of the agents that are allowed to move only later. Therefore the process of choosing a destination cell is done completely parallel by all agents, while the actual motion is a sequential process. In the following a *round* includes the decision for an exit as well as for a destination cell and all *steps*, while a *step* is the movement of an agent from one cell to one of the nearest neighbor cells i.e. a part of the path from the current toward the destination cell.

3.1.1 Choosing an Exit

An *exit* is defined as a bunch of *exit-cells* which are connected via common edges.

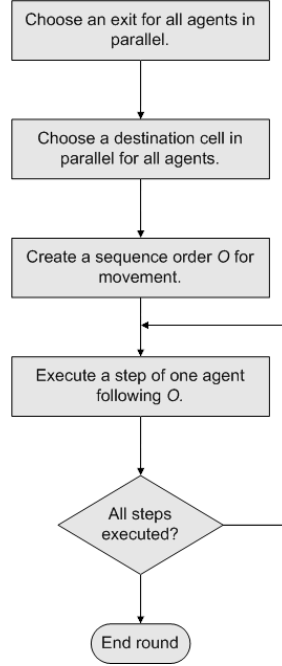


Figure 3.1: Structure of one round.

At the beginning of each round all agents choose one of the exits with the probability

$$p_E^A = N \frac{1 + \delta_{AE} k_E(A)}{S(A, E)^2} \quad (3.1)$$

with

- A numbering the agents,
- E numbering the exits agent A is allowed to use,
- $\delta_{AE} = 1$ if agent A chose exit E during the last round and $\delta_{AE} = 0$ otherwise,
- $k_E(A)$ being agent A 's persistence to stick with a once taken decision for one of the exits,
- $S(A, E)$ being the distance between the exit and the current position of agent A ,
- and N as normalization constant guaranteeing $\sum_E p_E = 1$.

The distance between agent and exit is squared so the probability is proportional to the inverse of the area of a circle around the exit with radius $S(A, E)$. Given a constant density of agents all over a scenario with high symmetry this area is proportional to the

number of agents which are closer to the exit than agent A . Therefore this is a measure of a possible queue before agent A at exit E .

There are plenty of possibilities to make this process of choosing an exit more elaborate. Very recently a model of information spreading in a crowd of evacuees has been published [60, 97], which could easily be incorporated. But as the focus in this work is more on the elementary dynamics, the exit choosing process was kept fairly simple intentionally.

3.1.2 Choosing a Destination Cell

In a model which is spatially and temporally discrete naturally an agent's dimensionless speed is the number of cells which he is allowed to move during one round. As the real-world interpretation of the size of a cell is fixed by the scale of the discretization, the real-time interpretation of one round fixes the real-world interpretation of such a dimensionless speed.

In the F.A.S.T.-model an agent chooses one cell he wants to move to out of *all* cells he would be able to reach during one round, except for those that are occupied by other agents. This concept can be used to combine the introduction of higher speeds with an improved symmetry and therefore a reduced dependence of the simulation results on the initial axis of discretization.

Moore and More - Higher Speeds

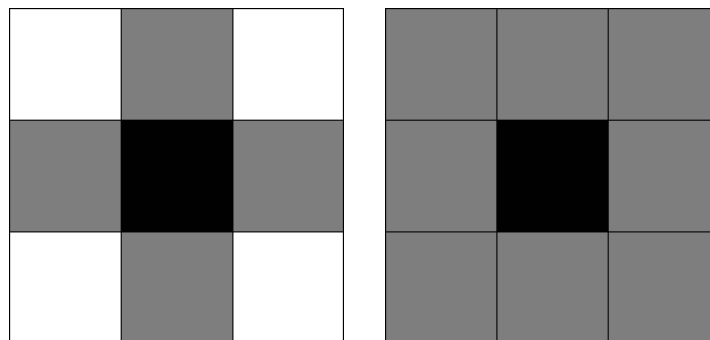


Figure 3.2: von Neumann- and Moore-neighborhood ($v_{max} = 1$).

Subsequent steps within one of the neighborhoods of figure 3.2, leave an agent to be either $\sqrt{2}$ times as slow or as fast moving into the diagonal direction than moving horizontally or vertically. One way to address this problem is given in [65], another in [51]. The F.A.S.T.-model, however, is based on another principle which is now going to be explained. It is sometimes suggested [98] to just extend the neighborhoods of figure 3.2 while keeping the shape, but to some extent the disadvantage of direction dependent speeds can be improved by a combination of a *mixture* of von Neumann and Moore neighborhoods to represent higher speeds. If for example an agent would be allowed

to do a total of five steps during one round, of which three are in von Neumann and two in Moore neighborhood, a *total neighborhood* of cells which can be reached during one round would result. The question is: Is there an *optimal total neighborhood* for a given speed? And can it be composed of von Neumann and Moore neighborhoods? In vertical and horizontal direction there is no doubt about the neighborhood: For a speed $v = v_{max}$ the neighborhood contains the cell of the agent's position and v_{max} cells into each horizontal or vertical direction. For any other direction there are cells for which it is not obvious if they should be part of the neighborhood. At the very beginning for $v_{max} = 1$ there is the question if one should use von Neumann or Moore neighborhood. (See figure 3.2).

Definition: *Complete neighborhoods* are four-fold symmetrical neighborhoods where all cells which do belong to the neighborhood are closer to the center cell than those which don't.

Example: There are three complete neighborhoods for $v_{max} = 2$ as well as for $v_{max} = 3$. (See figures 3.3 and 3.4.)

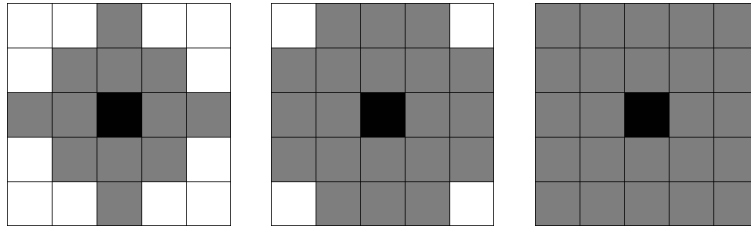


Figure 3.3: Example: Complete neighborhoods for $v_{max} = 2$.

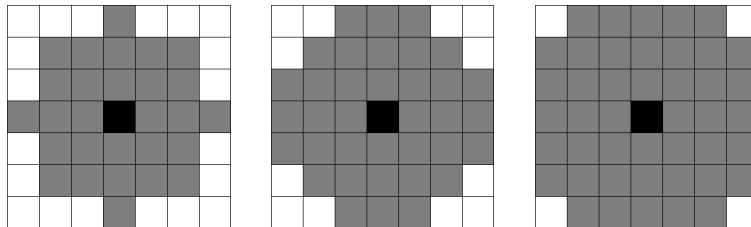


Figure 3.4: Example: Complete neighborhoods for $v_{max} = 3$.

Obviously one can limit the search for an optimal neighborhood to complete neighborhoods.

N.B.: In all of the following calculations a deterministic motion on the optimal path on an obstacle-free level is assumed. This implies that the distance of the cells is assumed to be the Euclidean distance of their centers.

The question is, which complete neighborhood represents the corresponding speed (=number of cells in horizontal and vertical direction) best. However there might exist other alternatives, the criteria chosen here are such that discretization effects concerning

the axis of discretization of the original plan are minimized. Therefore at first for each complete neighborhood the speed $v(\phi)$ into each direction has to be written down.

Then the direction-averaged speed is calculated.

$$v_{av} := \frac{1}{2\pi} \int_{\phi} v(\phi) d\phi \quad (3.2)$$

After that the squared deviation of speeds into each direction from this average is calculated.

$$\Delta v := \sqrt{\frac{1}{2\pi} \int_{\phi} (v(\phi) - v_{av})^2 d\phi} \quad (3.3)$$

The criteria for an optimal neighborhood are then

- The direction-averaged speed should be close to the corresponding integer.
- The relative deviation ($\Delta v/v_{av}$) from this average into different directions should be small.

Complete Neighborhoods up to $v_{max} = 10$: The neighborhoods are named by the maximum squared distance of a cell from the center, implying that neighborhood Y includes all cells of neighborhood $X \leq Y$. In table 3.1 the numbers (names) are shown in the second octant.

100	101	104	109	116			
81	82	85	90	97	106	117	
64	65	68	73	80	89	100	113
49	50	53	58	68	74	85	98
36	37	40	45	52	61	72	
25	26	29	34	41	50		
16	17	20	25	32			
9	10	13	18				
4	5	8					
1	2						
0							

Table 3.1: Names and squared maximal distances of the neighborhoods.

N.B.: Of those only the neighborhoods 1, 2, 4, 5, 8, 10, 13, 17, 20, 29, 34, 40, 45, 58, 80 and 97 can be composed of the corresponding number of subsequent steps within von Neumann and Moore neighborhoods. (Take N von Neumann and $M = v_{max} - N$ Moore steps and check how the largest possible neighborhood looks like.)

$v(\phi)$ - **the Variation of the Speed with the Direction of Motion:** Since all complete neighborhoods have a fourfold axis-symmetry it is sufficient to calculate $v(\phi)$ for $0 \leq \phi < \pi/4$.

$v(\phi)$ is continuously composed from different functions resulting from different ranges of ϕ . The structure of those ranges depends on the shape of the edge of the neighborhood. (See figure 3.5).

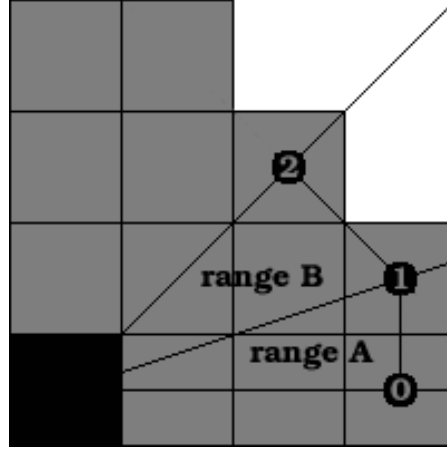


Figure 3.5: Example for calculating $v(\phi)$ for one of the $v_{max} = 3$ neighborhoods. The gray number within the black discs is the index i .

Definitions:

δx_i	Horizontal distance (in cells) of a border cell to the origin (the black cell in figure 3.5); with i starting with 0 at $\phi = 0$ (see the numbering in the black circles in figure 3.5)
δy_i	Vertical distance of a border cell to the origin; with i starting with 0 at $\phi = 0$
D	A large distance (far outside of the neighborhood)
ΔX	$D \cos(\phi)$
ΔY	$D \sin(\phi)$
N	Total (minimal) number of steps to reach a cell in distance D into direction $\arctan(\frac{\delta y_i}{\delta x_i}) \leq \phi_i < \arctan(\frac{\delta y_{i+1}}{\delta x_{i+1}})$
n	Number of steps into direction $(0/0) \rightarrow (\delta x_i/\delta y_i)$ to reach $(\Delta X, \Delta Y)$
$N - n$	Number of steps into direction $(0/0) \rightarrow (\delta x_{i+1}/\delta y_{i+1})$

To reach the point $(\Delta X, \Delta Y)$ an agent has to do n times a $(\delta x_i/\delta y_i)$ step and $(N - n)$ times a $(\delta x_{i+1}/\delta y_{i+1})$ step.

From that follows

$$n \delta x_i + (N - n) \delta x_{i+1} = \Delta X \quad (3.4)$$

$$n \delta y_i + (N - n) \delta y_{i+1} = \Delta Y \quad (3.5)$$

Solving this for N leads to

$$N = \frac{\Delta Y - r \Delta X}{\delta y_{i+1} - r \delta x_{i+1}} \quad (3.6)$$

where

$$r = \frac{\delta y_{i+1} - \delta y_i}{\delta x_{i+1} - \delta x_i} \quad (3.7)$$

In $\phi_i \in [0..\pi/4]$ r can only take the values ∞ (range A in figure 3.5) and -1 (range B) which in the former case in equation (3.6) has to be understood as limit. r is the local gradient of the border of the neighborhood.

Since speed is distance (in cells) over number of rounds to move that distance, from equations (3.6) and (3.7) one has

$$v(\phi) = \frac{D}{N} = \frac{\delta y_{i+1} - r \delta x_{i+1}}{\sin \phi - r \cos \phi} \quad (3.8)$$

See figure 3.6 for the speed's dependence on the direction of motion of all three complete $v_{max} = 2$ neighborhoods.

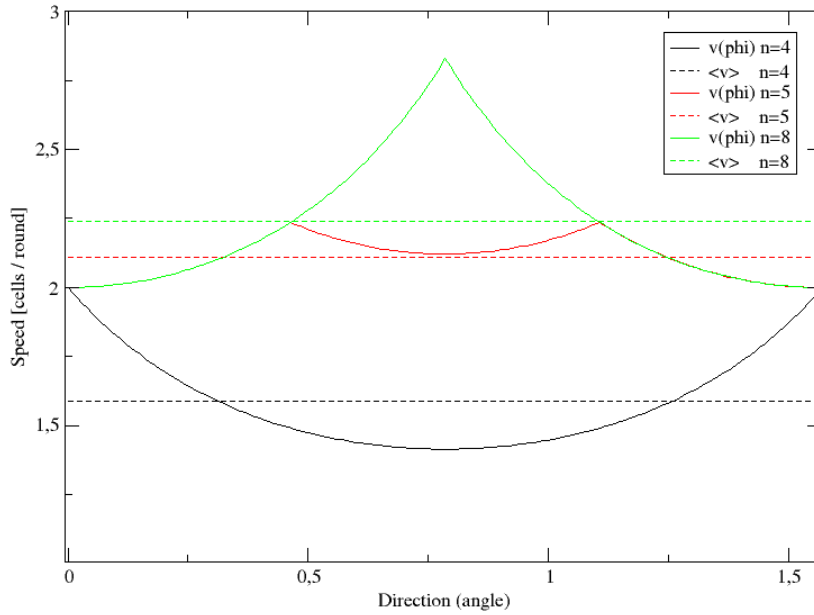


Figure 3.6: Example for the $v(\phi)$ dependence. ($v_{max} = 2$; neighborhoods 4, 5 and 8 as shown in figure 3.3.)

The Integrals for the Average Speeds and the Deviations: For a *range A* like range (vertical, see figure 3.5) to get the average one has to integrate:

$$I_i^A(\phi_i, \phi_{i+1}) = \int_{\phi=\phi_i}^{\phi_{i+1}} \frac{1}{\cos \phi} d\phi \quad (3.9)$$

$$= \ln \left(\frac{\tan(\frac{\phi_{i+1}}{2} + \frac{\pi}{4})}{\tan(\frac{\phi_i}{2} + \frac{\pi}{4})} \right) \quad (3.10)$$

$$= \ln \left(\frac{\sqrt{1 + \tan^2 \phi_{i+1}} + \tan \phi_{i+1}}{\sqrt{1 + \tan^2 \phi_i} + \tan \phi_i} \right) \quad (3.11)$$

and for a *range B* like range (diagonal):

$$I_i^B(\phi_i, \phi_{i+1}) = \int_{\phi=\phi_i}^{\phi_{i+1}} \frac{1}{\sin \phi + \cos \phi} d\phi = \frac{1}{\sqrt{2}} \ln \frac{\tan(\frac{\phi_{i+1}}{2} + \frac{\pi}{8})}{\tan(\frac{\phi_i}{2} + \frac{\pi}{8})} \quad (3.12)$$

$$= \frac{1}{\sqrt{2}} \ln \left(\frac{(\sqrt{2(1 + \tan^2 \phi_{i+1})} - 1 + \tan \phi_{i+1})(1 + \tan \phi_i)}{(1 + \tan \phi_{i+1})(\sqrt{2(1 + \tan^2 \phi_i)} - 1 + \tan \phi_i)} \right) \quad (3.13)$$

To get the average speed in that range additionally one has to normalize the integrals. The average for the whole first octant is the sum

$$v_{av} = \frac{4}{\pi} \sum_i I_i^X(\phi_i, \phi_{i+1}) \quad (3.14)$$

For the deviation integrals

$$(\Delta v)^2 = \int_{\phi=\phi_i}^{\phi_{i+1}} (v(\phi) - v_{av})^2 d\phi \quad (3.15)$$

the additionally needed integrals are

$$\int_{\phi=\phi_i}^{\phi_{i+1}} \frac{1}{(\cos \phi)^2} d\phi = \tan \phi_{i+1} - \tan \phi_i \quad (3.16)$$

and

$$\int_{\phi=\phi_i}^{\phi_{i+1}} \frac{1}{(\sin \phi + \cos \phi)^2} d\phi = \frac{1}{2} \left(\tan \left(\phi_{i+1} - \frac{\pi}{4} \right) - \tan \left(\phi_i - \frac{\pi}{4} \right) \right) \quad (3.17)$$

$$= \frac{1}{2} \left(\frac{1 + \tan \phi_{i+1}}{1 - \tan \phi_{i+1}} - \frac{1 + \tan \phi_i}{1 - \tan \phi_i} \right) \quad (3.18)$$

Results: Although all integrals are simple and analytic, the analytic results do not provide much insight and in the following only the numerical results are given. The results of the calculation of average speed and the deviations from it are shown in table 3.2.

Table 3.2: Average speeds and relative deviations (by angle) for all complete neighborhoods up to $v=10$

Neighb. (d_{max}^2)	Average speed	Relative deviation	Neighb. (d_{max}^2)	Average speed	Relative deviation
1	0.79	0.105	2	1.12	0.105
4	1.59	0.105	5	2.11	0.033
8	2.24	0.105	9	2.52	0.080
10	2.98	0.033	13	3.28	0.067
16	3.47	0.055	17	3.82	0.054
18	3.91	0.043	20	4.22	0.033
25	4.57	0.064	26	4.85	0.039
29	5.11	0.024	32	5.17	0.028
34	5.40	0.054	36	5.52	0.043
37	5.75	0.034	40	5.97	0.033
41	6.13	0.026	45	6.33	0.033
49	6.43	0.030	50	6.67	0.035
52	6.86	0.039	53	7.05	0.019
58	7.22	0.024	61	7.35	0.034
64	7.44	0.030	65	7.77	0.029
68	7.94	0.019	72	7.98	0.021
73	8.13	0.024	74	8.29	0.023
80	8.44	0.033	81	8.52	0.028
82	8.66	0.026	85	8.92	0.023
89	9.06	0.025	90	9.20	0.015
97	9.34	0.025	98	9.37	0.026
100	9.57	0.030	101	9.70	0.025
104	9.83	0.021	106	9.96	0.019
109	10.09	0.014	113	10.18	0.019
116	10.31	0.023	117	10.43	0.024

Speed	Neighborhood (d_{max}^2)
1	2
2	5
3	10
4	18
5	29
6	40
7	53
8	72
9	89
10	109

Table 3.3: Selected neighborhoods.

While there are ambiguities, these results nevertheless point to the choice of neighborhoods shown in table 3.3 (of which only the ones for the speeds 1, 2, 3, 5 and 6 can be composed out of the corresponding number of subsequent von Neumann or Moore steps).

This results in speed neighborhoods shown in table 3.4.

10	10	10	10							
9	9	9	10	10	10					
8	8	8	9	9	9	10				
7	7	7	8	8	9	9	10			
6	6	6	7	7	8	8	9	10		
5	5	5	6	7	7	8	9	9	10	
4	4	5	5	6	7	7	8	9	10	
3	3	4	4	5	6	7	8	9	10	10
2	2	3	4	5	5	6	7	8	9	10
1	1	2	3	4	5	6	7	8	9	10
0	1	2	3	4	5	6	7	8	9	10

Table 3.4: One quarter of the assignment “Neighboring cell \rightarrow maximum speed”. (An agent with maximum speed v_{max} can reach all cells with a number $\leq v_{max}$.)

Distance Toward the Exits - Dijkstra’s Algorithm on a Discrete Lattice

Dijkstra’s algorithm [30, 99] is used to find the shortest path of any node of a network to one or more source, exit, root (R), etc. points. The particular steps of the algorithm are:

- 1) Write down the distances of all pairs of nodes which are directly connected.
- 2) Add the root point R to C and all other points to U .
- 3) *RELAX* all nodes:
- 3a) Add those nodes which are directly connected to at least one node of C to N and delete them from U .
- 3b) Then calculate the (so far) shortest distance of those nodes to R .
- 4) Find the node of N which is closest to R .
- 5) Add that node to C and delete it from N .
- 6) Repeat 3) - 5) until U and N are empty.

With

C : Set of all nodes of which the shortest distance to R is known (connected).

N : Set of all nodes which are directly connected to one node of C (neighbored).

U : Set of all other nodes (unconnected).

RELAX: The distance to R can become smaller for a specific node while processing the algorithm if it is not the one (out of N) closest to R .

e.g.: If $\overline{RA} = 1$, $\overline{RB} = 5$, $\overline{AD} = 1$ and $\overline{BD} = 1$

B will be part of N after the first step, but its shortest distance to R will be 5 so far. Only when D is added to N and after that to C will the true shortest distance $\overline{RB} = 3$ unveil.

Finding the Necessary Nodes: To implement Dijkstra's algorithm efficiently in discrete space it is not necessary to make every cell a node. It's sufficient that every cell is visible from at least one correctly chosen *node cell*. Then one can calculate the shortest distance of the node cells to the exits R . After that the shortest distance of a non node cell is the minimum of all possible distances (distance to a node cell + distance of that node cell to R). To not overestimate a cell's distance toward the exit one has to choose the nodes carefully.

To find the optimal (minimal) number of node cells one would have to take a sophisticated look at the geometry of the considered room and do a detailed visibility analysis. The result would be a minimal visibility graph where the nodes are the convex corners of obstacles. As calculation times might rise, however accepting more nodes than necessary makes the task significantly simpler: One only has to look at nearest neighbors.

A *wall* is neither accessible by agents nor transparent, while *free* means an accessible and transparent cell.

So if a cell is a wall, it depends on the status (free/wall) of its direct neighbors which of the *free* neighbors will become nodes. This will result in a visibility graph which is not minimal - which has more nodes than necessary. The redundant nodes are nodes at corners which are locally convex but (sometimes due to the discretization) not on a larger scale.

A further simplification can be reached if the plan is smoothed in a way that no diagonal one layer walls are allowed (*forbidden neighborhood*). Respectively as seen in figure 3.7 one has to decide if there is a solid wall or a row of columns with intermediate spaces which agents can move on through.

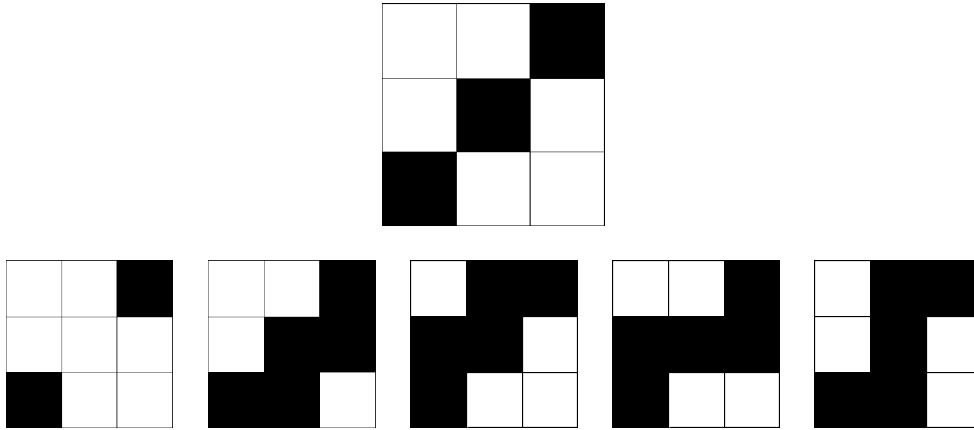


Figure 3.7: A forbidden neighborhood and its five possible smoothed versions

Accepting this restriction will make it very simple to decide which cell becomes a node cell:

1. Process each cell the following way:
2. Fix the cell as center cell.
3. If the center cell is a wall continue, otherwise process the next cell.
4. Mark each free cell in the von Neumann neighborhood of the center cell as node, if it does not share an edge or two corners with one or two wall cells other than the center cell within the Moore neighborhood of the center cell.

Expanded on actual neighborhoods this simple rule leads to six node generation neighborhoods (plus the ones that can be generated out of these by rotating and flipping them) of figure 3.8

With the constraint of a previously smoothed plan, processing the discretized plan this way results in a network where every non-node cell is visible to at least one node. This is due to the fact that if one tries to walk around a wall center cell as close as possible (shortest path) with diagonal steps allowed, a node cell is placed wherever one has to change the direction. Therefore a graph of all nodes which are mutually visible (visibility graph) will contain the shortest paths around arbitrary obstacles.

After the distances are calculated the distance of each cell is rounded to the next integer value. At first this measure might appear somewhat unmotivated, but subsection 3.2.2 of the discussion will explain it as one of the measures to reduce discretization effect.

For a labyrinth the resulting so called *static floor field* is shown in figure 3.9.

Probabilities for Eligible Destination Cells

Probabilities get assigned to each free and unoccupied cell in the neighborhood of an agent that corresponds to the maximum speed of that agent. In the following the

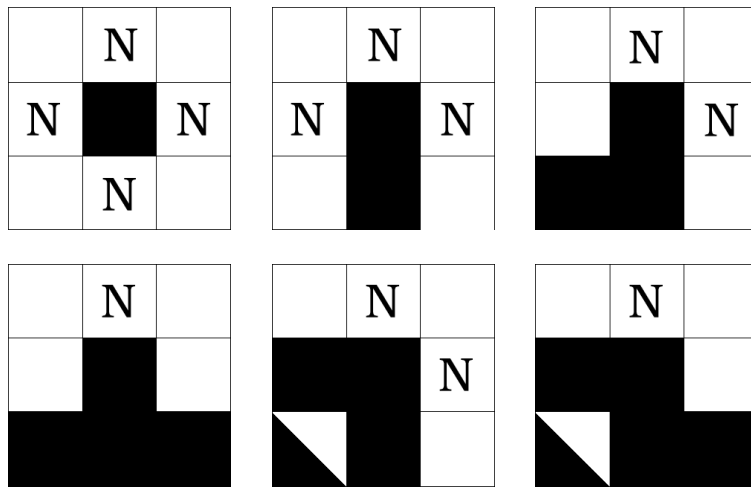


Figure 3.8: Node generating neighborhoods. The state of split cells does not matter.

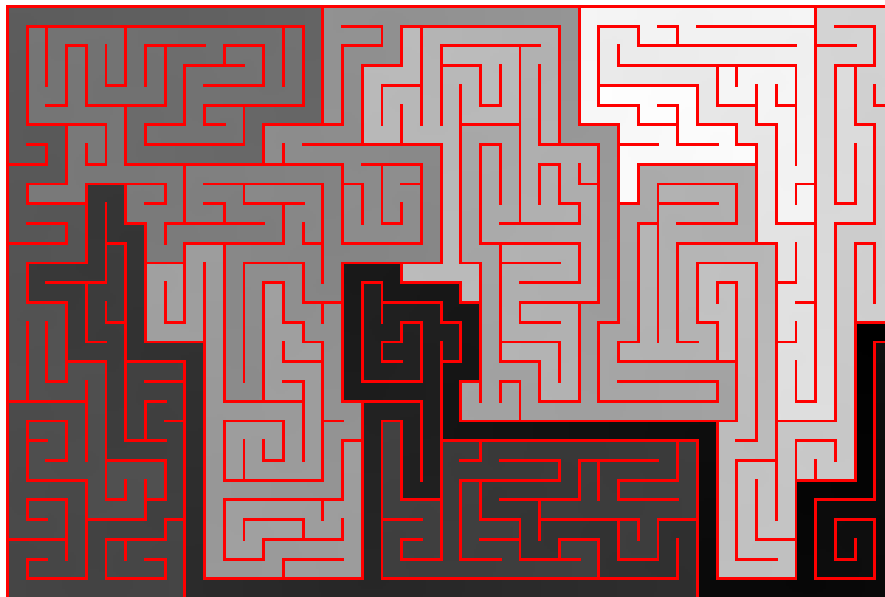


Figure 3.9: Static floor field calculated with Dijkstra's algorithm. The brighter a cell is, the larger is its distance toward the exit. The exit is in the center of the right edge

formulae of the different effects will only be listed briefly. Discussion and analysis will follow in section 3.2.

The probability that an agent chooses cell (x, y) is

$$p_{xy} = N p_{xy}^S p_{xy}^D p_{xy}^I p_{xy}^W p_{xy}^P \quad (3.19)$$

While N is a normalization constant, all p_{xy}^X are partial probabilities from the different influences on the movement of an agent.

1. p_{xy}^S is the influence of the *static floor field* which contains the information on the distance toward the exit.
2. p_{xy}^D is the influence of the *dynamic floor field* [100, 101] which contains the information of the motion of the other agents.
3. p_{xy}^I is the influence of inertia effects.
4. p_{xy}^W is the influence of nearby walls.
5. p_{xy}^P is the influence of nearby agents. Contrary to p_{xy}^D , p_{xy}^P depends on local densities not the motion of these agents.

These five influences will be introduced in more detail now.

Moving Toward the Exit - Following the Static Floor Field: With the static floor field p_{xy}^S is calculated for a certain cell at (x, y) :

$$p_{xy}^S = e^{-k_S S_{xy}^e} \quad (3.20)$$

With k_S being the *coupling strength* of an agent to the static floor field, knowledge as well as will to move are parametrized. All of the five influences are weighted against each other in their relative strengths by *coupling constants* k_X and all coupling constants are individual parameters of the agents, which are constant for an agent throughout the whole simulation. Time dependent coupling constants could evolve following ideas as presented in [32, 102]. However such ansatzes at the moment are in a very elementary stage and the agreement with reality has still to be tested. S_{xy}^e is the static floor field for exit e .

Herding Behavior - Following Others: Beside the main CA where the agents move, there is another CA - *the dynamic floor field* [29] - where agents leave a virtual trace whenever they move. This trace decays and diffuses with time. In the F.A.S.T.-model the dynamic floor field is a vectorial floor field. An agent who has moved from (a, b) to (x, y) adds $(x - a, y - b)$ at (a, b) to the dynamic floor field (D_x, D_y) after all agents have moved. The dynamic floor field does not change on intermediate cells, which the agents cross on their way from their source to their destination cell. After all agents have moved all values of both components of D decay with probability δ and diffuse with probability

α to one of the (von Neumann) neighboring cells. Since the vector components may be negative, decay means a reduction of the absolute value. Diffusion is only possible from x- to x- and from y- to y-component. Diffusion from a negative valued component means lowering the component value at the target cell whether it is positive or negative and vice versa for positive values.

The agents are influenced by the dynamic floor field:

$$p_{xy}^D = e^{k_D(D_x(x,y)(x-a)+D_y(x,y)(y-b))} \quad (3.21)$$

where (a, b) is the current position of the agent.

Inertia: Contrary to Newtonian physics, pedestrians experience de- and accelerating as being less arduous than walking through curves. Due to the shape and functionality of the human movement apparatus, pedestrians can de- and accelerate from and to their preferred walking speeds almost instantaneously compared to a timescale of one second. Yet deviating quickly by 90° e.g. from a certain direction while keeping up the walking speed is far more difficult. Therefore only centrifugal forces F_c are considered to have an influence on the motion of the agents:

$$p_{xy}^I = e^{-k_I F_c^{xy}} \quad (3.22)$$

On a circular motion for the centrifugal force holds

$$F_c \propto \frac{v^2}{r} \quad (3.23)$$

(Individual factors like the strength to resist centrifugal forces as well as coordinative abilities are summarized in k_I .)

The moment when a new destination cell is to be chosen is the point in the discrete world where no speed is defined. So there are basically three possibilities for speed v of equation (3.23):

- The speed of the last step,
- the hypothetical speed of the next step,
- or the average of both.

The F.A.S.T.-model makes use of the last possibility:

$$v = \frac{v_{last} + v_{next}}{2} \quad (3.24)$$

with v_{next} and v_{last} being integers determined by the neighborhood of speeds as defined in table 3.4.

Now, one has to think about the meaning of the radius r from equation (3.23) in discrete space: At some speed $v = v_{next}$ and a given angle $\Delta\phi$ between the movement of this and the last step, repeating this step with the same v and $\Delta\phi$ will lead to a

roughly regular polygon with n corners (n -gon). The radius of the circumcircle (r_{cc}) of this n -gon is taken for the radius r of the motion. Note: The choice of the circumcircle (and for example not the incircle) brings in some arbitrariness which has to be justified from the ability of the simulation to mimic reality afterwards.

Since the two equations

$$r_{cc} = \frac{v}{2 \sin \frac{\pi}{n}} \quad (3.25)$$

$$\frac{\pi}{n} = \frac{\phi}{2} \quad (3.26)$$

both hold for all regular polygons (see figure 3.10), here

$$r = \frac{v}{2 \sin \frac{|\phi|}{2}} \quad (3.27)$$

is also used as interpolation for all angles ϕ for which no regular polygon exists. The absolute value must be taken since $\phi = 0$ is meant to be the case of no deviation and of course there must be a symmetry between left and right turns. ϕ then is element of $(-\pi, \pi]$. And hence

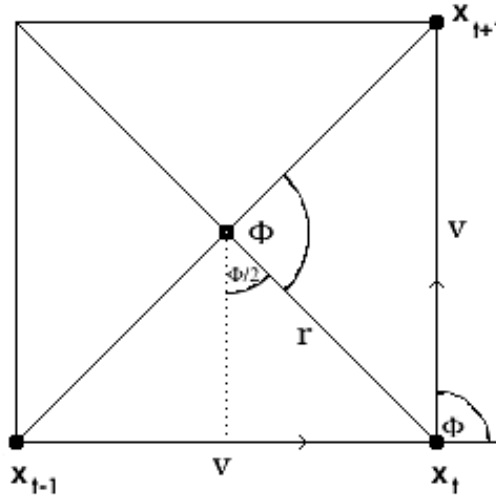


Figure 3.10: Example for calculating inertia.

$$F_c \propto 2v \sin \frac{|\phi|}{2} = (v_{next} + v_{last}) \sin \frac{|\phi|}{2} \quad (3.28)$$

leads to an inertia dependence of the movement probability

$$p^I(x_{t+1}, y_{t+1}) = e^{-k_I(v_{next} + v_{last}) \sin \frac{|\phi|}{2}} \quad (3.29)$$

$$\phi = \arctan \left(\frac{y_{t+1} - y_t}{x_{t+1} - x_t} \right) - \arctan \left(\frac{y_t - y_{t-1}}{x_t - x_{t-1}} \right) \quad (3.30)$$

with t counting the time steps. The agent is currently at position (x_t, y_t) .

Inserting ϕ from equation (3.30) in equation (3.29) results in

$$p^I(\Delta x_{t+1}, \Delta y_{t+1}) = \exp \left(-k_I (v_{next} + v_{last}) \sqrt{\frac{1}{2} \left(1 - \frac{\begin{pmatrix} \Delta x_{t+1} \\ \Delta y_{t+1} \end{pmatrix} \begin{pmatrix} \Delta x_t \\ \Delta y_t \end{pmatrix}}{\left| \begin{pmatrix} \Delta x_{t+1} \\ \Delta y_{t+1} \end{pmatrix} \right| \left| \begin{pmatrix} \Delta x_t \\ \Delta y_t \end{pmatrix} \right|} \right)} \right) \quad (3.31)$$

with

$$\begin{aligned} \Delta x_{t+1} &= x_{t+1} - x_t \text{hypothetical move} \\ \Delta y_{t+1} &= y_{t+1} - y_t \\ \Delta x_t &= x_t - x_{t-1} \text{last move} \\ \Delta y_t &= y_t - y_{t-1} \end{aligned}$$

Safety Distance Toward Walls: Exactly as in [30] this is considered via

$$p_{xy}^W = e^{(-k_W W_{xy})} \quad (3.32)$$

where W_{xy} is the distance of the cell (x, y) toward the closest wall.

For distances larger than a certain W_{max} , the effect vanishes completely and $p_{xy}^W = 1$.

Keeping some Distance Toward Other Agents: After each round for each cell (x, y) the number $N_P(x, y)$ of agents in its Moore neighborhood is counted. The more agents are immediately neighbored, the less another agent might want to choose this cell as his destination:

$$p_{xy}^P = e^{-k_P N_P(x, y)} \quad (3.33)$$

Figure 3.11 shows the effect of a non-zero k_P : The density at the border of a crowd

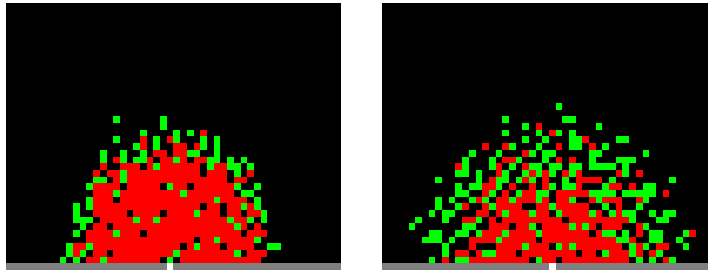


Figure 3.11: Situations after 200 rounds starting in a 100x100 cells room with 500 agents and $k_P = 0$ (left) respectively $k_P = 1$ (right)

changes less rapidly, while in the center of the crowd the density remains high since all free cells which an agent can reach during one round are surrounded by agents. Therefore the effect is canceled out. The strength of the effect depends on the ratio k_P/k_S and less on the absolute value of k_P .

3.1.3 Moving Toward the Destination Cell

Once all agents have chosen their destination cell there are many possibilities to actually move the agents. The various update schemes of the ASEP [103] must be reconsidered, supplemented and extended as there may appear conflicts during the motion process [90]. In the following a sample of possible movement update schemes will be described.

Jumping to the Destination Cell is the simplest way of moving the agents. This implies that the state of none of the cells between an agent and his destiny influences the agent on his way. However if a cell is chosen as destiny by two or more agents a *conflict* arises. Such a conflict remains unsolved with a probability μ , which is another parameter of the F.A.S.T.-model [2]. If a conflict remains unsolved none of the conflicting agents is allowed to move to the destination cell. All agents remain where they are. If a conflict is resolved one agent is chosen randomly who is allowed to move to the target cell, while all others remain on their cells.

Moving Cell by Cell is a more complicated, yet more realistic [87, 90] procedure with regard to the fundamental diagram. In this case an agent executes a sequence of steps within local Moore neighborhoods until he reaches his destination (or maybe does not). While doing so, each cell occupied by one agent during one step remains blocked for all other agents until the end of the round, even if the agent advances further and leaves this cell again during that round. To represent the *dynamic space requirement* [104] additional cells can be marked as blocked after an agent has taken one step (see figures 3.12 to 3.15). In this case blocked cells may overlap, yet only the agent who first blocked a cell is allowed to step on it in the future.

Annotation: In [90] it is suggested to fix the whole trajectories in advance and in [87] higher speeds are represented by doing the same decision algorithm for each step sequentially for each agent. The method chosen here to some extent lies between these two methods: The destination cell is fixed in advance, yet the cells which in the end form the trajectory are chosen sequentially, which implies that reacting to blocked cells is possible to some extent.

An agent deterministically steps on that unblocked cell in his neighborhood that is closest to his destination. This implies that whenever diagonal steps are necessary, they are executed first (see figure 3.16). If the cell closest to the destination cell is blocked, the next-closest cell is chosen and so on, as long as moving takes an agent closer to the destination cell. If two cells are equally close, the decision is done with equal probability.

With the blockage of once used cells, conflicts cannot only arise from common destination cells but also from crossing paths. The concept of unsolved conflicts is transferred in a way that each agent who shares his destination cell with other agents

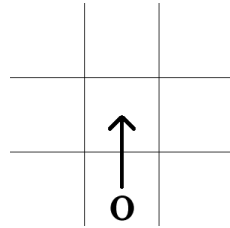


Figure 3.12: Variant 0 of cell blocking rules: Only the used cell gets blocked.

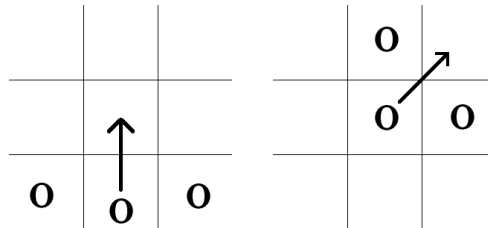


Figure 3.13: Variant 1 of cell blocking rules: The used cell and the next nearest neighbors orthogonal to the direction of motion get blocked.

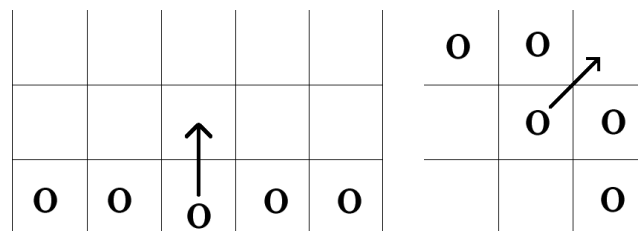


Figure 3.14: Variant 2 of cell blocking rules: The used cell, the next nearest and the next-to-next nearest neighbors orthogonal to the direction of motion get blocked.

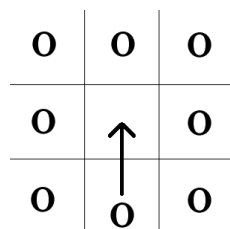


Figure 3.15: Variant 3 of cell blocking rules: All cells around the new position get blocked.

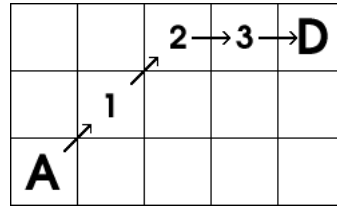


Figure 3.16: An agent's undisturbed path to his destination.

is not allowed to execute each of his steps with a probability $\sqrt[n]{\mu}/v$, where v is the current speed of the agent, n the number of competing agents and μ is the *friction* parameter. This leads to conflicts which may remain partially unresolved as each agent can take some of the steps into the direction of his destination cell. The n th root of the friction parameter is taken to make the conflict remain unresolved with probability μ for $v_{max} = 1$.

The Sequence of the Steps is the only statistical element in the process of moving toward the destination cell, at least it can be. The variants under consideration are:

- Ordered update* The sequence in which the agents execute their steps is the same in each round. An agent executes all of his steps before it is another agent's turn.
- Shifted update* The sequence in which the agents execute their steps is the same in each round, yet in each round the number of the agent who begins is shifted by a fixed or random amount. An agent executes all of his steps before it is another agent's turn. This is similar to the update scheme in [105].
- Shuffled update* The sequence in which the agents execute their steps is chosen randomly in each round. An agent executes all of his steps before it is another agent's turn.
- Full shuffle update* The sequence in which the agents execute their steps is chosen randomly in each round. So an agent does not execute all of his steps before it is another agent's turn. If nothing else is stated, this is the update scheme which was used for all further calculations. (See figure 3.17.)

Simulation Elements of Subordinate Priority are elements as stairs, attractors and connections between different floors, which do not influence the basic behavior of the model, but which are necessary in many real-life scenarios to produce realistic results.

Stairs reduce the average (horizontal component of the) speed of pedestrians by roughly 50% [104], regardless of the direction of motion. In addition to the results in literature own measurements were done, which can be found in section 4.2. The variety of possible motion behaviors on stairs is even broader than on a level. There is not one single

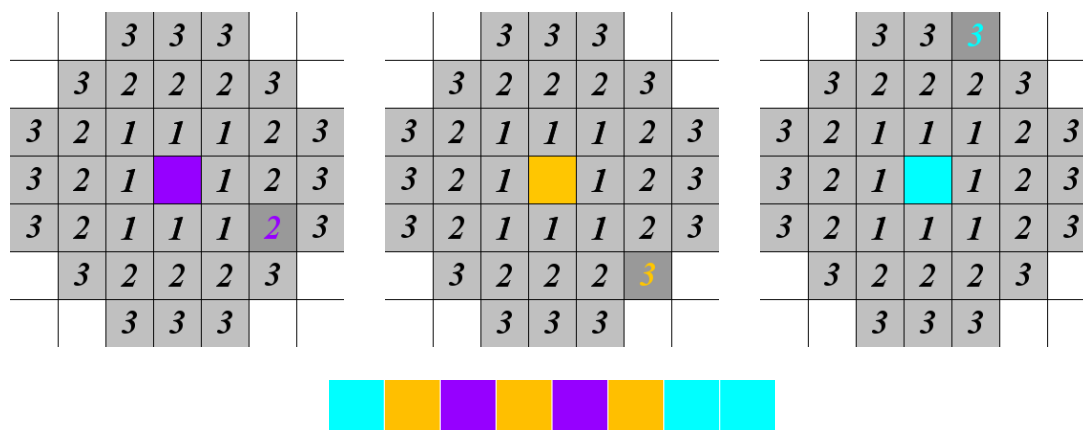


Figure 3.17: Three agents with destination cells and a possible sequence of steps in the full shuffle update scheme.

“correct” way to treat stairs. Therefore stairs are considered in quite a simple way such that an agent who is on a stair cell at the beginning of a round has his maximum speed reduced as table 3.5 shows. This speed reduction can be used as a rule of thumb to

$v_{max}...$...becomes v_{max} on stairs
1	1
2	1
3	2
4	2
5	3
6	4
7	4
8	5
9	5
10	6

Table 3.5: Speed \rightarrow Stair speed assignment.

model any uneven area that reduces walking speed in reality.

Attractors act like exits except that the agents can’t leave the building through them. Attractors are important to model routes that precede the actual evacuation process, e.g. passengers fetching life vests from their cabin before beginning the actual evacuation process. But also for basic tests (moving on a closed ring) they are important. For each attractor just like for an exit, a static floor field is calculated. Each group of agents then can have a list of tasks which will be processed one after the other. Each advice

consists of two numbers: The number of the attractor and the distance to that attractor at which an agent proceeds with the next advice. However if the first number is 0, the second number is interpreted as the number of rounds the agent will act as *random walker*. This concept appears to be simple, it is, however, quite flexible and opens a range of possibilities. In principle, a whole script language could be created to make more complex behavior possible as for example “Wait for agent no. $x!$ ”, “Wait for n agents!”, “Wait for announcement!”, “Keep close to agent $x!$ ” or “Search agent $x!$ ”. But as at least some of these orders only make sense on an individual basis, there also must be a good order-script-generation system available before or during the simulation. Or a practitioner would have to create an order-script “by hand” for all of the agents or at least for small groups. Ideas like this are necessary to implement, to make realistic simulations of complex scenarios. The basic properties with which this work deals must however not be forgotten over considerations on the consequences of the network structure of the society of a ship population or some other evacuee group.

Higher Floors have to be connected somehow. A real 3d-extension - a discretized volume - of the F.A.S.T.-model would at present be too expensive in terms of computer memory. Therefore, there are special cells which take agents who finish a round on them up or down one level. On the other level there are cells which act as entrance cells for agents who left another level through such a floor exit cell.

3.2 Discussion

In this section analytical and numerical results of different simulations in simple geometries are given. The particular factors that influence the motion are investigated separately.

3.2.1 Higher Speeds

Higher Speeds and the Fundamental Diagram

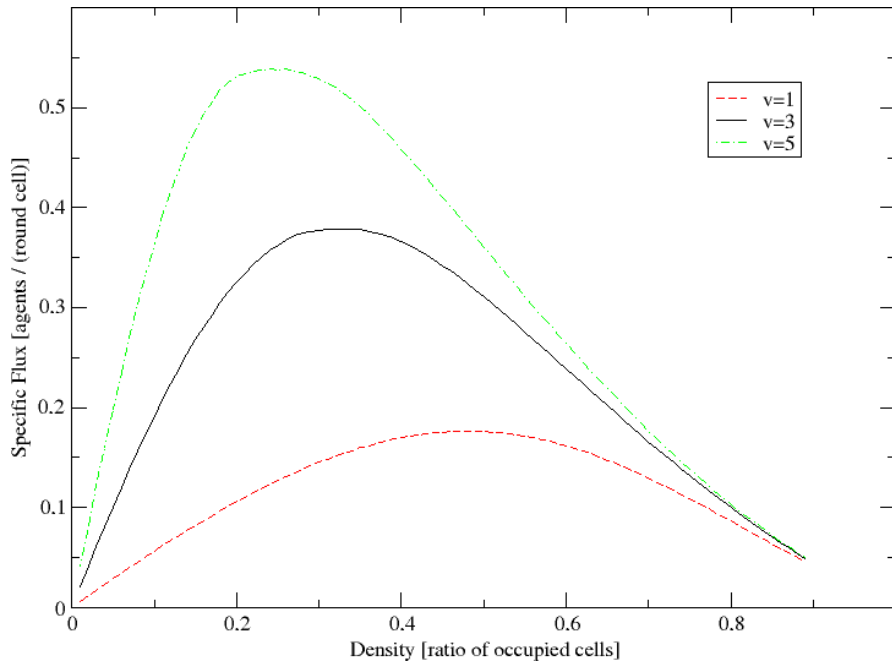


Figure 3.18: The specific fundamental diagram for $v_{max} = 1$, $v_{max} = 3$ and $v_{max} = 5$.

Figure 3.18 shows that the faster the agents can move the higher is the maximal flux. The position of the maximum varies greatly. Qualitatively this is something that is well known from particle hopping models as well as traffic models and phenomenology [85]. For $v_{max} = 1$ the maximum of the fundamental diagram is not located at $\rho = 0.5$. This is due to the fundamental diagram measured on a ring where the density is slightly larger near the inner than the outer wall. This and all further specific fundamental diagrams were calculated by letting the agents move on a ring with an inner radius of 990 and an outer radius of 1000 cells. So there are not only periodic boundary conditions but also a real curvature of the corridor. This opens an additional possibility to find deviations from symmetrical behavior of a model. For each round (time) the progress of each agent on the static floor field S (which is the speed orthogonal to the radius) is summed up and divided by the area of the ring. The density varies in steps of 0.01.

Note: In all further fundamental diagrams the “standard parameter set” is ($k_S = 1.0$, $v_{max} = 3$, all other $k_X = 0$). For comparison, in each diagram the corresponding “standard fundamental diagram” is drawn in black and with a solid line.

The Effect of Higher Speeds on the Symmetry of Walking Directions

Walking Speeds and Travel Times of Single Agents: To test the benefit of the considerations of subsection 3.1.1 for the equality of directions, several simulations were carried out where one agent moved a distance of 325 (the number < 1000 with the most integer solutions of Pythagoras: $325^2 = \Delta X^2 + \Delta Y^2$) cells into eight different directions with two different speeds. Each simulation was carried out 100 times. k_S has been set to 10.0 to make the simulation nearly deterministic. See table 3.6 for details and the corresponding figure 3.19. So the overall average evacuation time for $v_{max} = 1$ was 302.6

Δx	253	260	280	300	312	315	323	325
Δy	204	195	165	125	91	80	36	0
\rightarrow angle φ	38.9°	36.9°	30.5°	22.6°	16.3°	14.3°	6.4°	0°
$\langle T_{v=1} \rangle$	274.2	276.2	285.8	303.8	313.8	316.5	324.1	326.0
$\pm \sigma_T$	3.7	3.3	1.8	1.4	0.9	0.7	0.2	0.1
$\langle T_{v=5} \rangle$	67.4	67.0	66.0	64.9	65.0	65.2	66.0	66.0
$\pm \sigma_T$	0.5	0.2	0.2	0.4	0.4	0.4	0.0	0.0

Table 3.6: Scenarios and results.

rounds ± 7.00 rounds (2.30 %), while for $v_{max} = 5$ it was 65.9 rounds ± 0.30 rounds (0.46%). This means that the standard deviation of the overall average is roughly by the same factor smaller as the speed is larger. If one wants to interpret the agents moving in the two examples with 2 m/sec for $v_{max} = 1$, one round has to be interpreted as 0.2 seconds and for $v_{max} = 5$ one round would be one second. Then for $v_{max} = 1$ the time to move as far as 130 m would vary with the orientation of the discretization axis by more than 10 seconds ($(326.0-275.2) \cdot 0.2$), while for $v_{max} = 5$ it would be only 2.5 seconds (67.4-64.9).

A Radially Moving Crowd: 1948 agents were spread over 194812 cells of a circle area (radius 249 cells). With four exit cells in the center of the circle the agents started to move at once toward the center of the circle. The calculation was done twice: At first all agents had a maximum speed $v_{max} = 1$, during the second run, they had a maximum speed $v_{max} = 5$. See figure 3.20 for a comparison of how the initially rotationally symmetrical spatial distribution of agents evolves with time in the two cases.

Diagonal versus Horizontal Motion: As a last symmetry test, the simulated walking times of the two alternative routes (called A: Start $\rightarrow 2 \rightarrow 4 \rightarrow$ Exit and B: Start $\rightarrow 1 \rightarrow 3 \rightarrow 5 \rightarrow$ Exit) which are shown in figure 3.21 are compared. In reality route B is $\sqrt{2}$ times as long as route A and so should the walking times be for pedestrians with

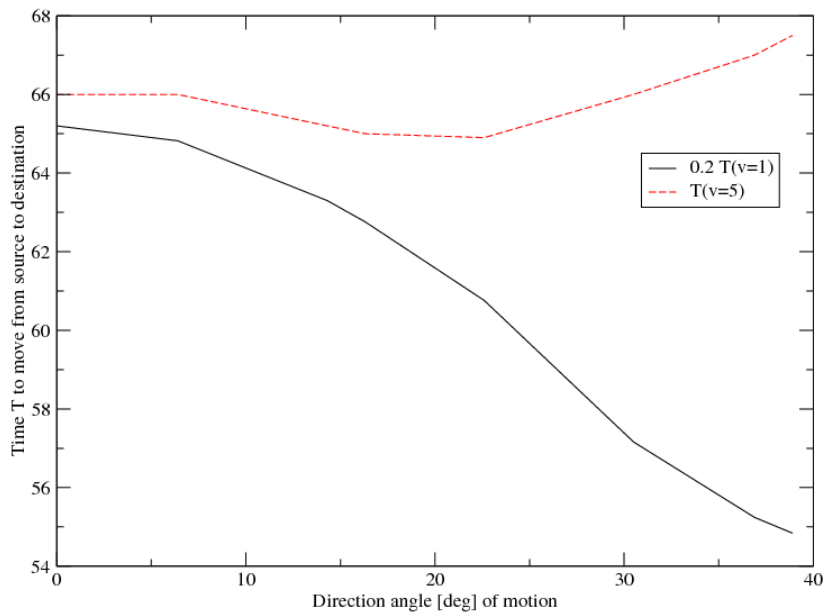


Figure 3.19: Influence of the direction of motion on the average speed.

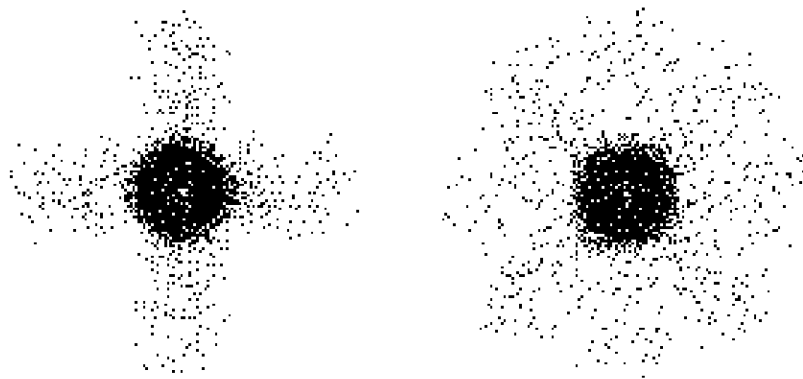


Figure 3.20: Comparison of two simulations with a crowd (black) moving to the center of a circle. The left image shows agents with $v_{max} = 1$ after 180, the right one agents with $v_{max} = 5$ after 36 rounds. In both cases there has been $k_S = 10.0$ and $k_P = 5$.

identical speeds. On the other hand, route A contains as many horizontal and vertical steps as route B contains diagonal ones. So agents with $v_{max} = 1$ are expected to take the same time on route A as on route B.

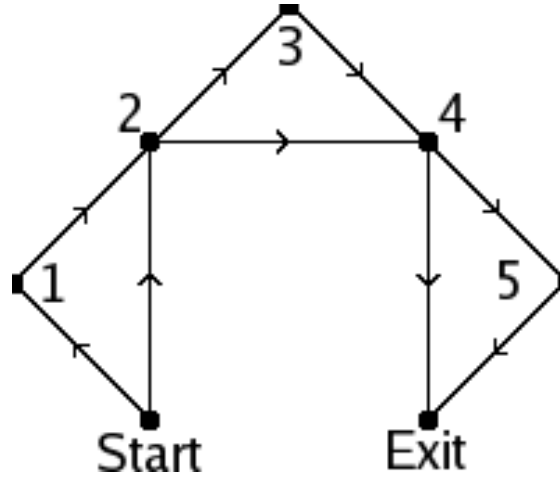


Figure 3.21: Two routes: Route A contains horizontal and vertical, route B diagonal parts.

The average (ten simulations) walking times for agents with a certain speed ($k_S = 10.0$) are shown in table 3.7. Because of the choice of speed neighborhoods,

	T_A	T_B	T_B/T_A	$T_B/(\sqrt{2}T_A)$
$v_{max} = 1$	291.1	328.4	1.13	0.80
$v_{max} = 2$	147.0	202.4	1.38	0.98
$v_{max} = 3$	98.6	155.2	1.57	1.11
$v_{max} = 4$	74.2	102.9	1.39	0.98
$v_{max} = 5$	59.4	86.7	1.46	1.03

Table 3.7: Walking times in dependence of v_{max} and the chosen path.

there is a tendency that the travel time is calculated more independently from the axis of discretization the faster (in terms of cells per round) the agents move. The reason why for $v_{max} = 1$ there is $T_B/T_A > 1.0$ is that for horizontal and vertical motion in the case of an integer-valued static floor field there are more possible paths that are chosen with equal probability even in the deterministic limit $k_S \rightarrow \infty$ and that do not lead to a delay in the arrival time. (See figure 3.22.) For a real valued static floor field there is one most probable path for each direction. Since a certain dispersion of the paths is much more realistic (see figure 3.24) this is an argument to keep the static floor field integer-valued.

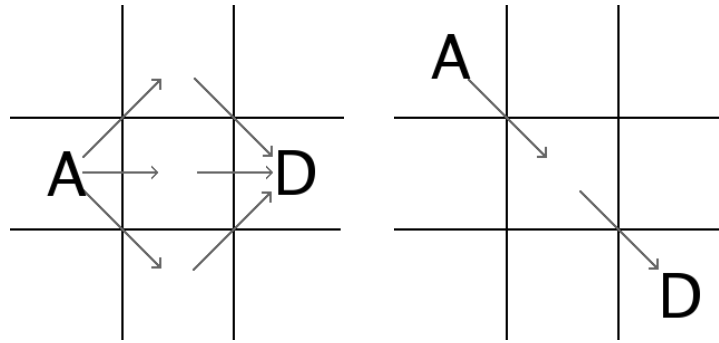


Figure 3.22: For horizontal motion there are three possibilities to move from A to D in two steps within a Moore neighborhood, and in the case of an integer-valued static floor field these paths often have an identical probability to be chosen. Yet for a diagonal path there is only one possibility.

3.2.2 The Static Floor Field

The Effect of an Integer-Valued Static Floor Field on the Symmetry of Walking Directions

If one rounds distances to integer values, small differences in distance are neglected. Therefore even large values of k_S do not lead to a totally deterministic behavior, since there might be - or in larger neighborhood probably will always be - a bunch of cells where $k_S S_{(x,y)}$ has the same value, which, if all other couplings are zero, leads to the same probabilities for the selection of the destination cell. If on the other hand the distances are not rounded, even the slightest difference in S will lead to deterministic behavior if k_S is chosen large enough. This has been considered in the scenarios of the last two paragraphs and will now be examined in more detail:

A Radially Moving Crowd: This time the shape of the crowd ($v_{max} = 1$; $k_S = 10$; $k_P = 5$) after 180 seconds is compared for integer- and for real-valued static floor fields.

Figure 3.23 shows that the dependence of the average speed on the direction of motion becomes even stronger for a real-valued static floor field.

Diagonal Motion in an Integer- and in a Real-Valued Static Floor Field: With identical parameters ($k_S = 10$) for the agents the occupancy (see section 3.4) differs quite a lot whether the static floor field is integer- or real-valued. Figure 3.24 shows that $k_S = 10$ leads to an almost deterministic behavior in a real-valued static floor field but that there always remains some statistical element in the motion governed by an integer-valued static floor field, not necessarily in the travel time of a single agent but at least in the chosen path.

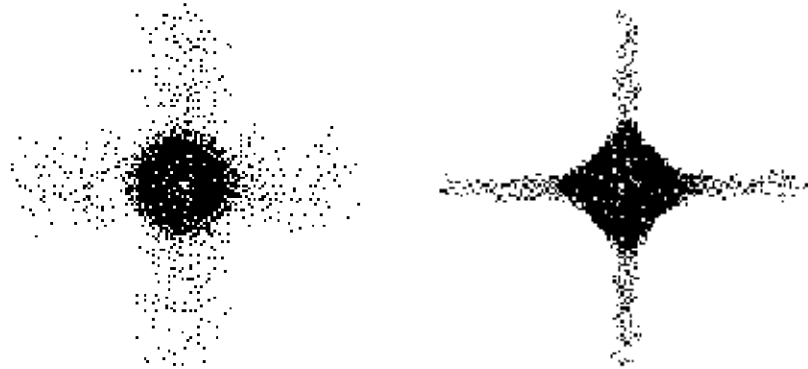


Figure 3.23: On the left: Situation with an integer-valued static floor field. On the right: situation with real-valued static floor field. Both snapshots show the situation after 180 seconds. Initially the agents ($v_{max} = 1$) were spread randomly over a circle area.

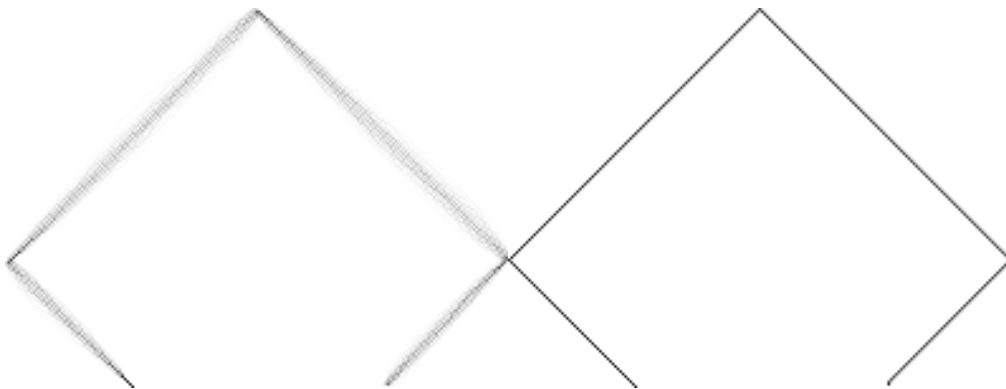


Figure 3.24: On the left: Occupancy with an integer-valued static floor field. On the right: Occupancy with a real-valued static floor field. Initially the agents ($v_{max} = 1$) were spread randomly over a circle area. The darker the pixel, the more often the cell was occupied by an agent in 1200 runs of the simulation.

The Static Floor Field and Average Speeds in a Narrow Corridor

At first one might think, that the results of a simulation with all agents moving at $v_{max} > 1$ and the interpretation of one round as $\Delta T = 1$ sec and a simulation with $v_{max} = 1$ and $\Delta T = 1/v_{max}$ sec will be the same. However this is not true as can be shown easily. This is especially interesting when one compares the F.A.S.T.-model to earlier models [28–30, 90, 96] which include a static floor field but where the speeds are equal to one.

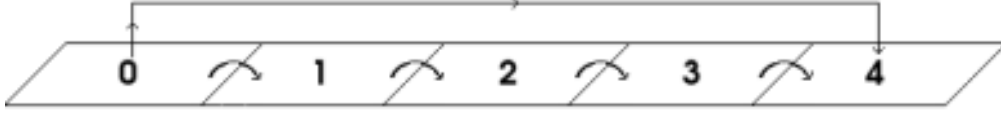


Figure 3.25: Single steps versus one large leap.

As a simplified model, the movement on a one-dimensional lattice is examined. Movement is governed by a static floor field which is growing linearly (one per cell) into the desired direction.

Walking and Planning Cell by Cell. It is assumed that stepping backwards is always allowed. For one step the probability to move one cell forward is

$$p_+ = N e^{k_S} \quad (3.34)$$

the probability to move backwards is

$$p_- = N e^{-k_S} \quad (3.35)$$

and the probability to rest is

$$p_0 = N \quad (3.36)$$

with N being the normalization

$$N = (e^{k_S} + 1 + e^{-k_S})^{-1} = \frac{1}{1 + 2 \cosh k_S} \quad (3.37)$$

The expectation value $\langle v \rangle$ for the speed v of a single step is then

$$\langle v \rangle = p_+ - p_- = \frac{2 \sinh k_S}{1 + 2 \cosh k_S} \quad (3.38)$$

Repeating this v_{max} times leads to the expectation value for the speed in dependence of the maximum speed:

$$\langle v(v_{max}) \rangle = v_{max} \frac{2 \sinh k_S}{1 + 2 \cosh k_S} \quad (3.39)$$

Let the number of steps forward (backward) be n_+ (n_-) and the number of rests be n_0 . Then (with $v = n_+ - n_-$ and $v_{max} = n_+ + n_0 + n_-$) the probability to move v cells for an agent with v_{max} is the sum over all possible combinations (n_+, n_0, n_-) :

$$p(v, v_{max}) = N^{v_{max}} \sum_{(n_+, n_0, n_-)} \frac{(n_+ + n_0 + n_-)!}{n_+! \cdot n_0! \cdot n_-!} e^{vk_S} \quad (3.40)$$

$$= N^{v_{max}} \sum_{(n_+, n_0, n_-)} \binom{v_{max} - n_0}{n_+} \binom{v_{max}}{n_0} e^{vk_S} \quad (3.41)$$

Which for $v_{max} - |v| = 2n$ (with $n \in \mathcal{N}_0$) is

$$p(v, v_{max}) = N^{v_{max}} \sum_{j=0}^n \binom{v_{max} - 2j}{n - j} \binom{v_{max}}{2j} e^{vk_S} \quad (3.42)$$

and for $v_{max} - |v| = 2n + 1$ is

$$p(v, v_{max}) = N^{v_{max}} \sum_{j=0}^n \binom{v_{max} - 2j - 1}{n - j} \binom{v_{max}}{2j + 1} e^{vk_S} \quad (3.43)$$

with the norm N as in equation (3.37).

Doing One Big Leap. If an agent is allowed to move any of $-v_{max} \leq v \leq v_{max}$ cells in one leap or at least choose one out of those cells as destination (plan ahead more than one cell), the probability to move v cells is

$$p = N e^{k_S v} \quad (3.44)$$

with the norm N

$$N = \left(\sum_{v=-v_{max}}^{v_{max}} e^{k_S v} \right)^{-1} = \frac{1}{1 + 2 \sum_{v=1}^{v_{max}} \cosh(vk_S)} \quad (3.45)$$

And so for the expectation value one has

$$\langle v(v_{max}) \rangle = N \sum_{v=-v_{max}}^{v_{max}} v e^{k_S v} = \frac{2 \sum_{v=1}^{v_{max}} v \sinh(vk_S)}{1 + 2 \sum_{v=1}^{v_{max}} \cosh(vk_S)} \quad (3.46)$$

A numerical illustration is given in table 3.8 and in figures 3.26 and 3.27.

v_{max}	$k_S = 0.5$			$k_S = 1.0$			$k_S = 2.0$		
	Steps	Leap	Ratio	Steps	Leap	Ratio	Steps	Leap	Ratio
1	0.32	0.32	1.00	0.575	0.58	1.00	0.85	0.85	1.00
continued...									

...continued									
v_{max}	$k_S = 0.5$			$k_S = 1.0$			$k_S = 2.0$		
	Steps	Leap	Ratio	Steps	Leap	Ratio	Steps	Leap	Ratio
2	0.64	0.91	0.71	1.15	1.45	0.79	1.70	1.84	0.92
3	0.96	1.68	0.57	1.73	2.42	0.71	2.55	2.84	0.90
4	1.28	2.56	0.50	2.30	3.42	0.67	3.40	3.84	0.89
5	1.60	3.50	0.46	2.88	4.42	0.65	4.25	4.84	0.88
6	1.92	4.48	0.43	3.45	5.42	0.64	5.11	5.84	0.87
7	2.24	5.47	0.41	4.03	6.42	0.63	5.96	6.84	0.87
8	2.56	6.46	0.40	4.60	7.42	0.62	6.81	7.84	0.87
9	2.88	7.46	0.39	5.18	8.42	0.62	7.66	8.84	0.87
10	3.20	8.46	0.38	5.75	9.42	0.61	8.51	9.84	0.86

Table 3.8: Comparison of average speeds between many steps and one leap strategy for different k_S . See also figure 3.26.

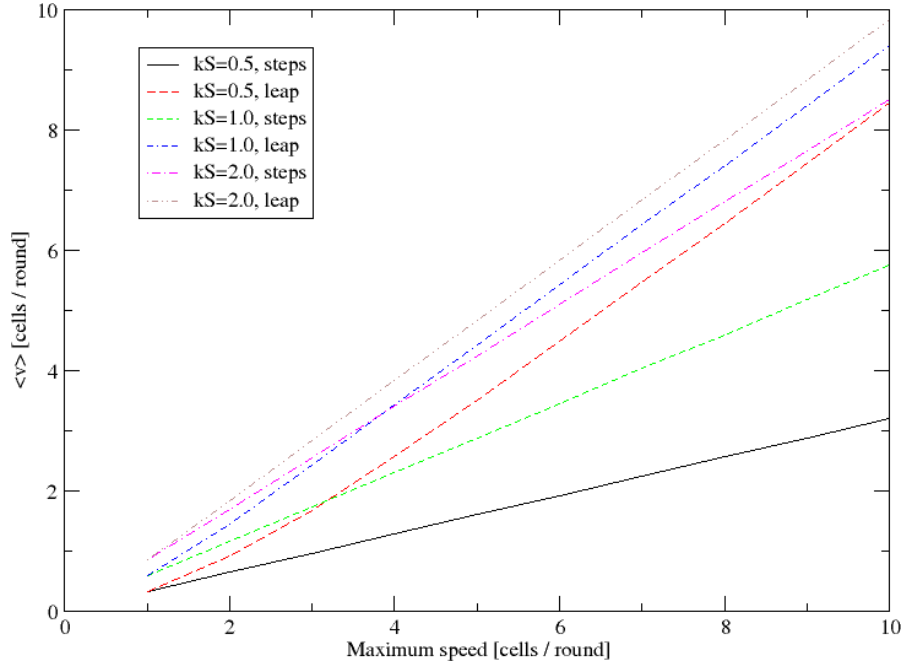


Figure 3.26: Comparison of average speeds for leap and for steps strategy.

A model where the agents can move v_{max} cells per time step at once will - at least in the case of small densities - lead to a more efficient behavior of the agents than a $v_{max} \equiv 1$ model where higher speeds are represented by the repetition of $v_{max} \equiv 1$ steps. This effect vanishes in the deterministic limit $k_S \rightarrow \infty$. While there are single steps

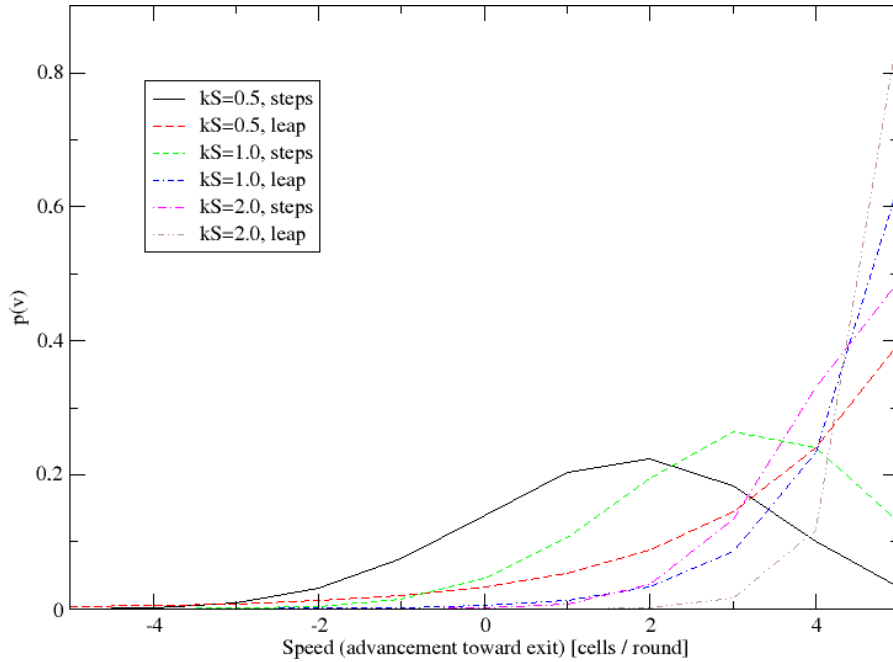


Figure 3.27: Probability to move v cells forward for $v_{max} = 5$.

from the initial toward the destination cell, the F.A.S.T.-model falls into the former category, as the planning process includes the whole area of movement.

Different Coupling Strengths to the Static Floor Field and their Influence on the Fundamental Diagram

Figure 3.28 shows how k_S influences the global specific flux in dependence of the global density. While for rising k_S the maximal flux increases significantly, the position of the maximum remains almost constant, which is in contrast to the dependence of the fundamental diagram on the maximum speed shown in figure 3.18.

3.2.3 The Dynamic Floor Field

The Vectorial Dynamic Floor Field as an Instrument of Analysis can be helpful, even with all agent's $k_D = 0$, since it can provide useful information on the state of the whole system. If one assigns each direction in the plain to a color from the color circle one can represent different directions by colors and thus not only get information where how many agents are as it is shown in a space-plot, but also gets information of something like a smeared first derivative of the space-plot.

The Dynamic Floor Field and the Fundamental Diagram Figure 3.30 shows that for moderate coupling constants $k_D < k_S$ the flux increases over the whole range of densities

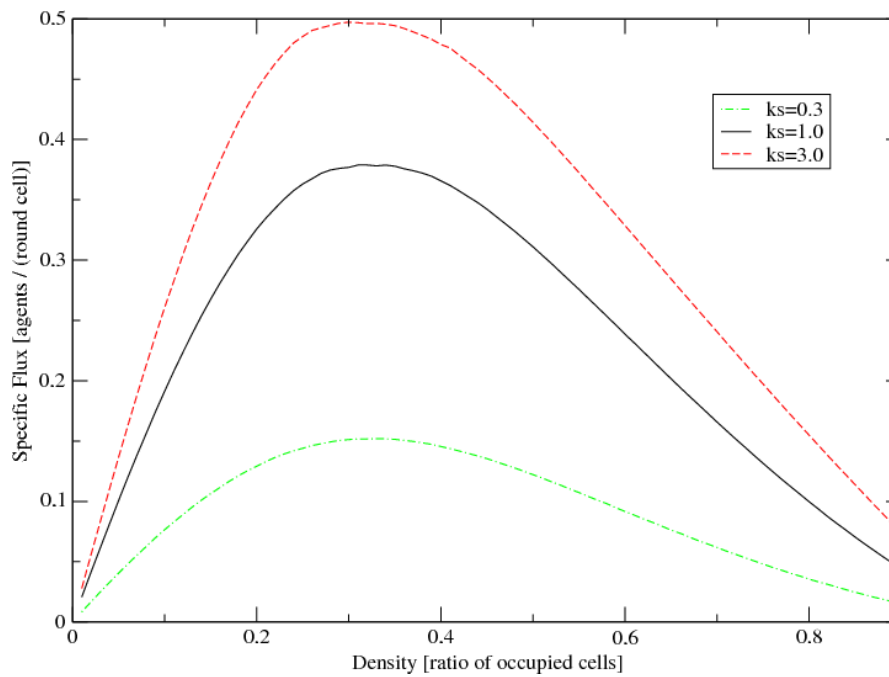
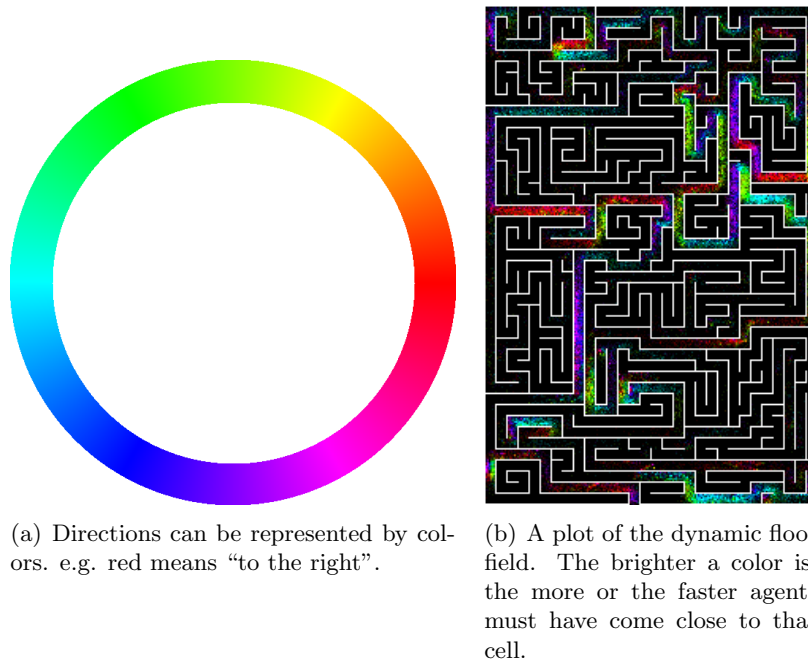


Figure 3.28: The specific fundamental diagram for $k_S = 0.3$, $k_S = 1.0$ and $k_S = 3.0$



(a) Directions can be represented by colors. e.g. red means “to the right”.

(b) A plot of the dynamic floor field. The brighter a color is, the more or the faster agents must have come close to that cell.

Figure 3.29: Directions and the dynamic floor field.

(compared to $k_D = 0.0$). The position of the maximum changes only slightly. The effect is similar to $k_S > 1.0$, but the shape of the fundamental diagram is slightly different.

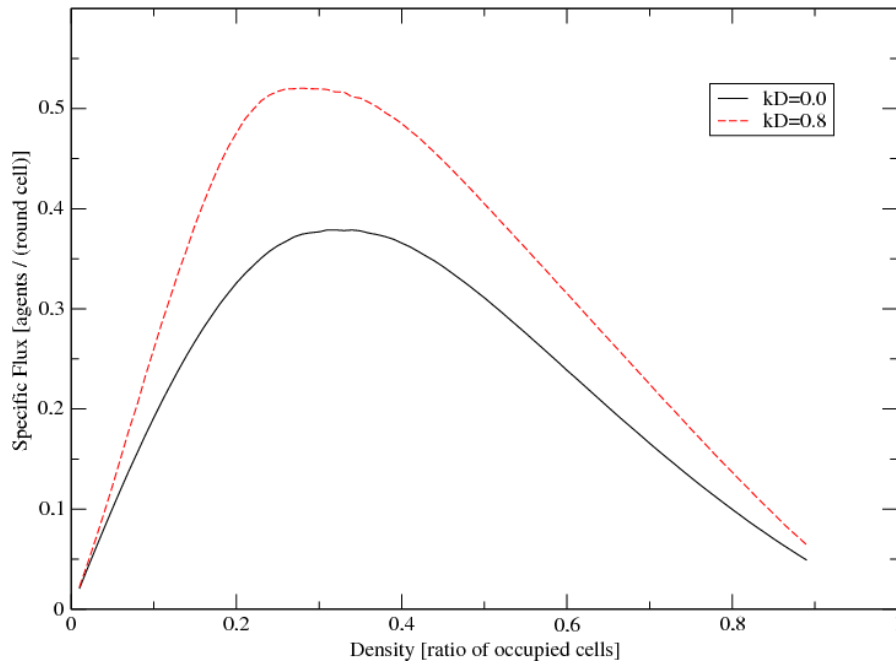


Figure 3.30: The specific fundamental diagram for $k_D = 0.0$ and $k_D = 0.8$, for which a significantly larger flux can be achieved.

Guided Evacuations can appear everywhere where there are two or more groups with different knowledge of the environment or different motivation to move like in kindergartens or on board of cruise ships at the beginning of the journey. In a simulation such situations can be modeled by creating two groups of agents. The first group (leaders) has a large k_S , a small k_D and a strong influence on the dynamic floor field, the second group (followers) has a small k_S , a moderate large k_D and a standard influence on the dynamic floor field. To demonstrate the effects of the vectorial dynamic floor field in such a situation, 100 leaders and 1000 followers were spread randomly in the maze from figure 3.9 and the egress process was calculated. This was compared with a scenario without a group of leaders. The parameters of the simulations are shown in table 3.9 and the results in table 3.10. The effect of a guiding group can be seen far better in the 95% quantiles (number of rounds when 95% of the agents have left the building) than in the average evacuation times. This is due to some agents who have their starting positions in remote parts of the labyrinth and who therefore are not guided toward an exit.

	Guided	Non-Guided
Leaders	100	0
Followers	1000	1000
k_S leaders	1.0	-
k_S followers	0.2	0.2
k_D leaders	0.0	-
k_D followers	0.2	0.2
Trace strength leaders	5	-
Trace strength followers	1	1
k_I, k_W	0.0	0.0
μ	0.0	0.0
k_P	0.0	0.0
α	0.8	0.8
δ	0.01	0.01
v_{min} leaders	2	-
v_{min} followers	2	2
v_{mean} leaders	2	-
v_{mean} followers	3	3
v_{max} leaders	2	-
v_{max} followers	4	4
v_{std} leaders	1	-
v_{std} followers	1	1
No. of runs	25	25

Table 3.9: Simulation parameters for guided and non-guided evacuations.

	Guided	Non-Guided
Fastest evacuation (#rounds)	11775	12389
Slowest evacuation (#rounds)	14133	14179
Average evacuation (#rounds)	12918.4	13241.3
St Dev. of average (#rounds)	664.2	463.9
Smallest 95% quantile (#rounds)	2511	3211
Largest 95% quantile (#rounds)	4905	6621
Average 95% quantile (#rounds)	3552.3	5503
St Dev. of average 95% quantile (#rounds)	755.9	859.2

Table 3.10: Simulation results for guided and non-guided evacuations.

3.2.4 The Effects of Inertia and Repulsive Walls

Inertia as well as repulsive walls have an influence on the way how a group of agents moves around a corner. The effects are similar in a way that they make the agents move around a corner in a wider circle (see figure 3.31). For small groups of agents a strong

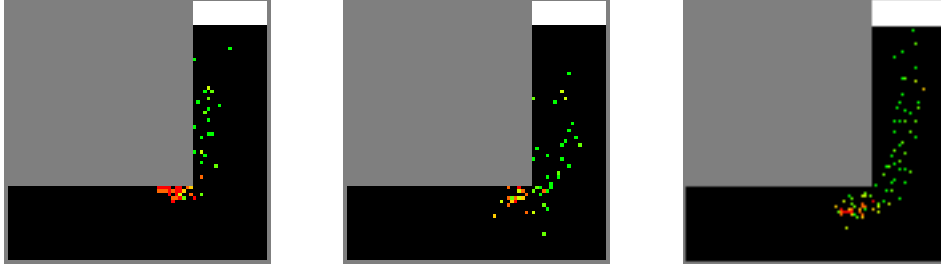


Figure 3.31: A group of 82 agents moving around a corner. From left to right: $k_I = k_W = 0$; $k_I = 1$ $k_W = 0$; $k_I = 0$ $k_W = 1$; with $k_S = 1$ and $v_{max} = 5$ for all three simulations

repulsion by walls leads to a higher value for the evacuation time, while for large groups it reduces the evacuation time. This is because the agents walk longer ways if they keep a certain distance toward the wall. Yet the fact that the repulsion by the walls decreases with distance prevents the agents from forming unphysical jams at the corner when all agents try to follow the shortest path.

	$k_I = 0$	$k_I = 1$	$k_I = 0$	$k_I = 1$
	$k_W = 0$	$k_W = 0$	$k_W = 1$	$k_W = 1$
82 agents	60.2	54.3	63.1	57.5
747 agents	316.9	263.5	282.2	246.6

Table 3.11: Average evacuation times (100 runs) for a small and a large group moving around a corner. The distance to walk has been about four times longer for the large group. All evacuation times differ mutually by more than the sums of their standard deviations.

The reduction of the walking time in simulations with $k_I = 1$ is not exclusively due to a larger effective width at the corner, since a decrease of the walking time of about 10% also happens in a straight corridor if k_I is set to $k_I = 1$ instead of $k_I = 0$. This is due to the proverbial fact that "the straight line is the shortest path". Once set on the direction toward the exit an agent with a value of k_I equal or close to the value of k_S will sway less and therefore have a higher effective speed toward the exit. For the large group however the reduction of the walking time is almost 17% and therefore clearly larger than the 10%-less-swaying-effect.

As for small groups the situations with $k_I = 1$ or $k_W = 1$ shown in figure 3.31 look more realistic, the slightly larger walking time does not obstruct setting k_I and k_W larger zero, as realistic does not have to be optimal behavior.

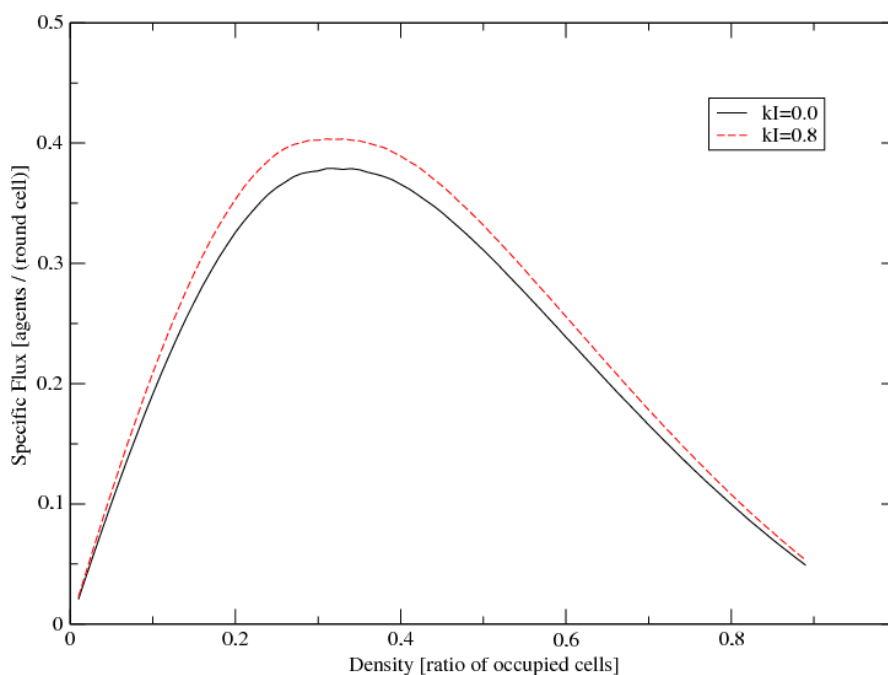


Figure 3.32: The specific fundamental diagrams for $k_I = 0.0$ and $k_I = 0.8$.

The fundamental diagram for repulsive walls - as shown in figure 3.33 - demonstrates that the effect of repulsive walls very much concentrates on the density range 0.1 to 0.5, as for very low densities every agent can freely choose to walk right in the middle of the corridor, while for high densities often all of the few free cells lie in the direct neighborhood of walls, which implies that the effect of reduced probability to choose such a cell as destination is given for all of the free cells and therefore canceled out mutually. Only in the intermediate range of density the agents start to compete for cells in the center of the corridor, raising the local density there.

3.2.5 The Effect of Inter-Agent Repulsion

The effect of inter-agent repulsion begins approximately at the density of highest flux. (See figure 3.34.) The effects of $k_P > 0$ can better be seen in the situation where two groups meet at an intersection than in the fundamental diagram. (See figure 3.35.) In the scenario each group consists of 300 agents who have to move through a corridor of a width of ten cells to an exit on the other side. Leaving by the exit of the other group is not allowed. The strong influence of the choice of k_P on the evacuation time for this process is shown in figure 3.36. The evacuation times for vanishing k_P appear to be

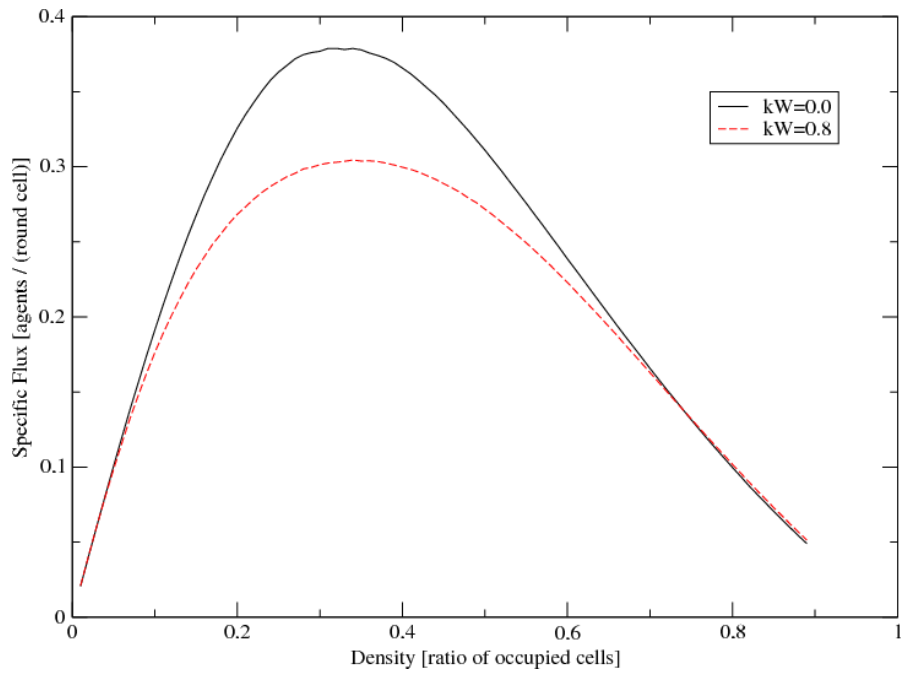


Figure 3.33: The specific fundamental diagrams for $k_W = 0.0$ and $k_W = 0.8$.

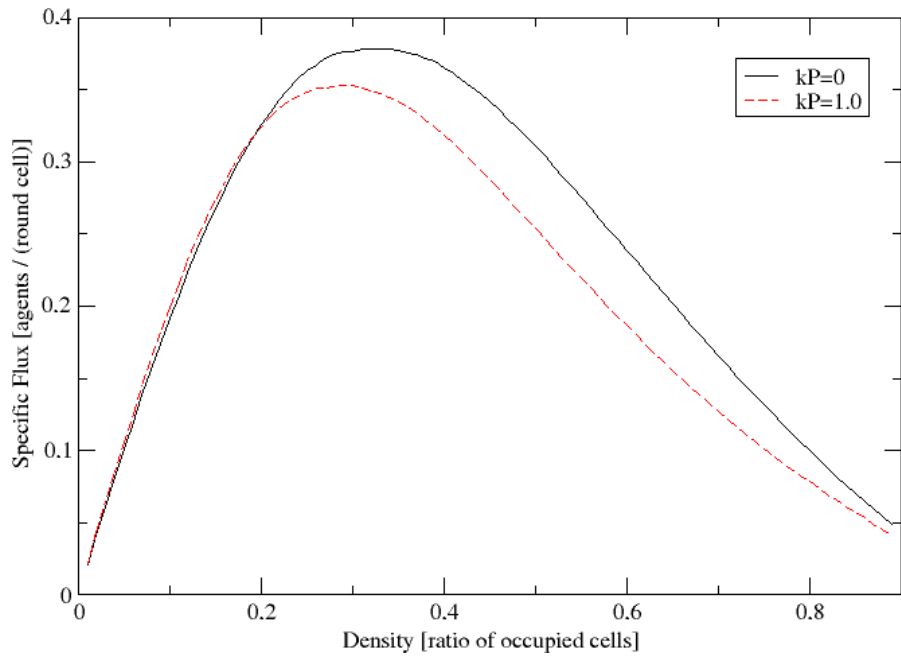


Figure 3.34: The specific fundamental diagrams without and with inter-agent repulsion

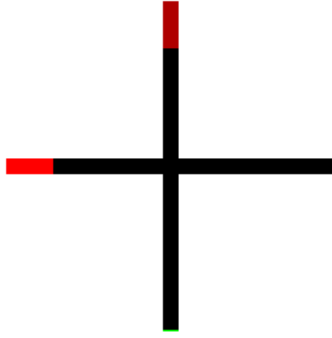


Figure 3.35: Floor plan with intersecting paths.

unrealistically large. Even without empirical data for comparison, one would suspect, that two groups in reality would need less time to pass mutually. This is fixed by setting $k_P \approx k_S/2$.

By this result one must not be misled to the assumption that k_P was an important parameter in any situation. For example, the simulation of an evacuation of 400 agents from an empty square-shaped room took 833.7 ± 7.4 rounds with $k_P = 0.0$ and 841.4 ± 7.9 rounds with $k_P = 1.0$ ($k_S = 1.0$ in both simulations).

3.2.6 The Influence of Friction

Friction effects become most important at narrow exits and narrowing corridors („bottlenecks”). Effects like “faster is slower” and “freezing by heating” as well as the idea of putting an obstacle in front of an exit to raise the outflow [106, 107] have attracted quite a lot of attention since they are counter-intuitive. A catalyzing effect of a pre-exit column has also been observed in a discrete model [88]. While similar effects have been observed in competitive situations [108], one question is at what level of competition or anxiety they become important or how a friction effect can or must be included into a model for normal or only slightly anxious behavior. The other question is what influence small details of the model in conjunction with details of the floor plan might have on the results of the simulation.

To demonstrate this reciprocal effect between model and floor plan, a crowd of a hundred agents leaving a room with an exit of width one cell was simulated. The exit was designed slightly differently during each simulation. All simulations were repeated 100 times with the same set of parameters. Figure 3.38 shows the way in which the floor plans were numbered. The average evacuation times were calculated as shown in table 3.12. Table 3.12 shows some remarkable effects. At first it appears that for different μ different exit designs appear to be optimal. This is not only a question of fitting best or fitting second best, but the difference is maximal. For example exit design 73 has for $v_{max} = 3$ the lowest of all evacuation times (quite a few of the others, however, lie within one standard deviation) if $\mu = 0.0$ and the largest if $\mu = 0.9$. For other exit designs,

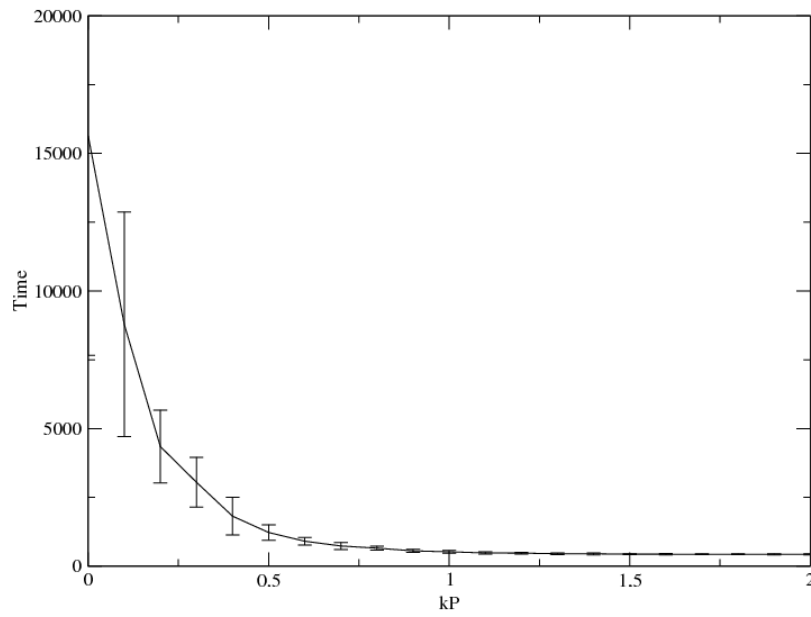


Figure 3.36: The time the crossing process takes decreases dramatically with increasing k_P at small k_P .

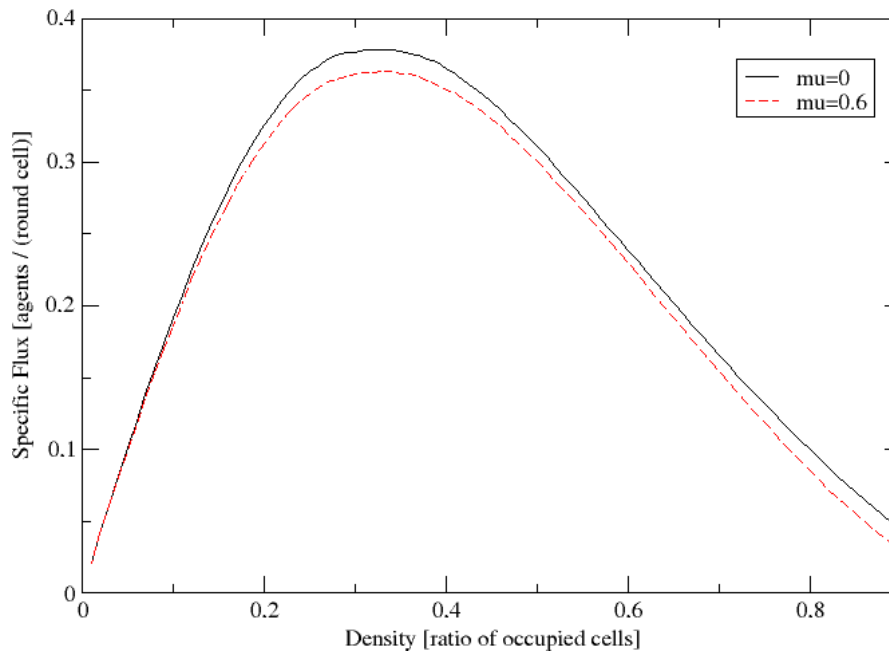


Figure 3.37: The specific fundamental diagram for $\mu = 0.0$ and $\mu = 0.6$. Friction reduces the flux for a broad range of densities.

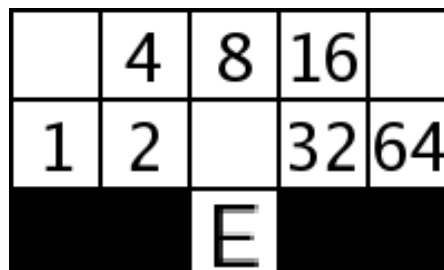


Figure 3.38: Exit designs: The number of the floor plan is the sum of numbers of cells which are blocked by a wall.

μ v_{max}	0.0		0.3		0.6		0.9	
	1	3	1	3	1	3	1	3
0	218.6	209.6	245.7	238.1	287.9	281.8	356.9	385.8
1	218.5	209.7	246.2	237.4	288.9	278.4	363.5	400.2
2	231.5	219.7	258.5	239.8	286.1	262.4	318.0	293.3
4	218.4	209.5	246.7	237.4	288.5	279.4	366.6	396.3
6	234.8	219.8	259.3	239.5	283.8	259.9	318.0	292.2
8	217.1	209.6	246.0	237.0	289.0	276.7	375.8	391.3
9	217.8	208.4	245.1	235.5	289.3	279.2	377.6	405.7
12	218.4	210.0	246.7	234.6	286.4	281.1	387.8	404.8
14	239.0	222.3	262.3	240.0	291.1	260.7	326.6	289.7
17	217.9	208.5	245.2	237.4	288.9	283.0	376.1	406.4
18	232.7	219.9	257.7	239.0	283.2	263.8	313.0	297.1
20	218.7	209.6	246.0	234.8	286.1	275.9	377.2	401.1
22	240.4	219.0	264.4	237.0	289.8	259.5	327.3	292.2
25	217.8	208.9	246.4	235.3	289.4	277.1	386.3	416.1
28	220.7	210.4	249.4	235.3	288.6	274.4	366.1	394.3
33	233.0	218.5	256.2	240.1	282.6	263.9	314.7	294.8
34	274.0	256.3	303.2	263.0	348.7	267.8	408.4	271.6
38	283.1	255.4	307.7	261.5	338.6	265.2	374.4	268.3
49	234.8	217.1	260.7	235.7	281.6	261.8	314.1	295.0
54	321.2	254.0	345.0	256.8	387.0	258.7	451.4	260.6
57	242.3	221.2	265.7	236.8	293.3	259.4	332.5	292.0
65	217.1	208.4	247.0	236.6	285.3	282.2	365.3	404.1
73	216.9	207.5	245.0	234.1	288.6	279.4	388.0	414.9
99	272.5	255.7	302.0	260.6	349.7	266.8	426.7	271.8

Table 3.12: Evacuation times in dependence of friction and exit design.

evacuation times develop similarly or contrarily if one changes μ . This is due to the fact that if the exit cell is visible and accessible from many cells it will be accessed with high probability if μ is small. An accessible exit cell on the other hand implies many conflicts, which slows down the evacuation process for larger μ . As there are more influences on the evacuation time, the effect does not show up best for exit design 0, in which the exit cell is most accessible. All this probably is more an artifact of the model not a prediction for reality. However one can make use of such information if one changes the plan for the simulation to distinguish a door of width 60 cm from one with width 40 cm or 80 cm. The safety advice for the practitioner would be not to experiment with exit designs and columns before exits, but to increase the width of an exit if a larger outflow is desired [108].

Another astonishing result is the evacuation time for simulations with $v_{max} = 1$ at exit design 54 and $\mu = 0$. A closer look at other evacuation times with $v_{max} = 1$ and $\mu = 0$ reveals that exit designs which contain a small corridor in front of the exit cell have a larger evacuation time than other exit designs. The reason for this is that in exit design 0 and others there are three cells from which the exit cell can be accessed. If there is a small corridor in front of the exit cell, the exit cell can only be accessed from one other cell. If an agent on this cell dawdles (chooses not to move) he will delay the whole evacuation process. In exit design 0 this only happens if all agents on cells neighboring the exit dawdle.

An Analytical Comparison of Two Exit Designs: For $v_{max} = 1$, $\mu = 0$ and exit design 34 which has a one cell shorter corridor than exit design 54, an analytical calculation can be done (see figure 3.39). It is assumed that whenever one of the three cells in front of the corridor is free, one of the agents that stands behind attempts to move on it during the very next round. The attempt is successful if there is no agent on the cell in the corridor who tries to step back. To compensate for that simplification the dawdling of agents is accounted for by a factor on the evacuation time which is the ratio of the evacuation times for a $k_S = 1.0$ and a $k_S = 10.0$ simulation within exit design 0. This factor is $218.6/201.3 = 1.086$ and not only contains situations where no agent from behind tries to advance but also situations where one of the agents on cells that are immediately adjacent to the exit moves sideways, denying advancement to an agent behind. Figure 3.39 shows the central agent advancing at the first step. Yet the meaning of this is “one of the three agents advances”.

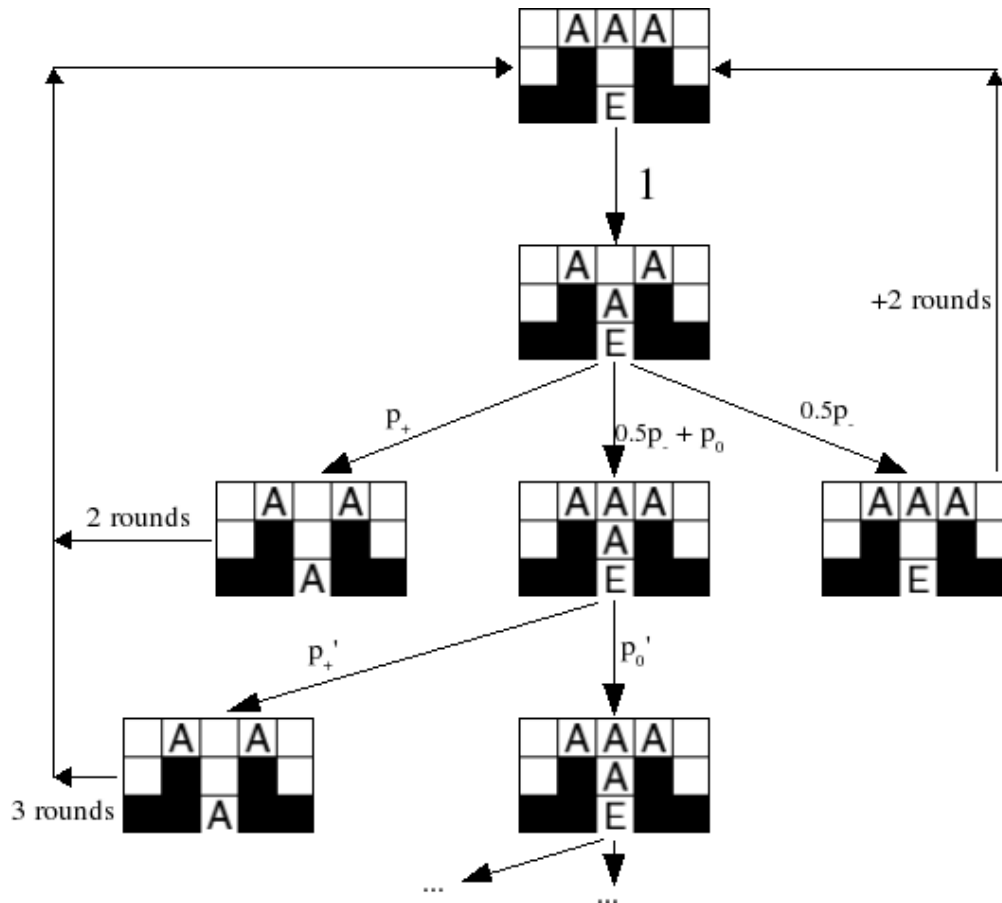


Figure 3.39: Exit design 34 - Transitions at exit together with the transition probabilities. The left and central branches show how the initial configuration reappears as one agent leaves the scenario after some rounds dawdling more or less, while the right branch shows how the configuration goes back to its initial state because an agent moves back on his initial position, implying that no agent leaves the scenario. Please note that the arrows that lead back to the initial state do not imply a progression of one round in time, while the other arrows do so.

The primed transition probabilities are those of situations where no back-stepping is possible. Therefore (with $k_S = 1$):

$$p_+ = \frac{e^{k_S}}{e^{k_S} + 1 + e^{-k_S}} \approx 0.665 \quad (3.47)$$

$$p_0 = \frac{1}{e^{k_S} + 1 + e^{-k_S}} \approx 0.245 \quad (3.48)$$

$$p_- = \frac{e^{-k_S}}{e^{k_S} + 1 + e^{-k_S}} \approx 0.090 \quad (3.49)$$

$$p'_+ = \frac{e^{k_S}}{e^{k_S} + 1} \approx 0.731 \quad (3.50)$$

$$p'_0 = \frac{1}{e^{k_S} + 1} \approx 0.269 \quad (3.51)$$

Since all dawdling effects which may appear in exit design 0 are also accounted for by the dawdling factor, the transition probability between the initial state and the second state has to be considered 1.

The agent in the corridor then has the choice of moving on to the exit cell, remain on the corridor cell or try to step back. In the latter case the conflict with the advancing agent will be won with probability 0.5. If the agent in the corridor moves on to the exit cell, he will be taken out of the simulation and the configuration before the exit returns to its initial state. The same holds if the agent manages to move backwards, adding two extra rounds on the evacuation time. If he remains on his cell, the same decision process will be repeated during the next round and the whole evacuation process will be delayed by one round.

The part of the expectation value for the evacuation time of an agent who dawdles a number of times is called T_l as it comes from the process shown in the left part of figure 3.39. The part of the expectation value for the evacuation time of an agent who moves forward and back again is called T_r . The expectation value for the evacuation time of $N = 100$ agents is then:

$$\langle T \rangle = N \cdot (T_l + T_r) \cdot (\text{dawdling factor}) \quad (3.52)$$

However this is not the full truth, since the dawdling of agents advancing from behind opens a second, third, or even more possibilities for a corridor agent to step back. This additional delay which cannot appear in exit design 0 evacuation processes and which therefore is not considered in the dawdling factor is hard to treat analytically, as there are already nine more cells involved. Therefore the following calculation gives a lower limit for the expectation value of the evacuation time.

$$\hat{p} := \frac{1}{2}p_- + p_0 \quad (3.53)$$

$$T_l = 2p_+ + 3\hat{p}p'_+ + 4\hat{p}p'_+p'_0 + 5\hat{p}p'_+p'_0{}^2 + \dots \quad (3.54)$$

$$= 2p_+ + \hat{p}\frac{p'_+}{p'_0{}^2}(1 + 2p'_0 + 3p'_0{}^2 + \dots - 1 - 2p'_0) \quad (3.55)$$

$$= 2p_+ + \hat{p}\frac{p'_+}{p'_0{}^2}\left(\frac{1}{(1-p'_0)^2} - 1 - 2p'_0\right) \quad (3.56)$$

$$\approx 2.306 \quad (3.57)$$

$$T_r = 2\sum_{n=1}^{\infty} n\left(\frac{p_-}{2}\right)^n \quad (3.58)$$

$$= 2\left(\frac{1}{(1-p_-)^2} - 1\right) \quad (3.59)$$

$$\approx 0.193 \quad (3.60)$$

$$\langle T \rangle \approx 100 \cdot (2.306 + 0.193) \cdot 1.086 = 271.4 \quad (3.61)$$

The sum in the term of T_r is not due to an agent who moves into the corridor, remains there for zero, one, two or more rounds and moves back again, but due to an agent moving ahead and backwards many times. The difference to the simulated 274.0 rounds in part must be due to the additional effects of dawdling described above. Another source of error is both, the beginning and the ending phase of the evacuation process as the assumption that there are always three agents on the three pre-corridor cells cannot hold during that phases. The simulation data furthermore show that in exit design 34 in average it takes 6.0 rounds until the first agent has left the room, while it is only 4.2 rounds in the case of exit design 0. With this correction one gets $\langle T \rangle = 273.2$ which is very well within the standard deviation of the simulation which has been 10.9 rounds for exit design 34 and 6.8 rounds for exit design 0.

For $v_{max} = 3$ the differences in the evacuation time are far smaller at $\mu = 0$. This is because an agent with $v_{max} = 3$ who stands on the center cell before a corridor can move into the corridor one two or three cells. As subsection 3.2.2 shows, he now will be much less likely to return to the cell before the corridor. For $\mu > 0$ exit designs with a corridor even show the slowest growth of evacuation times for $v_{max} > 1$, contrary to simulations with $v_{max} = 1$. The reason for this is that only the agent on the center cell can move more than one cell into the corridor, while his two neighbors at best could move onto the first cell of the corridor. A typical situation would be the central agent wanting to move three cells into the corridor and his two neighbors conflicting for the first corridor cell. In the random update scheme then there is a 2:3 chance for the central agent to be allowed to move first. If he is not allowed to do so he has the chance left that the conflict between his two neighbors remains unsolved. So there is a high chance that the central agent will reach his destination cell, because the symmetry between the three cells before the corridor is broken.

The conclusions one can draw are

- The large differences in the evacuation times for $v_{max} = 1$ are similarly unrealistic as is the fundamental diagram for $v_{max} = 1$. This is another reason to do simulations without $v_{max} = 1$ agents.
- At values of the friction parameter between $\mu = 0.6$ and $\mu = 0.9$, some dramatic changes in the evacuation times appear. Therefore it is very doubtful that values $\mu > 0.7$ are needed to reproduce any realistic situation.
- Since the simulation results vary with details of the model such as the decision if or if not an agent can choose a cell as destination which lies behind another agent and since it is very difficult and dangerous to reproduce situations with high friction in experiments, a general statement about an optimal exit design cannot be made easily. A simple solution to reduce evacuation times however is to widen the exit. The largest evacuation time in simulations with $v_{max} = 1$, $\mu = 0.9$ and an exit width of two cells, with all other parameters kept like in the calculations for table 3.12, was 171.0 rounds, which is smaller than all of the evacuation times calculated in scenarios with an exit width of only one cell. Additionally a reduced dependence of the evacuation time on the friction has been observed for wider exits: Instead of a 63.3% rise for $\mu = 0.9$ compared to $\mu = 0$ ($v_{max} = 1$, exit width 1) only a 20.2% larger evacuation time results for an exit width of five cells.

3.2.7 The Influence of the Blocking Variant on the Fundamental Diagram

The different blocking variants as shown in figures 3.12 to 3.15 lead to the fundamental diagrams of figure 3.40. The choice of the blocking variant changes the fundamental diagram at almost all densities. Just as in the case of the increased static space occupation (via $k_P > 0$), variants that shift the maximal flux toward higher densities also leads to larger, not smaller maximal fluxes. As interesting as these changes in the fundamental diagram may be, simulations that were done for section 3.2.8 all showed that no variant where more than actually once occupied cells were blocked lead to realistic results.

3.2.8 Comparison to Empirical Data

On page 54 of [104] a fit for the dependence of the speed of the density is given:

$$v = v_{free} \left[1 - e^{-g \left(\frac{1}{\rho} - \frac{1}{\rho_{max}} \right)} \right] \quad (3.62)$$

$$v_{free} = 1.34 \text{ m/s} \quad (3.63)$$

$$\rho_{max} = 5.4 \text{ persons/m}^2 \quad (3.64)$$

$$g = 1.913 \text{ persons/m}^2 \quad (3.65)$$

As the flux can easily calculated from the speed by multiplying it with the density ρ , this fit can be compared with fundamental diagrams as have been shown quite a few in

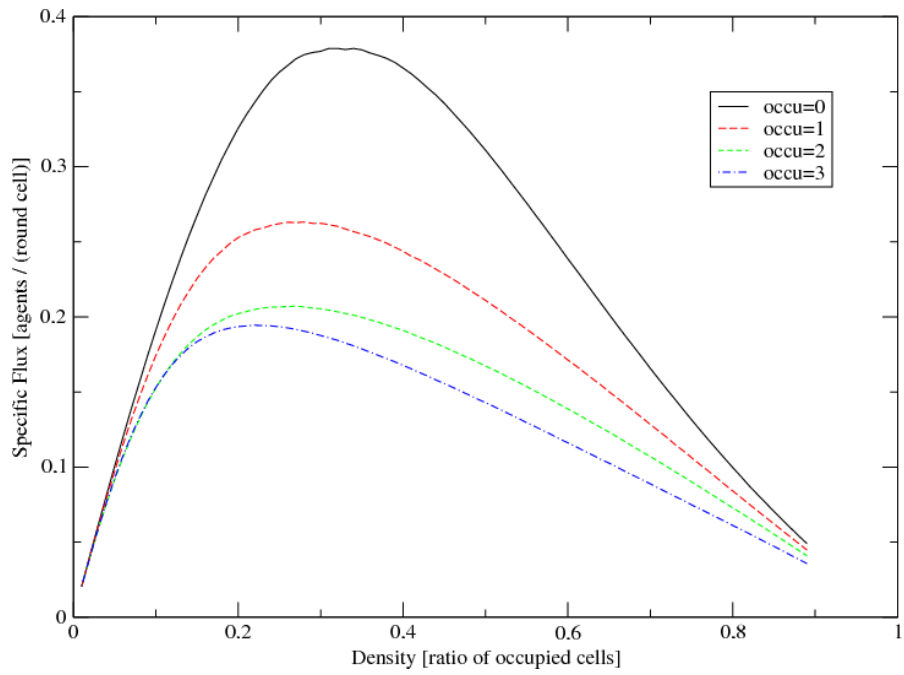


Figure 3.40: The specific fundamental diagram for the four cell blocking variants, as defined in figures 3.12 to 3.15

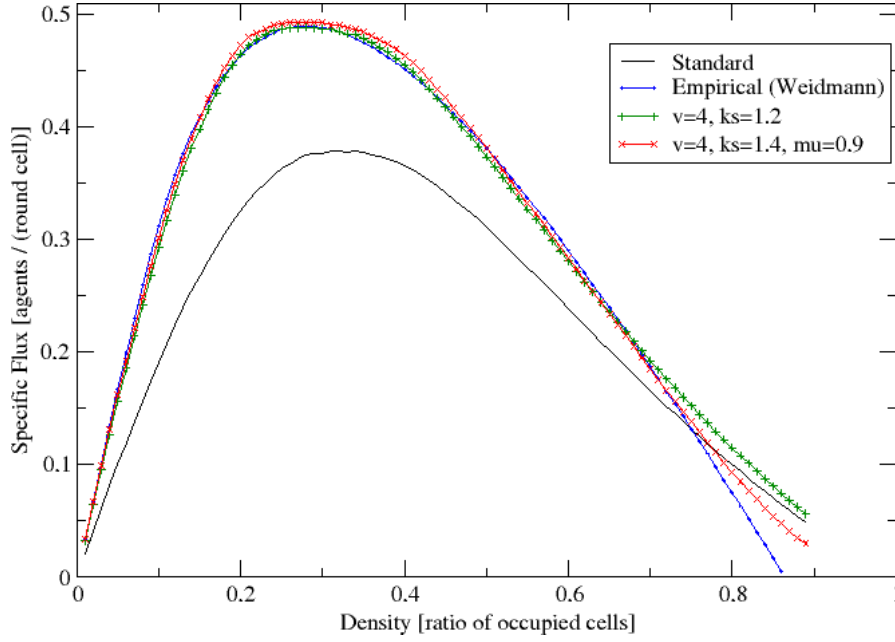


Figure 3.41: Comparison of two fundamental diagrams from simulations with the fundamental diagram that was fitted to a bunch of empirical data sets in [104]. All parameters that are not given explicitly are zero as in the standard set. The relative deviations are shown in figure 3.42.

this section. In addition one has to rescale the densities ρ and ρ_{max} , the free speed v_{free} and the gage constant g :

$$j = \rho v_{free} \left[1 - e^{-g' \left(\frac{1}{\rho} - \frac{1}{\rho_{max}} \right)} \right] \quad (3.66)$$

$$v_{free} = 3.35 \text{ cells/round} \quad (3.67)$$

$$\rho_{max} = 0.864 \text{ agents/cell} \quad (3.68)$$

$$g' = 0.30608 \text{ agents/cell} \quad (3.69)$$

There are probably many parameter sets in the F.A.S.T. that lead to fundamental diagrams that come close to this empirical one. In figure 3.41 two of them are shown. This flexibility is nice as far as it concerns the applicability of the model, as one can assume that it will probably be possible to reproduce a lot of different fundamental diagrams e.g. fundamental diagrams for only young or only elderly people, fundamental diagrams at different temperatures or times of day. From an epistemological standpoint this situation is not very nice, as one cannot find out - at least from looking at the fundamental diagram alone - how big the influence from friction or inertia *really* is. Finding one single “correct” parameter set is of course still possible by comparing the results of observations and simulations of other scenarios.

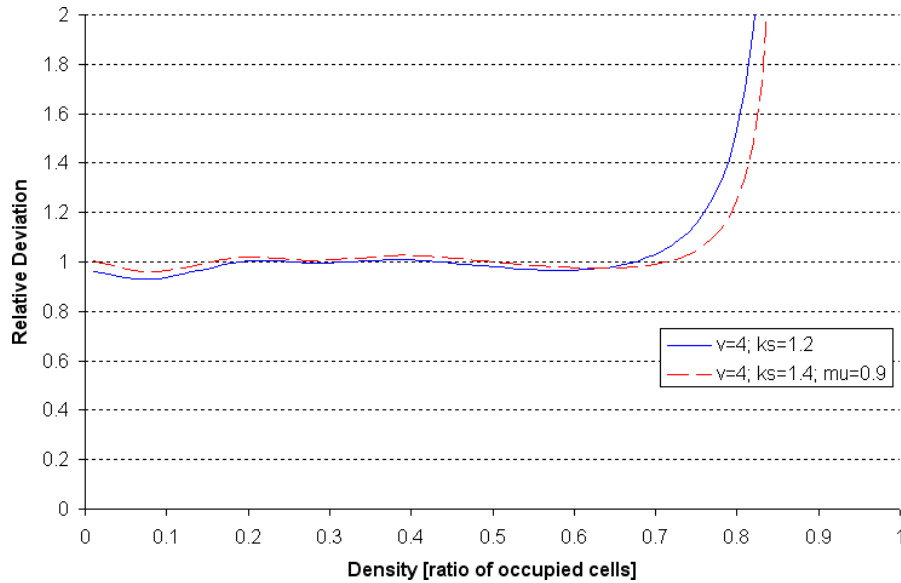


Figure 3.42: Relative deviations (simulation results) / (fit to empirical data) of the fundamental diagrams of figure 3.41.

It is obvious that for high densities there need to be deviations, since the interpretation of one cell as being $0.4 \cdot 0.4 \text{ m}^2$ allows motion at higher densities than the maximum density stated in [104] where the theoretical fit deviates most from the empirical curve for large densities. In addition one must assume that for large densities the amount of data that were used to produce the fit is far smaller than for small densities. For densities up to 0.7 ($4.375 \text{ persons/m}^2$) the deviation of the two simulated diagrams from the fitted one are smaller than the deviations of the fit from the empirical curve (compare figures 3.41 and 3.42 with [104], page 54).

3.2.9 Exit Strategies

An agent who finishes a round on an exit cell is taken out of the simulation after the choice of destination cells process of the next round. Therefore an exit cell can only be used by an agent each other round. With the cell width of 40 cm the maximal specific outflow therefore is $0.5/0.4 = 1.25$ agents per second and meter exit width. This is in principal in agreement with the 1.33 persons per second and meter stated as maximum outflow in [74] and the 1.22 persons per second and meter maximal flux in a corridor of [104]. However the theoretical maximal limit of the F.A.S.T model is typically not reached. This can lead to unrealistic jams in front of exits. Yet such jams do not necessarily have to be unrealistic. A steep or short staircase at an exit or a structural element of the door may reduce the outflow as well as people who have escaped already

but keep standing close to the door on the outside, or reduce their speed. Therefore a fine tuning of the outflow can be done:

- The “normal exit strategy” leads to the smallest outflow. (See figure 3.43.)
- If the depth of the exit group is increased up to the maximal speed, the agents decelerate less when approaching the exit. (See figure 3.44.) Since all exit cells are on the same height 0 of the static floor field, the probability to choose the cell in front is the same as for the cell most remote of an agent. This is why the outflow only increases slightly.
- If an agent approaches not an exit but an attractor that lies behind the exit, he is more likely to keep his speed than in the former strategy and the outflow is increased more. (See figure 3.45.)
- If the agents are not counted as being evacuated when they have left the simulation through an exit but when they have moved on a cell with a static floor field smaller than a certain value S_0 , the measurement stays uninfluenced of the doors that are placed behind the point of interest. (See figure 3.46.) One has to make sure that possible unrealistic jams from that exit do not reach back to the point of measurement. This strategy allows an agent to re-cross the line of measurement. It can also be used to measure the evacuation times of higher floors or certain areas in one simulation if S_0 is set on the smallest value of the static floor field in a certain floor or area.

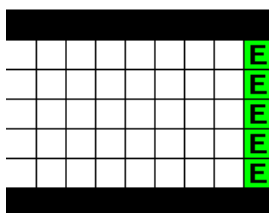


Figure 3.43: The “normal exit strategy” with only one row of exit cells at the true point of the exit leads to the smallest maximal outflow.

Another exit strategy would be to take an agent out of the simulation as soon as he reaches an exit cell instead of leaving him in the simulation until the next round. This clearly leads to the highest outflow, yet it is in a similar manner unrealistic as a general deceleration at an exit, since real persons do not simply disappear at exits. Note that if $k_W > 0$ and a wall is placed behind the exit cells the outflow becomes reduced. This of course cannot appear in the “extra floor exit strategy”. Figure 3.47 and a comparison with the results of [76] show that - concerning the evacuation time - the F.A.S.T.-model leads to more conservative results than the four commercially available software packages that were tested there, and that the results up to an initial density of 0.52 agents per

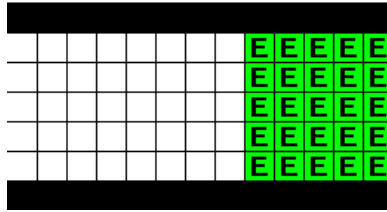


Figure 3.44: The “deep exit strategy” with up to $\max(v_{max})$ (maximum of all agents) rows of exit cells at the true point of the exit leads to a slightly increased outflow.

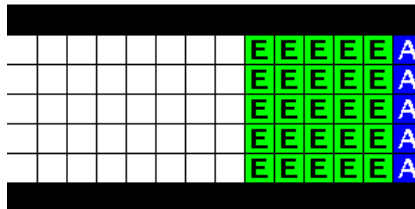


Figure 3.45: The “attractor exit strategy” with up to $\max(v_{max})$ rows of exit cells in front of an attractor that the agents head for increases the outflow even more.

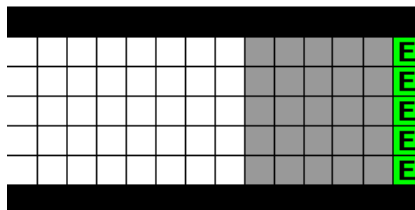


Figure 3.46: The “extra floor exit strategy” leads to the largest outflow. Here an agent is counted as having escaped if he is on a cell with a static floor field value of five or less.

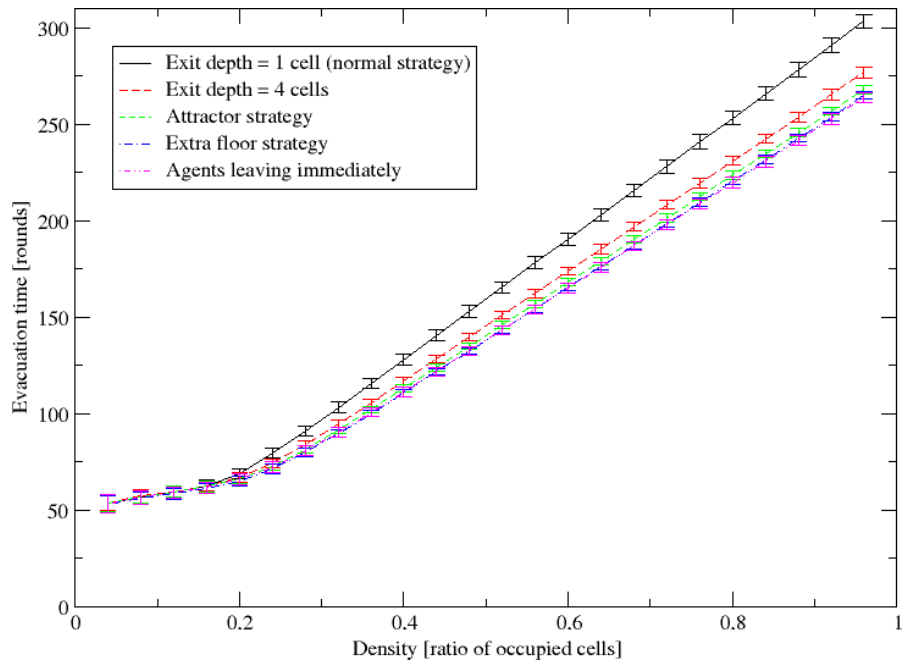


Figure 3.47: Evacuation times (averages and standard deviations of 1000 simulations for each scenario) from a corridor with a length of 125 cells (50 m) and a width of 5 cells (2 m). Note that the calculation is done to higher densities than in [76]. For comparison with the results of scenario 2 in [76] it is helpful to know that 4.0 persons per square meter is equivalent to 0.64 agents per cell.

cell (3.25 persons per square meter) lie well within the hand calculation area [109] for all exit strategies. Between 3.25 and 4 persons per square meter they lie above or within the hand calculation area, depending on the exit design .

3.2.10 Correlations in Oscillations at Bottlenecks

“*Oscillation*” is a widely used word, which here is understood to be the phenomenon that the direction of flow changes in certain intervals when two groups of particles compete for the right to move at narrow bottlenecks. Oscillations in pedestrian dynamics have been dealt with before [56, 110]. The aim of this subsection is to give a framework for an analytical and quantitative treatment of oscillations in observation, experiment and simulation.

There are three extreme types of oscillation: 1) The zipper principle: The flow direction changes after each particle. 2) No oscillation: The flow direction only changes after one group has completely passed the bottleneck. 3) Uncorrelated oscillation: The statistics of the flow direction is the same as for coin-tossing-experiments. While in the first two scenarios the whole process is completely determined as soon as the first particle has passed the bottleneck, there is absolutely no influence from one *event* to the next in the third scenario. Between those extremes there is a continuous spectrum of correlated oscillations with an influence from one event to the other but no full determination.

The Scenario

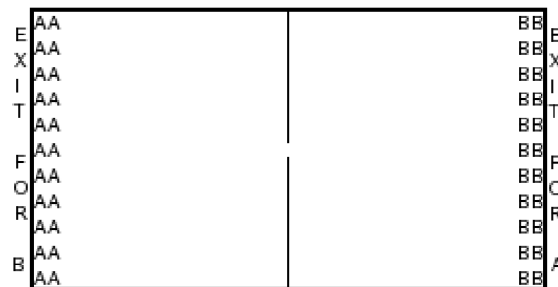


Figure 3.48: Initial positions of the agents in the scenario. (schematic view)

At the beginning of the simulation two groups (A and B) with $N_A = N_B = 202$ ($N = N_A + N_B$) agents each are placed in two rows as shown in figure 3.48. They have to pass the bottleneck with a width of one cell in the middle and proceed to the exit on the other side. An agent is counted as having passed as soon as he leaves the bottleneck cell in the direction of his exit. The possibility that he moves back into the bottleneck is given but neglected. Only the first $n = 100$ agents passing the bottleneck are taken into account to make sure that there are always two almost equally sized groups competing for passage. Of these $n = 100$ agents the number of agents of group A is called n_A and

of group B n_B . n cannot be chosen arbitrarily large, as at some size the crowds in front of the bottleneck become that dense that no passing is possible at all.

There are no new agents entering the scenario.

Observables

The Wald-Wolfowitz Test (also called “*runs test*”) can be used to check for correlations in time series whenever the statistic is dichotomous or can be dichotomized, i.e. when two kinds of events or data are present. The probabilities for the events to happen do not need to be equal. In this case those two kinds of events are “A member of group A passes the bottleneck” and “A member of group B passes the bottleneck”. The Wald-Wolfowitz test makes a statement about the expectation value and the variance of the number of runs (and other observables) if there are no correlations between the different events. In the terminology of the test a *run* is a series of events of one kind not interrupted by an event of the other kind.

The crucial values of the Wald-Wolfowitz test are:

- $\langle R(n_A, n_B) \rangle$ is - for given n_A and n_B - the expectation value of the number of runs for an uncorrelated series of - in this case - bottleneck passages.
- σ_R is the standard deviation of the expectation value of the number of runs.
- r is the number of runs in a certain simulation,
- $z = \frac{r - \langle R(n_A, n_B) \rangle}{\sigma_R}$ is the standardized test variable.

For $n_A, n_B \gg 1$ (at least $n_A, n_B > 10$) the distribution of the number of runs becomes comparable to the normal distribution which implies that the null hypothesis “The events are uncorrelated” can be rejected on an α -level of significance if $|z| > q(1 - \alpha/2)$, with $q(1 - \alpha/2)$ as quantile of the standard normal distribution for the probability $1 - \alpha/2$. For smaller n_A, n_B one has to make use of tables to decide about the rejection of the null hypothesis [111, 112].

For an uncorrelated process one has for given n_A, n_B

$$\langle R(n_A, n_B) \rangle = 2 \frac{n_A n_B}{n} + 1 = 2 \frac{n_A(n - n_A)}{n} + 1 \quad (3.70)$$

$$\sigma_R^2 = \frac{2n_A n_B (2n_A n_B - n)}{n^2(n - 1)} = \frac{(\langle R \rangle - 1)(\langle R \rangle - 2)}{n - 1} \quad (3.71)$$

The Wald-Wolfowitz test is independent of underlying distributions. Therefore it does not make use of deviations in the distribution of n_A in subsequently repeated simulations of a scenario. This additional information can be made use of by mapping the process onto a correlated random walk. This implies that one assumes that it is only the very last event that influences the next one.

In Correlated Random Walk Models [113, 114] the probabilities for the direction of the next step depend on the direction of the last step. The “correlated random walker” keeps his direction of motion with probability p and changes it with probability $1 - p$.

In the first step the direction is chosen with equal probability. In the thermodynamic limit ($n \rightarrow \infty$) one then gets a normal distribution $\mathcal{N}(n/2, \frac{p}{1-p}\sigma_A^2(p=0.5))$ for the probability that the walker made n_A of n steps to the right [115]. Here $\mathcal{N}(X_0, \sigma^2)$ is the normal distribution with maximum at X_0 and variance σ^2 , and $\sigma_A^2(p=0.5) = n/4$ is the variance for the number n_A of steps to the right in the case of uncorrelated random walk ($p=0.5$). The position x_n of the walker after n steps is $n_A - n_B$. Numerical calculations (see figure 3.49) show that for $n=100$ the thermodynamic limit is a good approximation (relative error for the standard deviation $< 1\%$) for $0.2 < p < 0.8$. The probability p to keep the direction should equal the sum of the correlation coefficients to find an event A directly followed by an event A and B directly followed by B .

$$p \approx cc_{\text{keep direction}} = cc_k = P(\langle AA \rangle_{\Delta \text{events}=1}) + P(\langle BB \rangle_{\Delta \text{events}=1}) \quad (3.72)$$

The events of the oscillation experiment are mapped on a special correlated walk – Gillis’ random walk in one dimension [116]:

- “An agent of group A passes the bottleneck.” \rightarrow “Random walker moves one step to the right.”
- “An agent of group B passes the bottleneck.” \rightarrow “Random walker moves one step to the left.”

Because of equation (3.70) there is a connection between $\langle R(n_A, n_B) \rangle$ - the expectation value of the number of runs - and σ_A . Since $\sigma_A = \sigma_B$ one has

$$\langle R(\sigma_A) \rangle \approx \frac{2}{n} \left(\frac{n}{2} + \sigma_A \right) \left(\frac{n}{2} - \sigma_A \right) + 1 = \frac{n}{2} + 1 - 2 \frac{\sigma_A^2}{n} \quad (3.73)$$

Values for an Uncorrelated Process

For $n=100$ and $N_A = N_B = 202$ the expectation value for n_A has to be 50 ($= n/2$) due to the symmetry of the scenario. Even if a finite group size effect would in a strict sense imply a correlation, here not only the values for an uncorrelated process with no finite group size effect, but also for an otherwise uncorrelated process with finite group size effect will be given. In the first case, where the passing order can be imagined to be determined by a guardian at the bottleneck who decides about the right of passage of some member of one of the two groups by throwing a coin, the basic distribution is binomial. (All numerical values are calculated for $n=100$ and $N_A = N_B = 202$)

$$P(n_A) = \binom{n}{n_A} 2^{-n} \quad (3.74)$$

$$\sigma_A = \frac{\sqrt{n}}{2} = 5 \quad (3.75)$$

$$\overline{\langle R \rangle} = \sum_{n_A=0}^n P(n_A) \langle R(n_A, n_B) \rangle = \frac{n}{2} + \frac{1}{2} = 50.5 \quad (3.76)$$

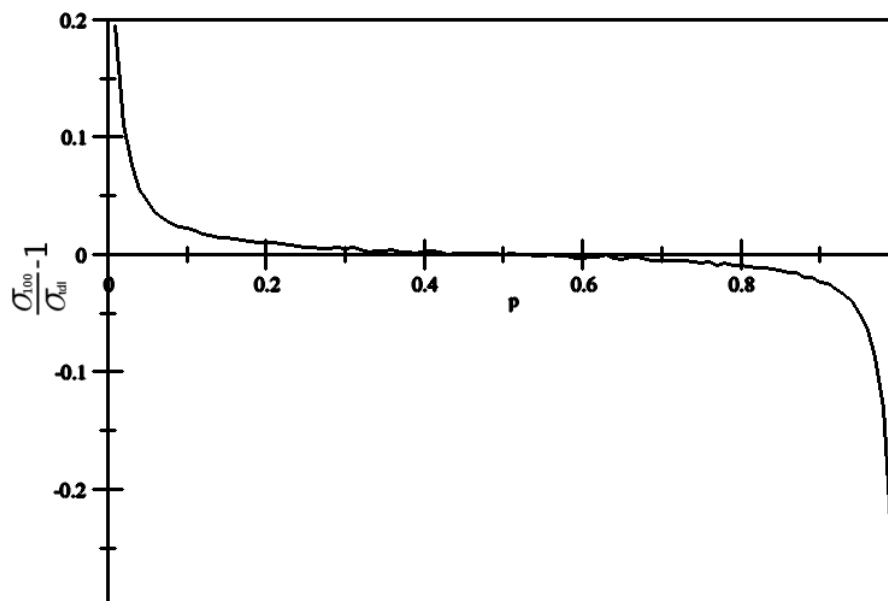


Figure 3.49: Relative difference of the numerically calculated standard deviation for the number of steps into a certain direction for $n = 100$ steps against the theoretical thermodynamic limit ($n \rightarrow \infty$) of the same standard deviation in dependence of the probability p to continue motion in the same direction.

The latter case, where the guardian decides about the right of passage with equal probability for each of the remaining individuals, is governed by the hypergeometric distribution.

$$P(n_A) = \frac{\binom{n}{n_A} \binom{N-n}{N_A-n_A}}{\binom{N}{N_A}} \quad (3.77)$$

$$\sigma_A = \sqrt{\frac{n}{4} \left(\frac{N-n}{N-1} \right)} = \sqrt{\frac{7600}{403}} \approx 4.34 \quad (3.78)$$

$$\langle R \rangle = \frac{n}{2} + 1 - \frac{1}{2} \frac{N-n}{N-1} = 50 \frac{251}{403} \approx 50.62 \quad (3.79)$$

It is assumed that the size of groups on both sides of the bottleneck has no influence on the movement probability as long as both groups have some minimal size which should be exceeded by construction during the counting process as the largest possible inequality is 102:202. However even if this was not the case, this comparison shows that the expectation values of the two possible cases of an uncorrelated process differ only slightly. These results can be taken as a basis for a comparison with the results of the simulations.

Oscillations without Dynamic Floor Field

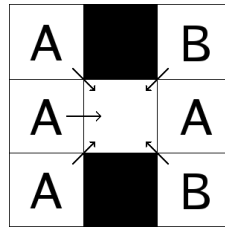


Figure 3.50: One of twelve possible situations after an agent has passed.

For $k_D = 0$ there is some sort of “intrinsic” correlation, which stems exclusively from the hard-core repulsion of the agents. As the last agent who passed occupies one of the three cells which are adjacent to the bottleneck cell, there are on average fewer agents on the adjacent cells on the side of the group that could not move than on the other side. Figure 3.50 shows the situation when there is the maximum of three agents of the group that moved last and the maximum of only two agents of the other group. Of course there can be other combinations (3:2, 3:1, 3:0, 2:2, 2:1, 2:0, 1:2, 1:1, 1:0, 0:2, 0:1, 0:0) and the group that moved last can have fewer agents adjacent to the bottleneck, but on average there will be more. Therefore on that side there will on average also be more agents that plan to move to the bottleneck cell and so also the probability that one of them wins a possible conflict is increased, as the winner of a conflict is chosen with equal probability out of all competitors. Note that this effect crucially depends on

the choice of von Neumann neighborhood or Moore neighborhood as neighborhood for $v_{max} = 1$.

For $k_S = 0.5$ the calculations for the three cases $v_{max} = 1$, $v_{max} = 3$ and $v_{max} = 5$ were repeated one-hundred times each. The tables 3.13 to 3.16 of this and the following subsection show the average number of runs that occurred, the average number of runs the Wald-Wolfowitz test predicts for uncorrelated behavior, average z-values as well as the number of times (out of 100) the z-value was smaller than -1.95 (5%-significance level) and smaller than -2.58 (1%-significance level), the standard deviation of n_A , the average evacuation time ($\overline{T_E}$) in rounds and the probability to continue in the same direction as calculated from σ_A (p) as well as calculated from correlation coefficients (cc_k). Note

v	\bar{r}	$\overline{\langle R(n_A, n_B) \rangle}$	\bar{z}	5%	1%	σ_A	$\overline{T_E}$	$p(\sigma_A)$	cc_k
1	37.04	50.51	-2.73	80	54	4.95	32945.9	0.49	0.64
3	37.47	50.26	-2.61	76	53	6.05	25676.0	0.59	0.63
5	37.94	50.36	-2.53	73	51	5.60	21395.4	0.56	0.63

Table 3.13: Results of simulations without dynamic floor field.

that $\overline{\langle R(n_A, n_B) \rangle}$ is the average of the values for $\langle R(n_A, n_B) \rangle$ calculated from the 100 simulation results for n_A respectively n_B using equation (3.70) and averaged in the way it is done in equation (3.76) however using the distribution of simulation results and not a theoretical distribution $P(n_A)$. The other averages are also averages over 100 simulations.

Oscillations with Dynamic Floor Field

For all simulations $k_D = 0.3$ and $k_S = 0.5$ has been set. This is quite a small value. However for $k_S = 1.0$ or even larger the crowds on both sides of the bottleneck become too dense, such that it becomes difficult for an agent to pass through them after he has passed the bottleneck. For each set of parameters the simulation was repeated 100 times. The largest deviations from the uncorrelated case are marked in the tables 3.14 to 3.16. (Also see figures 3.51 to 3.56.)

α	$v_{max} = 1, \delta = 0.03$								
	\bar{r}	$\overline{\langle R(n_A, n_B) \rangle}$	\bar{z}	5%	1%	σ_A	$\overline{T_E}$	$p(\sigma_A)$	cc_k
0.03	25.87	47.70	-4.69	98	95	12.84	5765.14	0.87	0.75
0.10	28.05	47.15	-4.15	94	84	13.84	6642.97	0.88	0.73
0.30	32.87	50.08	-3.52	93	86	6.75	13479.4	0.65	0.68
1.00	34.06	49.93	-3.26	90	75	7.32	13375.8	0.68	0.67

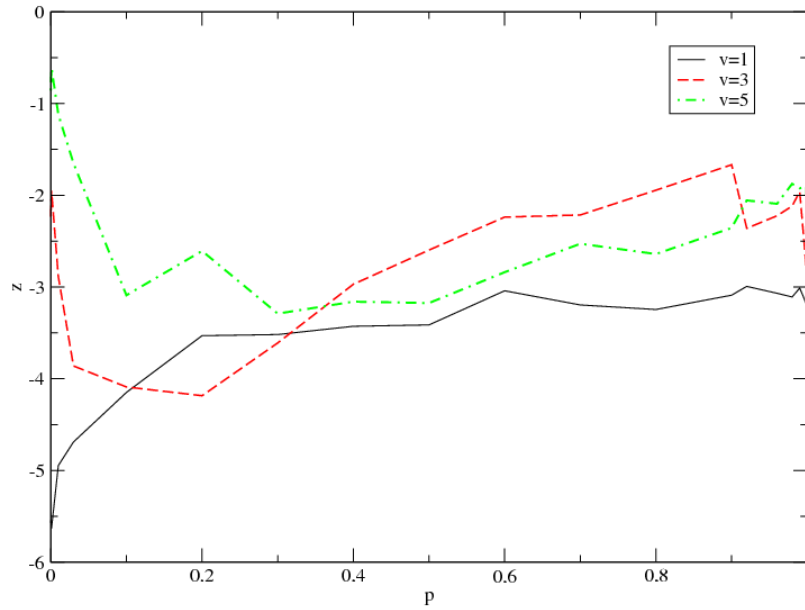
Table 3.14: Results of simulations with dynamic floor field and $v_{max} = 1$.

Other simulations showed that for $\delta > 0.1$ the effect begins to vanish as the dynamic floor field decays too fast to have a significant influence and for $\delta < 0.01$ the effect is

$v_{max} = 3, \delta = 0.03$									
α	\bar{r}	$\langle R(n_A, n_B) \rangle$	\bar{z}	5%	1%	σ_A	\bar{T}_E	$p(\sigma_A)$	cc_k
0.03	15.54	27.68	-3.86	74	69	34.06	2277.85	0.98	0.85
0.10	19.59	33.63	-4.09	81	73	29.47	2058.30	0.97	0.81
0.30	15.75	25.22	-3.61	74	65	35.79	1821.15	0.98	0.85
1.00	29.16	40.47	-2.86	74	58	22.94	2214.92	0.95	0.72

Table 3.15: Results of simulations with dynamic floor field and $v_{max} = 3$.

$v_{max} = 5, \delta = 0.03$									
α	\bar{r}	$\langle R(n_A, n_B) \rangle$	\bar{z}	5%	1%	σ_A	\bar{T}_E	$p(\sigma_A)$	cc_k
0.03	21.60	25.86	-1.65	40	28	35.34	2063.88	0.98	0.79
0.10	20.85	31.29	-3.09	61	55	31.34	1758.01	0.98	0.80
0.30	17.68	27.58	-3.29	64	57	34.18	1519.78	0.98	0.83
1.00	28.22	36.51	-2.41	57	46	26.87	1730.61	0.97	0.73

Table 3.16: Results of simulations with dynamic floor field and $v_{max} = 5$.Figure 3.51: Average z -value for different α at $\delta = 0.03$.

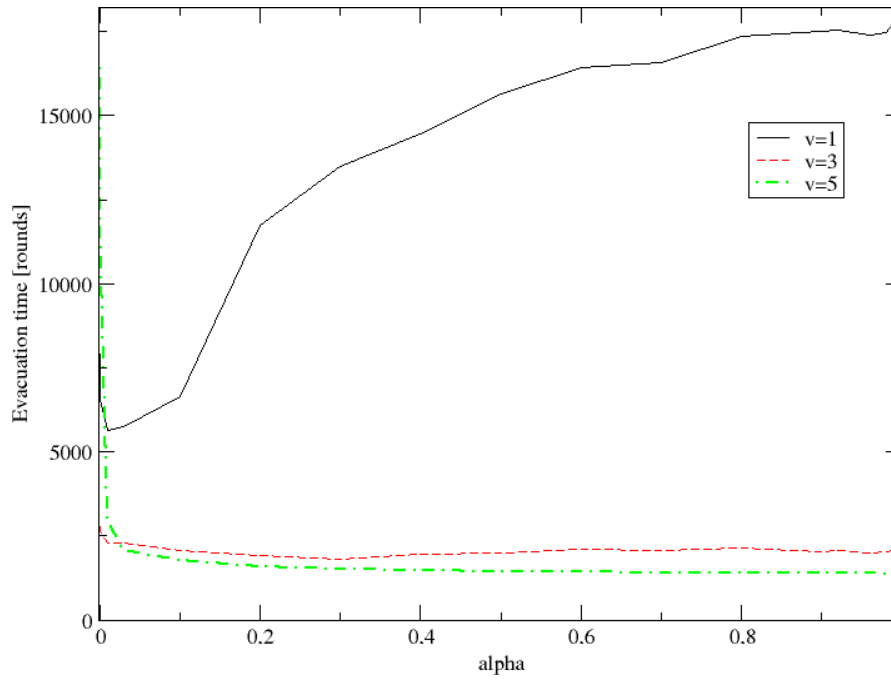


Figure 3.52: Average evacuation times for different α at $\delta = 0.03$.

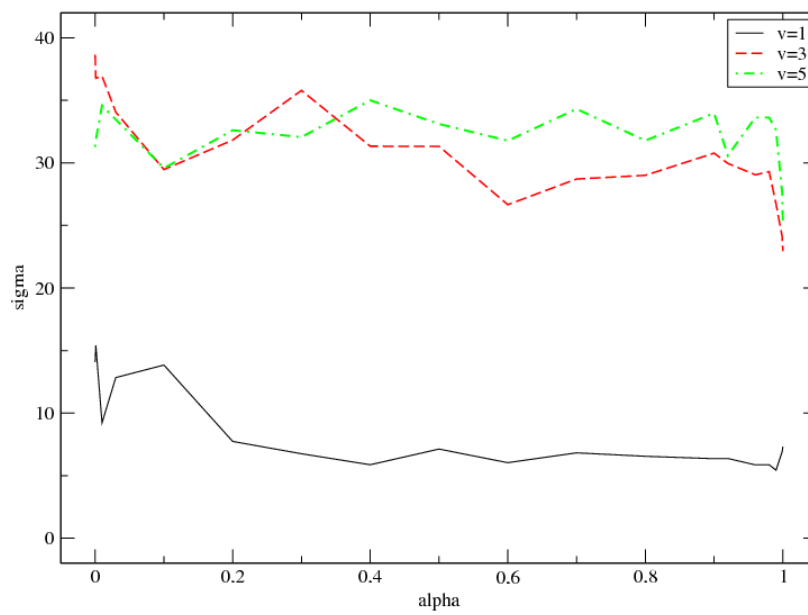


Figure 3.53: σ_A for different α at $\delta = 0.03$.

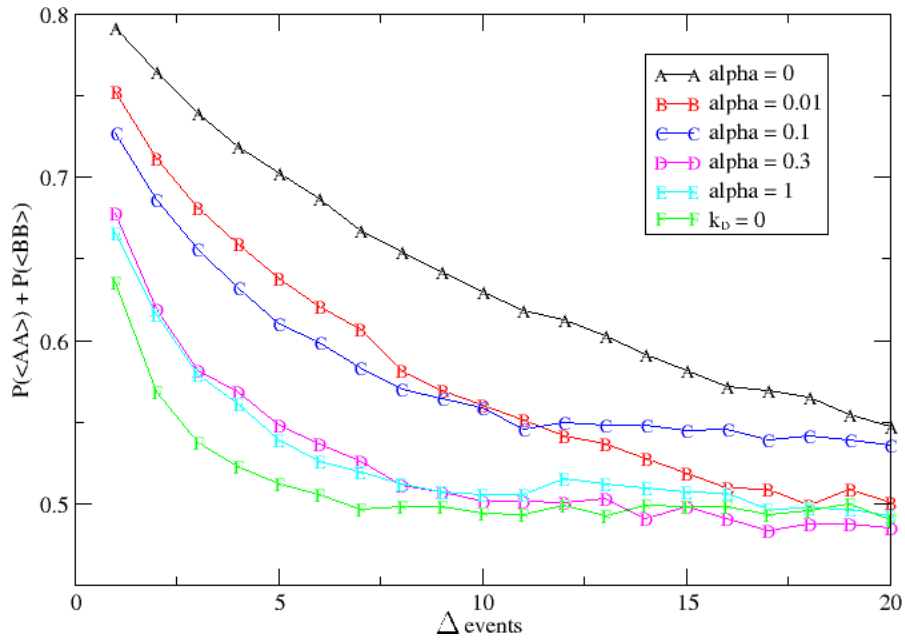


Figure 3.54: Correlation coefficients for different α and event distance at $v_{max} = 1$

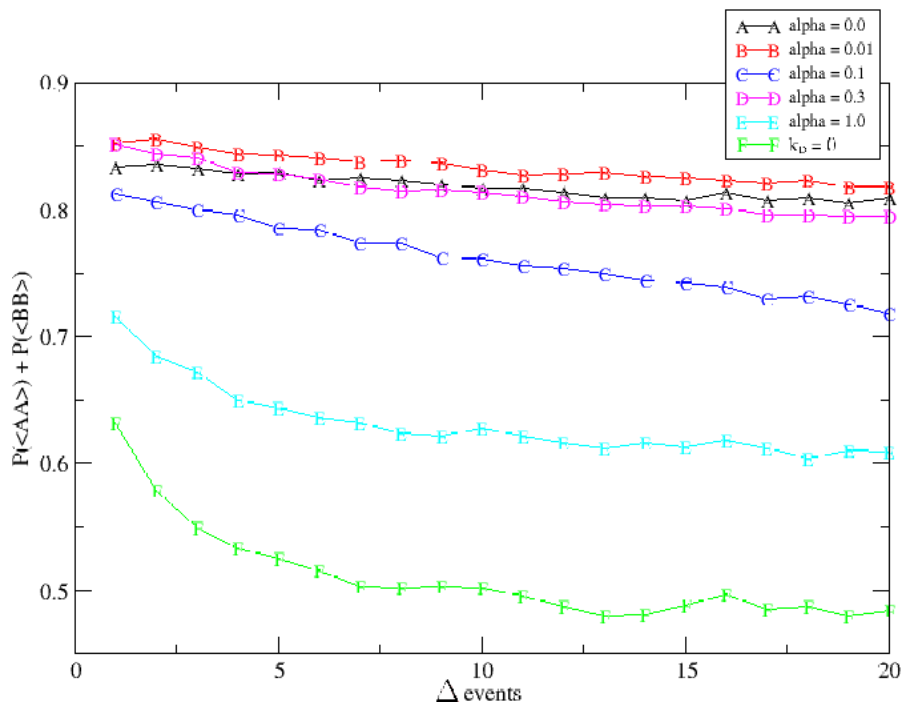


Figure 3.55: Correlation coefficients for different α and event distance at $v_{max} = 3$

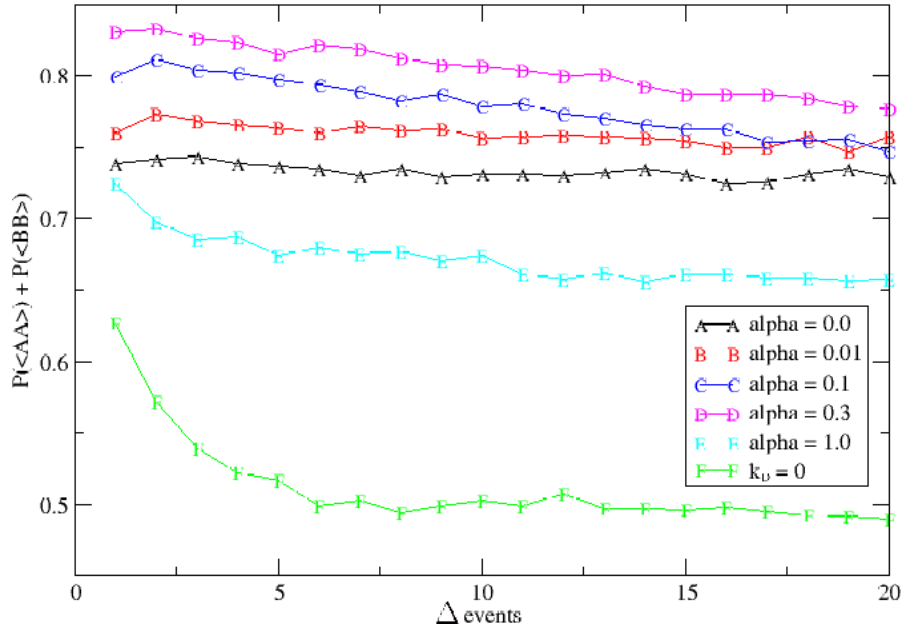


Figure 3.56: Correlation coefficients for different α and event distance at $v_{max} = 5$.

hidden by the dominant dynamic floor field that then induces irrational behavior. The agents begin to move in circles instead of heading to the bottleneck. Note that effects like this can also occur for too small α , if the dynamic floor field becomes too strong on some cells.

Compared to the case without dynamic floor field, the dynamic floor field with its time dependence brings in another dimension that can be analyzed: As long as the dynamic floor field has not reached a steady-state, the oscillation will be time dependent. This implies that the measured values either change with n or if n is kept constant but the measurement process starts not with the first event but later. For $\alpha = 1.0$, $v_{max} = 1$ and $n = 150$ $z = -3.92$ resulted, which is quite a difference to $z = -3.26$ for $n = 100$. However except for the case $\alpha = 0$, where they became slightly larger, the correlation coefficients did not change at all.

Discussion of the Resulting Data

Some observations made in the $k_D = 0.3$ data are:

- The evacuation time (in rounds) drops dramatically compared to $k_D = 0$ simulations. So it can be assumed that the larger groups of agents passing the door represent a more efficient behavior. This can be interpreted as less time being consumed by conflict solution processes at the bottleneck.
- The minimal z -value for each v_{max} is found at larger α for larger v_{max} . (See also figure 3.51.)

- The same holds for the minimum of the evacuation time. (See also figure 3.52.)
 - Correlations manifest themselves for $v_{max} = 1$ typically in smaller z -values and for $v_{max} = 5$ typically in larger σ_A .
 - σ_A for $v_{max} = 3$ and $v_{max} = 5$ are that large that ($n_A, n_B > 10$) is not always fulfilled.
 - For simulations with dynamic floor field, the correlations are stronger for $v_{max} = 3$ and $v_{max} = 5$ than for $v_{max} = 1$. This is due to the larger area of influence for higher speeds: More agents could choose the bottleneck cell as their destination cell. But due to the direction of the dynamic floor field mainly agents of the group that moved last indeed do choose the bottleneck cell as destination cell, which leads to a greater number of agents attempting to follow one of their group on the bottleneck cell compared to agents trying to change the direction of the flow, than in the case of $v_{max} = 1$.
 - Also for simulations with dynamic floor field $p(\sigma_A)$ is much larger than cc_k most of the time, but within each v_{max} -set of results there appears to be a tendency that cc_k and p are positively correlated. The difference points to a dynamic floor field that is too strong to reverse direction with only one agent passing. If for example after a sequence of agents of group A one agent of group B passes the bottleneck, a typical sequence will look like $AAAAAABAAAA$ if the dynamic floor field does not change direction with that single agent. If however it does change, a typical sequence would be $AAAAAABBBBB$. In the first case σ_A will grow, as the dominance of agents of one group outlasts the accidental event with small probability that one agent of the other group passes. In the latter case σ_A will be comparatively small since one long run of A s can be followed by an equally long run of B s and vice versa. The correlation coefficient cc_k however is much less affected by this phenomenon as it is not distinguished between AA and BB sequences. Take for illustration an A - B -symmetric $n = 11$ example: $(AAAAAABAAAA, BBBBBBABBBB)$ has $\sigma_A = 4.5$ and $cc_k = 0.8$ and $(AAAAAABBBBB, BBBBBBAAAAA)$ has $\sigma_A = 0.5$ and $cc_k = 0.9$. So while σ_A becomes larger with a stronger dynamic floor field, cc_k becomes smaller. Consequently a simulation with $v = 3$, $\alpha = 1$ and $\delta = 0.1$ resulted in $cc_k = 0.64$ and $p = 0.61$ instead of $cc_k = 0.72$ and $p = 0.95$ as for the $\delta = 0.03$ simulation. This shows that a comparison of p and cc_k can give a hint that δ was chosen too small, as for real pedestrians the passing of one individual is enough to completely change the odds.
 - Simulations without dynamic floor field gave values for σ_A and p that might make p look dependent on v_{max} . However the reason for this is a relatively broad distribution of the σ_A . In 20 additional $v_{max} = 1$ calculations of σ_A with $n = 100$ simulation repetitions, each σ_A varied between $\sigma_A = 5.34$ and $\sigma_A = 6.72$. This implies values for p between $p = 0.53$ and $p = 0.64$ with an average of $p = 0.575$. At the same time, cc_k remained relatively constant between $cc_k = 0.62$ and $cc_k = 0.64$. That p even at average remains smaller than cc_k probably results from a reduced
-

local density directly in front of the bottleneck if a group had a sequence of agents passing the bottleneck. The reduced local density then increases the probability of a change of the flow direction. This is an effect of the kind of a hypergeometric distribution that reduces the standard deviation (see above). Here p is much more affected than cc_k too, as cc_k is not affected by the relative total numbers of A s and B s within the first n events, but only by the number of changes of the flow direction.

The significant drop in the evacuation time compared to $k_D = 0$ is a sign that the dynamic floor field not only leads to a more efficient motion into the bottleneck but also out of the bottleneck and through the group on the other side.

It is not very surprising, that the effects of the dynamic floor field are strongest for larger v_{max} at larger α , since the larger neighborhood in which faster agents can move during one round makes it necessary that the dynamic floor field also diffuses faster to keep up with the agents.

If σ_A becomes too large, moderate z -values are no indicator that the events are uncorrelated. Contrary to that the scenario is just too small for such sets of parameters to make large z -values possible.

3.2.11 Counterflow in Corridors

Linked to “oscillations” are counterflow situations in (narrow) corridors. As is the case for oscillation situations two groups heading into opposite direction meet at and compete for small spaces. Counterflow situations with 10%, 30% and 50% of all agents moving into opposite direction were calculated in the same floor plan (ring) as were the single-directed fundamental diagrams presented up to this point. When there was no herding behavior ($k_D = 0$, figure 3.57) there was a jamming phase transition [117] at densities as small as $\rho \approx 0.1$. With $k_D = 0.8$ (figure 3.58), however, the jamming phase transition disappeared and the flux was significantly larger - compared to the $k_D = 0$ calculations - at almost all densities when there had been only 10% counterflow and also was larger at 30% and 50% counterflow. Yet in all three cases the flux appears to be somewhat unstable as the graphs in figure 3.58 are much less smooth than those in figure 3.57. While a higher flux for large k_D at only 10% counterflow could be explained with an increase of only the speed of the majority group and almost no progress of the small group, this cannot hold for 50% counterflow. There must be an effect that the two groups manage to pass each other more efficiently. Compared to the results presented in [118], however, this effect is rather small. The difference stems from the basics of the models as here no exchange of the positions of two agents is possible, whereas it is in the model of [118]. Since an exchange of position in dense crowds in reality is not that simple either that model probably overestimates the flow when there is no lane formation (at “interspersed” flows), while the F.A.S.T.-model underestimates lane formation, as for example in [104] it is stated that a reduction of the effective width due to counterflow is at maximum 10% as a consequence of lane formation. The appearance and disappearance of lanes has been described in [107] and compared to phase transitions

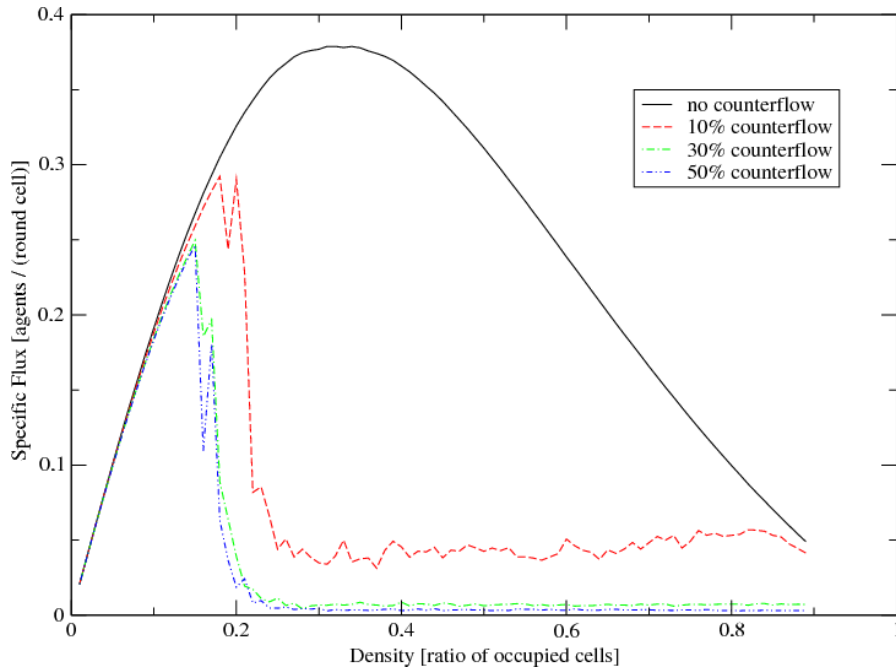


Figure 3.57: Fundamental diagrams at $k_S = 1.0$ and $k_D = 0$

of common matter. In section 4.3 some empirical results concerning lane formation are given.

3.2.12 Computation Times

To test the speed of the F.A.S.T. and the scaling of the computation time with the size of the scenario, the F.A.S.T.-model was used to simulate the evacuation from circle area with radius R cells where all of the cells at the edge were defined to be exits. All agents had speed $v_{max} = 3$, $k_S = 1.0$ and all other $k_X = 0$. They did not create a dynamic floor field. The computer used was an *AMD Athlon(tm) 64 X2 Dual Core Processor 4400+* with 2 GB of RAM, which at the end of the year 2005 was a very good workstation. Table 3.17 shows the computation times together with the predicted evacuation times. At constant initial density, the calculated evacuation time grows linearly with the way the agent who is furthest away from the exit has to move (radius). The computation time grows with $\mathcal{O}(R^3)$ of the radius which is $\mathcal{O}(N^{3/2})$ of the number of agents. As the agents' decisions are calculated serially (in contrast to the parallel calculation of reality), the number of agents grows with the area (if the initial density is kept constant) and the predicted evacuation time grows with the same order as the computation time, this also is the minimal possible scaling behavior. The point where the calculated evacuation time is equal to the computation time varies greatly with the parameters and the floor

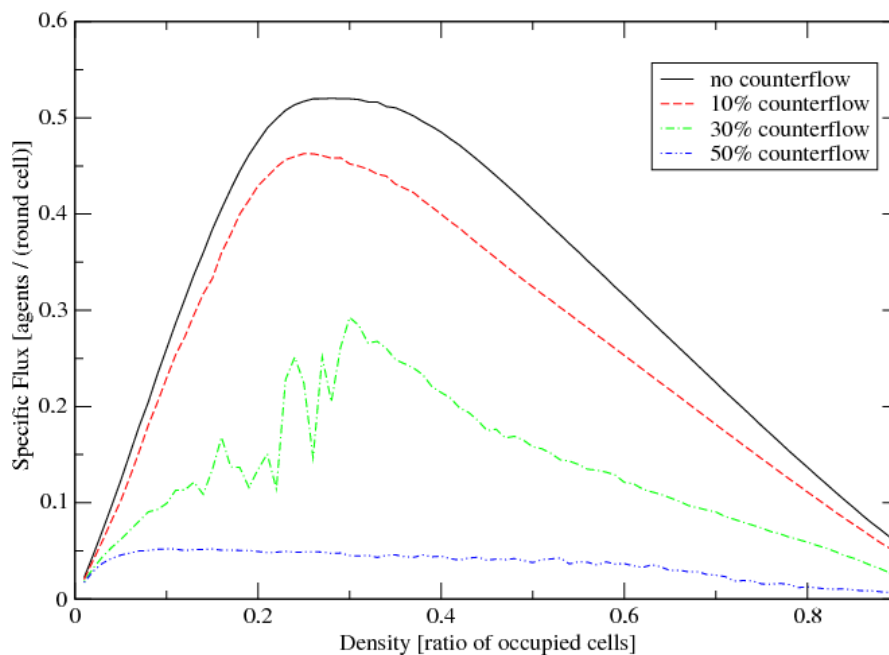


Figure 3.58: Fundamental diagrams at $k_S = 1.0$ and $k_D = 0.8$

R	Area (cells)	Agents	Computation time	Predicted evacuation time (rounds)
500	778,276	77,828	0:02:37	267
1000	3,127,382	312,738	0:21:56	515
2000	12,527,502	1,252,750	3:11:07	1028
3000	28,231,576	2,823,158	11:27:05	1523
3000	28,231,576	3,391,407	13:33:47	1516
3000	28,231,576	5,317,565	21:20:32	1541
3000	28,231,576	10,233,678	48:49:42	1567

Table 3.17: Computation times and predicted evacuation time. Compare figure 3.59.

plan. In this example with a regression calculation it can be found just under 130,000 agents.

For comparison: 3,391,407 was the number of inhabitants of the city of Berlin as of August 31st 2005, 5,317,565 the number of inhabitants of the Ruhr area as of October 1st 2004 and 10,233,678 the number of inhabitants of the Rhine-Ruhr metropolitan area as of December 31st 2004.

An additional calculation with 25,000,000 agents on a 5500 X 5500 cells large square took 234:39:11 hours and predicted 93 minutes for the evacuation time.

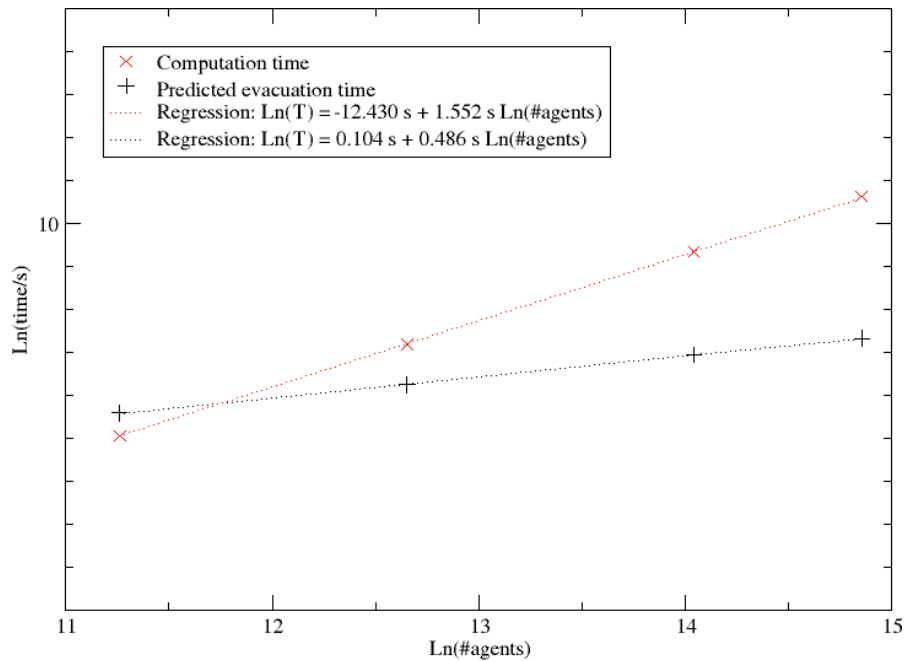


Figure 3.59: Comparison of computation time and predicted evacuation times in dependence of the number of agents and at constant initial density.

3.3 Fire and Smoke

3.3.1 The Model for the Spreading of Combustion Products: MRFC

The F.A.S.T can process the results of MRFC (Multi Room Fire Code) [119] calculations. In MRFC the concentrations of O_2 , CO_2 , CO , the temperature as well as some other parameters are calculated for an upper and a lower layer of smoke for every room in the considered scenario. Of course the height above floor level of the boundary layer is calculated too. What at present cannot be calculated with MRFC is the radiant heat as well as the HCN concentration, the latter one due to the fact that HCN concentrations strongly depend on the kind of burning materials. Yet there is a rule of thumb [120] which assumes a concentration ratio $[CO]:[HCN]$ of 12.5:1 for nitrogen containing ($> 2\%$ of fuel mass) fuels as furniture or clothing and 50:1 or less HCN for cellulosic or other materials which contain only few nitrogen.

The temporal (a value each 30 seconds) as well as the spatial discretization of MRFC are more coarse grain than the one of the F.A.S.T.-model. Concerning the evolution in time a simple linear interpolation has been made, while the cells only have been assigned to rooms and no smoothing at the boundaries of the rooms has been done.

3.3.2 Biological Impact of Physical Pollutant Concentrations: FED

The pure physical concentration data alone is not sufficient to calculate the effects of fire and smoke on evacuees. The biological impact of physical pollutant concentrations needs to be known in addition. This is done using the FED (fractional effective dose) model [121], which has been implemented earlier into software for evacuation simulation [26]. The FED model is based on the assumption of Haber's rule that "time equals concentration", which means that the biological harmfulness is a product of time and exposure to a certain concentration for that time. On the other hand the FED model takes into account that the uptake of toxic combustion products into the metabolism depends highly non-linear on the physical concentration. The FED model does not take into account recovering effects. During the typical time of an evacuation process this is surely correct for the effects of CO and HCN , yet in the absence of significant concentrations of CO and HCN a person can - to a certain point - quickly recover from a low concentration of O_2 due to an increased concentration of CO_2 and N_2 . The FED model norms all biologically active doses in a way that a person who has been exposed to a total of $F = 1$ suffers incapacitation. Fractional effective doses between three and five are described as deadly. The total fraction of an incapacitating dose of all combustion products is

$$F = \max((F_{CO,HCN} + F_{O_2}), F_{CO_2}, F_T) \quad (3.80)$$

with $F_{CO,HCN}$, F_{O_2} , F_{CO_2} and F_T being the summed up fractions of an incapacitating dose of $CO+HCN$, lack of O_2 , incapacitating dose of CO_2 and convecting heat:

$$F_{CO,HCN} = \sum_{t=t_0}^{t_1} \left(\left(\dot{F}_{CO}(t) + \dot{F}_{HCN}(t) \right) \cdot VCO_2(t) \right) \cdot \Delta t \quad (3.81)$$

$$F_{O_2} = \sum_{t=t_0}^{t_1} \dot{F}_{O_2}(t) \cdot \Delta t \quad (3.82)$$

$$F_{CO_2} = \sum_{t=t_0}^{t_1} \dot{F}_{CO_2}(t) \cdot \Delta t \quad (3.83)$$

$$F_T = \sum_{t=t_0}^{t_1} \dot{F}_T(t) \cdot \Delta t \quad (3.84)$$

The time derivatives $\dot{F}_X(t)$ are the so-called fractional effective doses. VCO_2 is the uptake increase factor due to an increased concentration of CO_2 (accelerated breathing). Since the effective dose is calculated each round Δt is the real time interpretation of one round. Light activity assumed [121] states:

$$\dot{F}_{CO}(\text{ppm } CO) = 4.61 \cdot 10^{-7} \cdot (\text{ppm } CO)^{1.036} \text{ per second} \quad (3.85)$$

$$\dot{F}_{HCN}(\text{ppm } HCN) = \exp(-9.490 + 0.023 \cdot (\text{ppm } HCN)) \text{ per second} \quad (3.86)$$

$$\dot{F}_{O_2}(\%O_2) = \exp(-1.062 - 0.54\%O_2) \text{ per second} \quad (3.87)$$

$$VCO_2 = \exp(0.2[CO_2]) \quad (3.88)$$

$$\dot{F}_{CO_2}(\%CO_2) = \exp(-6.1623 + 0.5189(\%CO_2)) \text{ per second} \quad (3.89)$$

$$\dot{F}_T(T) = 3.33 \cdot 10^{-10} \cdot T^{3.4} \text{ per second; with } T \text{ in } ^\circ\text{C} \quad (3.90)$$

With these equations it is a straight forward matter to sum up F for all agents individually. The results are given as described in subsection 3.4.4.

3.3.3 Reaction on Irritant Smoke

It is assumed that all evacuees follow the recommendation to move beneath the boundary layer between the two gas layers. However walking in a bent position or even creeping reduces the speed considerably. In the F.A.S.T.-model this is taken into account by the following speed reductions at certain boundary layer heights if the optical smoke density (following [122]) is above 0.11/m:

$$150 \text{ cm} < h : v = v_{max} \quad (3.91)$$

$$125 \text{ cm} < h \leq 150 \text{ cm} : v = \max(1, v_{max} - 1) \quad (3.92)$$

$$100 \text{ cm} < h \leq 125 \text{ cm} : v = \max(1, v_{max} - 2) \quad (3.93)$$

$$75 \text{ cm} < h \leq 100 \text{ cm} : v = \max(1, \min(2, v_{max} - 2)) \quad (3.94)$$

$$h \leq 75 \text{ cm} : v = 1 \quad (3.95)$$

3.3.4 Intrinsic Errors of the FED Model

Following the FED model even fresh air at 25 °C leads to incapacity after some time, which is

$$t^{\text{incapacity, fresh air}} = t^{ifa} = \frac{1}{\dot{F}_X(\text{conditions of fresh air})} \quad (3.96)$$

In detail these times are ($VCO \equiv 1$):

$$t_{CO}^{ifa} = \infty \quad (3.97)$$

$$t_{HCN}^{ifa} = 220 \text{ min.} \quad (3.98)$$

$$t_{O_2}^{ifa} = 3395 \text{ min.} \quad (3.99)$$

$$t_{CO_2}^{ifa} = 475 \text{ min.} \quad (3.100)$$

$$t_T^{ifa} = 883 \text{ min.} \quad (3.101)$$

3.3.5 Caveats

- The FED model is the product of one group of researchers. There appears to be no independent comparative study.
- The numerical values of the formulae for the fractional effective doses appear to be derived mainly or even exclusively from tests with animals. Precision up to four digits seems to be a little optimistic.
- Research on real behavior in smoke filled environments has not been done or at least only to very little extent: How large is the share of people who really immediately start moving beneath the boundary layer?
- The reaction of the boundary layer on moving people is not taken into account. Even without moving people is the evolution of the boundary layer subject to present and future research.
- The reduction of speed due to the height of the boundary layer is a qualitative consideration of the real effect. No empirical data is available concerning this issue.
- The intrinsic errors limit the simulation time on an equivalent of at maximum 220 minutes and this only if one accepts the simulation to predict incapacitated persons, where they in fact did not even have had contact to any smoke. If one only accepts intrinsic errors of e.g. $\Delta F < 0.1$, the limit would be 22 minutes.

For an application of this feature see section 5.5.

In total one has to be careful that the seeming possibility to prove the safety of a construction even under smoke conditions does not lead to reduced safety efforts of constructors or organizers. All three types of involved models (fire simulation, FED model, evacuation simulation) up to now include simplifications of reality. One therefore

should not calculate on the edge of incapacity but rather at the edge of smoke contact. Measures to improve the safety of a structure should not be taken when such a simulation results in incapacitated persons, but rather as soon as such a simulation claims that the boundary layer falls below some threshold height (e.g. 2.2 m) while there are still persons in the room.

3.4 Simulation Output

Besides a realistic theory of pedestrian motion and an efficient and correct implementation, what is important for simulation is the kind, amount and form of the output. One category for simulation output data is whether the data is or corresponds to an observable. The evacuation time for example is directly an observable. The dynamic floor field is not. “Frustration” (see below) at the moment cannot be measured.

3.4.1 Roundwise Output

Space Plots

Space plots are the most natural kind of output. They show the floor plan and the positions of the agents at the end of a certain round. The color of an agent indicates his current speed. See figure 3.60.

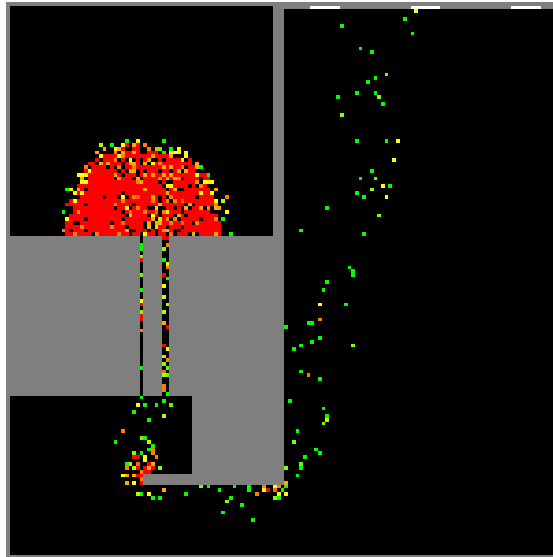


Figure 3.60: A space plot. Red agents stand still, green move with maximal velocity.

The State of the Dynamic Floor Field

Like the positions of the agents the state of the dynamic floor field can be plotted after each round, regardless of k_D being possibly zero. A plot of the state of the dynamic floor field can help to understand the situation shown in a single space plot, since the averaged direction of motion of the last few rounds is coded in the dynamic floor field. The hue of a pixel gives the direction of the field on the position of the corresponding cell, while brightness and saturation illustrate the strength of the field. See figure 3.61 below and figure 3.29 in subsection 3.2.3.

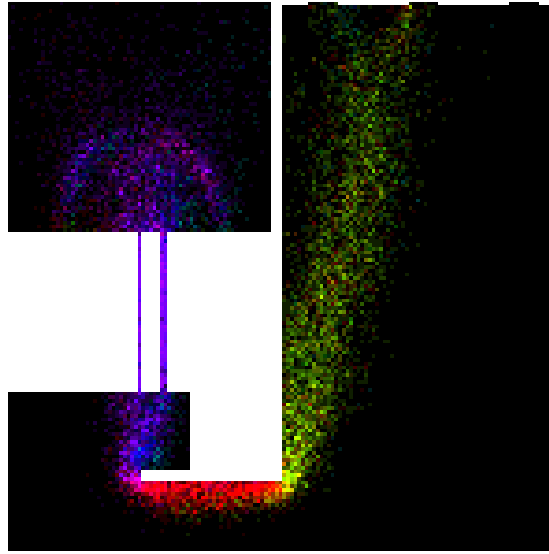


Figure 3.61: The dynamic floor field.

The Local Density

The number of persons on a Moore neighborhood is divided by the number of free cells in that neighborhood. Green (RGB=(0,255,0)) means density is zero, yellow (RGB=(255,255,0)) density=50% and red (RGB=(255,0,0)) density=100% of the theoretical maximum. See figure 3.62.

The Intermediate Range Density

The number of persons within one of the neighborhoods for speeds larger one is divided by the number of free cells in that neighborhood. The color scheme is the same as for the local density. Naturally the two density plots look alike, but offer slightly different insight into the situation. See figure 3.62.

3.4.2 Summarized Output

Occupancy

The number of rounds during which a cell was occupied by an agent divided by the total evacuation time (in rounds) is the occupancy of a cell. This can be normalized on the occupancy of the cell with the largest occupancy to show the most occupied cells. In such a relative occupancy plot the most often occupied cell is always colored red and all others over yellow to green accordingly. See figure 3.63.

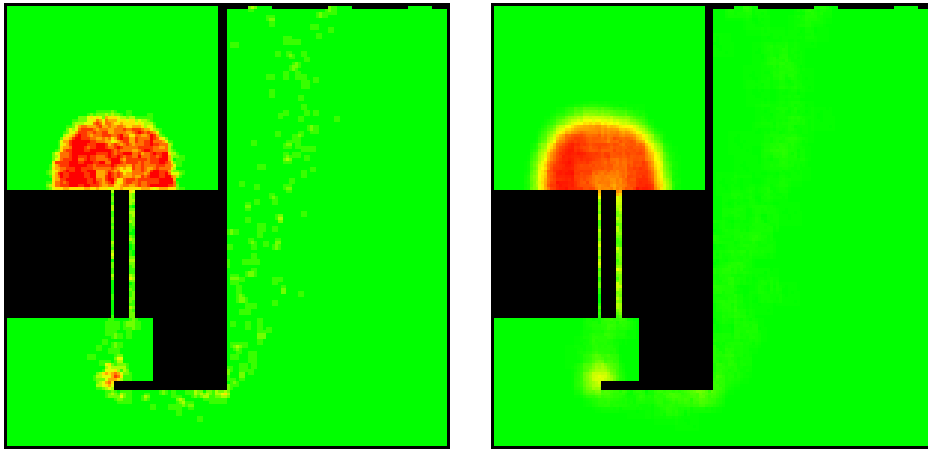


Figure 3.62: Local density (left) and intermediate range density averaged over $v_{max} = 5$ neighborhoods (right).

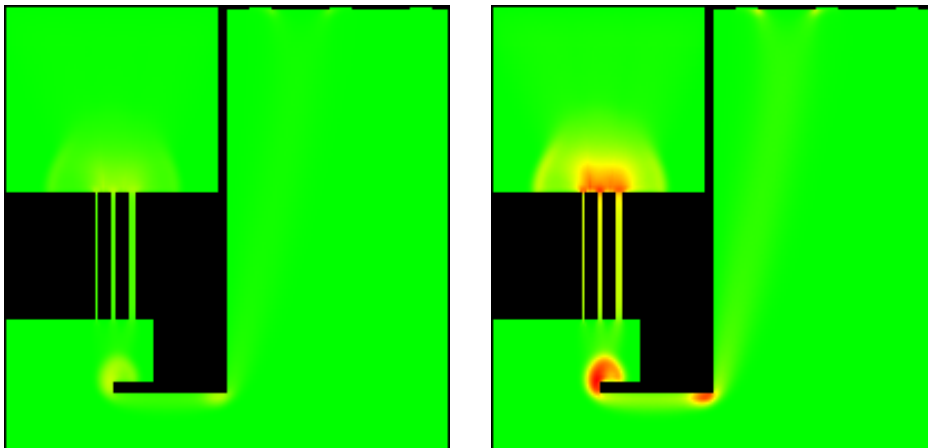


Figure 3.63: Absolute and relative occupancy.

Significant Congestion

In [74] a local density of more than four persons per square meter for more than 10% of the evacuation time is called a *significant congestion*. (See figure 3.64.) This definition makes sense as it considers density as well as congestion time. Therefore it is a measure for a spot's relative responsibility for delays. On the other hand faster evacuations can lead to the detection of significant congestions where there would be none for slower evacuations. So optimization can lead to "false alarms". A solution would be to define a threshold (e.g. 15 seconds) on how long a congestion must last before it is called significant. Furtheron, one could think of congestion volumes in two space and one time dimensions which must pass a threshold to call the congestion significant. A congestion of 2 persons/m² which extends over 100 m² and 15 seconds would be a threshold of 3000 persons · seconds for example.

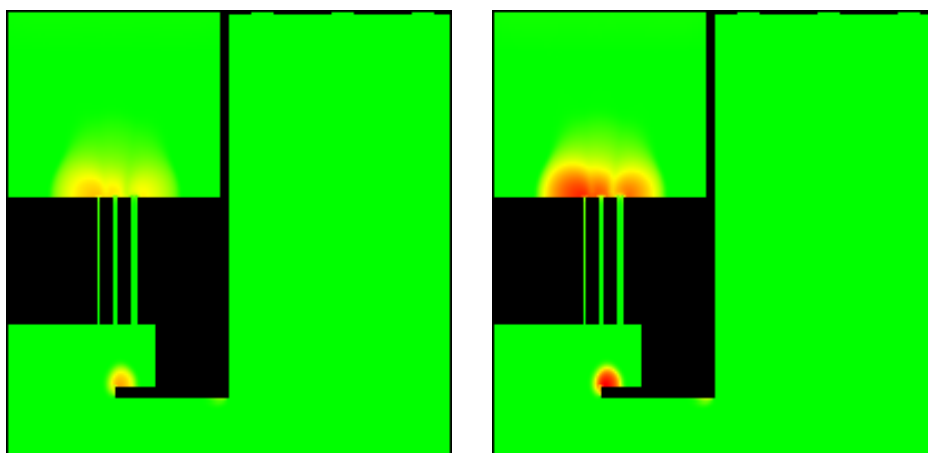


Figure 3.64: Absolute and relative significant congestions. A significant congestion is given for red values larger 51 (of a maximum of 255) in the absolute significant congestion plot.

Frustration

Whenever an agent finishes a round on a cell other than his destination cell, the frustration counter of that cell is raised by one. This is similar to switching between "happy" and "unhappy" in [28]. There however it is used as influence on motion, here it is used as part of analysis to find critical spots in a plan. The frustration plot is possible, since a clear desire of movement is calculated for each agent and separated from actual motion. Since frustration is defined as *denial of desires* and is derived from Latin *frustra* which means *in vain*, the term exactly describes what happens if an agent cannot reach his destination cell. Following the frustration-aggression-hypothesis [123] of psychology frustration leads or can lead to aggression. Therefore a model extension for example

could use the notion of frustration to vary μ or other parameters in time. However this is just a speculation since two issues have to be clarified before one could do so:

- Frustration can only occur if the desires have a subjective chance to be fulfilled. So it must be guaranteed that the destination cell choosing algorithm predominantly returns destination cells which in reality would be given a realistic chance to be reached within one second by real persons as well.
- The influence of many such tiny frustrations on the behavior of a person has to be quantified.

Frustration plots typically very much look like occupancy plots, as the chance for frustration is higher in dense crowds and in areas that are accessed frequently. There are differences, however. A heavily used narrow corridor for example can show up a high occupancy while the frustration level remains low, since overtaking is unrealistic and the next destination cell always lies at least one cell behind the preceding agent. A narrow corridor implies special dangers (e.g. a collapsed person), but the hot spots of danger typically lie before the entrance of a corridor. This difference between “heavily used without congestion and competition for the right to move” and “congestion spot” is illustrated slightly better by frustration than by occupancy plots. See figure 3.65 and compare to figure 3.63.

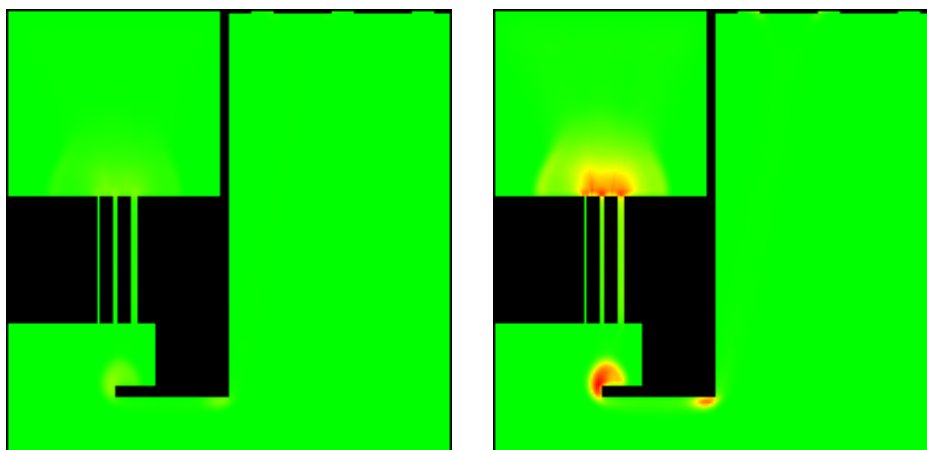


Figure 3.65: Absolute and relative frustration.

Blockage

If an agent is totally surrounded by walls and other agents, such that the only possible destination cell is his present cell he is counted as *blocked*. In the F.A.S.T.-model, blocked agents do not experience frustration, as they do reach their destination cell. Blockage plots therefore are a kind of supplement of frustration plots. Additionally this

is interesting as being blocked in reality for a certain time can cause anxiety. See figure 3.66.

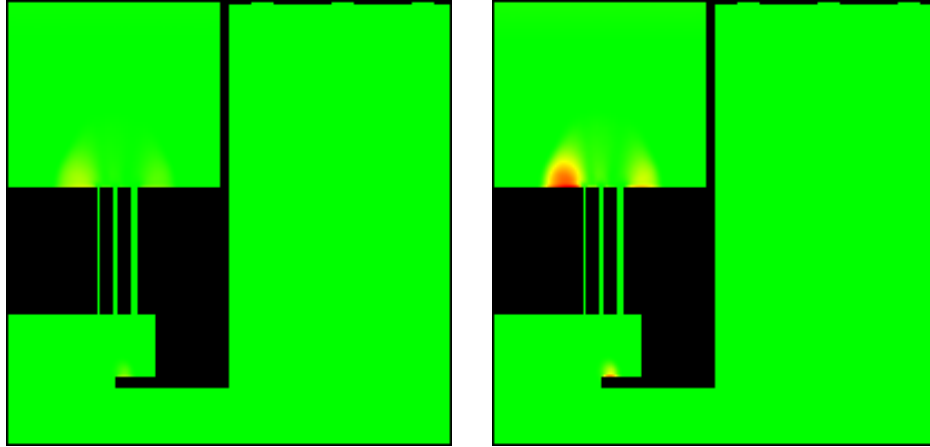


Figure 3.66: Absolute and relative blockage.

Evacuation Progress

The number of agents which have left the simulation at a certain point of time is shown in the evacuation progress plot. Typically this graph starts with slope zero. Then the slope rises to a constant value when the exits reach their full capacity until during the final phase of the evacuation the slope again falls down to zero as the latecomers approach the exit. Deviations from this form might give a hint that something is not optimal. One should also try to understand the reasons for minimum and maximum values that greatly differ from the average. See figure 3.67.

Distribution of Evacuation Times

For a large number (1000 or more) runs of a simulation a look at the distribution of evacuation times can give a good overview of the behavior of the system. See figure 3.68. The same plot can be produced for the times when 95% of the agents have escaped and for the individual egress times.

Average Speed and Flux

The average speed can be calculated by either using the number of the smallest speed neighborhood in which an agent moved during a round (absolute value of speed) or the reduction in the static floor field an agent could achieve (speed component into “correct” direction) during a round. If one multiplies these speeds with the number of agents which are still part of the simulation one gets a measure for the flux. A natural normalization then would be the number of free cells in the scenario. See figures 3.69 and 3.70. The

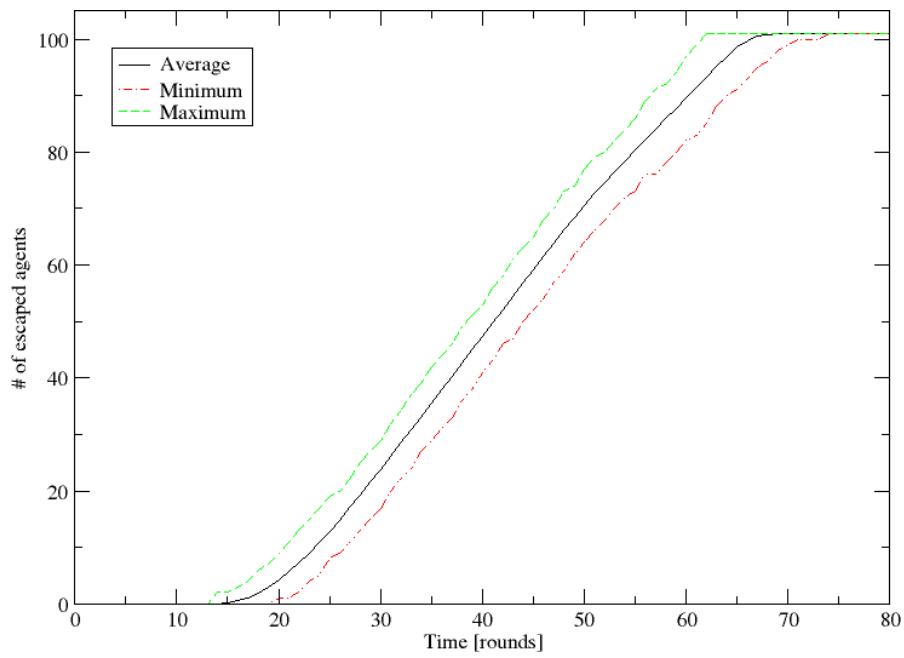


Figure 3.67: Evacuation graph.

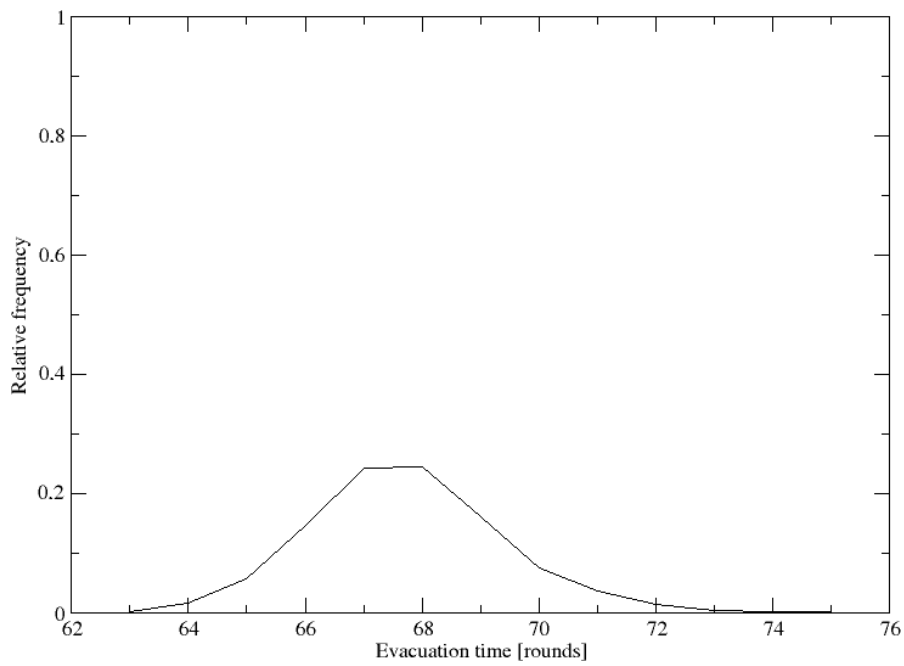


Figure 3.68: Distribution of evacuation times.

difference between the two ways to calculate the averages (speed or progress in S) is a measure for the effectiveness (concerning free behavior as well as congestions) of the process.

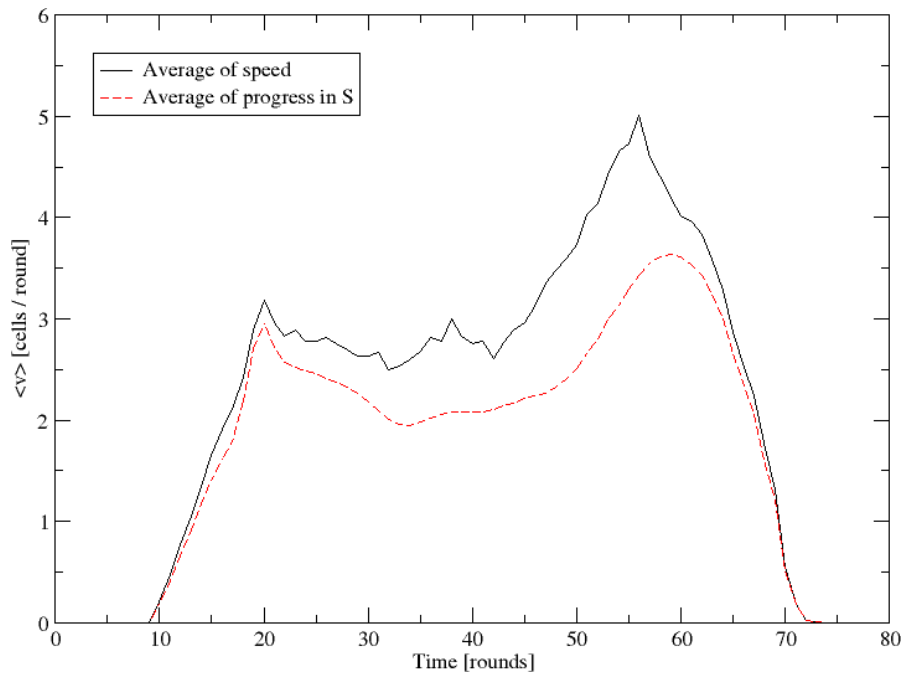


Figure 3.69: Average speed during the evacuation process. The averaging is done over the agents as well as over the simulation runs.

Exit Statistics

The total average number of agents who used an exit as well as the total average number of agents who used an exit-group are plotted, which can help to find unused capacities. See figures 3.71 and 3.72.

3.4.3 Statistics

The results also contain a number of numbers as

- The evacuation times (time needed for the whole process) of all runs plus the average, maximum, minimum and standard deviation.
- The average of the egress times of all agents for all runs plus the total average, maximum, minimum and standard deviation of these.

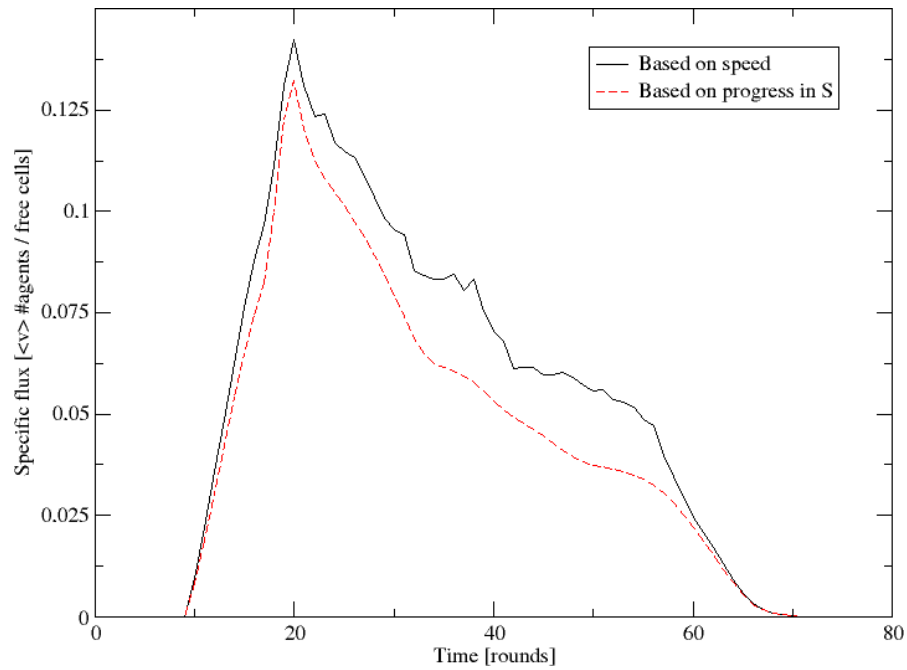


Figure 3.70: Average global flux during the evacuation process. The averaging is done over the agents as well as over the simulation runs.

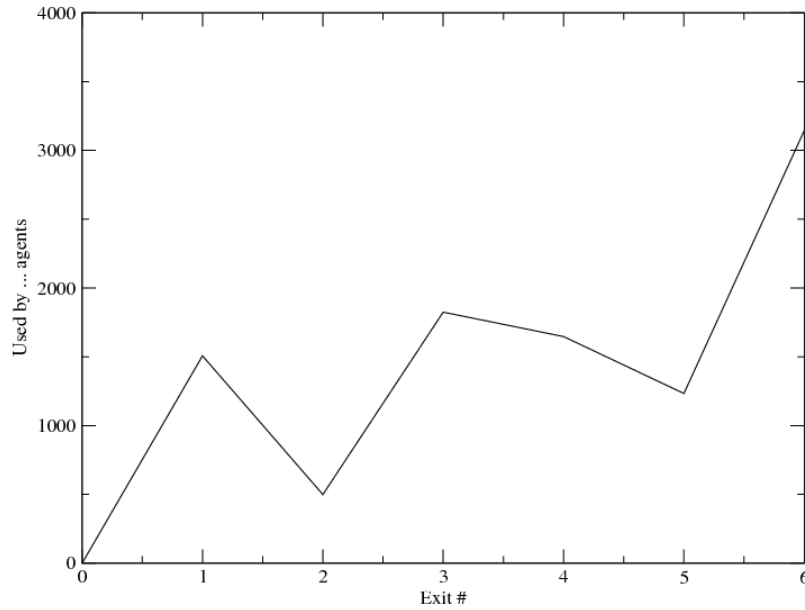


Figure 3.71: Statistics of exit-group usage behavior

- The 95 percentiles (number of rounds when 95% of the agents have left the simulation) of all runs plus the average, maximum, minimum and standard deviation of these.
- The group name of the last three agents who leave the simulation.

3.4.4 Additional Output in Simulations which Include Combustion Product Data

In fire and smoke scenarios additional space plots show the (in-)capacitation state of the agents. For each reason or combination of reasons of incapacitation an agent is colored in a special color as soon as he has passed the threshold value to incapacitation. See figure 3.73.

Endangerment on Different Starting Positions

If one repeats the simulation of a scenario very often one can get incapacitation probabilities for different starting positions. For certain fire sources and sizes in this way the positions are calculated from where self rescue appears to be possible. See figure 3.74.

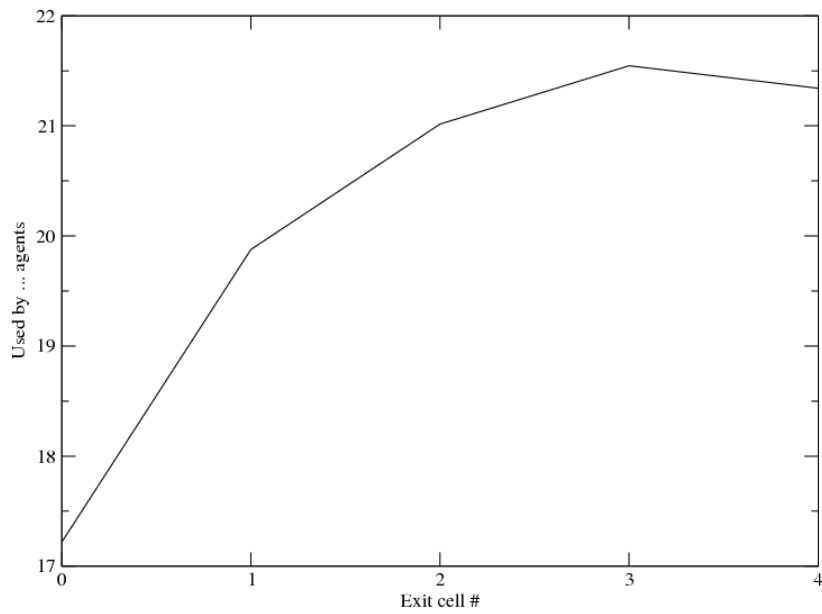


Figure 3.72: Statistics of exit usage behavior

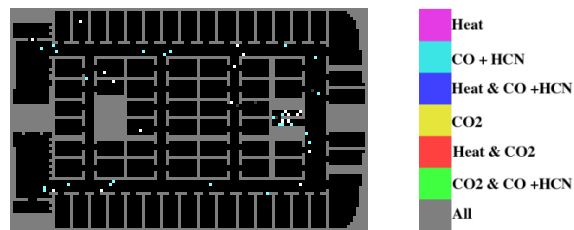


Figure 3.73: A space plot which shows the incapacitation state in presence of fire and smoke and the color table of reasons for incapacitation. Agents that do not suffer incapacitation are colored white.

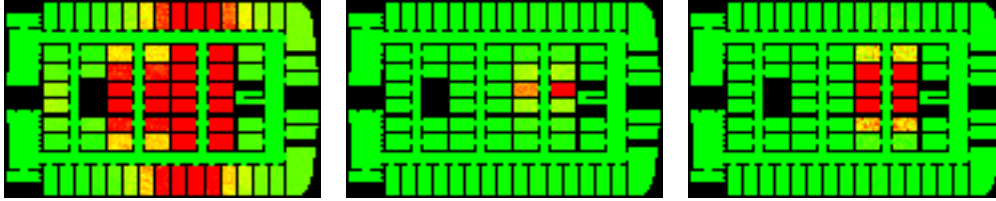


Figure 3.74: Risk of suffering incapacity if a person stands on a certain starting position due to $CO + HCN$ (left), CO_2 (center) and heat (right).

Temporal Development of the Number of Incapacitated Agents

As the ability to resist combustion products has been assumed to be the same for all agents this plot often gives a sharp value for a critical time after which one has to expect a rapid rise in the number of casualties. See figure 3.75.

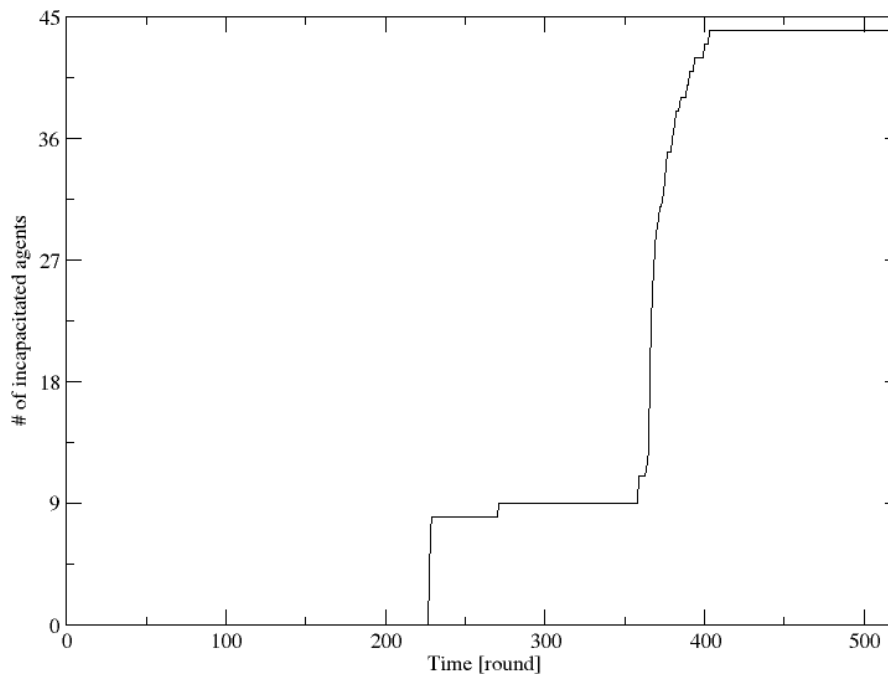


Figure 3.75: Development of the number of incapacitated agents with time.

Spatial Distribution of Incapacitation

This might be the most error-prone statement of the calculation but an information on the positions where rescue forces have to expect incapacitated people might be of some use. See figure 3.76.

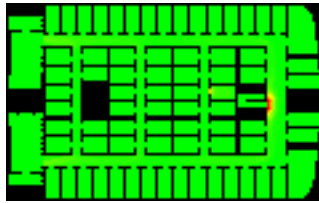


Figure 3.76: Positions where persons pass the threshold to incapacitation.

4 Empirical Results and Validation

In this chapter four empirical studies are discussed. The first one serves as validation of the model that was presented in the preceding chapter, while the results of the latter three have not yet implemented into the F.A.S.T.-model, as the results are very detailed and they include some real challenges for model building. At least to some extent they therefore stand for themselves and expand the perspective of this work, as up to now the focus was very much on the development and discussion of the F.A.S.T.-model. The general relation in which they are linked to this work so far is, the motivation for continued development of the F.A.S.T.- and other models.

4.1 Evacuation Exercise in a Primary School

The evacuation exercise that was reported about in [124] was repeated. However this time there were fewer pupils. The children were highly motivated, which was partly due to the presence of a camera team reporting for a children's news show on a German children's TV station. The exercise was repeated twice. The first time the music class did not become aware of the alarm as the bell in their class-room was broken and they were singing too loud to hear the bell from the floor. The school consists of two buildings: the main building and a newer second building. The music class was on the second floor in the main building. The main building consists of three (first, second and third floor), the second building of two floors (first and second floor). See figure 4.1.

In addition to the three cameras, the time for the last person to leave the third floor was measured. A person was counted as having exited the main building as he reached the last of the stairs outside the main building.

4.1.1 Results

The results (table 4.1) of the two exercises in the main building can hardly be compared since the music class only took part in the second exercise. The data of the second building however suggest that in the second run there either was a learning effect or that the pupils - at least some of them - were more aware of an alarm to come instead of having normal lessons interrupted by an alarm, since they reacted more quickly. See figures 4.2 and 4.5.

4.1.2 Comparison to Simulation Results

After the exercise was finished and the empirical data was evaluated, simulations were done with the aim to reproduce the empirical data of the first exercise as well as possible.

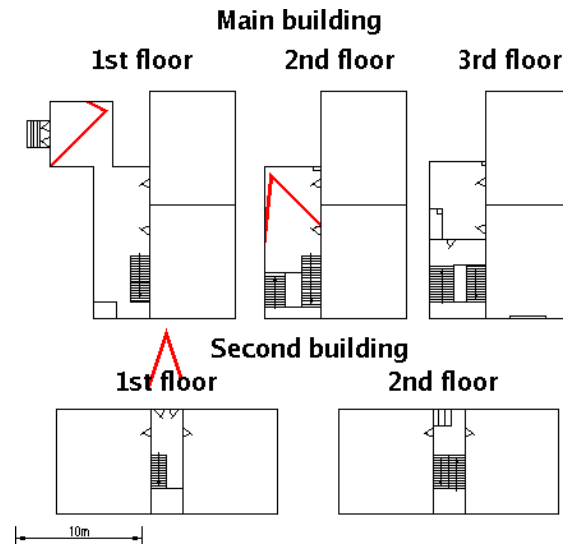


Figure 4.1: Floor plan without furniture. The approximate camera perspectives are drawn in red, the number of persons as counted on the day of the exercise in each class room in blue.

Time (in seconds) after alarm for...	First Exercise	Second Exercise
...the last person to leave the main building	65.4	69.9
...the first person to leave the main building	28.5	12.3
...the last person to leave the 2nd floor of the main b.	43.2	44.9
...the first person to leave the 2nd floor of the main b.	15.3	13.2
...the last person to leave the 3rd floor of the main b.	25	24
...the last person to leave the second building	60.5	56.5
...the first person to leave the second building	16.2	5.2

Table 4.1: Empirical results of the exercise.

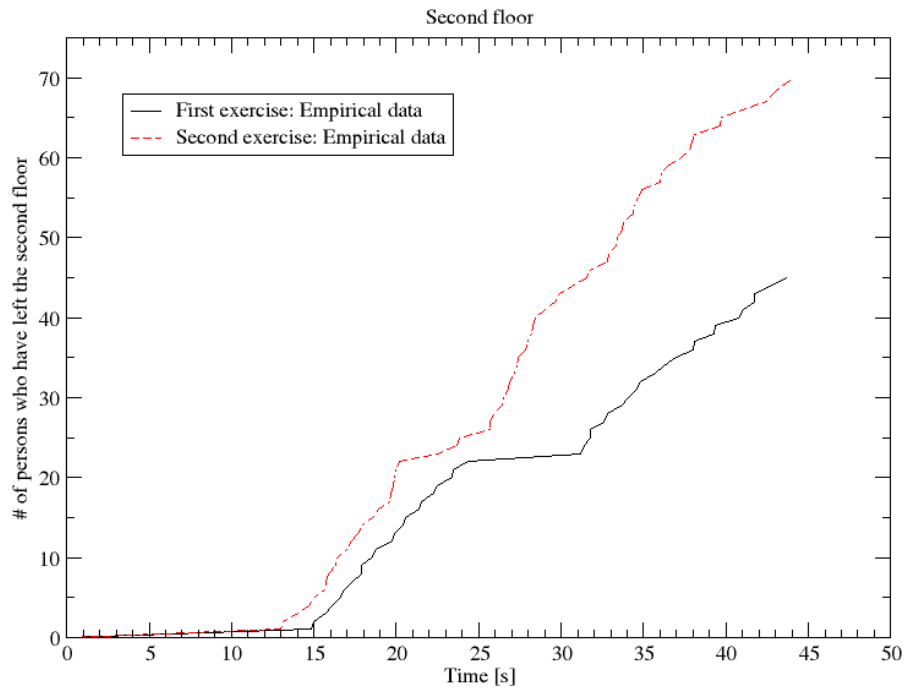


Figure 4.2: Evacuation graphs of both runs. The pupils were counted, when they left the second floor and moved down the first step of the stairway between second and first floor. In the first run (without the music class) the pupils on the second floor except the music class had left the second floor some time before the pupils of the third floor arrived. In the second run the pupils from the third floor arrived before all pupils of the second floor had left the second floor, but there was some dawdling of two pupils without apparent reason, leading again to an - in this case smaller - plateau in the evacuation graph.

This resulted in the evacuation graphs of figure 4.3. Due to technical reasons an empirical evacuation graph at the main exit could not be evaluated, but the total time - averaged over 1000 simulation runs - of the evacuation (until all pupils had completely left the main building) was 62.2 rounds at a standard deviation of 1.3 rounds. The smallest evacuation time that appeared during those 1000 simulation runs was 58 rounds, the largest 69 rounds. For the evacuation of the second floor those numbers were: 44.6 ± 1.4 rounds with all evacuation times between 42 and 52 rounds. The parameters have been

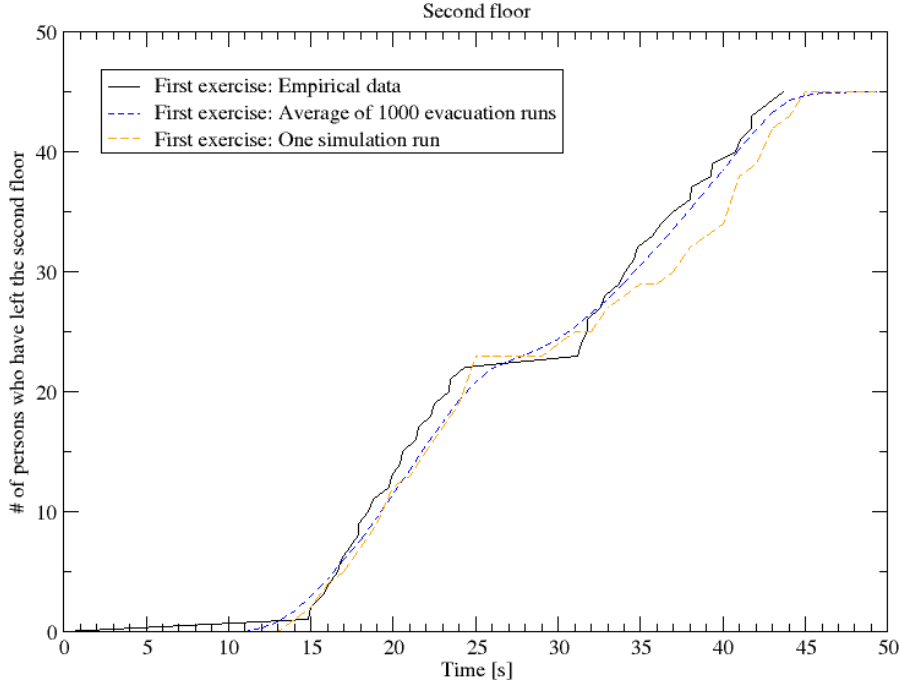


Figure 4.3: Comparison of empirical and simulation results. The simulations were done after the exercise, so this is not a prediction but a calibration of the simulation.

set as follows: $k_S = 3.0$, $k_D = 2.0$, $k_I = 2.0$, $k_W = 0$, trace strength: 6, $\alpha = 0.8$, $\delta = 0.5$, $\mu = k_P = 0$. For the reaction times of the teachers and the pupils on the third floor (fourth grade, oldest pupils of the school) the following distribution of reaction times was used: $t_r^{min} = 18$, $t_r^{av} = 19$, $t_r^{max} = 20$, $t_r^{std.} = 1$. The maximum speed was set to $v_{max} = 5$ for all of them, while for the other (younger pupils) the reaction time was set on smaller values for some of them $t_r^{min} = 10$, $t_r^{av} = 15$, $t_r^{max} = 20$, $t_r^{std.} = 5$ and the speed varied: $v_{max}^{min} = 4$, $v_{max}^{av} = 6$, $v_{max}^{max} = 8$, $v_{max}^{std.} = 1$. This corresponds to the following observations: Some of the younger pupils were highly motivated, speeds up to 3 meters per second were observed. The older pupils of the third floor stayed slightly closer together and appeared to be slightly less (but still highly) motivated and/or more disciplined. It might surprise that all pupils seem to have such a strong inertia, but k_I always has to

be set and seen in relation to k_S and it was indeed the case that the turnaround on the stairway slowed the pupils down significantly. Note: Even small variations in some parameters as the maximum speed, the reaction times, α , δ , the trace strength, k_D , k_I and to some extent k_S lead to a much smaller agreement between observation and simulation. It was especially difficult to find parameters that reproduce the plateau in the evacuation graph of figure 4.4.

Now these parameters have been used in simulations that include the music class. A comparison of observation and simulation is shown in figure 4.4. The total time - averaged over 1000 simulation runs - of the evacuation was 67.7 rounds at a standard deviation of 1.7 rounds. The smallest evacuation time that appeared during those 1000 simulation runs was 63 rounds, the largest 75 rounds. For the evacuation of the second floor those numbers were: 46.0 ± 1.7 rounds with all evacuation times between 42 and 56 rounds. While the parameters have been calibrated at the data of the evacuation of

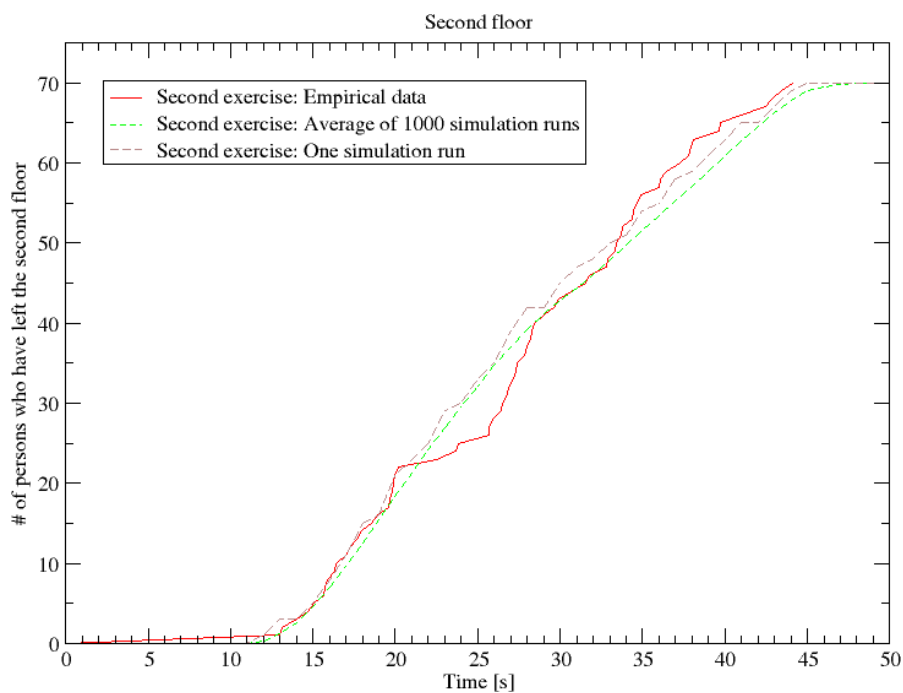


Figure 4.4: Comparison of empirical and simulation results for the second exercise.

the second floor and the first exercise, the results of the simulation for the evacuation of the whole building at the second exercise (67.7 ± 1.7 seconds, minimum 63, maximum 75 seconds) are also in good agreement with the corresponding empirical data (69.9 seconds). The fact that no set of parameters could be found that fully reproduces the high outflow from the second floor is probably due to the smaller size of the children compared to adults for which normally data is taken in experiments and observations.

The same applied to the second building (main exit) leads to an average simulated evacuation time of 56.0 ± 2.2 seconds. (See figure 4.5.) Compared to the first exercise the

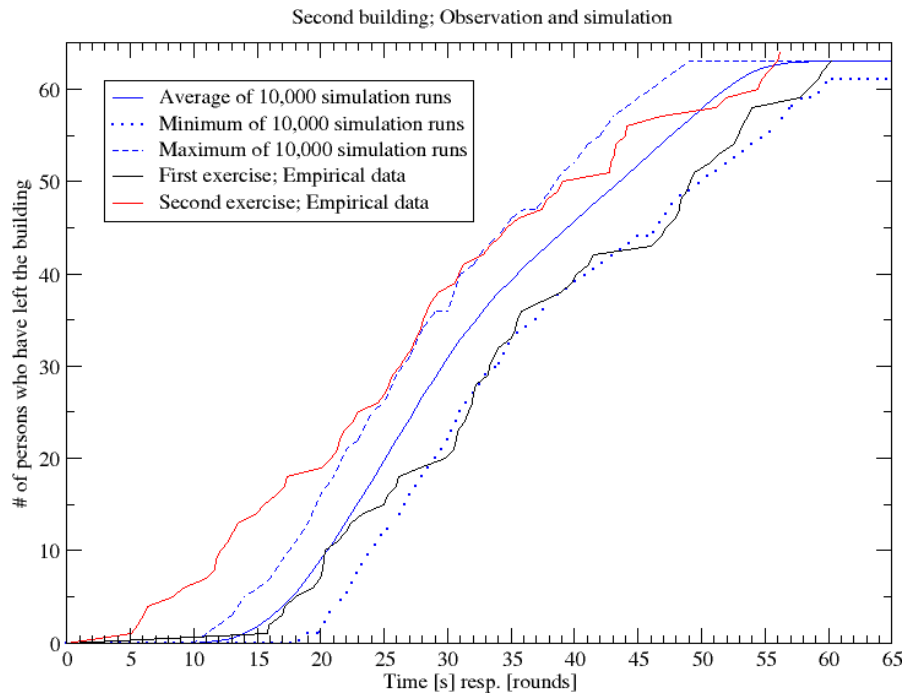


Figure 4.5: Comparison of empirical and simulations results for the second building. In the second exercise there was one person more in the building.

pupils in the second building performed better throughout the whole second exercise. The average of simulations at the beginning of the process yields results that are almost identical to the results of the first exercise and, at the end of the process, results that fit very well to the data of the second exercise.

Time (in seconds) after alarm for...	First Exercise	First Simulation	Second Exercise	Second Simulation
...the last person to leave the main b.	65.4	62.2 ± 1.3	69.9	67.7 ± 1.7
...the last person to leave the 2nd floor.	43.2	44.6 ± 1.4	44.9	46.0 ± 1.7
...the last person to leave the second b.	60.5	56.0 ± 2.2	56.5	same as first

Table 4.2: Overview of comparisons.

4.2 Upstairs Walking Speed on a Long Stairway

It is equally difficult as necessary to get data of upstairs walking speed distributions on long stairs. It is difficult as nowadays there do exist only few really long stairs without parallel elevators. If there is an elevator as an alternative to walking a long stair one has fewer people deciding to walk the stairs. And those who do so are a selection of the whole population of which one can assume to be physically fitter than the average of the population. It is on the other hand necessary to get data from long stairs as in cases of emergency no elevators are available and therefore sometimes long stairs have to be walked. Even downstairs evacuation in high-rise-buildings is often planned as “phased evacuation” partly since many people are not able to move downward a large number of stairs. Still the problem is not that urgent in most buildings, as typically people only have to walk downstairs. Therefore endurance abilities of the occupants only are of minor importance. However, there are structures where walking upstairs several floors can become necessary. On board e.g. of cruise ships there are situations where a non-negligible fraction of passengers linger at lower decks. Therefore they would have to walk several floors upstairs to reach the exits and life-boats. But also certain big underground garages or large underground stations would fall into this category. Here endurance does play a role and empirical data from short stairs is only of limited use for calculating walking times. Therefore the aim of this study was to find out the distribution of walking speeds on a stairway that is that long that even trained people would consider climbing it a matter of endurance.

4.2.1 Scenario, Methods and Materials

The Dutch pavilion at the Expo 2000 in Hannover, Germany (English spelling: “Hanover”) has had elevators, yet they were located some distance away from the entrance of the stairs. In addition the chance to oversee the area from some height might have attracted some people to walk the stairs instead of taking the elevator. The comparatively long stairs (total height 35.8 meters) were on the outside where quite good

observation conditions were given. Figure 4.6 shows that the observation region was shortly below the roof, implying that the observed persons already had climbed approximately 25 m high before their walking speeds were measured. The stair steps had (respectively have) a tread of 27.0 cm and a riser of 19.0 cm. This implies an angle of inclination of 35.1° . The stairs had a closed box design, and the railing a round shape that could be encompassed. To summarize these details: a special building code was raised for the Expo 2000 and the stairway in concern met all of these standards concerning riser, tread, slippery resistance, used materials, etc..



Figure 4.6: The walking times were measured at the part of the 18 stairs at the right to the triangle-shaped door (platform to platform). The whole stairway had this design of an alternation of stairs and platforms.

An objective measurement of the density was not possible. Therefore, each measurement was subjectively assigned by visual judgment to one of three categories based upon the potential influence of other nearby persons. These categories were:

- The individual in focus was walking obviously uninfluenced by anyone else. (Category A)

- Few people standing or moving around the individual in focus, but there were only small or even no visible influences from one to another. (Category B)
- High density situation, each person clearly influenced the others in the surrounding. (Category C)

The visitors moving upward were filmed [125] at a frame rate of 25 frames per second and the recordings were evaluated later on a frame by frame basis.

The comparison study on a short stairway took place at the World Team Cup tennis tournament 2004 at the Rochusclub in Düsseldorf. A total of 85 spectators walking upward and downward a stair were filmed and their walking speeds were measured. People obviously doing anything else than exclusively walking were not taken into the statistics. The details of the stairs were as follows: 12 steps with a tread of 36.7 cm and a riser height of 15.0 cm, the stairs were covered with a felt (or felt-like) carpet. The camera was the same as for the first study.

Weather Conditions

The recordings of the Expo study took place at the 31st July 2000 at about 8:30 pm. The temperatures at that day varied between 14.1°C and 20.6°C with an average of 15.9°C. The day was mostly cloudy however it did not rain throughout the day. There was a total of 4.5 hours of sunshine during the evening hours when the recordings took place and it was almost windless [126]. Besides these information, the weather conditions at the time of the recording can probably best be estimated by looking at figure 4.6, which is a frame taken from the footage that was actually used for evaluation. So, the weather conditions can be assumed to have been considered very comfortable by most people.

During the recordings for the comparison study on a short stair (May 19th, 2004) there were very comfortable conditions as well: approximately 24°C, good lighting conditions and no rain.

4.2.2 Results

The “Expo Stairway”

The walking speeds of 485 individuals were measured. The mean, median, maximum and minimum speeds within each category are listed in table 4.3. The relations between the types of speed are $v_{vertical} \approx 0.704 \cdot v_{horizontal}$ and $v_{slope} \approx 1.223 \cdot v_{horizontal}$. In more detail, figures 4.7, 4.8, and 4.9 show the distributions for the horizontal speed.

Comparison Study on Short Stairs

At the World Team Cup tennis tournament 2004 at the Rochusclub in Düsseldorf. The results are shown in table 4.4. The three largest speeds upstairs are larger than the largest speed downstairs. As well are the ten largest speeds upstairs larger than the third largest downstairs. For categories B and C even the mean walking speeds are larger upstairs than downstairs. This confirms that on shorter stairs one can sometimes

	Category A	Category B	Category C
# of persons	73	390	23
Mean horizontal speed	0.423	0.382	0.359
Standard deviation	0.130	0.075	0.040
Median horizontal speed	0.410	0.374	0.349
Minimum horizontal speed	0.22	0.13	0.27
Maximum horizontal speed	1.27	1.15	0.43
Mean vertical speed	0.298	0.269	0.253
Standard deviation	0.091	0.053	0.028
Median vertical speed	0.289	0.263	0.246
Minimum vertical speed	0.15	0.09	0.25
Maximum vertical speed	0.89	0.81	0.30
Mean slope speed	0.517	0.468	0.439
Standard deviation	0.159	0.091	0.048
Median slope speed	0.502	0.457	0.427
Minimum slope speed	0.27	0.16	0.43
Maximum slope speed	1.55	1.40	0.52
Mean # of stairs per second	1.567	1.416	1.331
Standard deviation	0.481	0.277	0.147
Median # of stairs per second	1.520	1.385	1.293
Minimum # of stairs per second	0.82	0.48	1.30
Maximum # of stairs per second	4.69	4.25	1.59

Table 4.3: Basic Results. All speeds and standard deviations in m/s respectively stairs/s.

	Category A	Category B	Category C	All
# of persons upstairs	10	62	19	91
# of persons downstairs	6	38	38	82
Mean upstairs	0.78 m/s	0.70 m/s	0.71 m/s	0.71 m/s
Mean downstairs	0.83 m/s	0.63 m/s	0.65 m/s	0.65 m/s
Minimum upstairs	0.13 m/s	0.41 m/s	0.53 m/s	0.13 m/s
Minimum downstairs	0.54 m/s	0.38 m/s	0.21 m/s	0.21 m/s
Maximum upstairs	1.43 m/s	1.86 m/s	1.29 m/s	1.86 m/s
Maximum downstairs	1.33 m/s	0.96 m/s	1.39 m/s	1.39 m/s

Table 4.4: Horizontal walking speeds on a short stair.

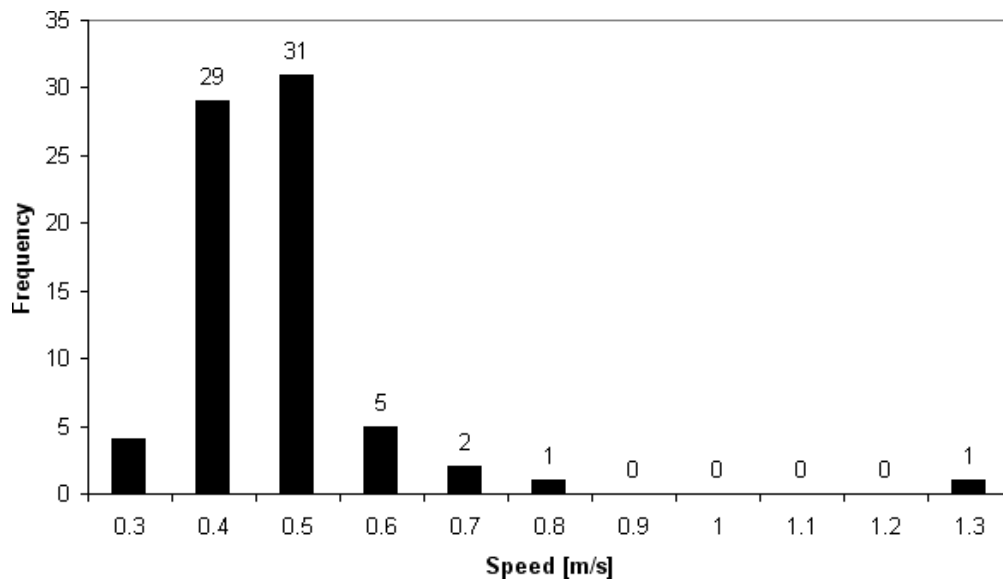


Figure 4.7: Histogram of the horizontal speeds for category A.

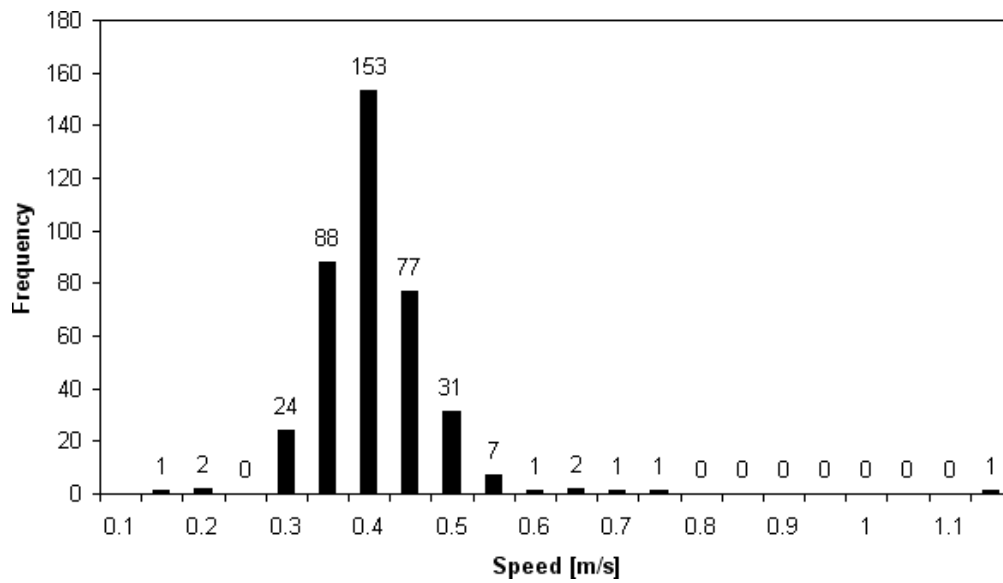


Figure 4.8: Histogram of the horizontal speeds for category B.

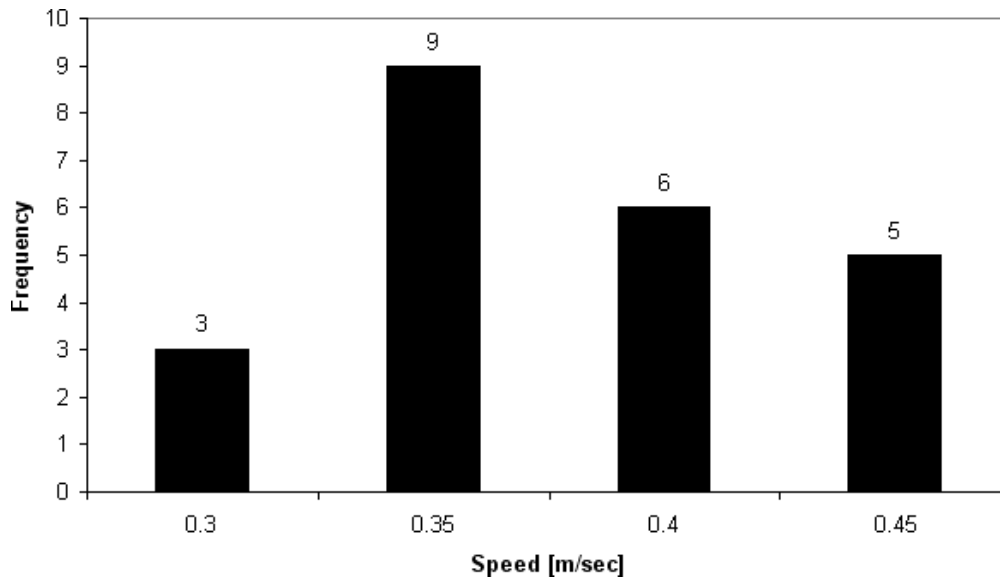


Figure 4.9: Histogram of the horizontal speeds for category C.

watch people, especially young people, accelerating when walking upstairs compared to them walking on horizontal ground or downstairs. Therefore the measurement of walking speeds on short stairways can not easily be used to predict walking times on longer stairways.

The reason why for category C the mean velocities are slightly larger than for category B may be due to people feeling urged to move on if others follow. Note that this was a very relaxed situation and people moved freely at their leisure and probably only rarely as fast as they would have been able to.

4.2.3 Discussion

Comparison to Earlier Studies

In comparison to various earlier measurements the walking speeds measured on the Expo stairway are quite small, yet they results for the short stairway is in agreement with the literature.

The many single studies typically measure different walking speeds with respect to one variable: conditions (comfortable, normal, dangerous) [109]; slope and age [127]; narrow/wide stairs [128]; age, motivation, and slope [129]. In addition there are some compilations or “meta studies”: [130] contains a list of capacity measurements in which some explicitly deal with upstairs motion and in [104] one can find an average of 58 single studies with an average horizontal upstairs speed of 0.610 m/s. There are also studies that examine those values for mobility impaired people [131]. There is also an

attempt to calculate the upstairs speed from the stair geometry (riser and tread) [132], neglecting the length of the stairway and the parameters of the population.

On the whole the wide variation of results in the literature and in this work shows how much the speed depends on the details of the situation as the age and sex of the persons, the motivation, and the length and slope of the stairway.

Caveats

There are some points one must consider when interpreting the results:

- The stairs were on the outside with fresh air and good lighting conditions. Depending on what assumes for indoor conditions, this might let one assume that on long indoor stairs walking speeds would be even slower.
- The recording time was in the evening. So one has to assume that most people had already been walking over the Expo area for some hours and were quite tired. This implies that the true walking speeds in an all-day-average would probably be faster.
- On the other hand this situation might also have led to some selection in a way that not only some visitors might have searched more insistently for elevators. But this also can mean that some visitors not aware of the elevators within the building might have passed the pavilion without visiting. This then would have changed the measured mean value compared to the total population toward faster speeds.
- However the stairway is long, this does not mean people moved without breaks. A break could have been used to take a view over the Expo area as well as to recover a bit and move on faster afterward. This again means that the true mean value of walking speeds would be smaller than measured.
- In cases of emergency people are willing to accept higher heart rates when moving, thus they would move faster even on stairs of that length. On long stairways this might only lead to a small increase of the speed. Even moderately increased upstairs speed can be experienced as a significant increase of the effort.
- The reduction of speeds in categories B and C compared to category A must not necessarily be due to density effects. It can also be caused by psychological effects of people belonging to the same group [87].

Conclusions

In this section the results of a measurement of the upstairs walking speeds of a sample of 485 visitors of the Expo 2000 in Hannover were presented and compared to measurements on a much shorter stairway. Nearly all circumstances must have let one suspected that one would find comparatively small walking speeds. While with a total mean horizontal speed of 0.387 m/s this proved to be true, one must assume that the true whole-population-average free walking speed on such a stair in such a situation would

be even smaller. On the other hand this was an extreme leisure situation; during an emergency higher speeds would probably be possible. The factor of increase, however, would depend on the height to be overcome. Altogether one can assume that the speed distributions measured for this work are sufficient for worst case calculations on stairs with an intermediate or short length and for mean calculations for long stairs. For the case of building simulation models with a high level of agreement in the details with reality the results of this section either demand a whole set of stair elements (short, intermediate, long) or the ability of the agents to plan ahead that far, that the length of a stairway ahead can be considered to set the speed accordingly.

4.3 Experiment: Counterflow in a Corridor

Pedestrian counterflow may occur in a number of situations: in rather narrow corridors on board of ships; in shopping areas at Christmas time; or at pedestrian traffic lights and most importantly in emergency situations if there are no separate routes for rescue forces and evacuees. Such situations may vary in the relative group size and differ in the time the counterflow situation exists: near equilibrium over comparatively large times in shopping areas while only for a few seconds at traffic lights. One-directional pedestrian flow has often been investigated and summarized into one common fundamental diagram [104]. For bi-directional pedestrian flow (counterflow) much less data are available [133, 134]. Yet there is a number of theoretical analyses [28, 56, 95, 117, 118, 135–139], and the study of counterflow is not limited to pedestrian counterflow, for example counterflow has recently attracted some interest on ant trails [140], the dynamics of motor molecules [141], and basic theoretical investigations [142].

4.3.1 The Scenario

The experiment, which follows test scenario 8 of [74], took place at the Sportschule Wedau in Duisburg and is one out of two experiments which have been conducted following [74]. The floor plan (see figure 4.10 and 4.11) consisted of a corridor of a width of 1.98 meters and a length of about 34 meters. 98 cm above the ground the corridor broadened by 40 cm on each side, increasing the effective width slightly as the participants could lean above this cornice to some extent. Three cameras with frame rates of 25 respectively 30 frames per second were used to obtain data. The one to the left and to the right were placed at a distance of 5 m next to the central camera. Two groups started walking five more meters outside the camera region after some acoustic signal.

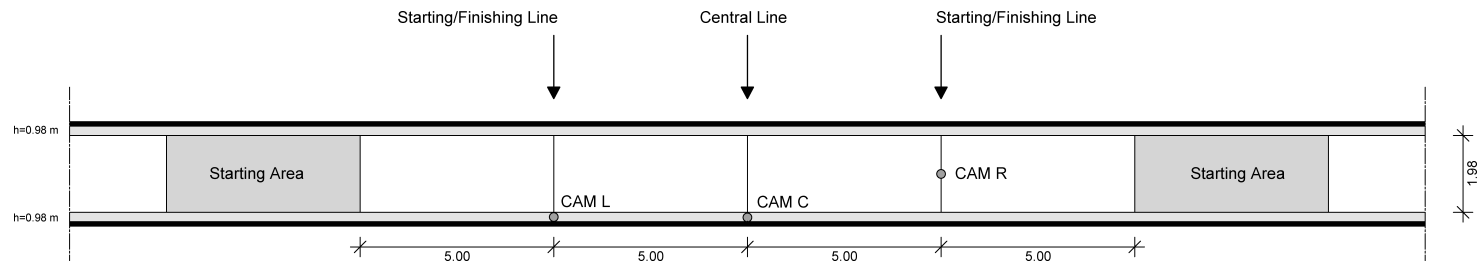


Figure 4.10: The floor plan. The participants initially stood within the “Starting Area”, without further advises how they should arrange there. The positions of the cameras are marked with “CAM L”, “CAM C”, and “CAM R”, of which the latter one filmed from above and the other ones from the side. The distance between the cameras is 5 meter, the height of the cornice 0.98 meter and the width (without the extra space above the cornice) is 1.98 meter.



Figure 4.11: A snapshot from the experiment.

Participants and Groups: The majority of the 67 participants (33 male and 34 female) were students of Duisburg-Essen University, mostly born in the eighties. The amount of counterflow, which is always given as a size of the counter-group of the group in focus divided by the total number of participants, always was (approximately) 0, 0.1, 0.34, or 0.5. Those values were not always met exactly due to rounding errors and participants needing to pause. While there were repeated runs with identical or very similar group size combinations, the assignment of the people to the two groups was changed each time. Appendix C contains the detailed statistics of the participants as well as the precise sequence of runs.

4.3.2 Results

The resulting data (passing time, walking speed and specific flux) will now be given, either in dependence of the group size for (approximately) identical counterflow fractions and in dependence of (exact) counterflow fractions.

Passing Times

The passing time is defined as the time a group needs to pass a certain spot. As would have been expected, for each counterflow fraction the passing time grows linearly with the group size. See figures 4.12 and 4.13. More interesting is a comparison of

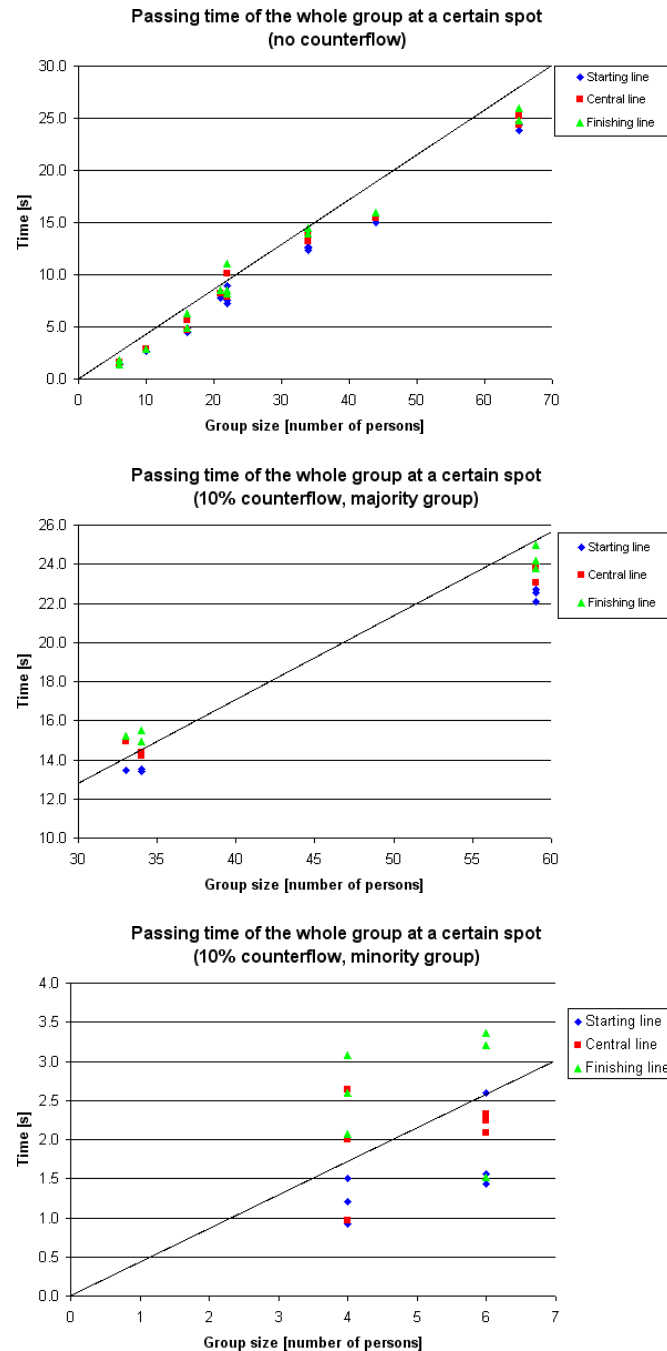


Figure 4.12: Passing times (part *i*). The first thing one observes in this and figure 4.13 is that the results vary significantly more in the presence of counterflow. Naturally this effect is most distinctive when the group is very small and the selection of the group members (e.g. due to varying body height) becomes important. It is a priori not obvious that for a counterflow situation the passing time increases linearly with the group size, as is in the case of no counterflow. Yet the results of the 50% counterflow situations (compare figure 4.13) justify this assumption and thus table 4.5.

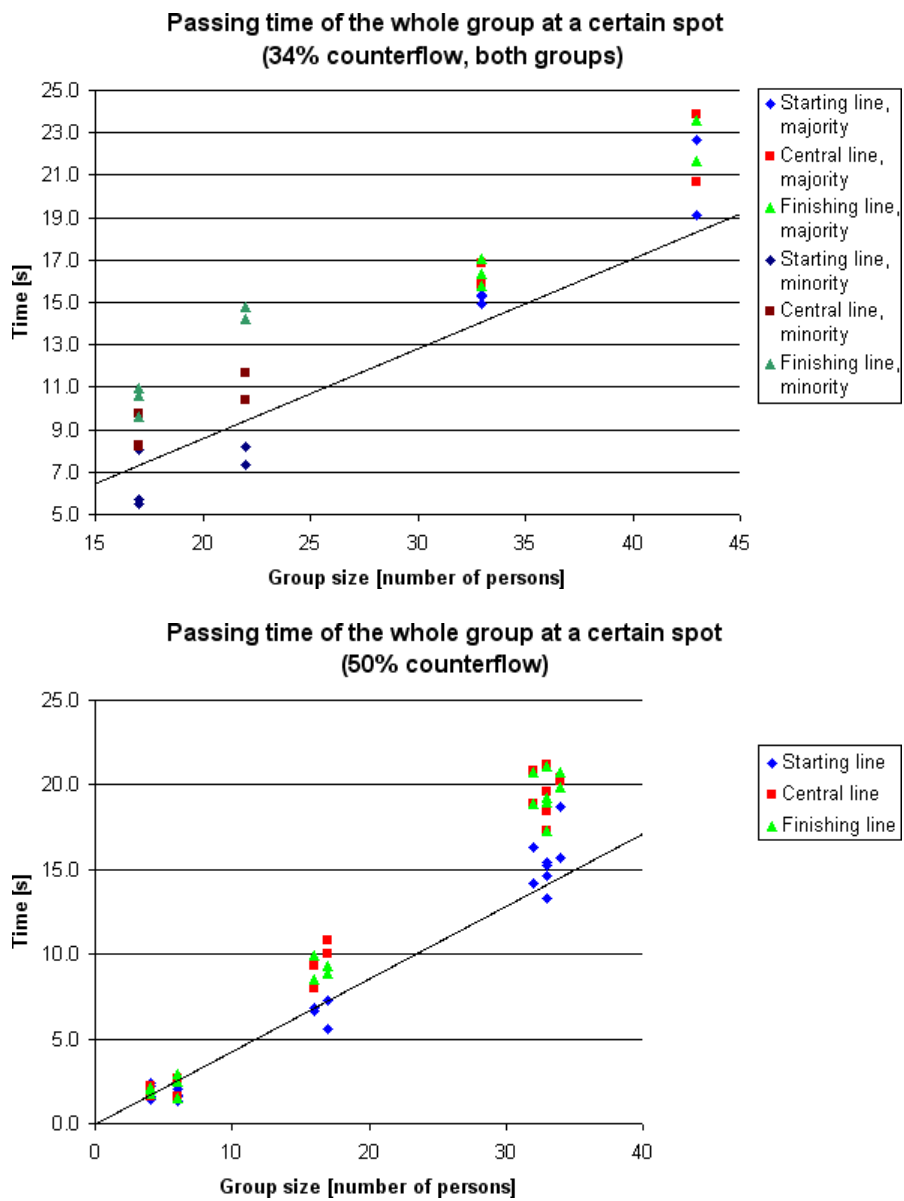


Figure 4.13: Passing times (part *ii*).

the gradients of the different counterflow fractions at the finishing line (see table 4.5), which have the dimension of an inverse flux. The large dispersion of the results for the minority group in the case of a counterflow fraction of 0.1 follows from the small group size and from the important role which the choice of individuals plays that form the minority group. Another interesting result is the comparison of passing times for

Fraction of counterflow	Offspring included		Offspring not included	
	Dependence	R^2	Dependence	R^2
0.00	0.39 $s/\text{pers}\cdot n$	0.98	0.40 $s/\text{pers}\cdot n - 0.28 s$	0.98
0.10	0.42 $s/\text{pers}\cdot n$	0.96	0.36 $s/\text{pers}\cdot n + 3.20 s$	0.99
0.34	0.51 $s/\text{pers}\cdot n$	0.92	0.62 $s/\text{pers}\cdot n - 4.14 s$	0.95
0.50	0.59 $s/\text{pers}\cdot n$	0.98	0.62 $s/\text{pers}\cdot n - 0.99 s$	0.99
0.66	0.64 $s/\text{pers}\cdot n$	0.90	0.81 $s/\text{pers}\cdot n - 3.43 s$	0.95
0.90	0.51 $s/\text{pers}\cdot n$	-0.49	0.06 $s/\text{pers}\cdot n + 2.36 s$	0.01

Table 4.5: Results of linear regressions for the dependence between passing time at the finishing line and group size, with and without forced inclusion of the offspring. n : number of persons. Note that a counterflow fraction of 0.90 denotes the minority group of an experiment with 10% counterflow. Compare figures 4.12 and 4.13.

constant majority group size in figure 4.14. The increase of the passing time even at the starting line from 0 to 0.1 counterflow shows that the participants reacted quite early to even just a few people approaching.

Walking Speeds

While the passing time is a time measurement at a certain spot, the walking speeds - to be more precise the speed of the front and the back of a group - relate events at different positions. Figures 4.16 and 4.17 show the results and figures 4.18 and 4.19 the quotients (speed factors) of the walking speeds of the last and first person. The speed factors in absence of counterflow never fall below 0.7, while in counterflow situations they can even be smaller than 0.5. This shows how counterflow situations can loosen walking groups by increasing the distance between the members. It's an interesting observation that the minority group in a 0.34 counterflow situation is more affected by this phenomenon than the majority group. In 0.1 counterflow situations, however, the minority group seems to be so small (no more than six persons) that they avoid being more loosened than the majority group. Yet, if one compares the speed factors of the majority group in the 0.1 counterflow case with those of groups of comparable size in the no counterflow case one finds them to be very similar, while the speed factors of the minority groups are smaller than in cases without counterflow. This on the contrary could let one conclude that it is the minority group that is affected more than the majority group by the counterflow situation.

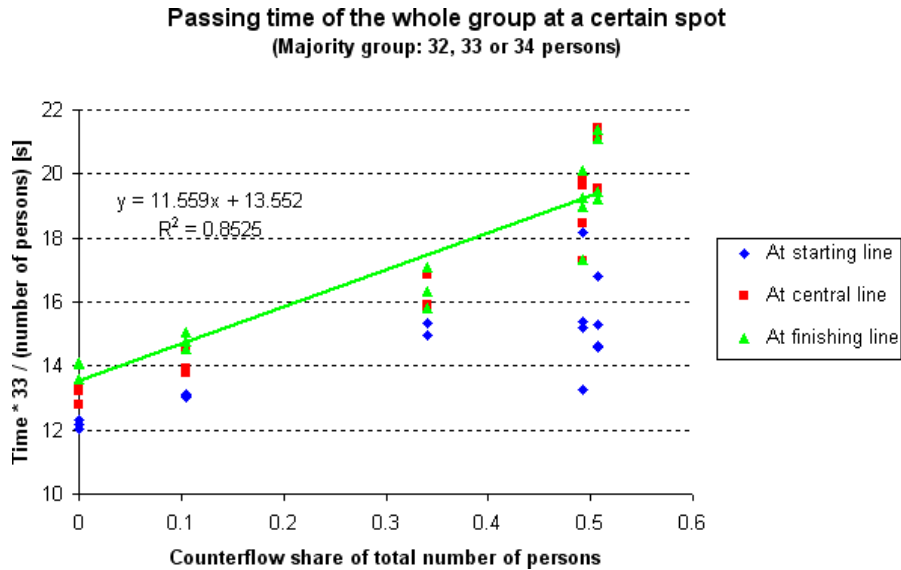


Figure 4.14: Comparison of passing times of a majority group with approximately constant group size. Since the size of the majority group varied slightly, the times were scaled accordingly. This figure demonstrates the significant influence some counterflow has on the passing time. However, the influence is not that big as one might assume at first: imagining the group to occupy a rectangle with the width of the corridor in the case of no counterflow and half of the width of the corridor in the case of 0.5 counterflow, one might guess, that the passing time at a spot behind the central meeting point of the two groups doubles. In fact it only increases by roughly 43%. Compare figure 4.15.

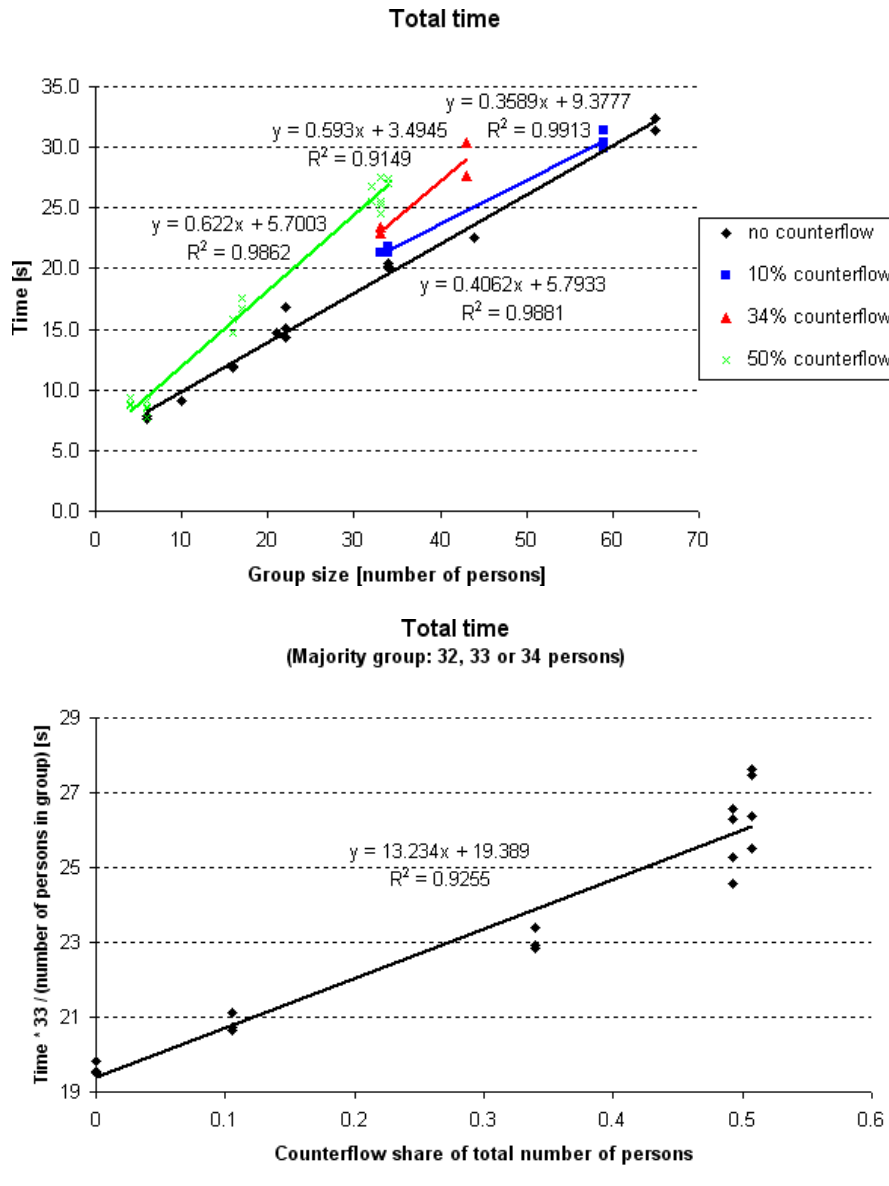


Figure 4.15: Comparison of total times: The total time is the time between the passing of the starting line by the first person until the time of the passing of the finishing line by the last person. The first figure shows the total times of the majority group. The second figure exhibits an influence of the counterflow on the total time, which with an increase of approximately 34% from no to 0.5 counterflow is slightly smaller than the influence on the passing time (compare figure 4.14). The absolute value of the slope of the regressionline, however, is bigger than in the case of the passing times. The reason for this is, that there is a minimum time larger than zero for the total time, while the passing time can get very close to zero for very small groups.

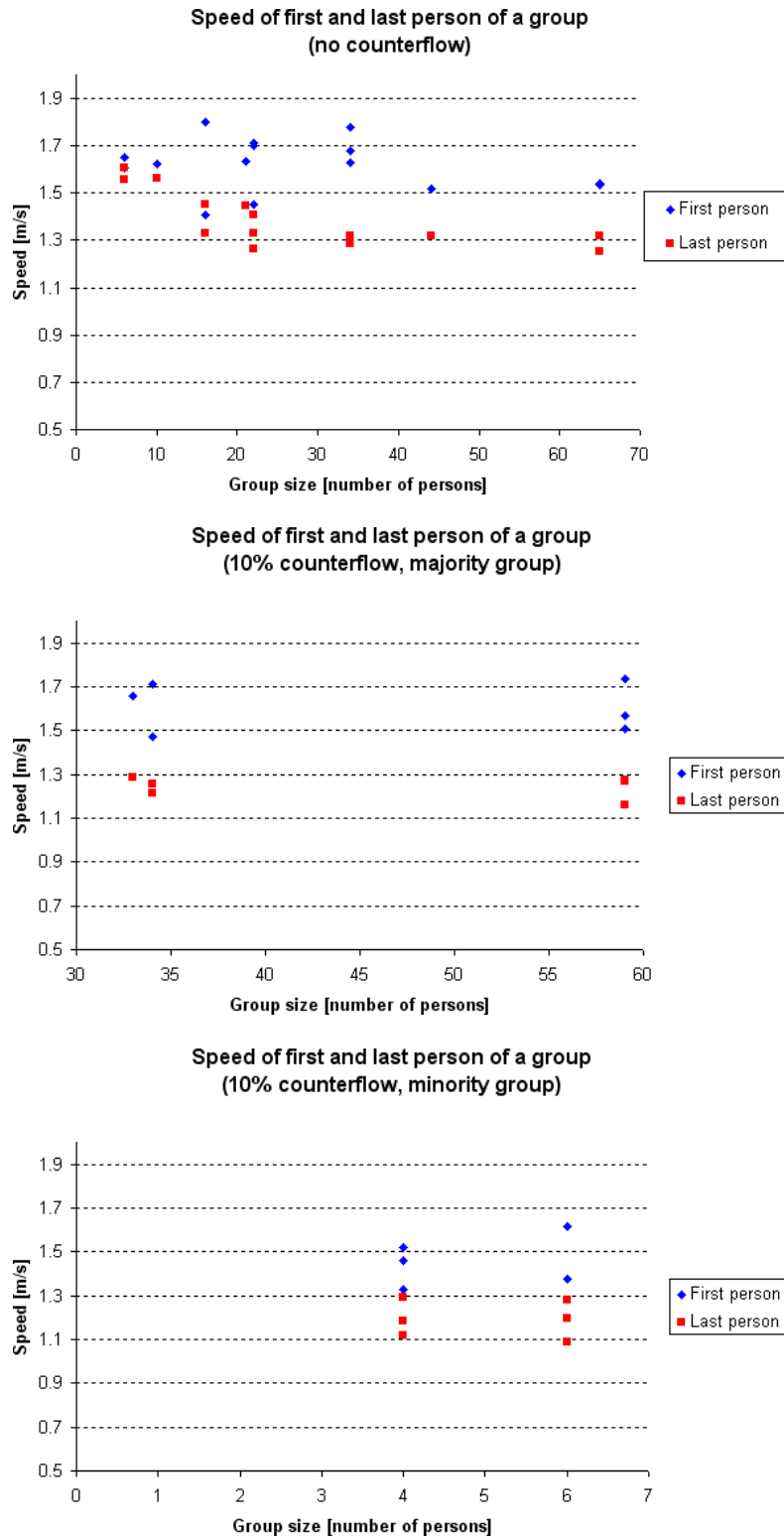


Figure 4.16: Walking speeds (part *i*). For no or only small counterflow there is only a small or even no influence of the group size on the walking times.

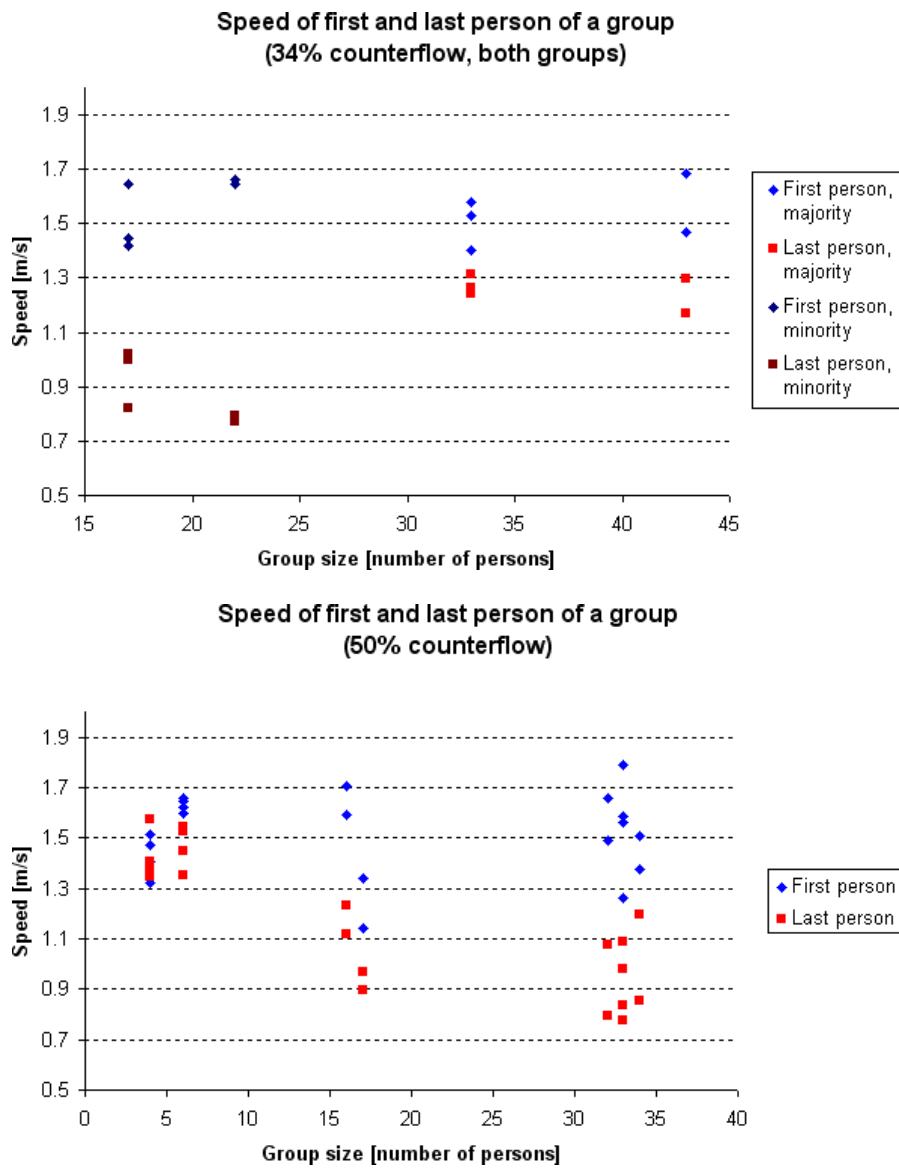


Figure 4.17: Walking speeds (part *ii*). The group size has an influence on the walking speed of the last person in the case of 0.5 counterflow and in terms of the variation of results as well on the speed of the first person.

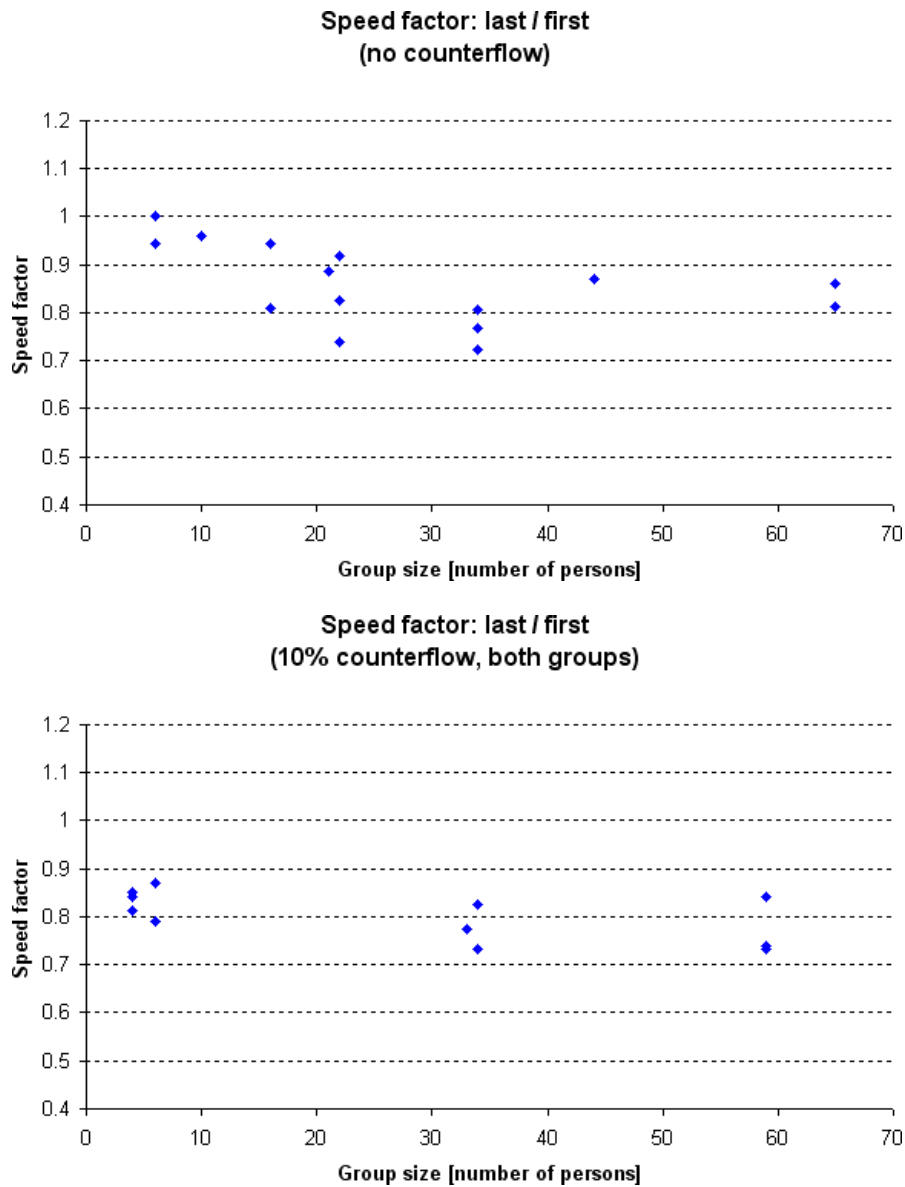


Figure 4.18: Walking speed factors (part *i*). This is the ratio of the time the first person needs to move from the starting to the finishing line by the same time the last person needs. Note that the last and first person may have changed on the way in some cases. For the majority group this ratio is if any then unrecognizably affected at 0.1 counterflow compared to no counterflow situations. For the minority group there is an effect denoting that some people (first of the minority group) may do better when walking against a flow than others (last of the minority group).

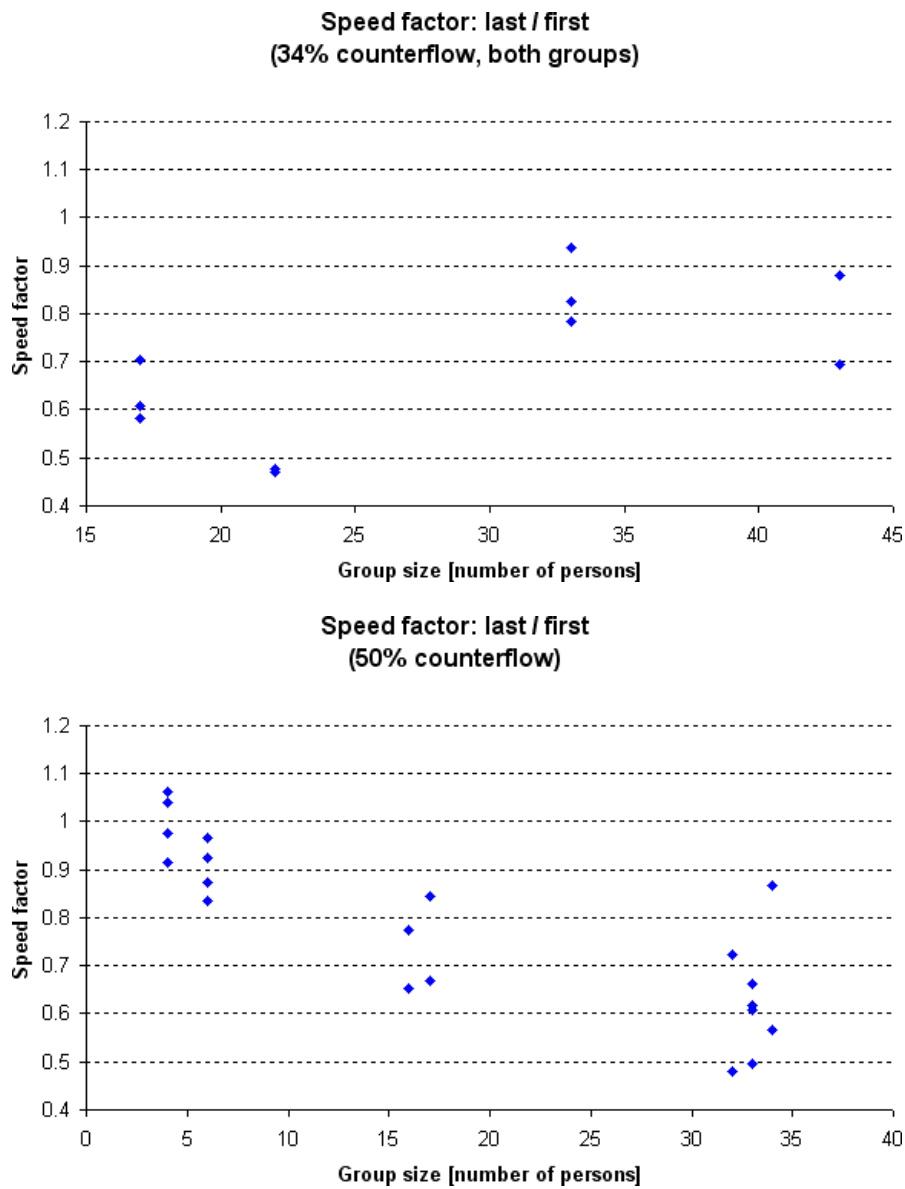


Figure 4.19: Walking speed factors (part *ii*). The walking speed factors outline, what has been foreshadowed in the walking speeds: the relative difference in the speed of the first and the last person is most distinctive for large groups and 0.5 counterflow. The figure for 0.34 counterflow shows, that the minority group in both cases is more affected than the majority group.

Fluxes

The specific flux is the number of persons that cross a certain spot divided by the width of the corridor and the (passing) time this process takes. A surprising result from figures 4.20 and 4.21 is that the flux in a 0.5 counterflow situation is larger than half of the flux in a no counterflow situation with the same total number of persons. (Also compare figures 4.22 and 4.23.) This is not very surprising at the starting line, i.e. before the two groups meet, as for this spot one effectively has a doubled width compared to no counterflow motion. But for the central line this is a clear indication that in open-boundary-no-counterflow-situations the density always remains well below the density of maximal flux in the fundamental diagram and that therefore an increased flux is possible for increased density.

If one looks at the specific flux as a function of the fraction of counterflow, one first notices a wide dispersion of the results. Only confining the displayed results to those runs where the majority group contained at least 20 persons shows some clearer trends. But even then the first trend is that the dispersion of results for the minority group (counterflow fraction > 0.5) is large, which might be simply due to the small size of the minority group. (The characteristics of the few individuals who form the group might be crucial.) Only an experiment with more participants would be able to bring more reliable results for counterflow fractions of 0.9. Therefore the impression that the specific flux has a minimum at a counterflow fraction of 0.5, which could arise from figure 4.22b, should not be regarded as definite result of this work. This demands further research, though.

A somewhat more evident result is that the flux at the finishing line linearly drops as the fraction of counterflow is increased. (See figure 4.22c.) With c_f as counterflow fraction the linear regression results in $1.181 \cdot \text{persons}/(s \cdot m) - 0.374 \cdot c_f \cdot \text{persons}/(s \cdot m)$ (with $R^2 = 0.232$) if one only considers runs with a majority group size of at least 20 people and $1.208 \cdot \text{persons}/(s \cdot m) - 0.687 \cdot c_f \cdot \text{persons}/(s \cdot m)$ (with $R^2 = 0.910$) for runs with a majority group size of 32, 33 or 34 people. Here it is interesting to note that the fact that the slope is larger than -1 can be interpreted in a way that a counterflow reduces the effective width by a factor smaller than the fraction of counterflow. This is a similar result as the finding that the flux in a 0.5 counterflow situation is larger than half of the flux in a no counterflow situation (see above).

Lane Formation

A famous phenomenon in counterflow - but also in some other crowd movement - situations is lane formation [28, 56, 143]. Pedestrians simply choose to follow closely behind some other person who moves into the same direction. The lanes that emerge in this way are stable for some time and then disappear, merge or split again.

NB: The terminology here is such that a lane can consist of several layers. Thus if two people can walk side by side without someone in between them who walks in opposite direction, it is still one lane, but two layers.

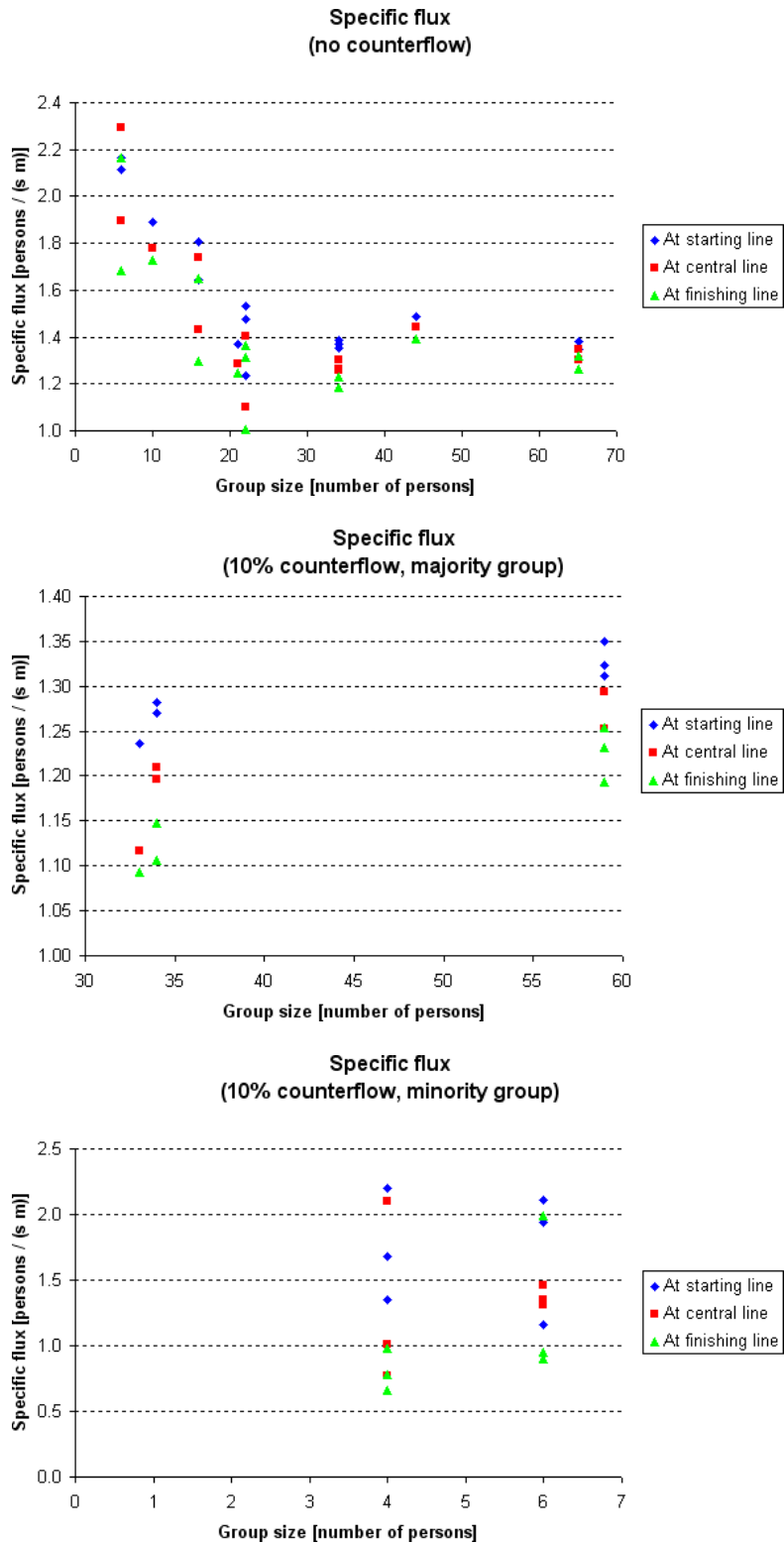


Figure 4.20: Specific fluxes (part *i*): Number of persons / (1.98 m · passing time).

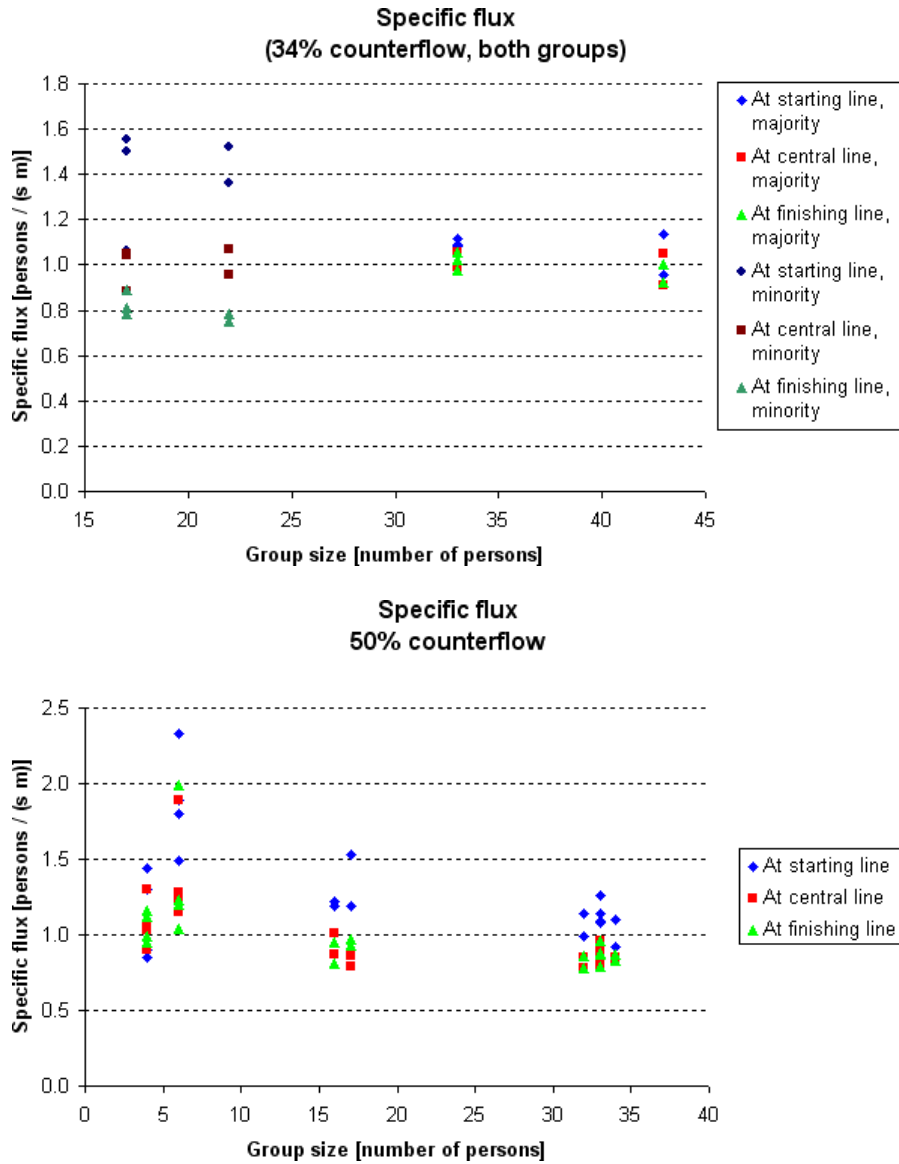


Figure 4.21: Specific fluxes (part *ii*): Number of persons / (1.98 m · passing time). As with the passing and total times, it also holds for the specific flux, that compared to no counterflow (compare figure 4.20) the performance in the 0.5 counterflow case is not reduced by a factor of two, but only by approximately a factor of 1.5 (slightly depending on the measurements taken for comparison).

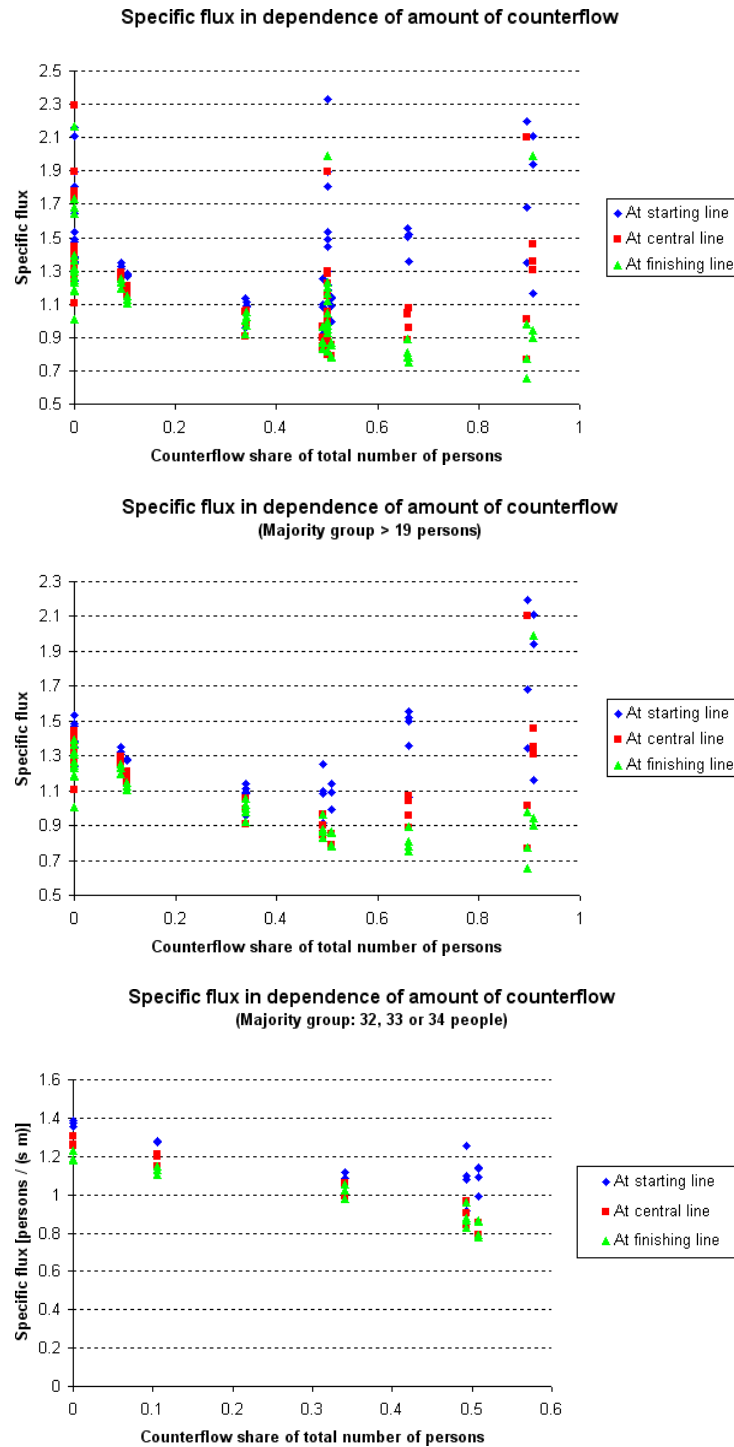


Figure 4.22: Comparison of specific fluxes. All results and selections. The third figure shows the results of the largest majority groups that could be formed and significantly less dispersed results than the rest of the data set. At the finishing line the specific flux was found to reduce from approximately 1.2 (no counterflow) to 0.9 persons per meter and second (0.5 counterflow).

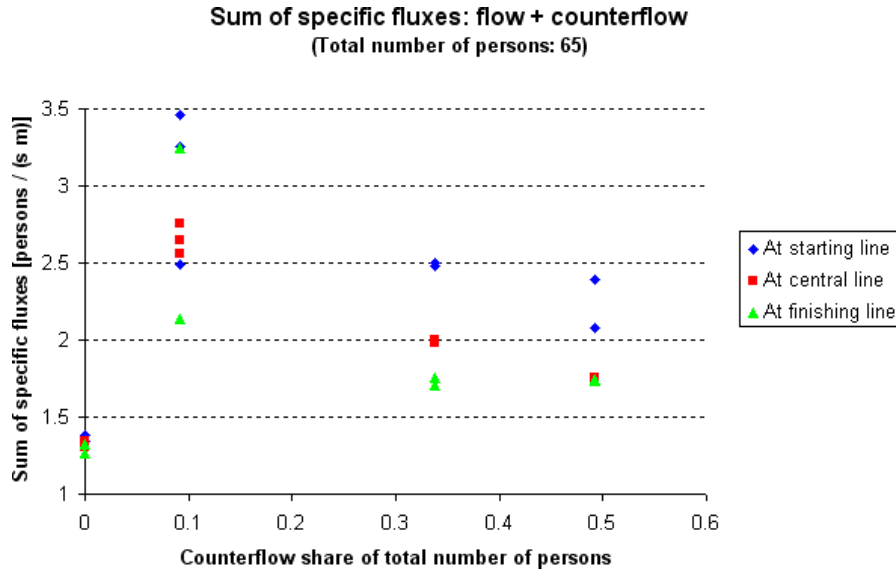


Figure 4.23: Comparison of the sum of specific fluxes. The sum of fluxes in counterflow situations is always larger than the flux in the no counterflow situations.

Number of Lanes: Figures 4.24 and 4.25 show that in the different runs of this experiment two, three as well as four lanes appeared. For adults this is probably the maximum of possible cases, as in the case of five lanes there would remain less than 40 centimeters for each person.

Left-Right-Asymmetry: While an odd number of lanes always exhibits a broken symmetry, in the case of an even number of lanes, the symmetry could be preserved, as long as right-hand traffic and left-hand traffic appear in equal shares. In the nine cases of an even number of lanes, however, left-hand traffic did not appear even once. The participants always “chose” right-hand traffic.

4.3.3 Summary and Conclusions

The results of this pedestrian counterflow experiment yield comparatively high speeds and fluxes, which probably is mainly due to the participants mostly being in their twenties. Compared to a situation without counterflow the performance - in terms of passing or total times, speed, and flux - of a group of walkers is never reduced as much as one would expect from the amount of counterflow. For example if there are two equally sized groups the passing time at a certain spot does not double, nor does the flux drop to 50%. However, the passing time increases and the flux decreases, the participants seemed to be able to compensate the existence of a counterflow to a certain point by accepting higher densities and using space more efficiently. This phenomenon can be summed up by saying that the sum of fluxes in a counterflow situation in this experiment was always

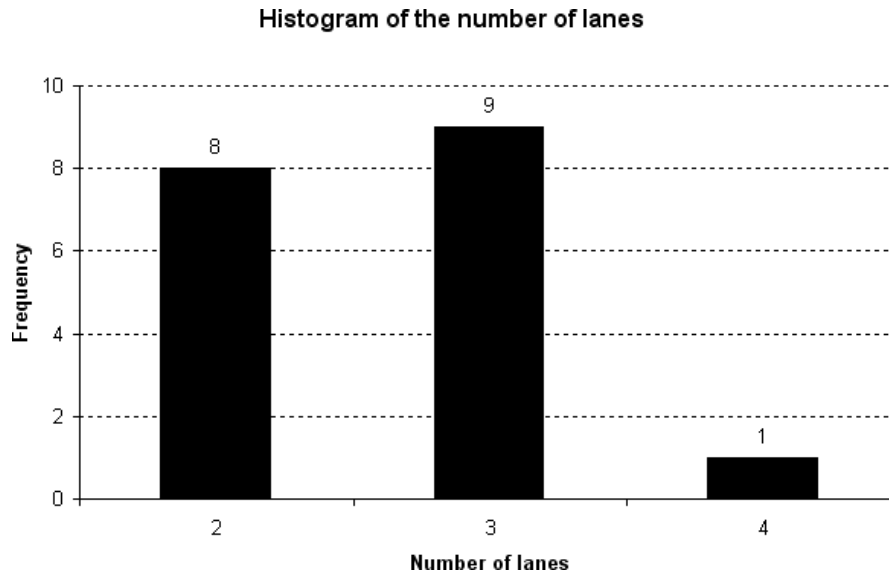


Figure 4.24: Histogram of the number of lanes. Only those runs were counted, where the number of lanes could be verified to be the same at CAM C and CAM R (compare figure 4.10).

found to be larger than the flux in any of the no counterflow situations. Implementing this high efficiency of real pedestrians to realistic simulation models of pedestrian dynamics will pose a challenge, as it seems that a lot of details and a significant amount of intellectual power have to be considered.

4.4 Experiment: Flow Through a Bottleneck

Bottlenecks are of interest in many systems as traffic [144–147], the internet [148], the ASEP [149, 150], evolution theory [151] and a lot more. A bottleneck typically denominates a limited area (in a general sense) of reduced capacity or increased demand (e.g. on-ramps on highways). This capacity reduction can be due to a forced speed reduction (speed limit in traffic), a reduced movement probability (ASEP, tunnel effect), a reduced bias or correlation in a dynamic process (ASEP, correlated random walks), or a direct capacity reduction (networks, blocked highway lanes). For pedestrians bottlenecks are usually formed by direct capacity reduction (door or corridor).

Bottlenecks are of fundamental importance in the calculation of evacuation times and other observables for buildings. This directly implies the need to understand the phenomenons that occur in junction with bottlenecks quite well to build reliable (simulation) models of pedestrian movement. Therefore there has been increasing interest into pedestrian flow through bottlenecks in recent years [2, 108, 143, 152–158]. Often such research has as one aim the construction of models of pedestrian dynamics or to



Figure 4.25: Two, three and four lanes.

create data or tools to validate such models. One set of very basic tests that aim at giving authorities and applicants criteria to evaluate such simulation models can be found in [74]. Deciding in what situations a precise reproduction of reality is essential is one thing, knowing the reality of these situations another. In the present situation there are much more simulation models (compare section 1.3) than empirically well investigated test scenarios. This section aims at closing this gap a little bit.

The outline of this paper is as follows. First the scenario is described in terms of the geometrical layout. Then the group of participants is described. The sequence of runs - in terms of the bottleneck's widths - might also be of some importance and concludes the description of the experimental setting. The section "Results" begins with an analysis of the starting phase and starting effects. From total times over fluxes, specific fluxes to the distribution of time gaps the results then proceed from macroscopic to microscopic data.

4.4.1 Experimental Setting

The Geometrical Layout

The experiment follows test scenario 4 of [74] but exceeds it in the amount of aspects considered. It took place in a building at the campus Duisburg of Duisburg-Essen University from 3 pm to 5 pm on the 15th of Mai 2006. The bottleneck was formed by two cabinets with a height of two meters and a depth of 40 centimeters. Note that especially compared to the experiments reported about in [143, 152], this bottleneck with a depth of 40 cm is rather short, i.e. it is rather comparable to a door than a corridor. The space in front of the bottleneck was about 4 meter wide and 9 meter deep with a slight increase of the width toward the back wall. At the beginning of each run, the participants stood right in front of the bottleneck, there was no mentionable free space between them and the bottleneck. The process was videotaped from above (see figure 4.26) and from the side. For analysis only the former one was used. The time distance between two frames and therefore the time resolution is 0.033367 seconds. Higher time resolutions would have been possible, yet it becomes difficult at some point to distinguish between "person has not yet passed" and "person has passed" if the frames are too similar. The criterion for "person has passed" was when the first frame showed that the head of a participant fully crossed the line shown in figure 4.26. Ten different widths of the bottleneck were examined: 40, 50, 60, 70, 80, 90, 100, 120, 140 and 160 centimeter. For each reconfiguration the width was measured with a laser distance measurement device and accepted if the difference to the exact value was 2 millimeter or below. The cabinets were weighed down (> 300 kg) to the point that the possibility of a displacement during a run was excluded.

The Participants

The majority of the 94 participants were students at Duisburg-Essen University (32 female, 62 male). Thus the group was rather homogeneous concerning age (six born before 1978, one after 1990, most around 1984) and level of fitness. Concerning body



Figure 4.26: A snapshot from the recordings at a bottleneck width of 40 cm.

height there was a “female frequency peak” around 170 cm and a “male frequency peak” around 180 cm with approximately ten guys being taller than 190 cm. A more detailed statistics can be found in appendix D.

The participants have been told to be vigilant and not to dawdle, but that they should not think of a competition or an emergency situation. The homogeneity of the group must let one suspect that they are able to estimate each other’s behavior quite well, which probably led to comparatively small time gaps. The fact that most of the participants are in the age of maximal physical fitness as well as maximal reactivity will probably have had the same effect.

Concerning the homogeneity of the group: one will probably quite often find groups (defined by spatial proximity) that are significantly more homogeneous than a random sample of the society. There is most often a reason, why individuals meet and move within groups and these reasons often have a selecting effect. In fact it is not implausible to assume that subsets of the population that are truly representative only rarely gather autonomously.

The Sequence of Runs

The sequence of runs is shown in table 4.6. For the bottleneck width of 100 cm, six repetitions were done for two reasons: 1) The participants were to get used to the

Bottleneck width	Number of runs
100 cm	6
90 cm	3
80 cm	3
70 cm	3
60 cm	3
50 cm	3
40 cm	3
120 cm	4
140 cm	3
160 cm	3

Table 4.6: The sequence of runs.

situation, especially to being filmed and 2) 100 cm is the width mentioned in [74]. For 120 cm an extra run was done unintentionally.

4.4.2 Results

During the planning process the aim was to have 100 participants. As finally 94 participants came to take part in the experiment, the idea was to fill the gap by telling the first six persons to walk around the cabinets in some distance and pass the bottleneck again. However due to the noise of the crowd this did not work out well in each case and so in the following the results considering the first 80 and - where possible - the first 100 persons are given.

The most direct measurement is the total time from the first to the last participant crossing the line shown in figure 4.10. This implies, that the total time is the sum of $n - 1$ time gaps, if there are n participants. The flux then simply is the inverse of the total time multiplied by the number of persons that walked through the bottleneck in this time. The specific flux is the flux divided by the bottleneck width. Finally the distribution and evolution of time gaps - the time distances between subsequent persons - will be given. But first the analysis will begin with the starting phase and therefore - to have a sufficiently detailed perspective - also with a look at the time gaps.

The Starting Phase

The question is whether the process needs some time to become static or if the measured observables are the same from start to end. A standard assumption would be an exponential relaxation of the time gaps T_G following equation (4.1).

$$\tilde{T}_G(t) = a \exp(-bt) + c. \quad (4.1)$$

The large dispersion of the data does not necessarily select the function of equation (4.1) and exclude other ones. It was chosen for reasons of simplicity as well as comparability

to [152]. The results for the three parameters are shown in table 4.7 and for two of them together with the original data and smoothed functions $\hat{T}_G(t)$ (following equation (4.2)) in figures 4.27.

$$\hat{T}_G(t) = \frac{\sum_{i=1}^{N_{max}} T_G^i \exp\left(-\frac{(t-t(T_G^i))^2}{\tau^2}\right)}{\sum_{i=1}^{N_{max}} \exp\left(-\frac{(t-t(T_G^i))^2}{\tau^2}\right)} \quad (4.2)$$

with t in steps of 0.1 seconds, N_{max} being the number of measurements and τ freely set to $\tau = 1$ second or $\tau = 10$ seconds.

Bottleneck width	a	b	c	RMS	adjusted R^2
40 cm	-0.127 s	0.018 1/s	1.191 s	0.208 s	0.011
50 cm	-0.086 s	0.192 1/s	0.986 s	0.180 s	-0.006
70 cm	-0.157 s	0.024 1/s	0.897 s	0.243 s	0.010
80 cm	-0.087 s	0.099 1/s	0.714 s	0.274 s	-0.005
100 cm	0.006 s	-0.062 1/s	0.511 s	0.296 s	0.021
120 cm	0.255 s	-0.016 1/s	0.103 s	0.246 s	0.086

Table 4.7: Results of a regression following equation (4.1) for the temporal evolution of the time gaps.

The large dispersion of measurements and the fact that no trend is recognizable concerning the dependence of a and b on the bottleneck width make the results for the parameters a and b seem to be not very reliable. The negative value of b at 100 and 120 cm indicate, that there is either no relaxation tendency for the first 100 participants or that at least if there is such a tendency it is obscured by another effect. The positive values for a and the negative ones for b have different causes for 100 and 120 cm. While for 120 cm this is probably caused by the tailback described at the beginning of the next section, this cannot be the cause at a width of 100 cm, since even for the first 18 seconds the fit revealed positive a and negative b . In addition, there is another local RMS-minimum for a width of 100 cm at $a = -0.618$, $b = 3.685$ and $c = 0.563$ with a RMS only slightly smaller than for the result given in table 4.7 and thus a sharp and quick relaxation on a time scale of $1/b = 0.27$ s, which is less than most time gaps. The most likely conclusion seems that for 100 cm there is neither a relaxation tendency nor some exponential increase. Due to the short time in which the runs for 120 cm are completed, besides the tailback a second reason for the evolution of time gaps at 120 cm could in principle be that the relaxation has not been completed before all participants have passed. In this case, however, one would expect that this trend somehow can already be identified for 100 or even 80 cm and thus would expect different results for 80 and 100 cm than have actually been measured: b is comparatively large for 80 cm and a is much smaller for all other widths than 120 cm.

For parameter c however, there is a nice trend except for the result for a width of 120 cm. As for positive b c is the static average on the long run, it is the parameter

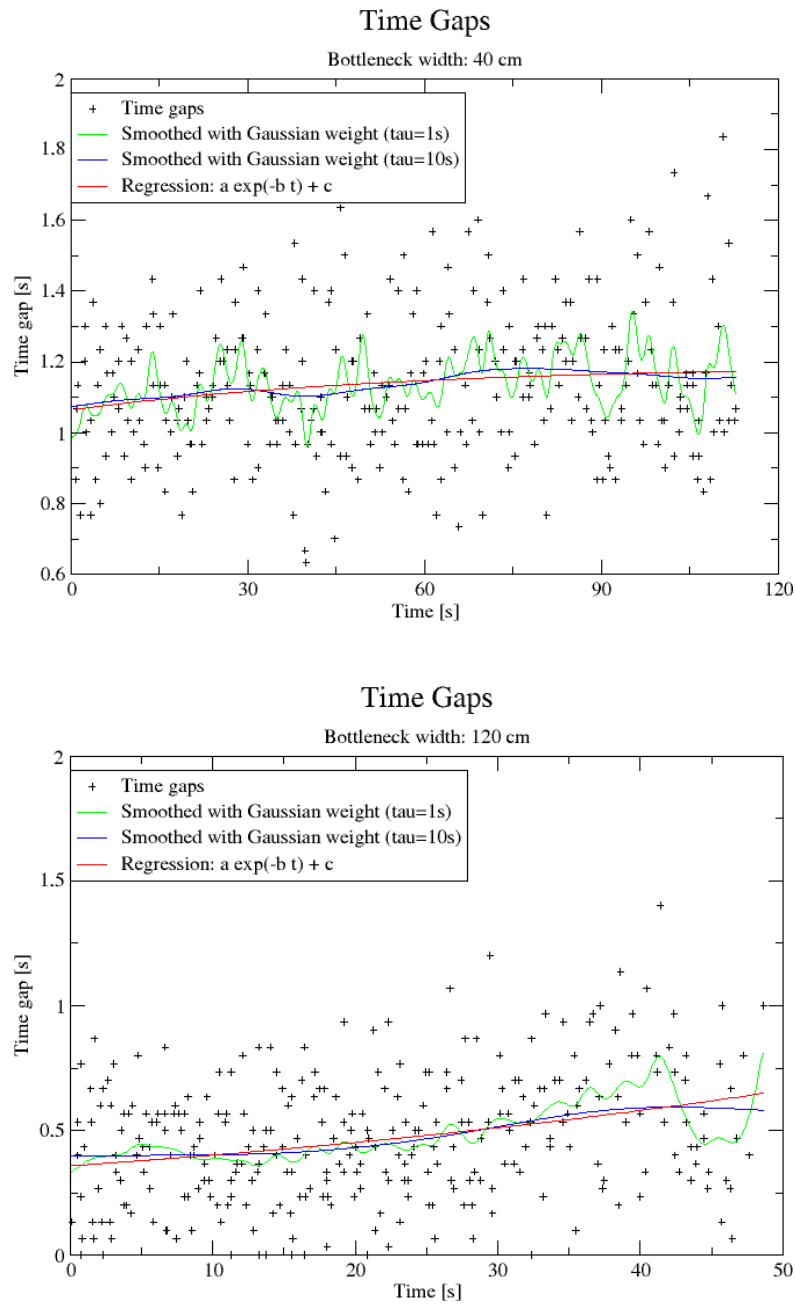


Figure 4.27: The original time gaps data (black “+”s) and from that data two smoothed functions (green and blue curves) and a regression following $\tilde{T}_G(t) = a \exp(-bt) + c$ for the widths 40 and 120 cm. The numerical values for a , b , and c can be found in table 4.7. The smoothing of the blue and green curve has been done using a Gaussian weight dependent on the time distance between the considered point in time and the time of the time gap (see equation (4.2)).

which should be easiest to fit. a and b are meant to show the deviation from the static process in the beginning. Therefore a much larger fraction of the measurements can be used to fit c compared to a and b .

Another possibility to estimate the time dependence of the time gaps is to watch the evolution of the average time gap between person $n - 1$ and person n . Averaging over six (100 cm) or three (rest) runs leads to far too large fluctuations to tell something about starting effects. Therefore one has to average over a few consecutive time gaps. A running average sample size of five was chosen. For smaller sample sizes the fluctuations were too large and for larger sample sizes possible starting effects might be averaged out too much. Figure 4.28 shows no starting effects with a possible exception at a bottleneck width of 100 cm. Or if there are trends in the beginning, they are not stronger than fluctuations that appear later on. Since the fluctuations remain larger than possible starting effects throughout the process anyway, there seems to be no need to take starting effects into account.

Total Times

If - as a first assumption - one assumes a linear increase of the flux with the bottleneck width, the total time is expected to depend like

$$T \approx c/(w - w_0) + t_1 \quad (4.3)$$

on the bottleneck width w , with w_0 as minimal bottleneck width where passage is possible, t_1 the time for one person to pass the bottleneck, and c as some constant. If one neglects the depth of the bottleneck (a person needs no time to cross the line), one can set $t_1 = 0$. This is what is assumed in this work: The total time for N persons consists of $N - 1$ time gaps between consecutive persons.

Figure 4.29 shows a decrease of the total time until the bottleneck width reaches 120 cm. That the decrease does not continue for wider bottlenecks is not only due to a normal $1/w$ behavior, which comes close to its static value, but at least partly due to participants who did not leave the area behind the bottleneck fast enough. The available area behind the bottleneck and the possibilities to leave this area were not sufficient to guarantee a fast efflux of the participants at those large bottleneck widths. Therefore the flux through the bottleneck is not limited by the bottleneck itself, but by a tailback. Figure 4.28 very clearly shows this effect. One can even guess quite precisely at what time the tailback reached the bottleneck. In other words: The bottleneck stopped being a bottleneck for widths of 120 cm and above, in a sense that the participants - due to some obstacles - couldn't leave the area behind the bottleneck fast enough to allow those passing the bottleneck to do this as fast as they could. Figure 4.30 shows the total times for those bottleneck widths for which a linear approximation appears to be possible. Please note that this is not a claim that there actually is a linear dependence of the total time on the bottleneck width. This - for reasons stated above - would not be possible over the whole range of widths anyway. Nevertheless an almost constant decrease of the total time should not be possible in a range from 50 or even 40 to 100 cm, if one assumes

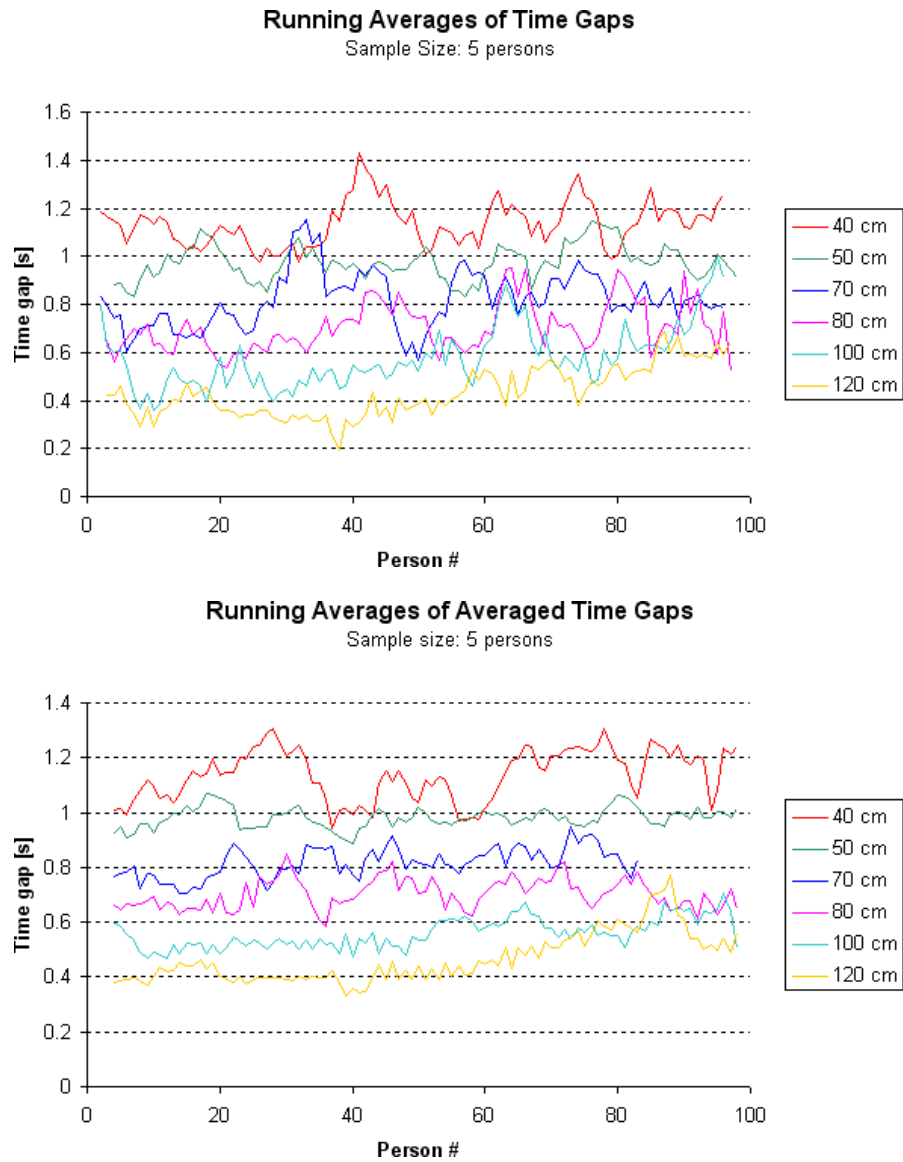


Figure 4.28: Running averages with a sample size of five. The upper diagram includes data of just one run, while for the lower one at first an average of the i -th time gaps of all runs of a certain bottleneck width has been done. A data point at position (i/\bar{T}_G) therefore has the meaning, that the average of the time gaps $i - 4$ to i was \bar{T}_G .

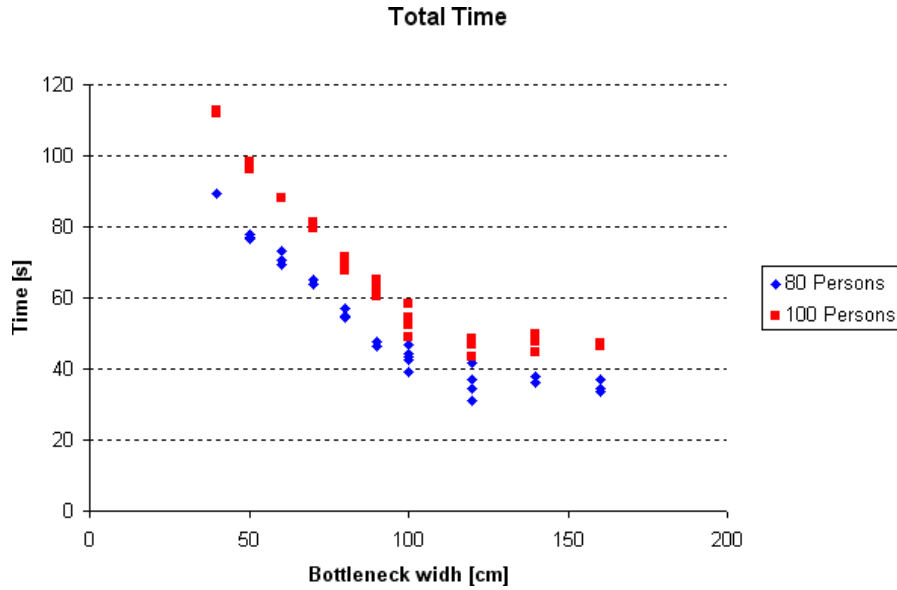


Figure 4.29: Total times for all runs.

equation (4.3) to be correct, even if one assumes $w_0 = 20$ cm, which would be rather small.

Fluxes

Figure 4.31 shows the fluxes of all runs. One of the first things noticeable is the increase in variation for bottleneck widths of 100 cm and above. This has at least two reasons: The first is trivial, as there were six instead of three runs. Second, one has to remember that the experiment started with a width of 100 cm. Maybe there has been some learning effect at the beginning of the experiment. The rather large variation of results for a width of 120 cm and the development of the specific fluxes during the 100 cm runs shown in figure 4.36 neither fully support nor fully exclude this possibility. And third there could indeed be a larger variation for widths of 100 cm and above that is reproducible in further experiments independently of the sequence of runs or other factors.

An interesting observation can be made in figure 4.32, where the data region is confined to bottleneck widths up to 100 cm. There seems to be some deviation from linearity: The specific flux (the slope in figure 4.32) appears to be smaller for bottleneck widths of 60 cm and below than for larger widths. This will now be examined in more detail. Further discussion of the flux itself will be made in section 4.4.3, where it is compared to the results of other experiments.

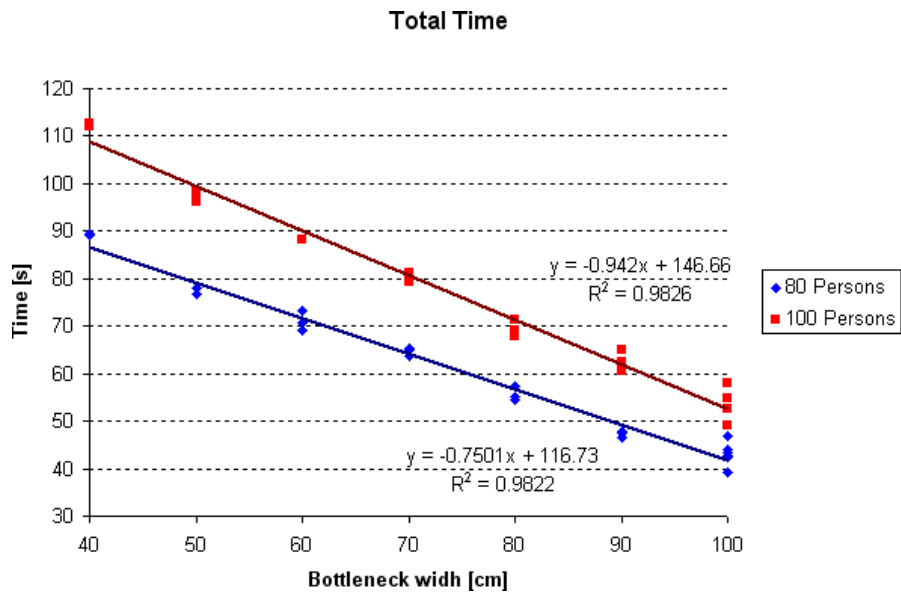


Figure 4.30: Total times for bottleneck widths between 40 and 100 cm.

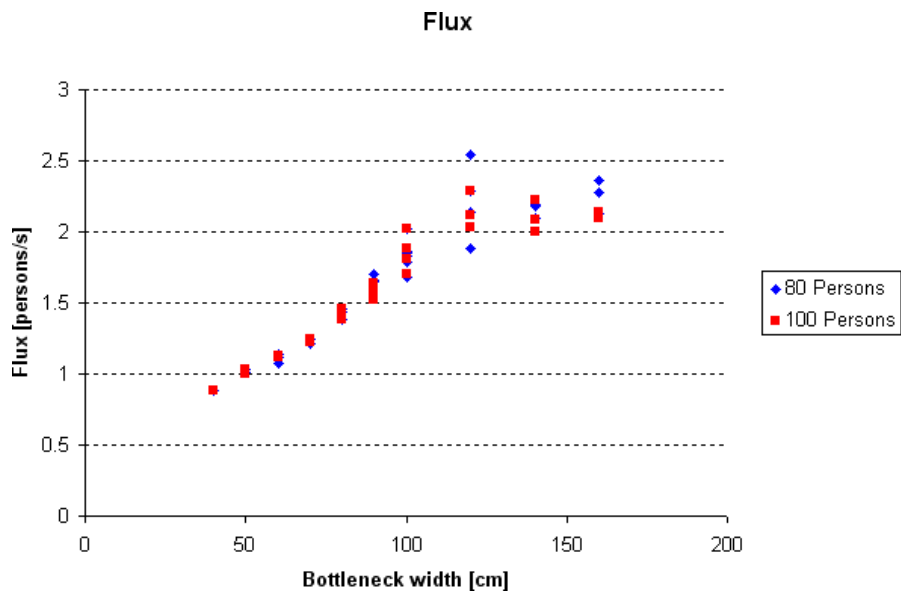


Figure 4.31: Fluxes for all runs.

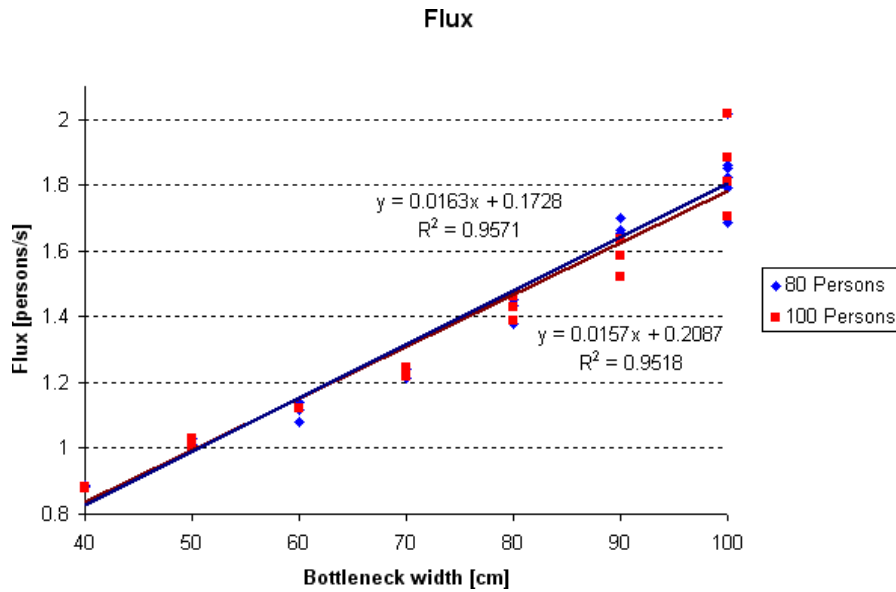


Figure 4.32: Fluxes for bottleneck widths between 40 and 100 cm.

Specific Fluxes

The diagram of specific fluxes (figure 4.33) shows a decrease until a width of 70 cm. It follows a plateau (see figure 4.35) or maybe even an small increase (see figures 4.33 and 4.34). A non-monotonic evolution is something one would not expect. Reasons for this could hardly be found. Furthermore one probably would rather trust a diagram showing the averages (plateau) than one with a large dispersion of results (showing what could be interpreted as small increase). So it seems more probable that it is a plateau with fluctuations unveiling a minimum by chance. Why in spite of this it might be that there is an unincisive minimum is discussed in subsection 4.4.2.

For small bottleneck widths of 60 cm and below the specific flux increases since the participants actively increase their width usage efficiency by rotating their body to the side. The reduction in the specific flux above 100 cm on the contrary surely is caused by the tailback, but maybe also by the participants not actively taking care of efficient motion, as the task of walking through a wide “bottleneck” may appear to be too simple to exert.

Bottleneck Width 70 cm

While for all other widths it appeared that the participants did not need to communicate before passage, hesitation caused by communication appeared a number of times at a width of 70 cm, as is shown in figure 4.37. This specialty of a width of 70 cm was already noticed by several people enlisted in the organization of the experiment and later confirmed from the video footage. The reason for this is, that at a width of 80 cm

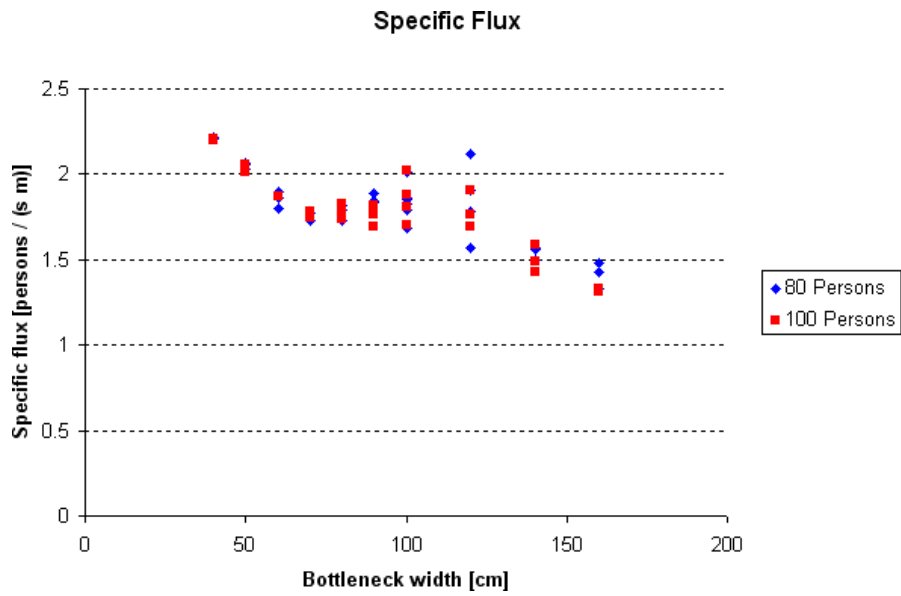


Figure 4.33: Specific fluxes for all runs.

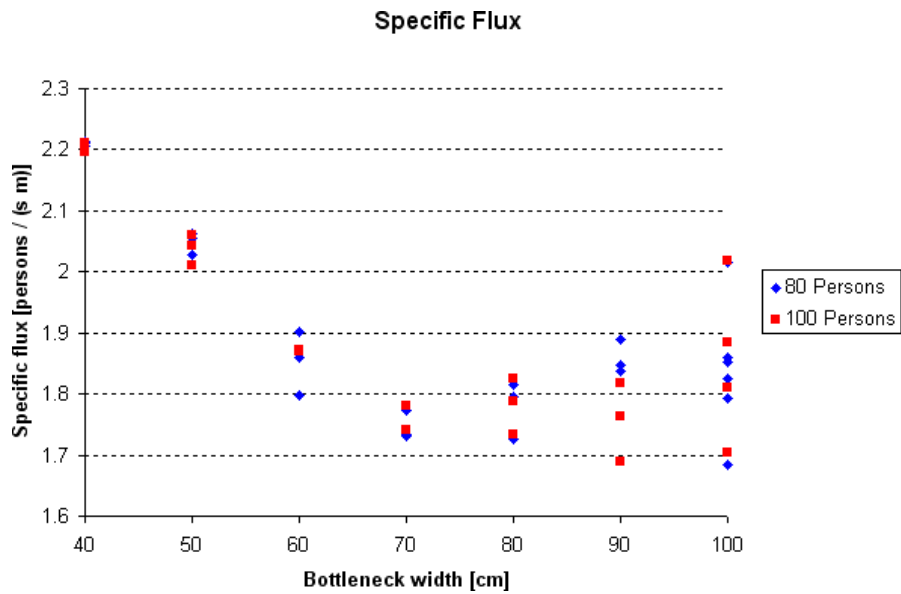


Figure 4.34: Specific fluxes for bottleneck widths between 40 and 100 cm.

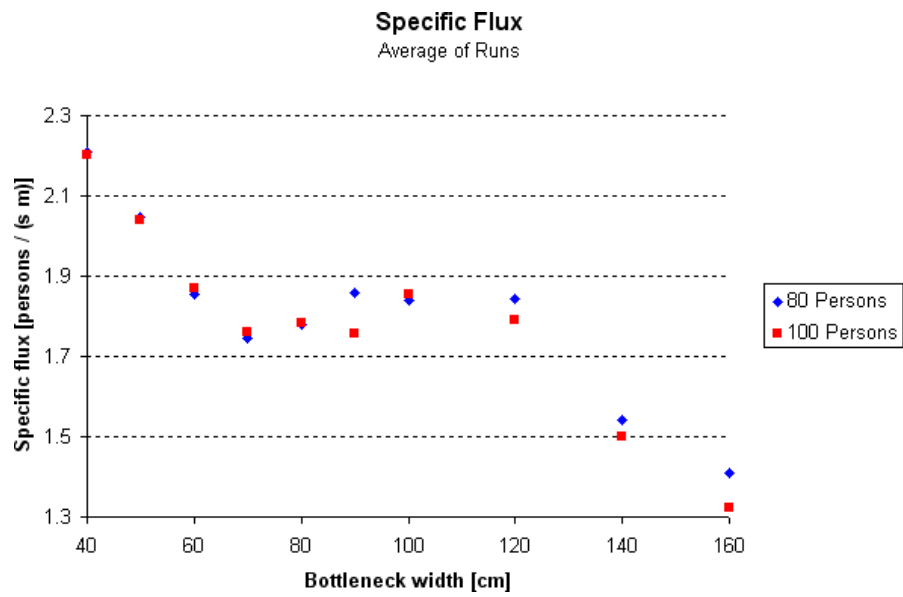


Figure 4.35: Average of specific fluxes.

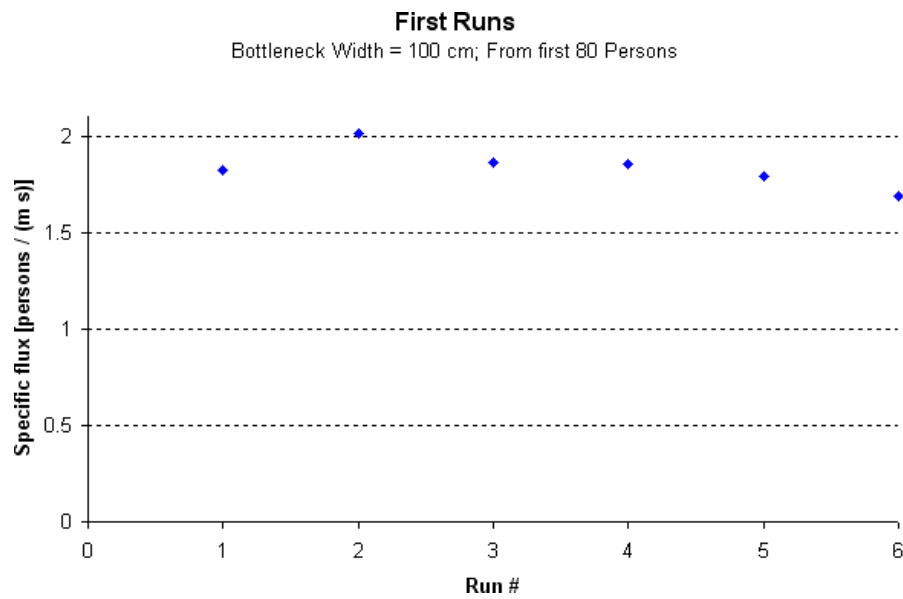


Figure 4.36: Specific fluxes (from the “80 persons data”) for the six runs with a bottleneck width of 100 cm in the chronological order of the runs.



Figure 4.37: Two participants dawdling in front of a 70 cm bottleneck.

the participants, while walking, displaced in a zipper-principle-like way: One participant rather on the left side, then one rather on the right side and again one rather to the left. For widths of 90 cm or above two or more participants were able to pass at the same time, sometimes, however, this was even possible at 80 cm. For widths smaller than 60 cm typically only one participant at a time passed. The transgression from two-at-once over zipper-principle to one-by-one at a width of 70 cm then caused those difficulties, as this appears to be the only width, where it is not obvious that typically only one person at a time can pass. So the reason for delay is not the time needed for communicate about earlier passage. If this was the case, the specific flux should be reduced for smaller bottlenecks even more. The true reason is the late awareness that communication is necessary and the communication therefore falls into a time when passing would already be possible, leading to a dawdling phenomenon.

It is interesting to compare this phenomenon to the results of [108]. There the evacuation time for competitive behavior quite sharply decreases between 70 and 80 cm and the evacuation time for non-competitive behavior increases slightly between 60 and 70 cm door width. One would have to compare the recordings to tell whether these two effects can be related to the need of communication about earlier passage. But in principle one could interpret this in the following way: If there is the need to communicate about earlier passage, the participants do so in the non-competitive scenario, which leads to dawdling effects. In the competitive scenario, however, they do not. This leads to some friction-like phenomenon which compensates or even overcompensates the in-

creased speed which follows from the higher motivation. As soon as there is no more need for communication the higher motivation in the competitive scenario can fully unfold and leads to smaller evacuation times than in the non-competitive scenario.

Distribution of Time Gaps

The distribution of time gaps (figures 4.38 and 4.39) outlines what has already been described in the last subsection. Where the process was a strict one-by-one sequence, the distribution looks rather symmetrical with a more or less distinct maximum at the center. The larger the width becomes, the flatter gets the distribution. It extends more to smaller time gaps, as passing the bottleneck side by side - in principle with a time gap of zero seconds - becomes possible.

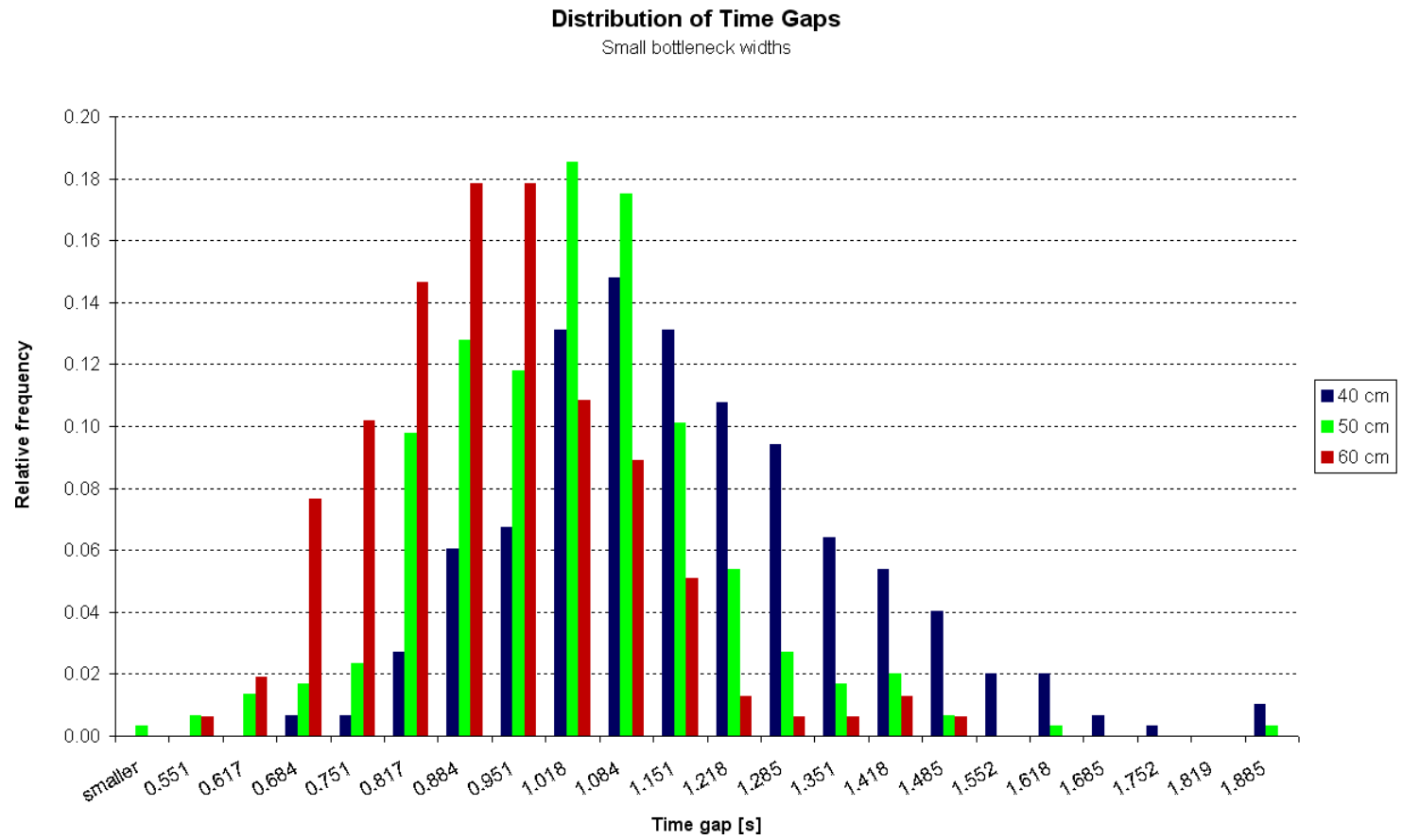


Figure 4.38: Distribution of time gaps: small bottleneck widths. The partitioning of the time gap categories is done such that each category contains two frames.

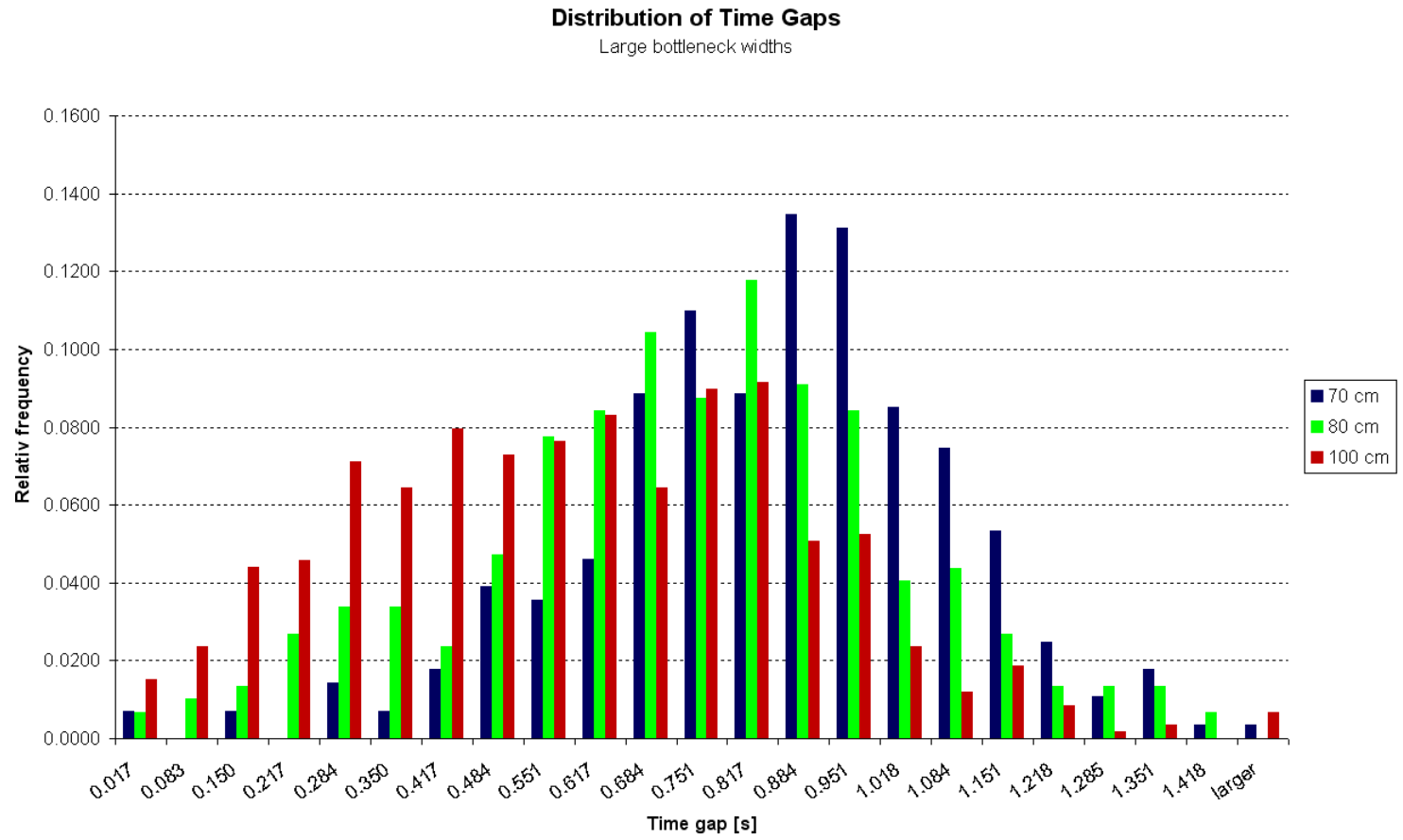


Figure 4.39: Distribution of time gaps: large bottleneck widths. The partitioning of the time gap categories is done such that each category contains two frames.

Apart from this observations, the averages, standard deviations, skewnesses and kurtoses of the time gaps can be found in table 4.8.

Bottleneck width	Average	Standard deviation	Skewness	Kurtosis
40 cm	1.14 s	0.21 s	0.59	0.59
50 cm	0.98 s	0.18 s	0.35	2.63
60 cm	0.87 s	0.18 s	-0.28	4.33
70 cm	0.82 s	0.25 s	0.11	2.33
80 cm	0.70 s	0.27 s	-0.14	-0.06
100 cm	0.56 s	0.30 s	0.70	2.86
120 cm	0.47 s	0.26 s	0.37	-0.06

Table 4.8: Averages, standard deviations, skewnesses, and kurtoses (defined such that the kurtosis of the normal distribution equals zero) of the time gaps.

The numbers of table 4.8 exhibit...

- ... as expected an anti-proportional dependence of the average time gap of the bottleneck width.
- ... in parallel to the development of the specific flux a considerable variation of the product (*bottleneckwidth*) · (*averagetimegap*) over the different widths (0.46 ms for 40 cm and 0.57 ms for 70 cm).
- ... an agreement of the average with the regression parameter *c* (compare table 4.7) that is better for small widths.
- ... standard deviations that become larger as soon as the zipper-principle applies. The reason for the standard deviation at 40 cm being larger than the ones of 50 and 60 cm might be, that for 40 cm the body size plays an important role in the effort of passing the bottleneck.
- ... mostly positive skewness which means - compared to the normal distribution - many small (normal behavior) and a few large time gaps (dawdling).
- ... mostly positive kurtoses which means a sharper maximum than in the normal distribution. The exception at 80 cm might be a reflection of the second peak visible in figure 4.39, indicating the two modes: two people side by side or one person walking in the middle, claiming the bottleneck alone. If one takes the values for 120 cm for granted, the kurtoses exhibit minima each 40 cm (at 40, 80 and 120 cm). One can suspect, that a small kurtosis exhibits a “perfect fit” of a certain number of lanes into the bottleneck. However, this needs confirmation from other experiments.

4.4.3 Comparison to Similar Studies

There is a number of studies which are related in some point or another to this one. These studies exceed what is reported in the following, yet the focus is on those parts

that are comparable to this experiment. In [157] the results of an evacuation exercise of a classroom are reported. The door in that experiment had a width of 50 cm. The maximal efflux was found to be as large as approximately 2 persons per second. In the present experiment at a width of 50 cm an average flux of almost exactly 1 person per second (compare figure 4.31) was measured and only one single time gap (compare figure 4.38) was smaller than 0.5 seconds. This implies that the flux observed in [157] as stable flux over a few seconds appeared only as an extreme value in the present experiment. This factor of 2 can be explained in its tendency, yet it might still appear surprisingly large: If the students were very young and far from being full-grown (as the focus is on the comparison with simulation results, neither the age nor the grade of the participants are stated) they would have used the available width even more efficiently than the students in the present experiment. The second reason might be that the depth of the door might have been noticeably smaller than 40 cm, allowing the pupils to wind around the bottleneck borders more efficiently than the students of the present study.

This is a suiting keyword to proceed to a comparison with [143]. In that experiment the flow through a bottleneck with a depth of 5 meter and different widths (1 and 2 meter) was measured. From the measurements it was concluded, that the flux is a step function with respect to the bottleneck width. This is something that could not be observed in the present experiment (compare figure 4.31). This is probably not due to the small overlap of widths (0.4 to 1.2 meter compared to 1.0 to 2.0 meter there) but either to the largely different depth (0.4 meter here compared to 5.0 meter there) or the conclusion of a step-function is not justified. The probability that the steps are obscured by the steps in which the bottleneck width was increased in the present experiment can be assumed to be very small. Aside from that for a bottleneck width of 1 meter a flux of 1.774 persons per second is reported. This is the result from a model calculation that is assumed to be in agreement with the measurement. Compared to the 1.33 persons/(m s) of [74] or the 4 persons/(m s) of [157] this result is quite close to the 1.85 (resp. 1.89) persons per second (compare figure 4.35 of the present work. The difference can maybe be understood as stemming from the participants, who are representative for the population in the experiment of [143].

The study most similar to the present one is probably [152] (participants: students, normal behavior), where between 20 and 60 participants walked through a bottleneck with a depth of 2.8 meter and widths between 0.8 and 1.2 meter. Aside the depth, differences to the present experiment include that the borders of the bottleneck could be overlooked by all participants and that the participants closest to the bottleneck started 3 meter ahead of it. Thus there may have been some kind of sorting (faster ones reach the bottleneck earlier) and maybe even some kind of “confusion” as the participants form the queue immediately in front of the bottleneck. In any case is this difference in the initial condition most probably the reason for the difference in the distinctness of the starting phase. With λ having the same meaning as the b from subsection 4.4.2, for the time gaps the difference with $0.16 < \lambda < 1.00$ compared to $0.01 < |b| < 0.20$ becomes evident. Concerning the flux there is quite a good agreement between both experiments. Especially if one considers the difference from the two ways to calculate the flux that is exhibited in [152]. There seems to be a tendency that for small widths the flux in the

present experiment is larger, while for larger widths it is larger in [152]. An explanation might be, that for a short bottleneck the participants have more possibilities to increase their performance in the case of narrow bottlenecks.

In another study [153] (participants: students, normal behavior) a significant dependence of the average flux from the initial density was found. The maximum efflux was measured for an initial density of 5 persons per square meter: approximately 3.3 persons per second for a width of 120 cm and approximately 1.7 persons per second for a width of 40 cm, which in the latter cases is almost twice as large as the result of the present experiment, but - in terms of the specific flux - not as large as the flux in [160] (see below for details) when a column is part of the scenario. It is particularly interesting, that the specific flux (4.25 p./ (m s) for 40 cm and 2.75 p./ (m s) for 120 cm) is larger for the smaller width, which is in agreement with the present experiment, however the relative difference is even larger in the experiment of [153] than in the present one.

As is stated in the introduction, the participants were remembered in the beginning, that the experiment is not a competition. Consequently, the experiment didn't exhibit any competitive characteristics. Creating [161] a situation that is competitive in some respect, however, is necessary to evoke maladaptive behavior in the sense, that the density in front of the bottleneck rises to values where the flow through the bottleneck is reduced [109, 162] significantly. Therefore, the present experiment neither examined this regime, nor does it make any claim about the probability and requirements for a bottleneck situation going "sub-optimal". However, contrary to the claim that panic-like situations reduce the efflux, the results of an experiment [160], where the participants were told to "force their way through the bottleneck as fast as possible" exhibit considerably smaller average time gaps than the present experiment (compare table 2 of [160] with table 4.8). The smallest average time gap (door width 82 cm) was found to be as small as 0.275 s, which is only a fraction of 0.39 of the overall average of 0.70 s for a width of 80 cm of the present experiment and it implies a specific flux as large as 4.43 persons per meter and second. For the panic experiments 1-6 (without obstacle) of [160] the absolute values of the standard deviations - rather than the relative ones - of the time gaps are comparable to the one stated in table 4.8.

4.4.4 Summary and Conclusions

Due to the participants being mostly in their twenties, comparatively large fluxes could be observed in this bottleneck experiment. To be precise: all specific fluxes were found to be larger than 1.33 persons/ (m s) , which is a value given in [74], comparable to those of [143, 152], but smaller than those found in [153, 157, 160]. If one takes all of the results together, one finds, that the specific flux seems to increase both with the motivation as well as the initial density. This might be in contradiction with [109] and the simulations of [162], where a reduction of the flux for large densities and/or over-motivation (panic) is reported. This contradiction could be resolved by assuming, that neither the initial density in [153] nor the participants' motivation in [160] were large enough to reduce the flux. Another possibility would be that arching and clogging exist for large initial densities and strong motivation, but they do not overcompensate the

effects of initial density and motivation themselves. This is, what is assumed in [153], where the saturation of the flux at large initial densities is attributed to clogging and not to the maximal capacity of the bottleneck. Third, in principle there could be some maximum which has not been measured yet. Appealing to the participants to go as fast as possible *as group* (i.e. minimize the total time) might help [161] to measure such a maximum, if it really exists.

Sometimes it is claimed explicitly [143], sometimes assumed implicitly [163], that the flux is a step function of the bottleneck width. This is something that is definitely not confirmed for bottlenecks with a smaller depth by the results of this work. While in principle it could be that there is a step function for the flux at deeper bottlenecks and a rather linear function for bottlenecks with depths compared to the one examined here, the agreement of this work with [152] excludes the step function.

The specific flux was found to be not a constant with regard to the width, but to increase with declining bottleneck width for widths smaller 70 cm. This can most probably be imputed to the participants moving more efficiently by turning their body ellipse when passing the bottleneck. This turning of the body ellipse will probably not occur for bottlenecks where the depth is that large that more than one or two lateral steps are necessary to pass the bottleneck.

Only a minor if not even no starting effect could be found insofar as its amplitude is much smaller than the typical variation of measurements.

Concerning model building, especially the combination of insights of the set of experiments discussed in section 4.4.3 impressively demonstrates the richness of phenomena and the number of influences that pose a challenge for any model builder. To mention just one example: the increased efficiency at short bottlenecks demands to consider the body ellipse. If this is implemented, a routine has to be modeled, that lets the agents in a simulation decide if they move toward a short or a deep bottleneck and if they therefore will turn their body ellipse or not.

5 Applications

5.1 Example Study on the Optimization of Egress Routes

This study was carried out at the ATP World Team Cup final at the area of the Rochus-club in Düsseldorf. 27 grandstands are built on the area of the club every year and dismantled again after the event. This, however, does not open possibilities to make fundamental changes in the plan since the area itself sets strong constraints on the construction of the grandstands and the catering infrastructure. Therefore the focus of this study was put on the evacuation plan. The capacity of the grandstands is slightly larger than 10,000 visitors. Additionally there are tickets which only grant access to the area but not to the grandstands. All visitors enter the area through one entrance by which they also leave in normal situations. Additionally, there are seven emergency exits. Without exception opposite to each grandstand exit there are signs pointing to the emergency exit the organizer would want to move the spectators in case of an evacuation. During the matches all grandstand entrances/exits are taken care of by security staff who in a case of emergency would also send the spectators into the desired direction. These measures make it likely that, contrary to the tendency to leave an area by the same exit that was used as entrance, the spectators indeed would move to the planned emergency exits. However, the question remains: Which is the optimal assignment of grandstands to exits (furthermore called “configuration”)? Theoretically, the number of such configurations is immense: In the F.A.S.T.-model one has to decide for each grandstand whether the spectators are allowed to use the exit. As at least one exit has to be allowed the number of configurations is $2^7 - 1 = 127$. Therefore the total number of configurations is $127^{27} \approx 6 \cdot 10^{56}$, which is - for comparison - roughly 100,000 times the number of baryons (protons and neutrons) that form planet earth. This makes it clear that even for this comparatively small scenario a full test of all configurations can never be done and that also a general automated optimization strategy appears to be very difficult to realize. Instead a preselection of configurations guided by human experience has to be done to create a set of configurations which all could be optimal. In further steps the best configurations of the first test can be changed slightly for a finer search of the optimal configuration. Finally the best configurations have to be retested, using different sets of coupling strengths to test the stability of the solution found. For the simulations only spectators on the grandstands were taken into account. Each simulation was repeated 25 times. At first the current de facto assignment of grandstands to exits was extracted from the exit signs (see table 5.1). From the simulation results of this (current) configuration alternative configurations were created and used as basis for further simulations. The evacuation times (see table 5.2) dropped in the simulations with all eight parameter sets. In five of these the difference was larger than both of the



Figure 5.1: Plan of the Rochusclub area with numbers of exits (1-7) and names of grandstands (A-ZF). Higher floors are moved to the right. Black pixels mark free cells, white and dark green walls. Exits are marked light green. Floor exits are drawn cyan and floor entrances magenta.

Grandstand	Current	Optimized
A	4 7	2
B	4 7	2 7
C	7	7
D	6 7	2 7
E	6 7	6 7
F	6	5
G	5 6	5
H	5 6	5
J	5	5
K	5	1 3
L	4 5	2 5
M	4	2
ZA	4	2
ZB	7	2
ZC	7	7
ZD	6 7	7
ZE	6 7	6 7
ZF	6	5 6
ZK	5	1 3
ZL	4 5	2 5
ZM	4	2
ZN	4	2
S	4	2 4
T	4	2 4
U	4	4
V	7	7
W	7	7

Table 5.1: Comparison of Current and Optimized Configuration.

standard deviations. Even clearer is the difference for the average egress times of single

Set of parameters	Current	Optimized
1 ($k_S = 1.0$, others: 0)	1550.0 ± 15.2	1530.7 ± 16.6
2 ($k_S = 5.0$)	1187.8 ± 7.2	1161.0 ± 7.1
3 ($k_W = 0.5$)	1541.2 ± 9.8	1538.2 ± 18.2
4 ($k_D = 0.5$)	1242.8 ± 43.6	1132.2 ± 14.4
5 ($\mu = 0.9$)	1680.7 ± 81.4	1650.2 ± 16.5
6 ($k_I = 0.5$)	1469.9 ± 15.4	1443.2 ± 16.5
7 (3-6 combined)	1317.9 ± 37.8	1261.2 ± 315.7
8 ($k_P = 0.5$)	1460.7 ± 11.5	1448.6 ± 11.6
Average	1431.4	1395.7

Table 5.2: Total evacuation times.

agents shown in table 5.3. This exemplary calculation shows how different configura-

Set of parameters	Current	Optimized
1 ($k_S = 1.0$, others: 0)	661.3 ± 3.2	576.3 ± 2.7
2 ($k_S = 5.0$)	522.0 ± 1.6	440.6 ± 1.0
3 ($k_W = 0.5$)	660.3 ± 3.3	586.7 ± 3.0
4 ($k_D = 0.5$)	504.1 ± 2.4	437.8 ± 1.7
5 ($\mu = 0.9$)	697.1 ± 3.0	608.2 ± 2.7
6 ($k_I = 0.5$)	628.4 ± 2.4	543.2 ± 2.4
7 (3-6 combined)	518.5 ± 2.6	468.1 ± 10.8
8 ($k_P = 0.5$)	623.7 ± 2.0	544.8 ± 1.8
Average	601.9	528.9

Table 5.3: Single egress times.

tions of egress routes can be analyzed by using pedestrian evacuation simulations to find the configuration for the shortest evacuation time. It does however demonstrate another thing: The optimized configuration can hardly be realized using simple exit signs. The spectators of grandstand L who turn into the direction of exit 5 mix up with the spectators of grandstand K. Sending both groups to exits 1 and 3 would be too much, so would be sending both to exit 5. Two exit signs at the branching could lead to unpredictable behavior. The best idea would be to print the way to the emergency exit on each ticket, so one could lead each group to a specified exit. This implies some kind of information campaign to make people realize the plan and study it in advance. The organizers of the tournament agreed to this idea independently of the concrete evacuation plan. Yet the obstacle to the realization of this idea is the online ticket trading. None of the big online ticket services supports this possibility to increase safety. It would have been only a small effort to force them to install the necessary infrastructure (possibility to upload

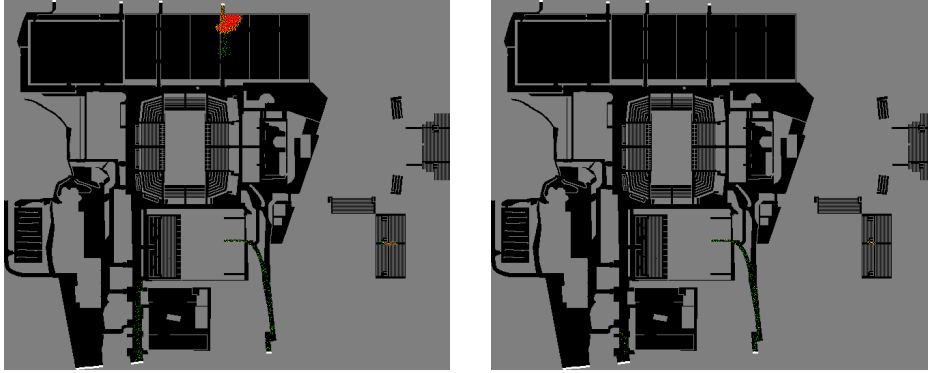


Figure 5.2: Situation after 960 rounds. On the left with the current configuration, on the right with the optimized configuration

the necessary plans) in connection with the soccer world championship in 2006. Yet this chance has been missed.

5.2 Example Study on the Optimization of a Floor Plan

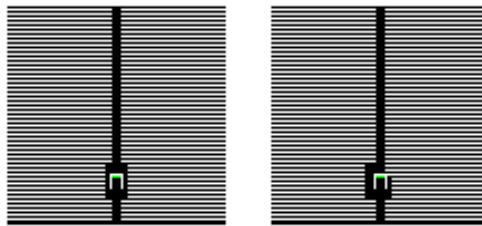


Figure 5.3: Two grandstands. Walkways are colored black

Figure 5.3 shows two grandstands which differ only by the surrounding of the exit. In the left one spectators coming from the higher seats can walk around the exit on both sides, while on the right grandstand there is only one way which however is as wide as the two on the left grandstand together and as wide as the exit itself. Tables 5.4 and 5.5 show that this difference in the construction in the simulation has an influence on the evacuation time.

The reason for this difference is the motion of the agents around the last corner before the exit. At this corner the width of the way is not used efficiently since typically the shortest path around the corner is preferred as shown in figure 5.4. Not only the stability of the difference for different parameters suggests that this is a real effect and not only one of the model, but also the fact that at the tournament of section 5.1 one of the grandstands had two exits of which one had the geometry of the left and one of

Set of parameters	Evacuation time	
	Left type of grandstand	Right type of grandstand
$(k_S = 1.0, \text{others: } 0)$	1199.4 ± 13.6	1447.1 ± 19.1
$(k_S = 1.0, k_W = k_I = 0.5)$	1170.4 ± 14.0	1361.7 ± 19.3
$(k_S = 1.0, k_P = 0.8)$	1173.9 ± 13.3	1309.4 ± 15.4

Table 5.4: Evacuation times.

Set of parameters	Average individual egress time	
	Left type of grandstand	Right type of grandstand
$(k_S = 1.0, \text{others: } 0)$	574.3 ± 6.0	662.7 ± 8.7
$(k_S = 1.0, k_W = k_I = 0.5)$	565.8 ± 5.8	632.5 ± 7.7
$(k_S = 1.0, k_P = 0.8)$	545.0 ± 5.0	587.6 ± 6.0

Table 5.5: Average individual egress times.

the right example. Almost always the queue at the right one existed longer and this was not because more people used it, but - as evaluations of the video footage showed - because the flux through the grandstand exit of the right type was smaller. Whenever there was obviously a queue before the exit, it was measured how long a certain number of people needed to leave the grandstand through the exit. There were seven (left type), respectively six (right type), measurements of which the averages are shown in table 5.6.

Type of average	Flux	
	Left type of grandstand	Right type of grandstand
1)	0.92	0.74
2)	0.94	0.73
3)	0.97	0.74

Table 5.6: Averages of measured fluxes (in persons per second; minimum number of people in a measurement: 10) through two types of grandstand exits. Type of average 1): Sum of people of all measurements divided by sum of times of all measurements; Average type 2); Average of all fluxes, regardless of the number of people; Average type 3): Average of fluxes weighted by number of people.

5.3 Obstacle in a Corridor

The results of the last section lead to a more fundamental question: Where is the best position if an obstacle - like for example a column or a fire extinguisher - needs to be

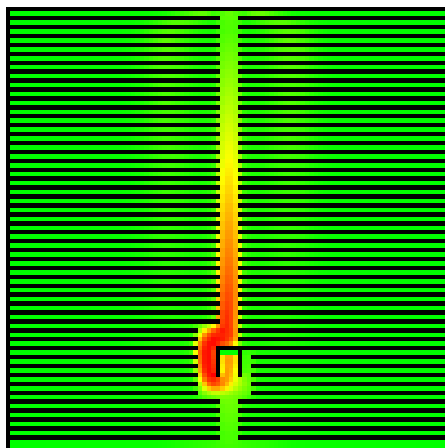


Figure 5.4: Occupancy: The corner in front the exit is not used efficiently.

placed into a corridor? At the edge or in the middle? Intuitively one would guess at the edge as one typically chooses to walk in the middle of a corridor if there are not many other people around. An obstacle in the middle then often is perceived as “standing in the way”.



Figure 5.5: A free corridor, four configurations of a corridor with an obstacle and a corridor which is narrowed on the full length.

Scenario: 300 agents with $v_{max} = 3$ move through a corridor with a width of ten cells. An obstacle with a width of four cells and a depth of one cell is placed into the corridor at different positions. (See figure 5.5). The results (see table 5.7) show that the possibility to pass an obstacle on both sides leads to a more efficient flow. This is in agreement with the results of the last section even if the grandstand scenario includes a turnaround which is not part of this scenario. For smaller obstacles the effect also becomes smaller but is present even for one-cell-obstacles.

5.4 Example Study on Organizational Optimization Potential

For the stadium shown in figure 5.4 the question was raised: “What would be the benefit, if the spectators distributed equally on two available exits instead of only using the one closest to the grandstands?”. The results as shown in table 5.8 at first might

Configuration	Evacuation time
Free	131.8 ± 1.9
Obstacle at edge	148.8 ± 2.5
One cell between obstacle and edge	144.8 ± 2.3
Two cells between obstacle and edge	140.4 ± 2.2
Central obstacle	140.1 ± 2.2
Free, width only six cells	179.5 ± 2.1

Table 5.7: Results

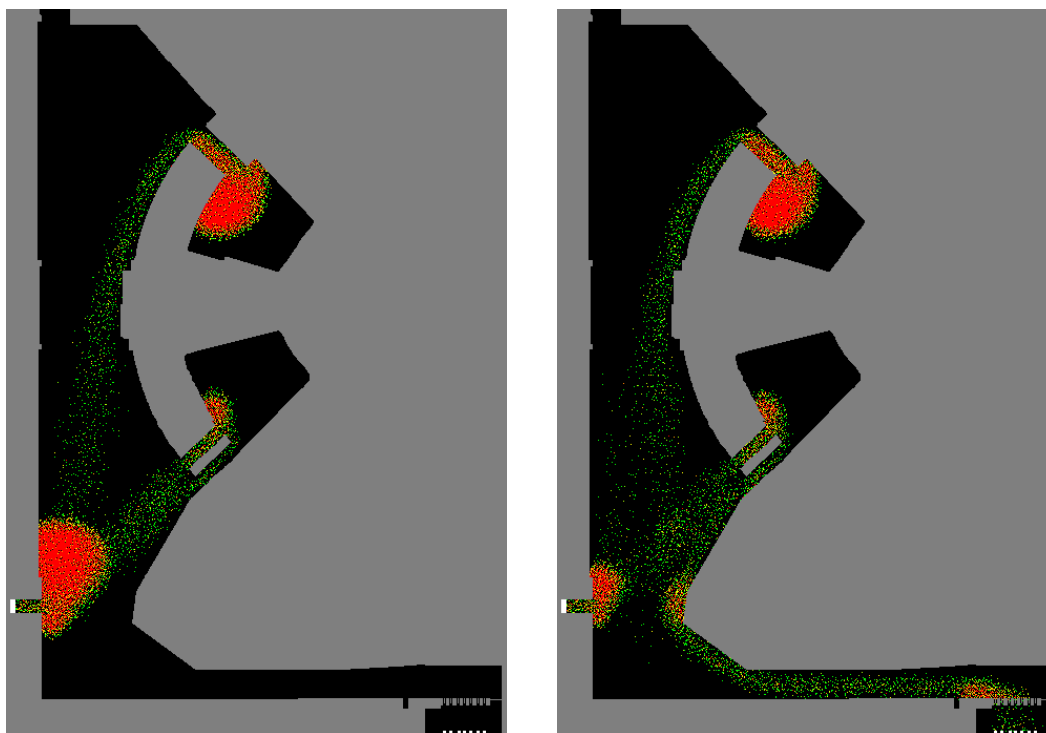


Figure 5.6: Outer area of a large stadium. 12.145 spectators leave the grandstands by two corridors. They then can choose to leave the whole area by one of two exits: on the lower left and on the bottom right corner. Both images are snapshots from ten minutes after the beginning of the evacuation process. In the left simulation all agents were sent to the left exit, which is closer to all of the agents' starting positions within on the grandstands. In the right simulation the agents distributed equally on the two exits, increasing the average path length but also the used capacity. Note: The interior of the stadium was explicitly not subject to the study and intentionally kept as simple as possible.

be surprising insofar as the average evacuation time is smaller if all agents leave by the same exit. The reason for this is that there is a share of agents with $v_{max} = 1$ who arrive at any exit only after all jams already have dissolved. If a few of these choose to take the exit on the right, then their path is longer and thus their travel time. As the evacuation time is the largest individual egress time this leads to an increase of the evacuation time compared to the situation when all agents choose to take one and the same (closest) exit. From this one has to conclude that the average individual egress time is the far

Observable	Using only left exit	Using both exits
Average evacuation time	2347.7 ± 7.3 rounds	2634.2 ± 50.3
Average individual egress time	1214.0 ± 2.5 rounds	812.7 ± 3.8

Table 5.8: Results of 100 simulation runs (each).

more important measurement. And here an optimization by approximately 33% or 401 seconds can be achieved. For all agents this sums up to a total of more than 56 days of saved time.

Some details: The exit choice behavior of the agents was entirely governed by the parameter k_E , the other parameters were in both cases $k_S = 1.0$, $k_D = 0.2$, $k_I = k_W = 0.4$, $v_{av}^{max} = 3.0125$, $v_{STD}^{max} = 0.80625$, $v_{min}^{max} = 1$, and $v_{max}^{max} = 5$. The computation time was between three and six minutes per simulation run equalling at least a sixfold realtime speed.

5.5 Example Study with Inclusion of Combustion Product Data

5.5.1 A Cabin Fire

Evacuation during a fire in a passenger cabin was simulated with 15,000 simulation runs. The production and spreading of the combustion products (CO_2 , CO , heat, smoke density) was calculated [164] using MRFC [119]. This data was used in evacuation simulations. The passengers all started in their cabins (see figure 5.7) and reacted to the alarm with a reaction time between 420 and 780 seconds (IMO night case). It should be noted that although these reaction times are prescribed by the IMO and may be realistic for night cases, the smoke detectors probably will react to the smoldering fire before the flash over and thus give the passengers more time for evacuation, which would allow to reduce the reaction times in the simulation. The problem is to determine the duration of the smoldering fire. Therefore the worst-case was assumed, that the alarm sounds at the time of the flash over.

It should be noted that the agents did not move at all before their reaction time was over. Therefore no one could move into a smoke-filled area in advance of the evacuation process. The fire and smoke simulation was done for seven different fire sectors, which included the burning cabin itself and six corridors (see figure 5.8). The conditions on

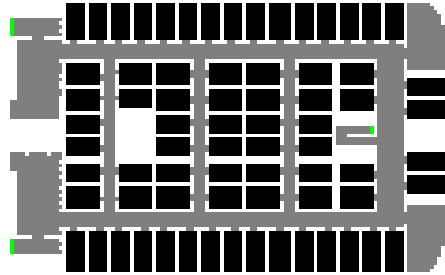


Figure 5.7: The passengers initially were spread randomly over the black area (cabin). The gray area marks free cells, which are not allowed as starting positions.

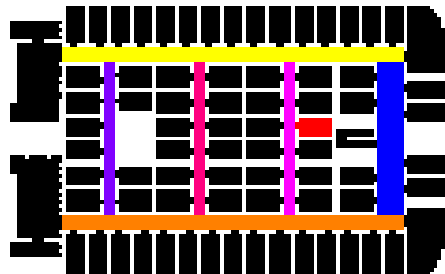


Figure 5.8: Each color marks a different fire sector. Black areas are assumed to be free of combustion products. The burning cabin is marked red.

all cells within a fire sector are identical. It showed up that conditions within the burning cabin become unsurvivable only few seconds after the flash over (see figure 5.9). Therefore whoever had not left the cabin at that point became incapacitated.

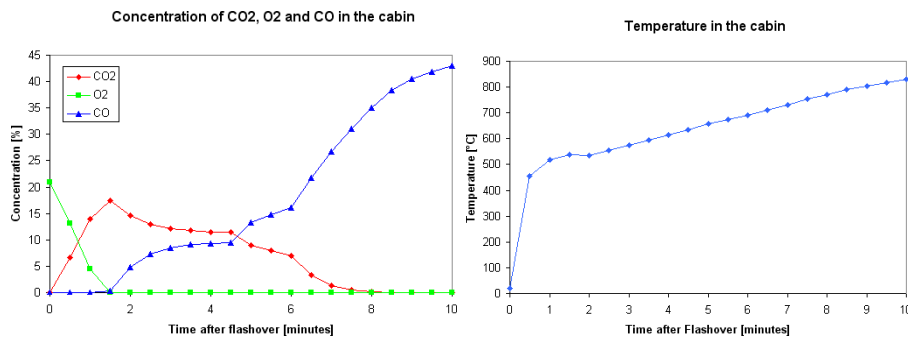


Figure 5.9: The conditions in the burning cabin do not allow survival shortly after the flash over. Based on data by [164].

The conditions on the corridors however were moderate (due to fire sprinklers and the air conditioning system), such that no one suffered incapacity in a corridor. Therefore there was only one moment (after 22 seconds) and one place (the burning cabin) when incapacitation occurred, which led to figure 5.10.

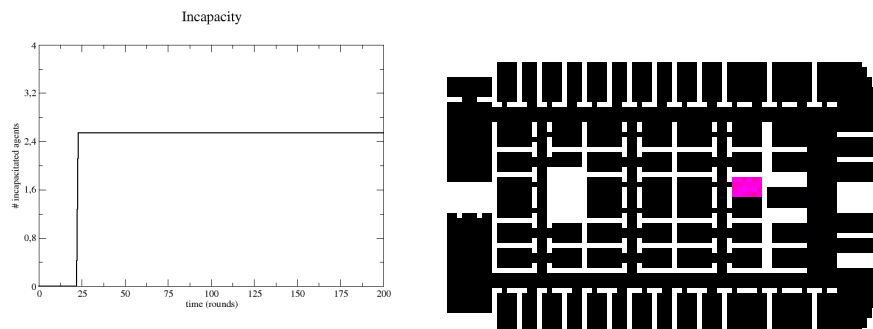


Figure 5.10: Incapacitation only occurred 22 seconds after the flash over and only in the burning cabin.

Cabin Occupation: the Worst Case

One would at first assume that the worst case is that the burning cabin is inhabited by the maximum of four passengers. However, since due to the idealizations of the different models as well as the kind of fire there are such sharp temporal and spatial transitions between possible and impossible self-rescue, one can show that this is not

necessarily the case. One only needs to assume a heterogeneous distribution of reaction times and cooperation: The first passenger to wake up is assumed to waken up all of his roommates. The additional time needed for this process is neglected and therefore it is assumed that all passengers of the burning cabin will survive if only one of them reacts timely. Let p be the probability that a passenger reacts timely and let n be the number of passengers in a cabin. Then the probability that none of them reacts timely is $(1-p)^n$ and the expectation value of incapacitated passengers is $n(1-p)^n$, which implies that n passengers in the cabin is the worst case, if $(n+1)^{-1} \leq p \leq n^{-1}$. For a maximal cabin occupation n_{max} the best case is $n = 1$ for $p \leq 1 - n_{max}^{(n_{max}-1)}$ and $n = n_{max}$ otherwise. See also figure 5.11.

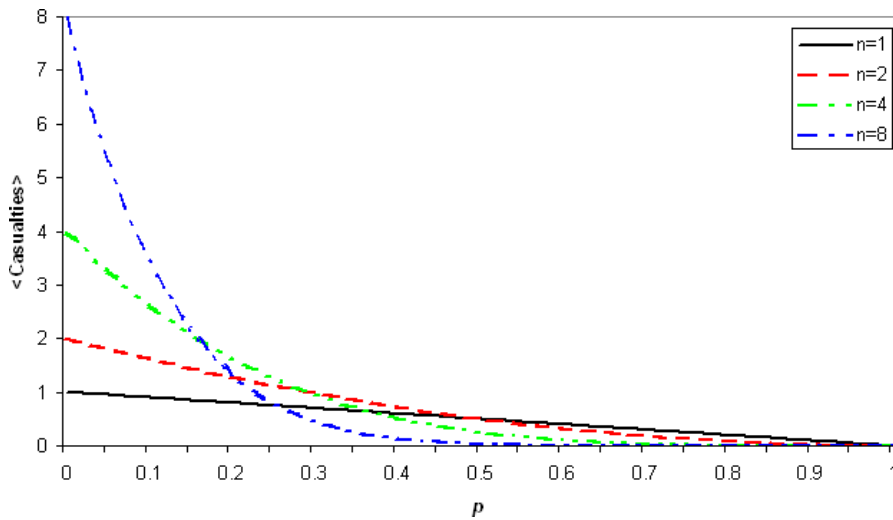


Figure 5.11: Expectation values for the number of incapacitated persons in dependence of the awakening probability p for different cabin occupation numbers n .

6 Outlook

6.1 Concerning the F.A.S.T.-Model

One of the main issues that will have to be dealt with is a more effective *lane-formation* and linked with that a higher flux in counterflow situations. There are a variety of possibilities that might serve to achieve this aim. Lane-formation at $v_{max} = 1$ in a rectangular corridor with an a priori classification of the agents into two species (depending on their constant main walking direction) has already been demonstrated in [28]. So a generalization of those methods for higher speeds and more complex geometries would be a natural attempt. In more details lane-formation might be achieved by integrating an explicit “follow-the-leader” mechanism. This would supplement the dynamic floor field. The difference, however, is that the dynamic floor field leads to an influence of an individual by a more or less large group, while in a “follow-the-leader” mechanism an influence of one individual on another would be present.

For the dynamic floor field itself one also could think of a bunch of variants, which were not investigated in this work. What for example would be the effect, if the dynamic floor field were not only influenced at the original cell, but also on all intermediate cells between original and destination cell? How would diffusion to more remote cells influence the results?

Another extension of the F.A.S.T.-model, that might also play a role in counterflow situations, but which is of more general interest, would be a more detailed *inter-agent repulsion*. An extension of the influence of “just being there” of an agent to a larger neighborhood might open a continuous path to a de facto finer space-discretization without giving up the advantages of an agent occupying only one cell at a time and without having to deal with the conceptual problems a finer space-discretization brings [90]. Another possibility would be to make such “*co-moving potentials*” or even “*precursory potentials*” dependent on the direction of motion. In the direction of motion the repulsion could be stronger (“bow wave”), while in the back of an agent it could even have an attractive effect (“stern wave” or “slip stream”), which would mean something like an implicit follow-the-leader mechanism that would neither be purely a one-one interaction nor an effect of large groups, but would be an effect of the few agents in the more or less direct neighborhood of an agent. Another idea would be, to consider the body ellipse and social distances [64, 165–167].

Similar to inter-agent repulsion, a more detailed elaboration of the *exit choice algorithm* would surely be possible. To mention just a few possibilities:

- The static floor field of an exit could be given an initial height, making it more or less attractive than the mere distance to an agent suggests.

- Not only the distance to an agent but also the width of an exit could influence the attractiveness an exit has on an agent, since a narrow exit might make an agent suspect a jam to exist in front of the exit.
- Being forced to move significantly slower than with v_{max} might make it more likely for an agent to choose another exit in the next round.
- The same might hold for being surrounded by a higher density of other agents.

The process of choosing an exit, however, has nothing to do with the elementary dynamics of the system. Therefore it lies a bit outside the scope of physics. Nevertheless is a realistic model of the exit choice process necessary for realistic simulations.

The discrepancy in figures 3.41 and 3.42 between the simulation and empirical data for high densities will surely be subject to theoretical as well as empirical future research.

Especially the investigation of the *oscillations at bottlenecks* in subsection 3.2.10 shows that sometimes realistic results can only be achieved with parameters that otherwise would only be used for somewhat extreme situations. Allowing an influence of the local environment on the parameters appears to be essential to guarantee realistic detailed results in arbitrary situations and scenarios. It might be a challenge to create an algorithm, that does not slow down the simulation too much and that, for example, automatically reduces k_S for an agent that encloses on a bottleneck, and that intends to pass it, while k_S for an agent who is at the same position, but does not intend to pass the bottleneck remains unchanged. A straight forward matter of implementation would be parameter-changing-fields that the user defines. However an exclusively spatial character of such fields would not distinguish between an agent who intends to move through a bottleneck and one who doesn't.

In subsection B.1 some recent progress in the research of emotion and especially fear contagion is mentioned. Up to now, it appears, that only the influence on the brain activity when the behavior of other people is observed is examined systematically. Little seems to be known on the influence on the behavior itself. Nevertheless might brain science and psychology produce results in the future that could be implemented into evacuation simulations. For the F.A.S.T.-model this might result in an algorithm for the evolution of the friction parameter μ instead of a static μ which is identical for all agents.

Something that is more interesting from an applicant's than from a scientist's point of view is the inclusion of special structural elements like elevators, escalators or different kind of doors including revolving doors into the F.A.S.T.. The elements, that have already been included can be worked out in more details as well. The interrelation of stairs and walls can serve as an example. While on level walking nearby walls is avoided, handrails typically provoke walking close to walls on stairs.

6.2 Concerning Experiments and Observations

With respect to stairways, an interesting observable to measure would be the distribution of break frequencies on long stairs. The number of stairs people are freely willing to move

without pausing and the time taken to pause could be a valuable hint for a maximum length of stairs that would pose no problems during evacuations. Furthermore would it be interesting to measure a) a full fundamental diagram for a given length of a stairway and b) the dependence of the walking speed on the length of the stairway by actually measuring walking speeds on stairways of different length. Additionally - in parallel to motion on a level - one could ask for the dependence of the speed or flux on the width of the stairway i.e. the specific flux.

The huge amount of influences on the outcome of a pedestrian experiment or an observation makes a large number of identical or similar experiments desirable. Only in this manner will it be possible to really identify the influences of age, temperature, time of day or other influences on basic parameters like the free speed as well as more elusive factors like a tendency toward aggression or cooperation.

For the experiments presented in this work a repetition with elderly participants and/or a more heterogeneous group is probably the first thing one can think of. How would the results change if the people carried luggage?

For the counterflow experiment a variation of the corridor width would not only be interesting in terms of the possible flux, but also answer the question how many lanes appear (at maximum, on average etc.) at what widths. Furthermore would it be interesting to conduct such an experiment with cyclic boundary conditions and constant global density on a ring area. More data on the left-right-asymmetry and a comparison to left-hand-traffic countries might attract interest also from outside the pedestrian researchers' community.

A variable of interest in the bottleneck experiment is the depth of the bottleneck. Increasing it above the 40 cm of the experiment presented in this work, would lead toward a into-and-through-a-corridor experiment, while reducing the depth comes closer to typical door depths.

Measuring the maximal possible flux in a bottleneck might be achieved by dividing the participants into to equally sized groups and differentiate the reward for participation with respect to which group as a whole was able to move faster through the bottleneck.

A Historical Overview of Crowd Disasters

It is always difficult to present facts of fatal events in tabulated form, summing up fatalities in plain numbers. However the purpose of the following table is not to induce panic or overemphasize dangers, but to list events of the past as a starting point for anyone who wants to learn from the past to prevent tragedies in the future. A risk analysis should be part of any preparation for an event including large crowds. However the possible events which can lead to catastrophic results are so numerous that it appears impossible to take each of them into consideration. Yet for ethical, pragmatic and public relations reasons each organizer can and should take past events as systematic starting points for his considerations on security issues to at least prevent a replay of catastrophes. The following list only contains events where the dynamic of the crowd was an important amplifying factor to the disaster or even the triggering factor itself without external danger. Although there are some printed compilations [106], most sources - especially compilations - can be found in the internet [168–172]. However those lists seem to include accidents where the dynamics of the crowd was not very important. Events where this appeared to be the case were not taken into the list below. Other sources were the homepages of newspapers, news magazines and broadcasters. For a quick survey the causes are only given as keywords. For a real understanding of the accident the details are crucial. Note that missing numbers for casualties do not necessarily imply that there were no casualties and that the number of injured can vary from source to source as there are injuries that are that slight that some observers would not even call them injuries.

Table A.1: Historical record of crowd disasters.

WHEN?	WHERE?	WHY?	CASUALTIES
1946 Mar 9th	Stadium in Bolton, England	Wall crushed	33 dead, >400 injured
1955 Mar 30th	Stadium in Santiago de Chile	Crowd dynamics	6 dead
1964 May 24th	Stadium in Lima, Peru	Disallowed goal	318 dead, 500 injured
1968 Jun 23rd	Stadium in Buenos Aires	Fans throwing burning newspapers into crowd	74 dead, 150 injured
1970 Nov 1st	Night club in St. Laurent-du-Pont	Fire, locked emergency exits	142 dead, \approx 40 injured
1971 Jan 2nd	Stadium in Glasgow, Scotland	Crowd dynamics	66 dead, 140 injured
1971 Mar 4th	Stadium in Salvador, Brazil	Fight on grandstand	4 dead, 1500 injured
1973 Apr 12th	Löwenbräukeller, Munich, Germany	Overcrowded venue, crowd dynamics	2 dead, several injured
1974 Feb 17th	Stadium in Cairo	Crowd dynamics	49 dead
1976 Dec 6th	Stadium in Port-au-Prince, Haiti	Firecracker	6 dead
1977 Apr 1st	Volksparkstadion in Hamburg	Hundreds stumbling down the stairs	1 dead
1979 Aug	Stadium in Nigeria	Floodlight failure	24 dead, 27 injured
1979 Sep 16th	Stadium in Medan, Indonesia	Crowd dynamics	12 dead
1979 Dec 3rd	Cincinnati, USA	Crowd dynamics during concert of "The Who"	11 dead
1981 Feb 8th	Stadium in Athens	Locked exit	21 dead
1982 Oct 20th	Stadium in Moscow	Reentering fans after last minute goal	340 dead (officially 77)
1982 Nov 18th	Stadium in Cali, Columbia	Fans urinating on grandstand	24 dead
1985 May 26th	Stadium in Mexico City	Crowd dynamics	10 dead, \approx 50 injured
1985 May 29th	Heysel stadium in Brussels, Belgium	English hooligans attacking other fans	39 dead, some 100 injured
1988 Mar 12th	Stadium in Katmandu, Nepal	Hailstorm, locked exits	93 dead, >100 injured
1989 Apr 15th	Stadium in Sheffield	Police pushing fans into a crowded block	96 dead, >700 injured
1990 Jul 2nd	Mecca	Tunnel crashed	1426 dead
1991 Jan 13th	Stadium in Orkney, South Africa	Crowd dynamics	>40 dead
1991 Jul 15th	Stadium in Nairobi, Kenya	Crowd dynamics	1 dead, 24 injured
1991 Dec 28th	New York	Crowd dynamics before basketball match	9 dead, 29 injured
1993 Jan 1st	Hong Kong	Crowd dynamics in open streets	21 dead
1994 Sep 27th	Baltic Sea, ferry ship Estonia	Technical defects	852 dead
1994 May	Stadium in Monrovia, Liberia	Result of the match	2 dead, 26 injured
1994 May 25th	Mecca	"Stoning the devil" ritual	270 dead
1995 Dec 23rd	School in Sirsa, India	Fire	\approx 400 dead
1996 Apr 11th	Düsseldorf airport	Fire, caused by welding	17 dead

to be continued on next page

Table A.1: Historical record of crowd disasters (continued).

WHEN?	WHERE?	WHY?	CASUALTIES
1996 Jun 16th	Stadium in Lusaka, Zambia	Crowd dynamics	9 dead, 78 injured
1996 Jul 31st	Station near Johannesburg, SA	Security using electric cattle prods	>15 dead
1996 Oct 16th	Stadium in Guatemala city	Overcrowded stadium	80 dead, 180 injured
1997 Jul 28th	Düsseldorf, Germany	Crowd dynamics at concert of “Die Toten Hosen”	1 dead, 60 injured
1997 Apr 15th	Mecca	Fire	343 dead, 1500 injured
1998 Apr 8th	Mecca	“Stoning the devil” ritual	>107 dead, 180 injured
1998 Apr 19th	Stadium in Zimbabwe	Fans trying to enter stadium at a free match	4 dead
1998 Oct 28th	Night club in Goteborg, Sweden	Fire, caused by arson	63 dead
1998 Dec 25th	Night club in Lima, Peru	Tear gas attack	9 dead, 7 injured
1999 Jan 11th	Stadium in Alexandria, Egypt	Crowd dynamics	8 dead
1999 Jan 14th	Sabarimala, India	Collapse of the sides of a hillock	53 dead, 100 injured
1999 May 29th	Railway station in Minsk, Belarus	Cloudburst	54 dead, 150 injured
1999 Dec 4th	Mount Isel, Austria	Crowd dynamics, location geometry, rain	5 dead, 5 cases of care of whom one died later
2000 Mar 24th	Night club in Durban, SA	Tear gas attack	13 dead, 44 injured
2000 Apr 16th	Night club in Lisbon, Portugal	Gas grenade induced panic	7 dead, 60 injured
2000 May 26th	Circus in Lahore, Pakistan	Overdrawn usage of force by private security	9 dead, >3 injured
2000 Jul 23rd	Stadium in Monrovia, Liberia	Crowd dynamics	at least 3 dead
2000 Jun 5th	Addis Abbeba, Ethiopia	Rainstorm during memorial ceremony	14 dead
2000 Jul 9th	Stadium in Harare, Zimbabwe	Police using tear gas	12 dead
2000 Jul 30th	Roskilde festival, Denmark	Crowd dynamics during “Pearl Jam” performance	9 dead, 26 injured
2000 Dec 30th	Stadium in Rio de Janeiro, Brazil	Overcrowded stadium	170 injured
2001 Jan 1st	Bar in Volendam	Fire	14 dead
2001 Jan 26th	Sidney, Australia	Crowd dynamics at “Big Day Out” festival	1 dead
2001 Mar 2nd	Station in Johannesburg, SA	Crowd trying to catch a train	7 dead, 9 injured
2001 Mar 5th	Mecca, Saudi-Arabia	“Stoning the devil” ritual	35 dead
2001 Mar 16th	Jakarta, Indonesia	Appearing of pop group “A1”	4 dead
2001 Apr	Pak Patten, Pakistan	Poor organization	36 dead, 150 injured
2001 Apr 11th	Stadium in Johannesburg, SA	Poor organization	43 dead, ≈200 injured
2001 Apr 29th	Stadium in Lubumbashi, Congo	Tear gas, locked exits	14 dead
2001 May 6th	Stadium in Sari, Iran	30000 in a 10000 capacity stadium	2 dead, 300 injured

to be continued on next page

Table A.1: Historical record of crowd disasters (continued).

WHEN?	WHERE?	WHY?	CASUALTIES
2001 May 9th	Stadium in Accra, Ghana	Police using tear gas	126 dead
2001 Jul	Akashi, Japan	Poor organization of a festival	10 dead, 120 injured
2001 Dec 18th	Aracaju, Brazil	Governmental Christmas gift giveaway	4 dead
2001 Dec 21st	Night club in Sofia, Bulgaria	Bad weather outside	7 dead
2002 Mar 11th	School in Mecca	Fire, locked doors	>14 dead, >50 injured
2003 Feb 11th	Mecca, Saudi-Arabia	“Stoning the devil” ritual	14 dead, 20 injured
2003 Feb 17th	Night club in Chicago, USA	Panic after Pepper spray attack	>21 dead
2003 Feb 20th	West Warwick, USA	Fire at “Great White” concert	100 dead, 190 injured
2003 May 14th	Stadium in Cotonou, Benin	Crowd dynamics at pop concert	>15 dead
2003 Aug 27th	Nasik, India	Crowd dynamics	>32 dead
2004 Jan 23rd	Srirangam, India	Fire	>51 dead
2004 Feb 1st	Mecca, Saudi-Arabia	“Stoning the devil” ritual	244 dead, ≈200 injured
2004 Feb 5th	Park in Beijing, China	Crowd dynamics during new year celebrations	37 dead
2004 Mar 13th	Stadium in Kameshli, Syria	Hooligans initiating panic	>5 dead, >100 dead
2004 Apr 12th	Uttar Pradesh, India	Distribution of free Saris	21 dead, 28 injured
2004 Mai 4th	Factory in Dhaka, Bangladesh	Erroneous fire alarm	>6 dead, >26 injured
2004 Sep 1st	Dshiddah, Saudi-Arabia	Giveaways at opening of an IKEA-store	3 dead
2004 Nov 20th	Lome, Togo	Crowd dynamics	>13 dead
2004 Dec 30th	Night club in Buenos Aires, ARG	Firecracker, fire, locked exits	174 dead, 410 injured
2005 Jan 25th	Wai, India	Slippery stairs	>250 dead
2005 Feb 27th	Ouagadougouh, West Africa	Rush for best positions at free film festival	2 dead
2005 Mar 25th	Stadium in Tehran, Iran	Crowd dynamics (without external reason)	5 dead, 40 injured
2005 Apr 6th	Bangladesh	Crowd dynamics	6 dead, several injured
2005 Aug 31st	Baghdad, Iraq	Rumors of suicide bombers in the crowd	1011 dead, 475 injured
2005 Sep 9th	Airplane	Stampede on board of airplane after bomb rumor	1 dead, several injured
2005 Dec 11th	Chennai, India	Heavy rain on a queue of 5000 people	42 dead, 37 injured
2005 Dec 23rd	Ljubljana, Slovenia	Crowd of 500 people pushing for entrance	2 dead
2006 Jan 12th	Mecca, Saudi-Arabia	“Stoning the devil” ritual	≥364 dead, many injured
2006 Feb 4th	Stadium in Manila, Philippines	Crowd misunderstanding closed gates to be open	≥73 dead, >300 injured
2006 Aug 8th	Rock festival in San Diego, USA	Crowd pushing toward stage	15 injured
2006 Sep 11th	Political rally in Taiz, Yemen	Crowd dynamics	≥4 dead, 10 injured

to be continued on next page

Table A.1: Historical record of crowd disasters (continued).

WHEN?	WHERE?	WHY?	CASUALTIES
2006 Sep 12th	Political rally in Ibb, Yemen	Counterflow at exit/entrance	≥ 51 dead, ≥ 238 injured

Commentary on the Events of December 11th 2005 and May 29th 1999: Both tragedies were mainly caused by heavy rain and an existing shelter (roof) that was too small. Both accidents included only a few thousand participants and lead to more than 50 casualties. The lesson that must be learned from this is that open air events must either include enough roofed space for all visitors or none at all. This is especially important as the extra space for rescue forces which is prescribed in Germany by the *Musterversammlungsstättenverordnung* [163] typically includes tents. These might become attractors for the crowd in the case of a cloudburst or hail storm. Surely those tents would not pose a threat as traps as they are flexible but only as attractors for people. The real danger would arise from the crowd itself.

Commentary on the Events of February 4th 2006: The accident in Manila happened when the people tried to enter (not leave) a stadium in Manila to attend a very popular annual TV game show. German newspapers reported someone shouting false warnings of suicide bombers to be the reason for the accident, while Anglo-Saxon media said this was wrong and that the true reason was that the crowd erroneously assumed the stadium doors were open and started to move forward. So there was not the slightest reason to escape from something. Instead the people moved for some gain. “In the desire to win money, she is the one I lost,” a man who lost his wife mourned [173]. Since no information was passed to the people behind about the closed doors in front, each person at the back by slightly moving forward contributed to creating a highly dangerous and finally deadly situation for the people in front. The organizer would have had no chance to prevent this accident from happening only by doing risk analysis of external dangers.

The Manila accident recalls another incident that happened in April 2005 before the kick-off of the Bundesliga soccer match Hertha BSC Berlin vs. FC Schalke 04. The match was postponed since the capacity of the security checks at the south gate of the Olympiastadion in Berlin was not sufficient to let everyone in early enough, yet the delay was not communicated to the waiting visitors in front of the gate and so they started to fear they would miss the first minutes of the match and continued to move forward, some of them getting angry. Compared to the event in Manila the gate was not totally closed, but the flux into the stadium was obviously very small. According to a newspaper report [174] this led to dramatic scenes. Additional research in web forums shows up at least one injured person (broken rib) and several statements like “I was scared about the life of my two kids”.

These two events seem to point one out of many mechanisms that may lead to crowd disasters. In this case a mechanism that may occur during a filling not an evacuation process:

- An event is scheduled to begin at a certain time.
 - Due to some reason the beginning of the event is postponed and with it the whole preparation, especially the filling process.
 - This delay is not communicated to the waiting crowds.
-

- The waiting people, acting as if the event was not postponed, may get nervous. As this is a typical “chance to gain” situation according to appendix B people are less likely to act cooperatively and more likely to act competitively.
- If the crowd is large enough and the back end of the queue does not become aware of the situation at the front end, the situation at the front end might escalate and become critical.

The process can be prevented from disastrous dimensions by a few and simple strategies: The first of course is reaching clear communication of possible delays. An additional technical element would be traffic lights that tell the crowd when not to move forward. These might prove helpful wherever crowds may gather in queues that are that large that it is not possible for any individual to gain an overall view of the whole crowd.

B Competition, Cooperation, Panic, and Altruism

The question which behavior emerges in which situation is on one hand important for the meaning of observations as well as experiments under normal conditions with regard to the case of emergency. First it is obvious that the results of simulations would be of much greater relevance, if one knew that the behavior of crowds changes only gradually, but not qualitatively under a great variety of external conditions, i.e. that competitive and irrational behavior occur only rarely and that cooperative behavior prevails in the majority of situations. Second, having the wrong idea of how other people would react in cases of emergency might trigger suboptimal if not disastrous behavior in an individual. In the worst case public ideas of crowds getting mad during emergencies could be a self-fulfilling prophecy, as they might trigger additional fear. Beside this, the purpose this chapter is to present the results of some literature research that was triggered by some passages in the examination of the stadiums for the soccer world championship 2006 done by the Stiftung Warentest [175] and the public reactions on it. This study attracted very much attention and commentaries of which approximately one half was much fierce criticism. Still, a claim like „Wie im Cowboyfilm, wo aus einer friedlich grasenden Büffelherde urplötzlich eine ziellos flüchtende, alles niedertrampelnde Masse wird, so verhalten sich auch in Panik geratene Menschen. Sie stürmen in der Regel kopflos nach vorn. Wer sich der Bewegungsrichtung zu widersetzen versucht, läuft Gefahr, überrannt und niedergetrampelt zu werden.“ (Engl.: Just like in a western movie, where a calmly grazing herd of buffalo suddenly turns into an aimlessly fleeing mass that tramples down everything which obstructs its path, so do act people in panic. Usually they storm ahead mindlessly. Whoever tries to resist the direction of motion, is in danger to be trampled down.), remained undiscussed and uncontradicted.

This chapter deals with human behavior. So it applies only to crowd situations, where behavior is still possible. If the density in a crowd becomes too large, the possibility to choose among alternatives disappears to a large extend or even completely and behavioral considerations become less important.

B.1 Panic

In the presence of an external danger, there are quite a few ways one could think of, how a crowd could behave:

- Calm, almost as under normal conditions; cooperative (harm no one to get out earlier), if not altruistic (help those who can't help themselves).
-

- Hasty, but orderly; people act similarly to normal conditions just quicker; cooperative, if not altruistic.
- Hasty, not altruistic, but still cooperative and therefore at least to some extent orderly.
- Hasty, non-cooperative, inconsiderately, maybe even a- or anti-social.

The Public Notion of “Panic”

The term “panic” (German „Panik“) is used equally frequently as thoughtlessly by the media and because of the media by the public when it comes to the point of describing or explaining the behavior of people in extreme and disaster situations.

“**Fear**” is an emotion that most or probably all people have experienced at some time in their life. There is a huge number of fear-inducing situations and reasons. Describing someone as being “fearful” does not rate the fearful person as overreacting to the fear-inducing reason. Additionally being “in fear” is often associated with a certain amount of passivity: Someone in fear is often imagined to need help as - due to the fear - he is not or at least less able to act himself against the fear-inducing situation.

“**Panic**” on the other hand surely is viewed as being related to fear. But saying that someone is “panicking” often implies that he overreacts to a reason that might justify some concern but not the kind of reaction the person shows - whatever that may be in a specific situation. Contrary to a fearful person a panicked person typically is imagined as being highly active. The kind of activity of a panicked person is often described as irrational (walking in circles) or selfish and anti-social, at least highly competitive. Everyone in a panicked crowd is believed to care for only one thing: One’s own rescue - presupposed there is enough rationality left.

This public idea of panic is also the basis of the examination of the stadiums for the soccer world championship 2006 done by the Stiftung Warentest [175] . The public reactions to it exhibited the notions described above.

“Panic” in Psychology

In psychology the terms “*panic disorder*” and “*panic attack*” are known as special form of an “*anxiety disorder*” and well defined. There do exist treatments for both phenomena. A closer look shows that the public understanding of the symptoms of “panic” comes quite close to the scientific medical definition of a “panic attack” with the difference that from a medical point of view someone either suffers more or less frequently from panic attacks or he does not. It is possible that someone who did not suffer from panic attacks starts to do so and that also someone can be cured. Therefore in psychology “panic disorder” and “panic attack” are rather viewed as illnesses than as reaction pattern to disastrous situations of all human beings.

From this one can follow that, if there is no general pattern that people panic - in the public meaning of the word - during dangerous situations, irrational and anti-social behavior should occur much less often in extreme situations than it is often assumed. This is supported by the results of many disaster examinations [176–181]. Maybe it is helpful to quote the essence of the phenomenological research of one of these [176]:

Concerning irrational behavior:

“After five decades studying scores of disasters such as floods, earthquakes and tornadoes, one of the strongest findings is that people rarely lose control.”

Concerning cooperation and altruism:

“When danger arises, the rule as in normal situations is for people to help those next to them before they help themselves.”

Concerning “panic”:

“Most survivors who were asked about panic said there was none. Instead there were stories of people helping their spouses, flight attendants helping passengers, and strangers saving each other’s lives.”

Note, that these sentences do neither stem from some theoretical considerations, nor from some ideal world ideology, but from a long experience of investigating incidents.

It is hard to understand, why the results of these empirical panic researchers are ignored so persistently when the behavior in cases of emergency is discussed and why on the other hand researchers, who are well known for their theoretical work, are not only accepted but properly pushed to take a role as authority concerning these empirical issues as well.

Fear and Crowds

Terminology

There are some subtle differences between German and English in the vocabulary that is used to describe panic phenomenons within crowds.

„Stampede” also in German is exclusively used as terminus technicus to describe stampedes of big gregarious animals as buffaloes, elephants or rhinos. In such stampedes the whole herd suddenly begins to run into the same direction, trampling down everything obstructing the way. In English “stampede” is additionally used for incidents where a crowd gets critical and people trample over each other, often with fatal results. While a stampede can be a good defense strategy for really big animals, it is doubtful that it would be for humans. Each individual is just too small to guarantee a stampede by humans the same success as an animal stampede. But if it cannot be successful, it is very unlikely that it has developed as a behavioral pattern during evolution. Therefore in this case the use of the English language is at least imprecise and the existence of the phenomenon doubtful.

„**Massenpanik**“ is the word typically used in German for human crowd disasters. It is quite strictly bound to panic in pedestrian crowds, while the direct English translation “**Mass Panic**” or “**Collective Hysteria**” sometimes is used to refer to other phenomena for example at the stock market as well.

„**Massenpanik**“ - “**Mass**” and “**Panic**”

What is the essence of the word “mass” before “panic”? Is there anything substantially new? To some extent independent from the precise implications of panic for the behavior of the individuals there are three possible implications the “mass” can have:

- Many people that face a dangerous situation together, react in the same way and “panic” individually. In this case there would be no substantially new phenomenon. The special difficulty for rescue forces would simply lie in facing many times the same problem: a “panicked” person.
- Panic (or fear) as phenomenon that is somehow contagious without panicked persons being a threat for surrounding people. If panicked persons act irrational yet not anti-social this case would imply increased danger for individuals in a group as the probability to “panic” of a certain person would be increased.
- Panic (or fear) as contagious phenomenon due to highly competitive and anti-social as well as irrational behavior of panicked persons. In this case the individuals of a group would impose direct physical danger toward each other by their competitive behavior and by that mutually increase their probability to “panic”.

Mirror Neurons and Fear Contagion

The existence of mirror neurons [182] has first been discovered in the brain of monkeys [183] and slightly later also in the brain of humans [184]. Mirror neurons are neurons that are not only active when an individual is actually performing an action, but also when the same individual is observing the same action performed by another individual. Recently there have been observations that watching whole-body expressions of fear induces activity in brain areas that are associated with emotions and not only - as the existence of mirror neurons suggests - in motor areas of the brain [185]. It is known [186] that a healthy human as adult has learned to control activations that have been induced to his motor areas by the actions of other people via his mirror neurons - but only to some extent. So, to what extent watching a fearful person can induce fear in a spectator is a somewhat open question of neuro-biology, but if this is the case in a non-negligible amount, fear and panic could indeed be viewed as gaining a new quality in a group or a “mass”. Beyond that “mass panic” is merely a term of everyday life language and has no background in human social sciences.

Reasons for the widespread Use of the Word “Panic”

In all probability there is a whole bunch of reasons, why the cause for many casualties in disasters is often identified to have been “panic”. At first the popular view of panic as being a general pattern of irrational behavior and therefore a wrong way to act in dangerous situations makes “panic” a scape goat concept to move responsibility for casualties from organizers and authorities to the victims themselves [187]. The second reason is probably the self-energizing interaction of the expectation of the public how people have to act in a dangerous situation and the way (Hollywood) action films present such situations to their spectators. The more dramatic and fearful the actors act, the more emotional is the film. This then ensures a spectator that his ideas of panic are correct and therefore sets expectations for the next disaster movie and so on. The third and especially in German-speaking countries important reason is a misinterpretation of Darwin’s theory of natural selection in the sense of an almost Hobbesian idea of human nature: a “struggle for survival”, a “war of all against all”. In German-speaking countries the situation in this aspect is worsened as “survival of the fittest” is often misinterpreted as “survival of the strongest”, since “fitness” is a loanword in German that is exclusively used in the sense of “physical fitness”. As humans frequently act competitive, and as competition is a way to gain something, the conclusion is that humans surely would act this way if the own life is at risk. In this case highly competitive or even anti-social behavior would be a somewhat consequent and rational behavior. But then the idea of panic generating irrational *and* anti-social behavior would include a contradiction.

B.2 Altruism and Cooperation in Evolutionary Biology

Identifying the mechanisms how the inaccurate public idea of panic could develop is one thing. To have a chance to correct this inaccurate idea one in addition needs an explanation why altruism and cooperation in dangerous or even life-threatening situations could be reasonable, even if this means or might increased danger for oneself is something different. For such explanations one always ends up thinking about the mechanisms of evolution, since all other possible explanations that at first might not appear to be related to evolutionary issues, typically can be summarized as elements of culture. The details of culture however can - due to the complexity of the relations - maybe not be explained by evolution in a strict sense, but it is obvious that culture interacts in many ways with evolution.

Darwin

The wrong perception of Darwin’s evolution theory can probably best be corrected by Darwin himself as he wrote on page 132 of [188]:

A tribe including many members who, from possessing in a high degree the spirit of patriotism, fidelity, obedience, courage, and sympathy, were always ready to aid one another, and to sacrifice themselves for the common good, would be victorious over most other tribes; and this would be natural selection.

However, only two pages earlier Darwin on the contrary wrote:

It is extremely doubtful whether the offspring of the more sympathetic and benevolent parents, or of those who were the most faithful to their comrades, would be reared in greater numbers than the children of selfish and treacherous parents belonging to the same tribe. He who was ready to sacrifice his life, as many a savage has been, rather than betray his comrades, would often leave no offspring to inherit his noble nature. The bravest men, who were always willing to come to the front in war, and who freely risked their lives for others, would on an average perish in larger numbers than other men. Therefore it hardly seems probable that the number of men gifted with such virtues, or that the standard of their excellence, could be increased through natural selection that is, by the survival of the fittest; for we are not here speaking of one tribe being victorious over another.

Darwin describes two antagonistic mechanisms of which one leads to more altruism and the other to increased selfishness. Altruism can appear among the individuals of a group if this group competes with other groups, if this makes the group function more efficiently. At the same time the individuals may face conflicts and competition within their group. First of all, the crucial point is that Darwin's evolution theory allows evolution toward altruism under certain conditions and that altruistic and cooperative behavior are not necessarily considered to be unfitting. But the theory of evolution did only begin and not end with Darwin. Darwin neither tried to quantify the importance of these two antagonistic mechanisms, nor did he bother to think about the definition of a "group" in the framework of evolution theory.

In biology an act of altruism is defined as "behavior that increases the fitness of a recipient organism while it decreases the fitness of the donating one". This definition applies whenever someone renounces the possibility to leave a dangerous situation as fast as possible, if remaining in danger for longer increases the chance to suffer from some disadvantage. Be it whether he renounces pushing other people aside or whether he chooses to remain in danger longer than necessary to actively help others. In recent decades there have been mainly three perspectives ("gene-level perspective", "individual-level perspective" and "group-level perspective") in evolution theory how cooperation and altruism could evolve. Over the years the group-level perspective first dominated the discussion, then was received sceptically by a vast majority of researchers, but is regaining some importance recently. One has to understand that the advocates of each perspective consider(ed) the mechanisms of their perspective to be the absolutely predominant and therefore the three perspectives today still compete fiercely. In any case notable is the fact that - contrary to public perception - the scientific discussion for decades is about *how* altruism could evolve by the laws of evolution and not *if* it did evolve. What is important at this point of the debate is not a definite answer of how it comes to cooperation and altruism, but that it is possible to have rational explanations that they could occur and that therefore there does not necessarily have to be a quasi deterministic development toward selfish and anti-social behavior, not even in the presence of some external danger.

In the following the three perspectives on evolution are surveyed only briefly, as the subtleties cannot be discussed here anyway.

The Individual-Level Perspective

Reciprocal Altruism [189] is altruism that hopes for future rewards from the beneficiaries of one's own altruism. It is a trade initiated by one individual, unrequested by the other, where the payment is not fixed in advance and postponed to a later time. The trade-like character of this kind of altruism makes some people deny that it is true ("genuine") altruism. Yet for subjects like the behavior during disastrous situations the psychological motivation is of less interest.

Tit for Tat [190, 191] is a simple strategy in game theory: In the iterative prisoner's dilemma where the players in each event have to decide between a cooperative or a defective strategy, "tit for tat", which means "cooperate at the first meeting with another player and later do as the other one did before" showed up to be the most successful strategy under certain, not very strict conditions of which the most important is that the importance of future benefits must not be weighted too small compared to immediate benefits (discount parameter). There are arguments that "tit for tat" is in fact an element of the group-level perspective.

The Gene-Level Perspective

In the gene-centric perspective the genes are viewed as the main or even only competitors for reproductive success [192, 193], while the fact that they are bound into groups within individuals is recognized but given a smaller priority. With this perspective altruism and cooperation mainly evolve among relatives.

Kin Selection, also called "Inclusive Fitness" [194] is the idea that an individual does not need to live on itself or to reproduce itself or for the reproductional success of its genes, but that helping other individuals whose genes resemble their own (relatives) or in an extreme case sacrificing one's own life to save them can also be a successful strategy. Therefore actions that at first may appear to be very altruistic, can show up to simply be the most successful option for the reproduction or continued existence of the genes of the individual.

The Group-Level Perspective

Beside of genes and individuals one can also think of groups of individuals competing for evolutionary success.

Group Selection [195, 196] as driving force of the evolution implies the possibility that traits can exist and prevail that are disadvantageous for an individual but that make

individuals behave as to improve the evolutionary fitness of their group. As already Darwin noticed (see above), this is a loop-hole by which altruism can evolve. This idea has at least in its early formulations one major problem: Even if a group successfully grows due to the altruistic behavior of some of its members, the share of those unselfish members within the group will probably decrease as selfish group members will exploit the selfless ones and thus reduce their reproductional success within the group. A comprehensive criticism of group selection theory in its early form can be found in [197].

Multilevel Selection Theory [198, 199] is a more recent concept that incorporates, unifies, and advances earlier ideas and concepts, and therefore in a sense represents a “return to Darwin”. Multilevel group selection theory tries to incorporate selection effect on many levels. The authors of multilevel selection theory stress the complexity of the field and that the theory has only started to be developed: *“Evolution is a notoriously messy process that defies single explanations. Nothing is perfectly adaptive or a product of only one level of selection.[...] All of the hypotheses [...] have at least some merit; our challenge is to discover their relative importance.”* ([200], chapter 1). Discovering the relative importance of within and in between group selection is what Darwin left to his scientific descendants, when he just put the two quotes from above side by side without weighing them against each other. The three elementary questions of multilevel selection theory for the prediction what will evolve from a system are: “What would evolve if only individual selection would exist?”, “What would evolve if only group selection would exist?” and “At what point between these extremes is the system placed?” However difficult the third question might be to answer, the fact that it is raised makes multilevel selection theory immune against justified criticism of pure group selection. Compared to the controversy of the preceding decades the main change in thought is that not one mechanism must be the one and only dominating one, but that contrary to that in each system one has to determine the relative importance anew. Finally it is worth mentioning that the authors of multilevel selection theory claim [200] a close relationship of their theory to the “Social Identity Theory” [201], which will also be of some importance in later plausibility considerations.

The Price Equation [202] is the mathematical justification and backup for multilevel selection theory. For a long time it did not get proper attention until recently it was pulled back to the attention of scientific public [203]. Whatever holds for multilevel selection theory also holds for the Price equation. In addition one of the most important findings of the Price equation is, that it is not kinship (in the sense of “common ancestry”) which matters in the evolution of altruism, but statistical associations in the genotype of donor and recipient [203]. This is something that fits well with the third quote from phenomenological incident research above. One must keep in mind, however, that the Price equation does not tell what evolves, but what could evolve, if only reality holds enough similarities to suiting models on which the Price equation can be applied. For example did the Price equation not only help to understand kin selection and the altruism evolving from that better, but it also gave the first idea of how spiteful

behavior (hurt oneself to hurt someone else more) could have evolved. While the Price equation probably grants the best insight to evolution in general so far (after all it is mathematics), its downside is, that for the aim of changing the imagination the public has of evolution, it is probably of only minor use (after all it is mathematics).

In detail the price equation describes the alternation Δz of a trait z - which influences the fitness w - from one generation to the other:

$$w\Delta z = \text{cov}_i(w_i, z_i) + E_i(w_i\Delta z_i) \quad (\text{B.1})$$

The values with no index denote averages over the corresponding ones with indices. For the operators covariance (cov) and expectation value (E) therefore the index over which they are calculated is also given in the operator name. The interesting thing now is, that the Price equation can recursively be inserted into itself by adding one more index:

$$w\Delta z = \text{cov}_i(w_i, z_i) + E_i(\text{cov}_j(w_{ij}, z_{ij}) + E_j(w_{ij}\Delta z_{ij})) \quad (\text{B.2})$$

As long as there does not appear to be some $\Delta z_{i_1 i_2 \dots}$ which is always zero, the Price equation is able to take into account groups and sub-groups and sub-sub-groups and so on to arbitrary depth. By this the group structure which was already estimated by Darwin to play an important role in the evolution of altruism is naturally taken into account and modeled by the Price equation. It is a straight forward task then to construct a model, where w_{ij} (the fitness) depends in such a way on z_{ij} (the amount of altruism exhibited by an individual j toward its group i), that Δz increases. What can not be discussed here - as it would by far exceed the scope of this appendix - is the relevance of any such model as well as the precise definition of a "group". Therefore one cannot follow that altruism and cooperative behavior must have evolved. This would be a conclusion that could easily be shown to be wrong, as there are many species which do not show the slightest such behavior. However, the aim of this appendix was to give a survey over concepts that are able to explain how it could have evolved and that assuming that altruism and cooperative behavior are intrinsically irrational in the framework of evolution theory is absolutely wrong.

B.3 Concepts of Altruism and Cooperation with Respect to Crowd Disasters

If the claim of multilevel selection theory is true that it depends on the situation, whether evolution is driven by within or by between group selection, and if both kinds of situations occurred frequently during the course of evolution, and if it is true that between group selection favors the evolution of cooperative while within group selection favors the evolution of competitive behavior, then it is almost self-evident to assume that both kinds of behavior can occur. It furthermore is self-evident as well to assume that it is situation dependent which kind of behavior is the more likely one to be exhibited. This then raises one question: "Which are the decisive factors for the exhibition of a certain kind of behavior during a critical crowd situation?" A very popular (also in the

literal sense) strategy is, to derive such factors from man once being a hunter and/or a gatherer. Yet, as the whole process of evolution is very complicated, this is not the way chosen here. Instead a more phenomenological ansatz is chosen: drawn from the study of the events of appendix A, in the following three hypotheses are stated:

Hypothesis 1: *In situations that include or could include competitive elements a dynamical process sets the border between “Us” and “Them” in the mind of the participants (compare “Social Identity Theory” [201, 204, 205] and extensions [206]). Depending on factors like genetic disposition, cultural imprint, experience of life and the details of the situation, the “Us” can range from “Just Me” to “All of the people here” and can be different for any of the participants. Each participant will then behave cooperatively or even altruistically toward those persons he includes into the set of “Us”.*

It is here where a blind spot of past research emerges, for what has often been examined are situations, where it is obvious that not all participants can gain some reward or avoid punishment respectively losses [108, 161]. That is, what has been done is research on systems that - however with tiny gains and losses - model the situation of an airplane that is inescapably going to crash and on board of which there are only half as many parachutes as passengers. Such a situation can easily be imagined as to create tiny sets of “Us” and therefore for the appearance of cooperation and altruism this is the worst situation one can think of, since being altruistic essentially means consciously deciding to die so someone else can survive, respectively as participant in an experimental game to reject the whole concept of the game. But this is not the nature of most crowd disaster situations. A fire normally does not crawl at constant speed from behind toward a door killing everyone who is not out after a certain time. And even if it would, estimating the speed of the fire front would not be that simple that each evacuee necessarily knows that those n out of N evacuees that have not passed the exit exactly after time T are inescapably going to die.

The history of crowd disasters shows that it is not necessarily a danger of life that initiates a disaster: The cause of motion and competitive behavior can be the flight from a real external danger like a fire or an inconvenience like a heavy rain, but also the hope for some reward like a good position within the crowd of a concert audience, arriving timely for the kick-off of a soccer match or being one of the persons to be gifted at a give-away campaign of a company. For all of these causes the chance that all members of the crowd can avoid a loss or gain a reward varies in addition to the type of reward or loss:

Hypothesis 2: *Crucial in the first place for the emergence of cooperation and altruism is the assumption of the members of the crowd that there is a reasonable - however, maybe only just small - chance that everyone can avoid loss or gain the same reward, rather than the type and amount of loss or reward.*

Hypothesis 3: *Large dangers respectively risks of large losses are more prone to produce cooperation and altruistic behavior than small dangers or rewards.*

The second hypothesis is trivial if one assumes a somewhat extreme situation and assumes completely rational behavior: If all members of a crowd assume that all of them can gain the exactly same (maximal) reward or avoid loss there is no necessity to act competitive.

The claim of the third hypothesis has quite a few causes: Small rewards like being timely for a kick-off and small losses like getting wet in a rain are underestimated concerning their potential to generate large damages. The problem here simply is the unawareness of the public about the dynamics of large crowds. In addition one must think of social control: It is socially fully accepted even expected to compete for minor gains, but at the same time it is as well expected to support any competitor for such minor gains, if he is in danger of life.

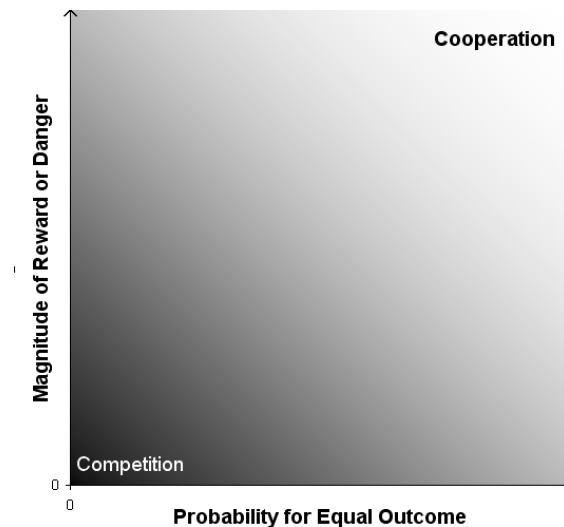


Figure B.1: Schematic view of (some of) the factors that influence the behavior during emergency situations. Note that other factors of which some are stated above as for example the degree of relatedness (kin selection) of the whole or parts of the group have an influence as well.

It maybe would not be exactly the same as these three hypotheses to say that it is “greed” and not “panic” which is likely to produce the behaviors typically ascribed to “panic”, but it would probably come much closer to correctly describing and understanding what actually led to many of those accidents that are described in appendix A.

An Example

As one of many possible examples the reports of two incidents will now be compared, which fit quite well for this purpose as they have many things in common: The near-accident at the entrance of the Olympiastadion in Berlin (23rd of April 2005) and the

disaster at the concert of the band „Great White” on Rhode Island (20th of February 2003). Both incidents happened at an event of popular culture (soccer and rock music). The authors of both reports [174, 207] can be assumed to consider themselves as fans within the general scene (soccer and rock music). In a more specific sense both authors are fans in a way that they would sympathize with the affected fans and rather not sympathize with the organizers of the event: Wolf can be found on the homepage of his company to be a fan of Schalke 04 - and not of Hertha BSC Berlin where the match took place - and Breusch is journalist for a magazine for fans and musicians and less for organizers. The events happened at a time distance of only two years and two months. Additionally for reasons stated above one should mention that both authors are Germans.

However similar the background of the authors might be, the course of events was different for the two (near-)accidents. What happened in Berlin is already explained in appendix A. Initially it is interesting to mention that all fans in front of the south gate were fans of Schalke 04 (just like the author Wolf). So they formed a similarly homogeneous group as the fans in the club on Rhode Island. For Rhode Island the events are summarized by saying that an element of the pyro show ignited the club during the show and the fire spread very quickly. 99 people died.

At first some of the most important and most impressive passages from both reports are given now. From the Olympiastadion report [174]:

„Weinende und schreiende Kinder an der Hand ihrer verzweifelten Eltern, ältere Menschen, die nach Luft rangen und fürchteten, zerquetscht zu werden - weil andere wütende Zuschauer, die Einlass haben wollten, von hinten schubsten und drängelten. Das war das schockierende Szenario vor dem Südtor der Arena.”

English translation:

“Weeping and screaming children at the hands of their desperate parents, elderly people, who were grasping for air and feared to be crushed - because other spectators, who demanded admittance, pushed and pressed from behind. This was the shocking scenario in front of the southern gate of the arena.”

From the Rhode Island report [207]:

„Christopher Arruda, einem LKW-Fahrer, wurde seine Uneigennützigkeit zum Verhängnis. Er stürzte insgesamt dreimal zurück in den Club, um Leute herauszuholen; beim dritten Mal kam er nicht mehr zurück. Matthew Darby, ein örtlicher Maler, Bildhauer und Galerist, der unverletzt ins Freie gekommen war, holte mindestens zwölf Menschen aus den Flammen, bevor er selbst nicht mehr den Weg nach draußen fand.”

English translation:

“Christopher Arruda, a truck driver, became victim to his own altruism. He rushed back into the club three times to help out other people; at the third

time, he did not come back. Matthew Darby, a local painter, sculptor and gallery owner, who managed to get out unharmed, helped at least twelve people out of the flames, before he himself did no more find the way back out.”

One has to keep in mind that surely not everyone in the Rhode Island disaster acted altruistically, and that it is more interesting to report about heroes than about some average guy who fled and stayed outside afterward. And most probably there was also much helping among the fans within the most dangerous area (in terms of density) in Berlin. But even then it remains obvious that some share of fans in the Rhode Island incident and in the Berlin incident acted differently, differently in the amount of cooperation and altruism they showed. The reward on Rhode Island was to survive, in Berlin to see the kick-off of the match. The punishment for wrong behavior was death on Rhode Island and to miss the kick-off in Berlin. What then did make some (many?, all?) fans on Rhode Island make to act so much more cooperatively and even altruistically than in Berlin? Is it the difference Americans vs. Germans or rock fans vs. soccer fans or most specific: fans of “The Great White” vs. fans of Schalke 04? Is it the time of day that leads to different states of mind or the time of the year, the weather, temperature, air pressure? Additionally one could think of the two authors being biased and reporting selectively. For example if one expects people to stay polite if there is nothing more to gain than to watch some kick-off, one might feel more need to report about those who did not stay polite. But Wolf explicitly describes fractions of the crowd (“*spectators [...] pushed and pressed*”) and not individuals. Therefore his report is not about some individuals who behaved exceptional. This is the big difference to Breusch whose report focuses on individuals. It could be that everyone else acted in the highly competitive way of the common public idea. But this would be an extreme assumption itself, however one could here as well argue that if one expects people to act competitive one might only feel the need to report about those individuals who did not do so. Finally one can fill this gap in the line of argumentation by referring to the disaster researchers cited above and conclude that all of these objections and probably some more cannot be excluded from the data and the reports available, but the interrelations and reasons described in this chapter should be given the highest probability to be the crucial ones.

Summary

The public notion and even the notion of some experts does not match with many results disaster researchers found during the past decades. From an evolutionary point of view these results can maybe not be derived from theory, but they fit into a modern theory like multilevel selection theory and do not contradict it. The behavior of individuals in a crowd appears to be governed by rules that at first may seem somewhat counter-intuitive, but which themselves fit well into the framework of multilevel selection theory. For application, one could think of laws that demand cooperation-fostering measures or at least that forbid intentional initiation of artificial competitions within large crowds.

C Details of the Experiment “Counterflow in a Corridor”

C.1 The Participants

The majority of the 67 participants were students of Duisburg-Essen University. The statistics of participants are shown in figure C.1.

After the experiment was finished the participants were asked two things: to compare their attitude in the first and the last run as well as to check how they experienced the situation during the experiment. The distribution of answers can be found in figure C.2.

The following answering possibilities had the topic „Selbsteinschätzung” (self-assessment).

- Ich betreibe aktiv Laufsport. (I actively practice running.)
- Ich betreibe aktiv einen Sport, bei dem gelaufen wird. (I practice some sports where running is included.)
- Wenn ich in einer Gruppe gehe, ist mir das Tempo üblicherweise eher zu langsam. (When I walk as part of a group, normally I feel the group walks too slowly.)
- Wenn ich in einer Gruppe gehe, ist mir das Tempo üblicherweise eher zu schnell. (When I walk as part of a group, normally I feel the group walks too fast.)
- Ich fühle mich im Vergleich zu meinen Altersgenossen nicht gut zu Fuß. (I think I am no good walker compared people my age.)
- Keine Ahnung. (No idea.)

The following statements did not have a topic. They concern the comparison between first and last run.

- Im Vergleich zum ersten Durchgang war beim letzten Durchgang kein Unterschied. (There was no difference between the first and the last run.)
 - Im Vergleich zum ersten Durchgang war ich beim letzten Durchgang müde. (Compared to the first run, I felt tired during the last one.)
 - Im Vergleich zum ersten Durchgang habe ich mich beim letzten Durchgang beeilt. (Compared to the first run, I was in a hurry during the last one.)
-

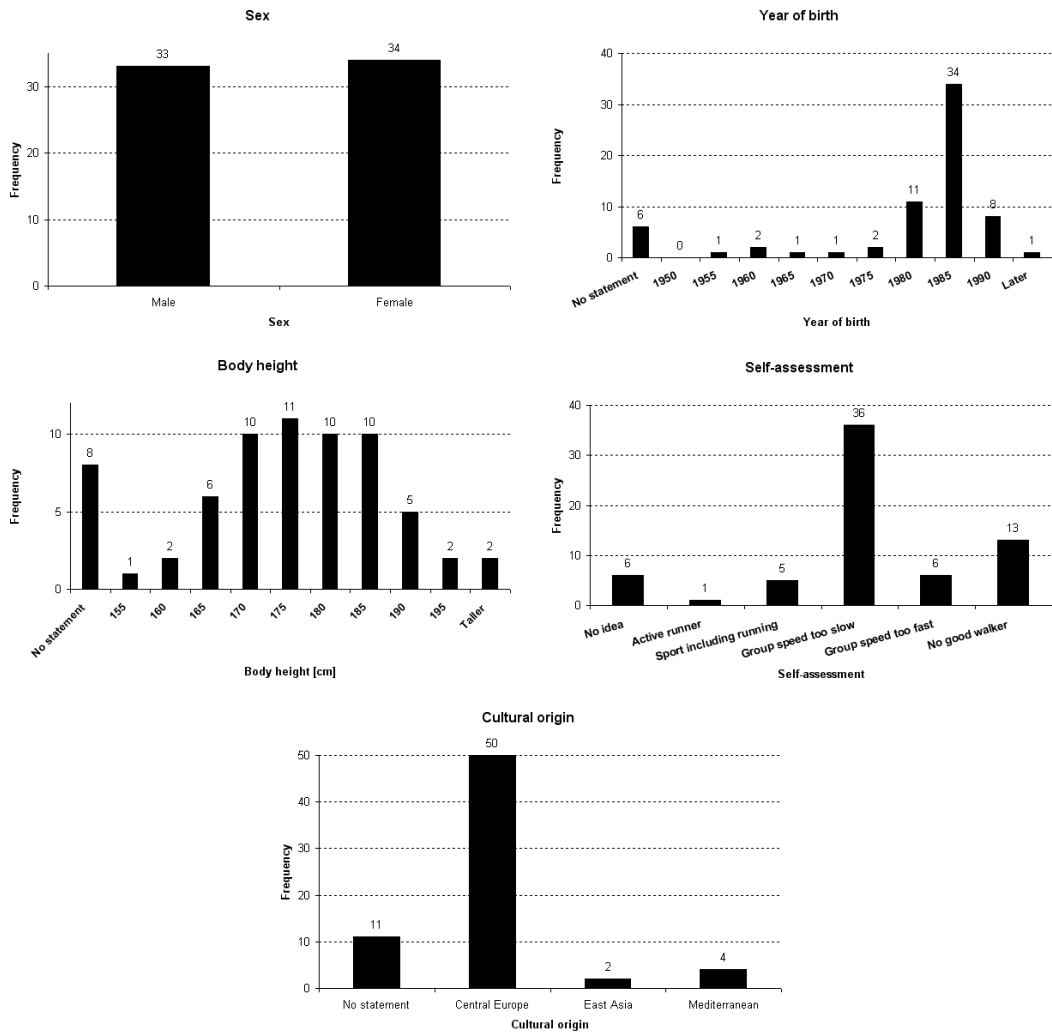


Figure C.1: Participant statistics.

- Im Vergleich zum ersten Durchgang war ich beim letzten Durchgang gelangweilt. (Compared to the first run, I felt bored during the last one.)

Concerning the commentary (topic: „Kommentar“) on the experiment:

- Das Experiment verlief aus meiner Sicht absolut problemlos. (From my point of view there were no problems during the experiment.)
- Es war zwischenzeitlich recht eng. (Sometimes it was quite cramped.)
- Ich habe mich regelrecht unwohl gefühlt. (I felt downright bad.)

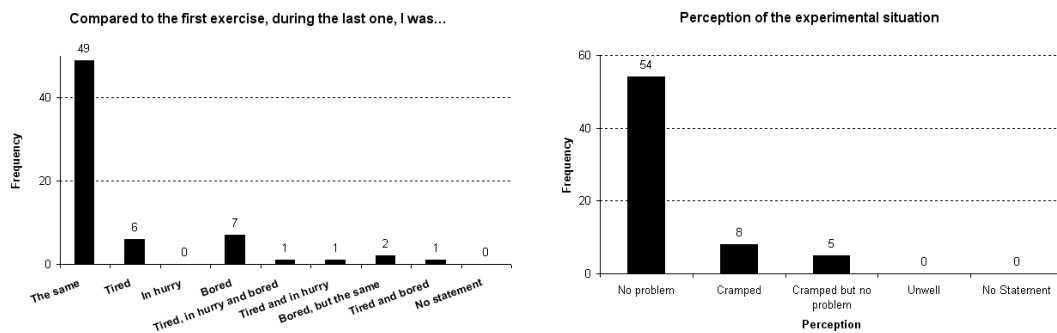


Figure C.2: Results of the participant poll.

C.2 The Script

At first the participants were asked to walk through the corridor one by one. This was done to have the first movement in front of the cameras not included in the experiment, as the participants did not walk in a natural way at the beginning. The sequence of runs that followed this initial process is shown in table C.1.

Size of majority group	Size of minority group	Counterflow fraction
65	0	0.000
65	0	0.000
6	0	0.000
59	6	0.092
6	6	0.500
59	6	0.092
6	6	0.500
59	6	0.092
6	0	0.000
22	0	0.000
43	22	0.338
21	0	0.000
43	22	0.338
22	0	0.000
44	0	0.000
10	0	0.000
33	32	0.492
16	16	0.500
33	32	0.492
34	33	0.493
17	17	0.500
34	33	0.493
16	0	0.000
33	17	0.340
16	0	0.000
33	17	0.340
16	0	0.000
33	17	0.340
33	4	0.108
4	4	0.500
34	4	0.105
4	4	0.500
34	4	0.105
34	0	0.000
34	0	0.000
34	0	0.000

Table C.1: The sequence of runs.

D Participants' Details of the Experiment “Flow Through a Bottleneck”

The majority of the 94 participants were students at Duisburg-Essen University. The statistics of participants are shown in figure D.1.

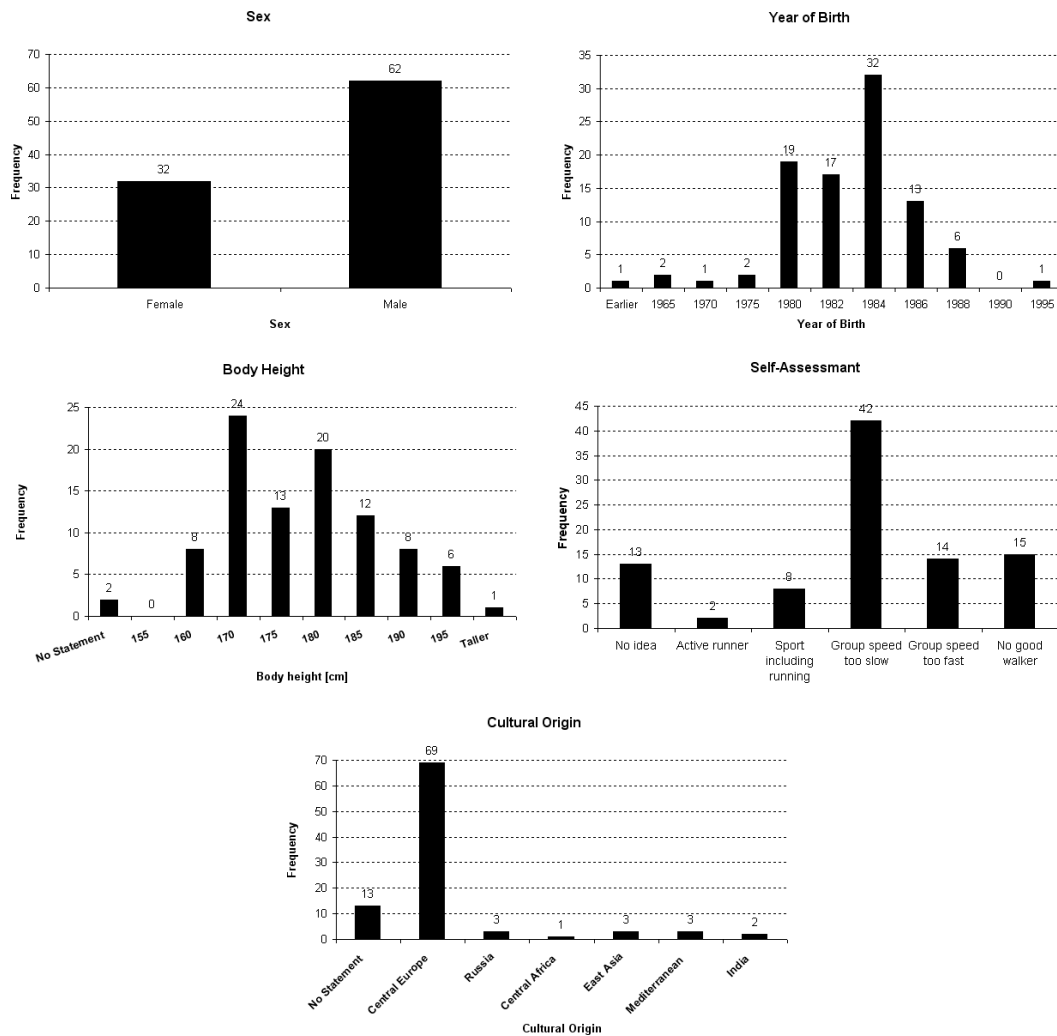


Figure D.1: Participants' statistics.

After the experiment, the participants were asked two questions: to compare their attitude during the first and the last run as well as to check how they experienced the situation during the experiment. The distribution of answers can be found in figure D.2. The exact (German) wording of the possible answers to these questions as well as the

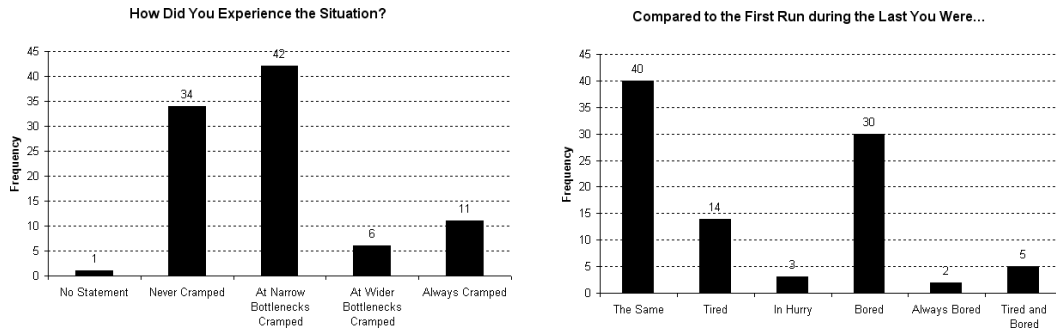


Figure D.2: Participant poll.

self-assessment was as follows.

The following answers had the topic „Selbsteinschätzung“ (self-assessment).

- Ich betreibe aktiven Laufsport. (I actively practice running.)
- Ich betreibe aktiv einen Sport, bei dem gelaufen wird. (I practice some sports where running is included.)
- Wenn ich in einer Gruppe gehe, ist mir das Tempo üblicherweise eher zu langsam. (When I walk as part of a group, normally I feel the group walks too slowly.)
- Wenn ich in einer Gruppe gehe, ist mir das Tempo üblicherweise eher zu schnell. (When I walk as part of a group, normally I feel the group walks too fast.)
- Ich fühle mich im Vergleich zu meinen Altersgenossen nicht gut zu Fuß. (I think I am no good walker compared to people my age.)
- Keine Ahnung (No idea.)

The following statements did not have a topic. They concern the comparison between first and last run.

- Im Vergleich zum ersten Durchgang war beim letzten Durchgang kein Unterschied. (There was no difference between the first and the last run.)
- Im Vergleich zum ersten Durchgang war ich beim letzten Durchgang müde. (Compared to the first run, I felt tired during the last one.)
- Im Vergleich zum ersten Durchgang habe ich mich beim letzten Durchgang beeilt. (Compared to the first run, I was in a hurry during the last one.)

- Im Vergleich zum ersten Durchgang war ich beim letzten Durchgang gelangweilt. (Compared to the first run, I felt bored during the last one.)

Concerning the commentary (topic: „Kommentar“) on the experiment:

- Aus meiner Sicht kam es nie zu einem „Gedränge“ vor dem Durchgang. (From my point of view it was never cramped in front of the bottleneck.)
 - Aus meiner Sicht kam es nur vor den schmaleren Durchgängen zu einem „Gedränge“. (From my point of view it was cramped in front of the narrow bottlenecks.)
 - Aus meiner Sicht kam es nur vor den breiteren Durchgängen zu einem „Gedränge“. (From my point of view it was cramped in front of the wider bottlenecks.)
 - Aus meiner Sicht war das immer ein „Gedränge“. (From my point of view it was always cramped in front of the bottleneck.)
-

Bibliography

- [1] The Executive Director of the Agency. *ED Decision 2003/16/RM on Certification Specifications for Large Rotorcraft*. European Aviation Safety Agency, November 2003. http://www.easa.eu.int/doc/Agency_Mesures/Certification_Spec/decision_ED_2003_16_RM.pdf.
 - [2] A. Kirchner, H. Klüpfel, K. Nishinari, A. Schadschneider, and M. Schreckenberg. Simulation of competitive egress behavior: comparison with aircraft evacuation data. *Physica A*, 324:689–697, Jun 2003. DOI:10.1016/S0378-4371(03)00076-1.
 - [3] Tagesschau. Evakuierungstest für A380 erfolgreich, 3 2006. (in German) http://www.tagesschau.de/aktuell/meldungen/0,1185,0ID5367204_REF1,00.html.
 - [4] P. Gattermann. Grundlagen von Entfluchtungskonzepten. Annotation in a talk at the Brandschutz-Fachtagung in Melk, 2005.
 - [5] Germanischer Lloyd, 2002. <http://www.gl-group.com/maritime/newbuilding/shipsafety/aeneas/3614.htm>.
 - [6] A.W. Heskestad, G. Jensen, O. Meland, and E. Torlen. ALLSAFE: An Engineering Tool for Evacuation Safety Design. In *Proceedings of the Fire Safety by Design Conference*, 1995.
 - [7] V. Schneider and S. Habip. ASERI, 1993. <http://www.ist-net.de/>.
 - [8] F.I. Stahl. BFIRES / Version 2: Documentation of Program Modifications. Technical Report NBSIR 80-1982, U.S. Dept. of Commerce, National Bureau of Standards, 1980.
 - [9] F. Ozel. A Stochastic Computer Simulation of the Behavior of People in Fires: An Environmental Cognitive Approach. In *Proceedings of the International Conference on Building Use and Safety Technology*, 1985.
 - [10] V.J. Blue and J.L. Adler. Cellular Automata Microsimulation of Bi-Directional Pedestrian Flows. *Transportation Research Record, Journal of the Transportation Research Board*, 1678:135–141, 2000. <http://www.ulster.net/~vjblue/CA-TRB99.pdf>.
 - [11] D.C. Brogan and J.K. Hodgins. Group Behaviors for Systems with Significant Dynamics. *Autonomous Robots*, 4:137–153, 1997. DOI:10.1023/A:1008867321648.
-

-
- [12] D.C. Brogan and N.L. Johnson. Realistic Human Walking Paths. In *16th International Conference on Computer Animation and Social Agents*, pages 94–101. IEEE Computer Society, 2003. DOI:10.1109/CASA.2003.1199309, ISBN: 0-7695-1934-2.
- [13] A. Treuille, S. Cooper, and Z. Popović. Continuum Crowds. *ACM Transactions on Graphics*, 25:1160–1168, 2006. DOI:10.1145/1141911.1142008.
- [14] S.P. Hoogendoorn, P.H.L. Bovy, and W. Daamen. Microscopic Pedestrian Wayfinding and Dynamics Modelling. In Schreckenberg and Sharma [215], pages 123–154. ISBN:3-540-42690-6.
- [15] K. Boyce, J. Fraser-Mitchell, and J. Shields. Survey Analysis and Modelling of Office Evacuation Using CRISP Model. In *Human Behaviour in Fire – Proceedings of the 1st International Symposium*, pages 691–702, 1998.
- [16] J. Dijkstra, J. Jessurun, and H. Timmermans. A Multi-Agent Cellular Automata Model of Pedestrian Movement. In Schreckenberg and Sharma [215], pages 173–179. <http://www.ddss.nl/Eindhoven/publications/193>.
- [17] E. Kendik. Methods of Design for Means of Egress: Towards a Quantitative Comparison of National Code Requirements. In Grant and Pagni [208], pages 497–511. ISBN:0-891-16456-1.
- [18] N. Ketchell. A Technical Summary of the AEA EGRESS Code. Technical report, AEA Technology, 2002. <http://www.aeat-safety-and-risk.com/Downloads/Egress%20Technical%20Summary.pdf>.
- [19] H.A. Donegan, A.J. Pollock, and I.R. Taylor. Egress Complexity of a Building. In Kashiwagi [210], pages 601–612. ISBN:1-88627-900-4.
- [20] E. Reisser-Weston. Simulating Human Behaviour in Emergency Situations. In *RINA, International Conference of Escape, Fire, and Rescue*, 1996.
- [21] T.M. Kisko, R.L. Francis, and C.R. Nobel. *EVACNET4 User's Guide, Version 10/29/98*, 1998. <http://www.riskinfo.dk/IT/EVAC4UGFM.pdf>.
- [22] L.S. Poon. EvacSim: A Simulation Model of Occupants with Behavioural Attributes in Emergency Evacuation of High-Rise Buildings. In Kashiwagi [210], pages 681–692. ISBN:1-88627-900-4.
- [23] D. Vassalos, H. Kim, G. Christiansen, and J. Majumder. A Mesoscopic Model for Passenger Evacuation in a Virtual Ship-Sea Environment and Performance-Based Evaluation. In Schreckenberg and Sharma [215], pages 369–391. http://www.safety-at-sea.co.uk/evi/publications/PED_Duisburg2001.pdf.
- [24] R.F. Fahy. *User's Manual, Exit89 v 1.01, An Evacuation Model for High-Rise Buildings*. Quincy, MA, 1999.
-

-
- [25] B.M. Levin. EXITT - A Simulation Model of Occupant Decisions and Actions in Residential Fires. In Wakamatsu et al. [209], pages 561–570. ISBN:0-89116-864-8.
- [26] E.R. Galea and J.M. Perez Galparsoro. *EXODUS: An Evacuation Model for Mass Transport Vehicles*. UK CAA Paper 93 006, 1993. ISBN:0-86039-543X <http://fseg.gre.ac.uk/exodus/>.
- [27] W.E. Feinberg and R.J. Norris. Firescap: A Computer Simulation Model of Reaction to a Fire Alarm. *Journal of Mathematical Sociology*, 20:247–269, 1995.
- [28] C. Burstedde, K. Klauck, A. Schadschneider, and J. Zittarz. Simulation of pedestrian dynamics using a 2-dimensional cellular automaton. *Physica A*, 295:507, 2001. DOI:10.1016/S0378-4371(01)00141-8.
- [29] A. Kirchner and A. Schadschneider. Simulation of Evacuation Processes Using a Bionics-inspired Cellular Automaton Model for Pedestrian Dynamics. *Physica A*, 312(1-2):260–276, September 2002. DOI:10.1016/S0378-4371(02)00857-9.
- [30] K. Nishinari, A. Kirchner, A. Namazi, and A. Schadschneider. Extended Floor Field CA Model for Evacuation Dynamics. *IEICE Trans. Inf. & Syst.*, E87-D:726–732, 2004. OAI:arXiv.org:cond-mat/0306262.
- [31] S. Deal. Technical Reference Guide for FPETool Version 3.2. Technical report, Natl. Inst. Stand. Technol., 1995. <http://fire.nist.gov/bfrlpubs/fire95/PDF/f95153.pdf>.
- [32] N. Fridman and G. Kaminka. Modeling Crowd Behavior Based on Social Comparison Theory: Extended Abstract. In El Yacoubi et al. [222], pages 694–698. ISBN:3-540-40929-7.
- [33] J. Funge, X. Tu, and D. Terzopoulos. Cognitive modeling: knowledge, reasoning and planning for intelligent characters. In *Proceedings of the 26th annual conference on Computer graphics and interactive techniques*, pages 29–38. ACM Press/Addison-Wesley Publishing Co., 1999. DOI:10.1145/311535.311538, ISBN:0-201-48560-5.
- [34] M. Bensilum and D.A. Purser. GridFlow: An object-oriented building evacuation model combining pre-movement and movement behaviours for performance-based design. In Evans [217], pages 941–952.
- [35] M. Katuhara, H. Matsukara, and S. Ota. Evacuation Analysis of Ship by Multi-Agent Simulation Using Model of Group Psychology. In Fukui et al. [214], pages 543–548. ISBN:3-540-40255-1.
- [36] F. Lamarche and S. Donikian. Crowd of Virtual Humans: a New Approach for Real Time Navigation in Complex and Structured Environments. *Computer Graphics Forum*, 23(3):509–518, 2004. DOI:10.1111/j.1467-8659.2004.00782.x.
-

-
- [37] D. Connor. Legion, 2003. <http://www.legion.biz/>.
- [38] S. Okazaki and S. Matsushita. A Study of Simulation Model for Pedestrian Movement with Evacuation and Queing, 2004. <http://www.anc-d.fukui-u.ac.jp/~sat/simu.html>.
- [39] Y. Murakami, K. Minami, T. Kawasoe, and T. Ishida. Multi-agent Simulation for Crisis Management. In *IEEE Workshop on Knowledge Media Networking*, pages 135–139, 2002.
- [40] S. Regelous. Massive Prime, 2002. <http://www.massivesoftware.com/>.
- [41] K. Teknomo. Micro-PedSim, 2002. <http://people.revoledu.com/kardi/>.
- [42] K. Teknomo. *Microscopic Pedestrian Flow Characteristics: Development of an Image Processing Data Collection and Simulation Model*. PhD thesis, Graduate School of Information Sciences Tohoku University, Japan, 2002. <http://people.revoledu.com/kardi/publication/Dissertation.pdf>.
- [43] S.R. Musse and D. Thalmann. A Model of Human Crowd Behavior: Group Inter-Relationship and Collision Detection Analysis. In W. Purgathofer, W.T. Hewitt, and Hansmann W., editors, *Computer Animation and Simulation '97*, pages 39–52, 1997. http://ligwww.epfl.ch/Publications/pdf/Musse_Thalmann_CAS_97.pdf, ISBN:3-211-83048-0.
- [44] G.K. Still. Myriad, 1992. <http://www.crowddynamics.com/>.
- [45] N. Ohi, M. Ikai, and K. Nishinari. Simulations of Evacuation Using Small World Network. In Fukui et al. [214], pages 555–559. ISBN:3-540-40255-1.
- [46] J. Cappucio. Pathfinder: A Computer-Based, Timed Egress Simulation. *Fire Protection Engineering*, 8:11–12, 2000.
- [47] J. Kerridge and N. McNair. PEDFLOW - A System for Modelling Pedestrian Movement in Occam. In B.M. Cook, editor, *Proceedings of WoTUG-22: Architectures, Languages and Techniques for Concurrent Systems*, volume 57 of *Concurrent Systems Engineering*, pages 1–18, Amsterdam, 1999. IOS Press.
- [48] Halcrow. Paxport, 1998. <http://www.halcrow.com/software/solutions/paxport.asp>.
- [49] H. Klüpfel and T. Meyer-König. PedGo Users' Manual, 2002. <http://www.traffgo-ht.com/>.
- [50] N. Pelechano, K. O'Brien, B. Silverman, and N. Badler. Crowd Simulation Incorporating Agent Psychological Models, Roles and Communication, 2005. electronic publication, presented at V-Crowds'05 http://www.seas.upenn.edu/~npelecha/Pelechano_V_CROWDS05.pdf.
-

-
- [51] M. Schultz, S. Lehmann, and H. Fricke. A discrete microscopic model for pedestrian dynamics to manage emergency situations in airport terminals. In Waldau et al. [219], pages 389–395. ISBN:3-540-47062-X.
- [52] S.M. Lo, Z. Fang, P. Lin, and G.S. Zhi. An Evacuation Model: the SGEM Package. *Fire Safety Journal*, 39:169–190, 2004. DOI:10.1016/j.firesaf.2003.10.003.
- [53] W. Shao and D. Terzopoulos. Autonomous pedestrians. In Anijyo and Faloustos [223], pages 19–28. DOI:10.1145/1073368.1073371.
- [54] P.A. Thompson and E.W. Marchant. Simulex; Developing New Computer Modelling Techniques for Evaluation. In Kashiwagi [210], pages 613–624. ISBN:1-88627-900-4.
- [55] Savannah Simulations AG. Simwalk, 2004. <http://www.simwalk.ch/>.
- [56] D. Helbing and P. Molnar. Social force model for pedestrian dynamics. *Phys. Rev. E*, 51:4282–4286, 1995. DOI:10.1103/PhysRevE.51.4282.
- [57] N.A. Hoffmann and D.A. Henson. Simulating Transient Evacuation and Pedestrian Movement in Stations. In *3rd International Conference on Mass Transit Management*, Kuala Lumpur, Malaysia, 1997.
- [58] Y. Sugiyama, A. Nakayama, and K. Hasebe. 2-Dimensional Optimal Velocity Models for Granular Flow and Pedestrian Dynamics. In Schreckenberg and Sharma [215], pages 155–160. ISBN:3-540-42690-6.
- [59] M. Sung, L. Kovar, and M. Gleicher. Fast and accurate goal-directed motion synthesis for crowds. In Anijyo and Faloustos [223], pages 291–300. DOI:10.1145/1073368.1073410.
- [60] C.M. Henein and T. White. Macroscopic effects of microscopic forces between agents in crowd models. *Physica A*, 373:694–712, Jan 2006. DOI:10.1016/j.physa.2006.06.023.
- [61] K. Takahashi, T. Tanaka, and S. Kose. An Evacuation Model for Use in Fire Safety Design of Buildings. In Wakamatsu et al. [209], pages 551–560. ISBN:0-89116-864-8.
- [62] S.S. Harrington. TIMTEX: A Hydraulic Flow Model for Emergency Egress. Technical report, MS Department of Fire Protection Engineering, University of Maryland, 1996.
- [63] V.O. Shestopal and S.J. Grubits. Evacuation Model for Merging Traffic Flows in Multi-Room and Multi-Storey Buildings. In Kashiwagi [210], pages 625–632. ISBN:1-88627-900-4.
- [64] J. Wąs, B. Gudowski, and P.J. Matuszyk. Social Distances Model of Pedestrian Dynamics. In El Yacoubi et al. [222], pages 492–501. DOI:10.1007/11861201.57.
-

-
- [65] K. Yamamoto, S. Kokubo, and K. Nishinari. New Approach for Pedestrian Dynamics by Real-Coded Cellular Automata (RCA). In El Yacoubi et al. [222], pages 728–731. ISBN:3-540-40929-7.
- [66] E.D. Kuligowski. Review of 28 Egress Models. In Peacock and Kuligowski [221], pages 68–90. <http://fire.nist.gov/bfrlpubs/fire05/PDF/f05008.pdf>.
- [67] G. Santos and B.E. Aguirre. Critical Review of Emergency Evacuation Simulation Models. In Peacock and Kuligowski [221], pages 27–52. <http://fire.nist.gov/bfrlpubs/fire05/PDF/f05012.pdf>.
- [68] H. Klüpfel, M. Schreckenberg, and T. Meyer-König. Models for Crowd Movement and Egress Simulation. In Hoogendoorn et al. [218], pages 357–372. <http://www.traffgo-ht.com/downloads/pedestrians/downloads/publications/Kluepfel2004a.pdf>.
- [69] N. Waldau. RiMEA - Richtlinie für Mikroskopische Entfluchtungsanalysen/Evakuierungsanalysen. In *Brandschutz-Fachtagung 2005*, pages 112–118, St. Pölten, February 2005. FSE Ruhrhofer & Schweitzer OEG. (in German) <http://www.fse.at/>.
- [70] S. Gwynne, E. Galea, M. Owen, P. Lawrence, and L. Filippidis. A Review Of The Methodologies Used In The Computer Simulation Of Evacuation From The Built Environment. *Building and Environment Journal*, 34:741–749, 1999. DOI: 10.1016/S0360-1323(98)00057-2.
- [71] S.M. Olenick and D.J. Carpenter. An Updated International Survey of Computer Models for Fire and Smoke. *Journal of Fire Protection Engineering*, 13:87–110, 2003. DOI:10.1177/1042391503013002001 with updates on URL: <http://www.firemodelsurvey.com/EgressModels.html>.
- [72] B. Beken and G. Beken. Fire and Smoke Egress Design Software, 2006. http://www.iklimnet.com/hotelfires/fire_egress_software.html.
- [73] N. Waldau and T. Meyer-König. RiMEA - Richtlinie für Mikroskopische Entfluchtungsanalysen. *HLK-Zeitschrift 4/1 A, Sonderausgabe Facility Management*, April 2004. (in German) <http://www.rimea.de/>.
- [74] IMO correspondence group. Interim Guidelines for Evacuation Analyses for New and Existing Passenger Ships. Technical Report MSC/Circ. 1033, International Maritime Organisation (IMO), June 2002. http://www.imo.org/includes/blastData.asp/doc_id=2188/1033.pdf.
- [75] A. Seyfried, B. Steffen, W. Klingsch, T. Lippert, and M. Boltes. Steps Toward the Fundamental Diagram - Empirical Results and Modelling. In Waldau et al. [219], pages 397–409. ISBN:3-540-47062-X.
-

-
- [76] C. Rogsch. Vergleichende Untersuchung zur dynamischen Simulation von Personenströmen. Master's thesis, Bergische Universität Wuppertal, 2005. (in German) <http://hdl.handle.net/2128/483>. Some results were published in English in [77].
- [77] C. Rogsch, A. Seyfried, and W. Klingsch. Comparative Investigation of the Dynamic Simulation of Foot Traffic Flow. In Waldau et al. [219]. ISBN: 3-540-47062-X.
- [78] J. Wahle. *Information in Intelligent Transportation Systems*. PhD thesis, Mercator Universität Duisburg, 2002. <http://www.ub.uni-duisburg.de/ETD-db/theses/available/duett-09252002-194258/unrestricted/wahle.pdf>.
- [79] M. Gardner. The fantastic combinations of John Conway's new solitaire game "life". *Scientific American*, 223:120–123, 1970. <http://www.ibiblio.org/lifepatterns/october1970.html>.
- [80] S. Wolfram. *A New Kind of Science*. Champaign, IL: Wolfram Media, 2002, 2002. ISBN:1-579-55008-8, <http://www.wolframscience.com/nksonline/toc.html>.
- [81] S. Wolfram. *Theory and Application of Cellular Automata*. World Scientific, Singapore, August 1986. ISBN:9-971-50123-6.
- [82] M. Machtey, K. Winkelmann, and P. Young. Simple Gödel Numberings, Isomorphisms, and Programming Properties. *Siam Journal on Computing*, 7:39–60, 1978. DOI:10.1137/0207003.
- [83] B. Martin. A Universal Cellular Automaton in Quasi-linear Time and its S-m-n Form. *Theoretical Computer Science*, 123:199–237, 1994. DOI:10.1016/0304-3975(92)00076-4.
- [84] J. Albert and K. Culik II. A Simple Universal Cellular Automaton and its One-way and Totalistic Version. *Complex Systems*, 1:1–16, 1987.
- [85] K. Nagel and M. Schreckenberg. A Cellular Automaton Model for Freeway Traffic. *Journal de Physique I*, 2:2221–2229, December 1992. DOI:10.1051/jp1:1992277.
- [86] K. Nagel. Particle Hopping Models and Traffic Flow Theory. *Phys. Rev. E*, 53:4655–4672, 1996. DOI:10.1103/PhysRevE.53.4655.
- [87] H. Klüpfel. *A Cellular Automaton Model for Crowd Movement and Egress Simulation*. PhD thesis, Universität Duisburg-Essen, 2003. <http://www.ub.uni-duisburg.de/ETD-db/theses/available/duett-08012003-092540/>.
- [88] A. Kirchner. *Modellierung und statistische Physik biologischer und sozialer Systeme*. PhD thesis, Universität zu Köln, 2002. (in German) http://www.thp.uni-koeln.de/~eb/phys/data/diss_aki.pdf.
-

-
- [89] A. Schadschneider and M. Schreckenberg. Garden of Eden States in Traffic Model. *J. of Phys. A*, 31:L225–L231, 1998. DOI:10.1088/0305-4470/31/11/003.
- [90] A. Kirchner, H. Klüpfel, K. Nishinari, A. Schadschneider, and M. Schreckenberg. Discretization Effects and the Influence of Walking Speed in Cellular Automata Models for Pedestrian Dynamics. *J. Stat. Mech.*, P10011, 2004. DOI:10.1088/1742-5468/2004/10/P10011.
- [91] L. Correia and T. Wehrle. Beyond Cellular Automata, Towards More Realistic Traffic Simulators. In El Yacoubi et al. [222], pages 690–693. DOI:10.1007/11861201_80.
- [92] H. Dreyfuss. *The Measure of Man - Human Factors in Design*. Whitney Library of Design, New York, 1967. ISBN:B-000-7EJK6-0.
- [93] A. Keßel, H. Klüpfel, and M. Schreckenberg. Microscopic Simulation of Pedestrian Crowd Motion. In Schreckenberg and Sharma [215], pages 193–202. http://www.ptt.uni-duisburg.de/fileadmin/docs/paper/2002/ped_kessel.pdf.
- [94] A. Schadschneider. Cellular Automaton Approach to Pedestrian Dynamics - Theory. In Schreckenberg and Sharma [215], pages 76–85. OAI:arXiv.org:cond-mat/0112117.
- [95] C. Burstedde, K. Klauck, A. Schadschneider, and J. Zittarz. Cellular Automaton Approach to Pedestrian Dynamics - Applications. In Schreckenberg and Sharma [215], pages 87–97. OAI:arXiv.org:cond-mat/0112119.
- [96] A. Kirchner, K. Nishinari, and A. Schadschneider. Friction Effects and Clogging in a Cellular Automaton Model for Pedestrian Dynamics. *Phys. Rev. E*, 67(056122), 2003. DOI:10.1103/PhysRevE.67.056122.
- [97] C.M. Henein and T. White. Information in Crowds: The Swarm Information Model. In El Yacoubi et al. [222], pages 703–706. DOI:10.1007/11861201_83.
- [98] H. Hamacher and S. Tjandra. Mathematical Modelling of Evacuation Problems - A State of the Art. In Schreckenberg and Sharma [215], pages 227–266. <http://www.itwm.fraunhofer.de/zentral/download/berichte/bericht24.pdf>.
- [99] E.W. Dijkstra. A Note on Two Problems in Connexion with Graphs. *Numerische Mathematik*, 1:269–271, 1959. <http://www.digizeitschriften.de/index.php?id=ppn&PPN=GDZPPN001163248&L=2>.
- [100] A. Schadschneider. Bionics-Inspired Cellular Automaton Model for Pedestrian Dynamics. In Fukui et al. [214], pages 499–509. <http://www.thp.uni-koeln.de/~as/MyPage/PSfiles/pede1.ps>.
- [101] A. Kirchner and A. Schadschneider. Cellular Automaton Simulations of Pedestrian Dynamics and Evacuation Processes. In Fukui et al. [214], pages 531–536. <http://www.thp.uni-koeln.de/~as/MyPage/PSfiles/pede2.ps>.
-

-
- [102] S. Bandini and S. Manzoni. Towards Affective Situated Cellular Agents. In El Yacoubi et al. [222], pages 686–689. DOI:10.1007/11861201_79.
- [103] N. Rajewsky, L. Santen, A. Schadschneider, and M. Schreckenberg. The Asymmetric Exclusion Process: Comparison of Update Procedures. *Journal of Statistical Physics*, 92:151–194, 1998. DOI:10.1023/A:1023047703307.
- [104] U. Weidmann. Transporttechnik der Fussgänger. Schriftenreihe des IVT 90, ETH Zürich, 1992. (in German).
- [105] M. Wölki, A. Schadschneider, and M. Schreckenberg. Asymmetric Exclusion Processes with Shuffled Dynamics. *J. Phys. A: Math. Gen.*, 39:33–44, 2006. DOI:10.1088/0305-4470/39/1/003.
- [106] D. Helbing, I.J. Farkas, P. Molnar, and T. Vicsek. Simulation of Pedestrian Crowds in Normal and Evacuation Situations. In Schreckenberg and Sharma [215], pages 21–58. ISBN:3-540-42690-6.
- [107] D. Helbing, I.J. Farkas, and T. Vicsek. Freezing by Heating in a Driven Mesoscopic System. *Phys. Rev. Lett.*, 84:1240, 2000. DOI:10.1103/PhysRevLett.84.1240.
- [108] H.C. Muir, D.M. Bottomley, and C. Marrison. Effects of Motivation and Cabin Configuration on Emergency Aircraft Evacuation Behavior and Rates of Egress. *Intern. J. Aviat. Psych.*, 6:57–77, 1996. DOI:10.1207/s15327108ijap0601_4.
- [109] W.M. Predtetschenski and A.I. Milinski. *Personenströme in Gebäuden . Berechnungsmethoden für die Projektierung*. Verlagsgesellschaft Rudolf Müller, Köln-Braunsfeld, 1971. ISBN:3-481-16844-6, (in German, translation from Russian).
- [110] D. Helbing, R. Jiang, and M. Treiber. Analytical Investigation of Oscillations in Intersecting Flows of Pedestrian and Vehicle Traffic. *Phys. Rev. E*, 72(046130), Jul 2005. DOI:10.1103/PhysRevE.72.046130.
- [111] W.W. Daniel. *Applied Nonparametric Statistics*. Wadsworth Publishing, 2nd edition, 1989. ISBN:0-534-38194-4.
- [112] J.V. Bradley. *Distribution-Free Statistical Tests*, chapter 12, pages 271–282. Prentice Hall, 1968. ISBN:0-132-16259-8.
- [113] J. Gillis. Correlated Random Walk. *Proc. Camb. Phil. Soc.*, 51:639–651, 1955.
- [114] A. Chen and E. Renshaw. The Gillis-Domb-Fisher Correlated Random Walk. *Journal of Applied Probability*, 29:792–813, 1992. DOI:10.2307/3213286.
- [115] N. Konno. Limit Theorems and Absorption Problems for One-dimensional Correlated Random Walks. *ArXiv Quantum Physics e-prints*, October 2003. OAI:arXiv.org:quant-ph/0310191.
-

-
- [116] N. Guillotin-Plantard. Gillis' Random Walks on Graphs. *J. App. Prob.*, 42:295–301, 2005. DOI:10.1239/jap/1110381390.
- [117] M. Muramatsu, T. Irie, and T. Nagatani. Jamming transition in pedestrian counter flow. *Physica A*, 267:487–498, May 1999. DOI:10.1016/S0378-4371(99)00018-7.
- [118] V.J. Blue and J.L. Adler. Flow Capacities from Cellular Automata Modelling. In Schreckenberg and Sharma [215], pages 115–121. ISBN:3-540-42690-6.
- [119] U. Max and C. Lebeda. *Referenzhandbuch MRFC*. Arbeitsgemeinschaft Brandsicherheit (AGB), Bruchsal/Wien, 1998. (in German).
- [120] D.A. Purser. Occupant Behaviour and Toxic Fire Hazards in Engineering Design of Buildings. Garston, Watford, England, UK, 2004.
- [121] D.A. Purser. *Toxicity Assessment of Combustion Products*, chapter 2-6, pages 2.83–2.171. Volume 1 of , DiNenno [216], 3rd edition, 2002. ISBN:0-877-65451-4.
- [122] DIN. DIN 5056.1.
- [123] J. Dollard, L.W. Doob, N.E. Miller, O.H. Mowrer, and R.R. Sears. *Frustration and Aggression*. Greenwood Publishing Group, 1980. ISBN:0-313-22201-0.
- [124] H. Klüpfel, T. Meyer-König, and M. Schreckenberg. Comparison of an Evacuation Exercise in a Primary School to Simulation Results. In Fukui et al. [214], pages 549–554. <http://www.traffgo-ht.com/downloads/research/bypass/evakuebung-rahm-en.pdf>.
- [125] A. Keßel, H. Klüpfel, and T. Meyer-König, 2000.
- [126] DWD. online, 2000. <http://www.wetterzentrale.de/archive/k1/2000/20000731.png>.
- [127] J.J. Fruin. *Pedestrian planning and design*. Metropolitan Association of Urban Designers and Environmental Planners, New York, USA, 1971.
- [128] H. Frantzich. *Study of movement on stairs during evacuation using video analysing techniques*. Department of Fire Safety Engineering, Lund Institute of Technology, Lund University, March 1996.
- [129] T. Fujiyama and N. Tyler. Pedestrian Speeds on Stairs - An Initial Step for a Simulation Model. In *Proceedings of 36th Universities Transport Studies Group Conference*, Life Science Centre, Newcastle upon Tyne, UK, January 2004. http://eprints.ucl.ac.uk/archive/00001241/01/2004_19.pdf.
- [130] E. Graat, C. Midden, and P. Bockholts. Complex evacuation; effects of motivation level and slope of stairs on emergency egress time in a sports stadium. *Safety Science*, 31:127–141, 1999. DOI:10.1016/S0925-7535(98)00061-7.
-

-
- [131] K.E. Boyce, T.J. Shields, and G.W.H. Silcock. Toward the Characterization of Building Occupancies for Fire Safety Engineering: Capabilities of Disabled People Moving Horizontally and on an Incline. *Fire Technology*, 35:64, 1999. DOI:10.1023/A:1015335132296.
- [132] J. Templer. *The Staircase*. MIT Press, Massachusetts, USA, 1992. ISBN: 0-262-70057-3.
- [133] M. Isobe, T. Adachi, and T. Nagatani. Experiment and simulation of pedestrian counter flow. *Physica A*, 336:638–650, 2004. DOI:10.1016/j.physa.2004.01.043.
- [134] R. Nagai, M. Fukamachi, and T. Nagatani. Experiment and simulation for counterflow of people going on all fours. *Physica A*, 358:516–528, Dec 2005. DOI:10.1016/j.physa.2005.04.024.
- [135] M. Fukui and Y. Ishibashi. Self-Organized Phase Transitions in Cellular Automaton Models for Pedestrians. *Journal of the Physical Society of Japan*, 68(8): 2861–2863, Aug 1999. DOI:10.1143/JPSJ.68.2861.
- [136] D. Helbing. Traffic and related self-driven many-particle systems. *Rev. Mod. Phys.*, 73(4):1067–1141, Dec 2001. DOI:10.1103/RevModPhys.73.1067.
- [137] V.J. Blue and J.L. Adler. Cellular Automata Microsimulation For Modeling Bi-Directional Pedestrian Walkways. *Transportation Research B*, 35(293), 2001. DOI: 10.1016/S0191-2615(99)00052-1.
- [138] S.A.H. AlGadhi, H.S. Mahmassani, and R. Herman. A Speed-Concentration Relation for Bi-Directional Crowd Movements with Strong Interaction. In Schreckenberg and Sharma [215], pages 3–20. ISBN:3-540-42690-6.
- [139] Y. Tajima, K. Takimoto, and T. Nagatani. Pattern formation and jamming transition in pedestrian counter flow. *Physica A*, 313:709–723, 2002. DOI: 10.1016/S0378-4371(02)00965-2.
- [140] A. John, A. Schadschneider, D. Chowdhury, and K. Nishinari. Collective effects in traffic on bi-directional ant trails. *Journal of Theoretical Biology*, 231:279–285, 2004. DOI:10.1016/j.jtbi.2004.06.022.
- [141] S. Klumpp and R. Lipowsky. Phase transitions in systems with two species of molecular motors. *Europhys. Lett.*, 66:90–96, 2004. DOI:10.1209/epl/i2003-10155-6.
- [142] M.R. Evans, D.P. Foster, C. Godrèche, and D. Mukamel. Spontaneous Symmetry Breaking in a One Dimensional Driven Diffusive System. *Phys. Rev. Lett.*, 74: 208–211, 1995. DOI:10.1103/PhysRevLett.74.208.
- [143] S.P. Hoogendoorn and W. Daamen. Pedestrian Behavior at Bottlenecks. *Transportation Science*, 39(2):147–159, May 2005. DOI:10.1287/trsc.1040.0102.
-

-
- [144] V. Popkov, L. Santen, A. Schadschneider, and G.M. Schütz. Empirical evidence for a boundary-induced nonequilibrium phase transition. *J. Phys. A: Math. Gen.*, 34(6):L45–L52, 2001. DOI:10.1088/0305-4470/34/6/103.
- [145] R. Barlovic, T. Huisinga, A. Schadschneider, and M. Schreckenberg. Open boundaries in a cellular automaton model for traffic flow with metastable states. *Phys. Rev. E*, 66(4):046113, Oct 2002. DOI:10.1103/PhysRevE.66.046113.
- [146] B.S. Kerner and S.L. Klenov. Probabilistic Breakdown Phenomenon at On-Ramp Bottlenecks in Three-Phase Traffic. *ArXiv Condensed Matter e-prints*, 2005. OAI:arXiv.org:cond-mat/0502281.
- [147] S. Yamamoto, S. Hieida, and S. Tadaki. Effects of Bottlenecks in Vehicle Traffic. *ArXiv Physics e-prints*, 2006. OAI:arXiv.org:physics/0604072.
- [148] S. Sreenivasan, R. Cohen, E. López, Z. Toroczkai, and H.E. Stanley. Communication Bottlenecks in Scale-Free Networks. *ArXiv Computer Science e-prints*, 2006. OAI:arXiv.org:cs/0604023.
- [149] S.A. Janowsky and J.L. Lebowitz. Finite-size effects and shock fluctuations in the asymmetric simple-exclusion process. *Phys. Rev. A*, 45(2):618–625, Jan 1992. DOI:10.1103/PhysRevA.45.618.
- [150] S. Klumpp and R. Lipowsky. Asymmetric simple exclusion processes with diffusive bottlenecks. *Phys. Rev. E*, 70(066104), 2004. DOI:10.1103/PhysRevE.70.066104.
- [151] M. Nei, T. Maruyama, and R. Chakraborty. The Bottleneck Effect and Genetic Variability in Populations. *JSTOR*, 29(1):1–10, 1975. DOI:10.2307/2407137.
- [152] T. Rupprecht. Untersuchung zur Erfassung der Basisdaten von Personenströmen. Master’s thesis, Bergische Universität Wuppertal, FB D - Abt. Sicherheitstechnik, 2005. (in German) <http://www.fz-juelich.de/zam/ZAMPeople/seyfried-teaching>. Some results were published in English in [159].
- [153] R. Nagai, M. Fukamachi, and T. Nagatani. Evacuation of crawlers and walkers from corridor through an exit. *Physica A*, 367:449–460, Jul 2006. DOI:10.1016/j.physa.2005.11.031.
- [154] T. Itoh and T. Nagatani. Optimal admission time for shifting the audience. *Physica A*, 313:695–708, Oct 2002. DOI:10.1016/S0378-4371(02)00979-2.
- [155] Y. Tajima, K. Takimoto, and T. Nagatani. Scaling of pedestrian channel flow with a bottleneck. *Physica A*, 294:257–268, May 2001. DOI:10.1016/S0378-4371(01)00109-1.
- [156] Y. Tajima and T. Nagatani. Scaling behavior of crowd flow outside a hall. *Physica A*, 292:545–554, Mar 2001. DOI:10.1016/S0378-4371(00)00630-0.
-

-
- [157] D. Helbing, M. Isobe, T. Nagatani, and K. Takimoto. Lattice gas simulation of experimentally studied evacuation dynamics. *Phys. Rev. E*, 67(067101), 2003. DOI:10.1103/PhysRevE.67.067101.
- [158] W. Daamen, S.P. Hoogendoorn, and P.H.L. Bovy. First-order Pedestrian Traffic Flow Theory. *Transportation Research Board Annual Meeting*, pages 1–14, 2005. <http://www.pedestrians.tudelft.nl/publications/TRB05d%20tft.pdf>.
- [159] A. Seyfried, T. Rupperecht, O. Passon, B. Steffen, W. Klingsch, and M. Boltes. New insights into pedestrian flow through bottlenecks. *ArXiv Physics e-prints*, 2007. OAI:arXiv.org:physics/0702004.
- [160] D. Helbing, L. Buzna, A. Johansson, and T. Werner. Self-Organized Pedestrian Crowd Dynamics: Experiments, Simulations, and Design Solutions. *Transportation Science*, 39(1):1–24, 2005. DOI:10.1287/trsc.1040.0108.
- [161] A. Mintz. Non-adaptive Group Behavior. *Journal of Abnormal and Normal Social Psychology*, 46:150–159, 1951.
- [162] D. Helbing, I. Farkas, and T. Vicsek. Simulating dynamical features of escape panic. *Nature*, 407:487–490, 2000. DOI:10.1038/35035023.
- [163] Argebau - Fachkommission Bauaufsicht. *Musterverordnung über den Bau und Betrieb von Versammlungsstätten (Muster-Versammlungsstättenverordnung – MVStättV)*, June 2005. <http://www.versammlungsstaettenverordnung.de/>.
- [164] S. Nusser, 2006. Data produced by Germanischer Lloyd (GL) for the PeSOS project. The corresponding diagrams have been published first on the PeSOS-Homepage: <http://www.ptt.uni-duisburg.de/projekte/pesos/>.
- [165] J. Waś, B. Gudowski, and P.J. Matuszyk. New Cellular Automata Model of Pedestrian Representation. In El Yacoubi et al. [222], pages 724–727. ISBN: 3-540-40929-7.
- [166] E.T. Hall. *The Silent Language*. Anchor Books, New York, 1959. ISBN: 0-313-22277-0.
- [167] E.T. Hall. *The Hidden Dimension*. Anchor Books, New York, 1966. ISBN: 0-844-66552-5.
- [168] AP. Major Stadium Disasters. *CNN Sports Illustrated*, 5 2001. http://sportsillustrated.cnn.com/soccer/world/news/2000/07/09/stadium_disasters_ap/.
- [169] Emergency & Disaster Management Inc. Sports Disasters. *www.emergency-management.net*, 2004. http://www.emergency-management.net/sport_ev.htm.
- [170] Hamburg-Mannheimer. Schreckenstage. *Die Zeit*, 28, 7 2004. (in German) http://www.zeit.de/2004/28/G-Beist_9fck-Sportevents.
-

-
- [171] Crowd Management Strategies. Crowd Management Strategies - The Rock'n'Roll Wall of Shame. *www.crowdsafe.com*, 2004. URL: <http://www.crowdsafe.com/thewallmemorials.html>.
- [172] Crowd Dynamics. Crowd Disasters. *www.crowddynamics.com*, 2004. <http://www.crowddynamics.com/Main/Crowddisasters.html>.
- [173] BBC. Manila stadium stampede kills 73. *BBC news*, 2 2006. <http://news.bbc.co.uk/2/hi/asia-pacific/4680040.stm>.
- [174] M. Wolf. Schockierende Szenen am Südtor. *Berliner Zeitung*, 4 2005. (in German) <http://www.berlinonline.de/berliner-zeitung/archiv/.bin/dump.fcgi/2005/0425/sport/0035/index.html>.
- [175] Unknown author(s). Viermal die rote Karte. *Stiftung Warentest*, 2006. (in German).
- [176] L. Clarke. Panic: Myth or Reality? *contexts*, 1(3), 2002. http://www.contextsmagazine.org/content_sample_v1-3.php.
- [177] J.L. Bryan. *Smoke as a Determinant of Human Behavior in Fire Situations (project people)*. National Bureau of Standards, University of Maryland, Washington, DC, 1977. Report No. NBS-GCR-77-94.
- [178] P.G. Wood. The Behaviour of People in Fires. *Fire Research Note*, 953, 1972.
- [179] J.P. Keating and E.F. Loftus. The logic of fire escape. *Psychology Today*, 15:14–19, 1981.
- [180] G. Ramachandran. Human behavior in fires: a review of research in the United Kingdom. *Fire Technology*, 26(2):149–155, 1990. DOI:10.1007/BF01040179.
- [181] E.L. Quarantelli. Panic Behavior in Fire Situations: Findings and a Model from the English Language Research Literature. In *Proceedings of the 4th Joint Panel Meeting, The U.J.N.R. Panel on Fire Research and Safety Tokyo: Building Research Institute*, pages 405–428, 1981.
- [182] V. Gallese, L. Fadiga, L. Fogassi, and G. Rizzolatti. Action Recognition in the Premotor Cortex. *BRAIN*, 119(2):593–609, 1996. DOI:10.1093/brain/119.2.593.
- [183] G. di Pellegrino, L. Fadiga, L. Fogassi, V. Gallese, and G. Rizzolatti. Understanding Motor Events: A Neurophysiological Study. *Experimental Brain Research*, 91(1):176–180, 1992. DOI:10.1007/BF00230027.
- [184] G. Rizzolatti, L. Fadiga, V. Gallese, and L. Fogassi. Premotor Cortex and the Recognition of Motor Actions. *Brain research. Cognitive brain research.*, 3(2):131–141, 1996. DOI:10.1016/0926-6410(95)00038-0.
-

-
- [185] B. de Gelder, J. Snyder, D. Greve, G. Gerard, and N. Hadjikhani. Fear Fosters Flight: A Mechanism for Fear Contagion when Perceiving Emotion Expressed by a whole Body. *Proceedings of the National Academy of Sciences (PNAS)*, 101(47):16701–16706, November 2004. <http://www.pnas.org/cgi/reprint/101/47/16701.pdf>.
- [186] J. Bauer. *Warum ich fühle, was Du fühlst - Intuitive Kommunikation und das Geheimnis der Spiegelneurone*. Hoffmann und Campe, Hamburg, 2005. ISBN: 3-455-09511-9, (in German).
- [187] J.D. Sime. *The Concept of Panic*, chapter 5, pages 63–81. John Wiley & Sons Ltd., 1980.
- [188] C. Darwin. *The Descent of Man and Selection in Relation to Sex*. John Murray, London, 1st edition, 1871. <http://darwin-online.org.uk/>.
- [189] R.L. Trivers. The Evolution of Reciprocal Altruism. *Quarterly Review of Biology*, 46:35–37, 1971. DOI:10.1086/406755.
- [190] R. Axelrod. *The Evolution of Cooperation*. Basic Books, New York, NY, 1985. ISBN:0-465-02122-0.
- [191] R. Axelrod. *The Complexity of Cooperation*. Princeton University Press, Princeton, New Jersey, 1997. ISBN:0-691-01568-6.
- [192] R. Dawkins. *The Extended Phenotype*. Oxford University Press, Oxford, 1982. ISBN:0-192-88051-9.
- [193] R. Dawkins. *The Selfish Gene*. Oxford University Press, Oxford, 2nd edition, 1989. ISBN:0-192-17773-7.
- [194] W.D. Hamilton. The Genetical Evolution of Social Behaviour, I and II. *Journal of theoretical biology*, 7:1–52, 1964. DOI:10.1016/0022-5193(64)90038-4.
- [195] A.E. Emerson. *The Evolution of Adaptation in Population Systems*, pages 307–348. Chicago University Press, Chicago, 1960. ISBN:0-226-79088-6.
- [196] V.C. Wynne-Edwards. *Evolution through group selection*. Blackwell Scientific Publications, Palo Alto, CA (USA), 1986. ISBN:0-632-01539-X.
- [197] G.C. Williams. *Adaption and Natural Selection: A Critique of Some Current Evolutionary Thought*. Princeton University Press, Princeton, NJ, 1996/1966. ISBN:0-691-02615-7.
- [198] D.S. Wilson and E. Sober. Re-Introducing Group Selection to the Human Behavioral Sciences. *Behavioral and Brain Sciences*, 17:585–654, 1994. preprint: <http://www.bbsonline.org/Preprints/OldArchive/bbs.wilson.html>.
-

-
- [199] E. Sober and D.S. Wilson. *Unto Others : The Evolution and Psychology of Unselfish Behavior*. Harvard University Press, Cambridge, Massachusetts, 1998. ISBN:0-674-93046-0.
- [200] D.S. Wilson. *Darwin's Cathedral : Evolution, Religion, and the Nature of Society*. University Of Chicago Press, Chicago, 2002. ISBN:0-226-90134-3.
- [201] H. Tajfel and J.C. Turner. *The Social Identity Theory of Intergroup Behavior*, pages 7–24. Nelson-Hall, Chicago,IL, 1986. ISBN:0-830-41075-9.
- [202] G.R. Price. Selection and Covariance. *Nature*, 227:520–521, 1970. DOI:10.1038/227520a0.
- [203] S.A. Frank. George Price's Contributions to Evolutionary Genetics. *J. theor. Biol.*, 175:373–388, 1995. DOI:10.1006/jtbi.1995.0148.
- [204] H. Tajfel. Experiments in Intergroup Discrimination. *Scientific American*, 223:96–102, 1970.
- [205] B. Simpson. Social Identity and Cooperation in Social Dilemmas. *Rationality and Society*, 18:443, 2006. DOI:10.1177/1043463106066381.
- [206] J.C. Turner, M.A. Hogg, P.J. Oakes, S.D. Reicher, and M.S. Wetherell. *Rediscovering the social group. A Self-Categorization Theory*. Basil Blackwell, New York, NY, 1987. ISBN:0-631-14806-X.
- [207] M. Breusch. Die Brandkatastrophe von West Warwick, Rhode Island. *Rock Hard Magazine*, 192, 2003. http://www.rockhard.de/home.php3?rubrik=1&grafik=1&inc=detail_147.inc&ihid=30696&suche=1.
- [208] C. Grant and P. Pagni, editors. *Fire Safety Science - 1st international Symposium Proceedings*, 1985. The International Association for Fire Safety Science, Interscience Communications Ltd, West Yard House, Guildford Grove, London. ISBN:0-891-16456-1.
- [209] T. Wakamatsu, Y. Hasemi, A. Sekizawa, P. Seeger, C. Grant, and P. Pagni, editors. *Fire Safety Science - 2nd international Symposium Proceedings*, 1988. The International Association for Fire Safety Science, Interscience Communications Ltd, West Yard House, Guildford Grove, London. ISBN:0-89116-864-8.
- [210] T. Kashiwagi, editor. *Fire Safety Science - 4th international Symposium Proceedings*, 1994. The International Association for Fire Safety Science, Interscience Communications Ltd, West Yard House, Guildford Grove, London. ISBN:1-88627-900-4.
- [211] D.E. Wolf, M. Schreckenberg, and A. Bachem, editors. *Traffic and Granular Flow*, Jülich, 1996. World Scientific Publishing. ISBN:981-02-2635-7.
-

-
- [212] D.E. Wolf and M. Schreckenberg, editors. *Traffic and Granular Flow '97*, Duisburg, 1998. Springer-Verlag Singapore. ISBN:981-3083-87-5.
- [213] D. Helbing, H.J. Herrmann, M. Schreckenberg, and D.E. Wolf, editors. *Traffic and Granular Flow '99*, Stuttgart, 2000. Springer-Verlag Berlin Heidelberg. ISBN:3-540-67091-2.
- [214] M. Fukui, Y. Sugiyama, M. Schreckenberg, and D.E. Wolf, editors. *Traffic and Granular Flow '01*, Nagoya, 2003. Springer-Verlag Berlin Heidelberg. ISBN:3-540-40255-1.
- [215] M. Schreckenberg and S.D. Sharma, editors. *Pedestrian and Evacuation Dynamics*, Duisburg, 2002. Springer-Verlag Berlin Heidelberg. ISBN:3-540-42690-6.
- [216] P. DiNenno, editor. *The SFPE Handbook of Fire Protection Engineering*, volume 1. National Fire Protection Association, One Batterymarch Park, Quincy, Massachusetts, USA, 3rd edition, 2002. ISBN:0-877-65451-4.
- [217] D. Evans, editor. *Fire Safety Science - 7th international Symposium Proceedings*, 2002. The International Association for Fire Safety Science, Interscience Communications Ltd, West Yard House, Guildford Grove, London.
- [218] S.P. Hoogendoorn, S. Luding, P.H.L. Bovy, M. Schreckenberg, and D.E. Wolf, editors. *Traffic and Granular Flow '03*, Delft, 2005. Springer-Verlag Berlin Heidelberg. ISBN:3-540-25814-0.
- [219] N. Waldau, P. Gattermann, H. Knoflacher, and M. Schreckenberg, editors. *Pedestrian and Evacuation Dynamics '05*, Vienna, 2006. Springer, Berlin. ISBN:3-540-47062-X.
- [220] A. Schadschneider, T. Pöschel, R. Kühne, M. Schreckenberg, and D.E. Wolf, editors. *Traffic and Granular Flow '05*, Berlin, 2007. Springer, Berlin. ISBN:3-540-47640-7.
- [221] R.D. Peacock and E.D. Kuligowski, editors. *Workshop on Building Occupant Movement During Fire Emergencies*, 2005. National Institute of Standards and Technology, Gaithersburg, MD.
- [222] S. El Yacoubi, B. Chopard, and S. Bandini, editors. *Cellular Automata - 7th International Conference on Cellular Automata for Research and Industry, ACRI 2006*, Perpignan, France, September 2006. Springer, Berlin Heidelberg. ISBN:3-540-40929-7.
- [223] K. Anijyo and P. Faloustos, editors. *Proceedings of the 2005 ACM SIG-GRAPH/Eurographics symposium on Computer animation*, New York, NY, USA, 2005. ACM Press. ISBN:1-7695-2270-X.
-

Ausblick

F.A.S.T.-Modell

Eine Hauptaufgabe wird eine effizientere Spurbildung und als Auswirkungen ein erhöhter Strom in Gegenstromsituationen sein. Es gibt eine Reihe von Möglichkeiten dieses Ziel zu erreichen. Spurbildung mit $v_{max} = 1$ in einem rechteckigen Korridor und mit einer von der Laufrichtung abhängigen a-priori-Aufteilung der Agenten in zwei Spezies wurde bereits in [28] demonstriert. Ein nahe liegender Versuch wäre daher eine Verallgemeinerung dieser Methode, so dass sie auch in komplexeren Geometrien und bei höheren Geschwindigkeiten funktioniert. Im Detail könnte die Integration eines expliziten „Follow-the-leader“-Mechanismus den gewünschten Erfolg bringen. Ein solcher Ansatz würde das dynamische Bodenfeld ergänzen. Der Unterschied läge darin, dass im Konzept des dynamischen Bodenfeldes hauptsächlich große Gruppen von Agenten andere Agenten beeinflussen, bei einem „Follow-the-leader“-Mechanismus explizit jedoch 1:1-Wechselwirkungen vorliegen.

Im Bezug auf das dynamische Bodenfeld kann man sich eine Reihe von Varianten vorstellen, die in dieser Arbeit nicht untersucht wurden. Was würde sich ändern, wenn das dynamische Bodenfeld nicht nur die Ursprungszellen, sondern auch Zwischen- und Zielzellen beeinflussen würde? Wie würde sich Diffusion über mit größeren Geschwindigkeiten bemerkbar machen?

Eine weitere mögliche Erweiterung des F.A.S.T.-Modells, die ebenfalls Auswirkungen auf Gegenstromsituationen-Situationen haben könnte, jedoch von allgemeinerem Interesse ist, ist eine detailliertere Ausarbeitung der Abstoßung zwischen den Agenten. Eine Ausweitung des Einflusses der bloßen Anwesenheit auf einer Zelle auf eine größere Zellnachbarschaft könnte ein kontinuierlicher Weg hin zu einer de facto feineren räumlichen Diskretisierung sein, ohne dass man die Vorteile aufgeben müsste, die das Eine-Zelle-Ein-Agent Prinzip mit sich bringt und ohne mit den konzeptionellen Schwierigkeiten [90] kämpfen zu müssen, die eine tatsächliche feinere Diskretisierung mit sich bringt. Solcherart „mitbewegte Potentiale“ oder gar „vorauslaufende Potentiale“ könnten in einem weiteren Schritt von der Bewegungsrichtung abhängig gemacht werden. In Bewegungsrichtung wäre die Abstoßung größer („Bugwelle“), im Rücken der Agenten könnte sie sogar als attraktive Wechselwirkung („Windschatten“) konstruiert sein, was einer Art impliziten „Follow-the-leader“-Prinzip nahe käme und weder eine absolut reine 1:1-Wechselwirkung wäre, noch an das Vorhandensein großer Zahlen von Agenten gebunden, sondern eine Wechselwirkung zwischen wenigen Agenten in mehr oder weniger unmittelbarer Nachbarschaft wäre. Eine weitere Idee in diesem Zusammenhang ist die Berücksichtigung der ellipsenähnlichen menschlichen Körperform sowie von „sozialen Abständen“ [64, 165–167].

Wie die Abstoßung zwischen den Agenten könnte auch der Algorithmus zur Wahl eines Ausgangs verfeinert werden. Als Beispiel seien nur einige der zahlreichen Möglichkeiten genannt:

- Dem statischen Bodenfeld eines Ausgangs könnte eine Anfangshöhe gegeben werden. Dies würde die Attraktivität dieses Ausgangs verstärken oder abschwächen.
- Neben dem Abstand zum Ausgang könnte auch die Breite desselben einen Einfluss auf die Wahl haben. Da ein schmaler Ausgang mitunter zu der Vermutung führen könnte, dass sich dort eher Stauungen bilden als vor einem breiten Ausgang.
- Für Agenten, die über mehrere Runden hinweg gezwungen sind, sich langsamer als mit v_{max} zu bewegen, könnte die Wahrscheinlichkeit erhöht werden, dass sie in der nächsten Runde einen anderen Ausgang wählen.
- Gleiches gilt für den Fall, dass ein Agent von einer hohen Agentendichte umgeben ist.

Der Ausgangswahlprozess ist kein Teil der elementaren Dynamik des Systems. Aus diesem Grund liegt diese Fragestellung ein wenig abseits des Themas dieser Arbeit und solcherlei Überlegungen wurden nicht umgesetzt. Dies ändert nichts an der Tatsache, dass ein realistisches Modell des Ausgangswahlprozesses für realistische Simulationen notwendig ist.

Die Diskrepanz für hohe Dichten zwischen Simulation und empirischen Daten in den Abbildungen 3.41 und 3.42 wird sicherlich Gegenstand zukünftiger Forschung sein, sowohl theoretischer als auch empirischer Art.

Besonders die Untersuchung der Oszillationen an Engstellen in Unterabschnitt 3.2.10 zeigt, dass manchmal realistische Resultate nur mit Parametern erreicht werden, die sonst allenfalls für extreme Situationen geeignet wären. Es erscheint unerlässlich, einen Einfluss der lokalen Umgebung auf die Parameter zuzulassen, um in beliebigen Situationen und Szenarien realistische Resultate erzielen zu können. Es ist wohl eine große Herausforderung, einen schnellen Algorithmus zu erstellen, der beispielsweise k_S automatisch reduziert, falls ein Agent, sich einer solchen Engstelle nähert, diese auch tatsächlich passieren will, wohingegen dies bei einem anderen Agent, der das nicht möchte nicht passiert. Einfacher wäre es, solche Bereiche vom Benutzer der Simulation von Hand kennzeichnen zu lassen. Der ausschließlich räumlicher Charakter dieser Lösung würde jedoch das Problem noch nicht lösen, dass für Agenten am gleichen Ort mit unterschiedlichen Plänen unterschiedliche Parameter realistisch sind.

In Unterabschnitt B.1 werden einige neuere Fortschritte in der Forschung zur „Ansteckung“ von Emotionen, insbesondere Angst, in Menschenmengen erwähnt. Zum heutigen Tag scheint es so zu sein, dass im Wesentlichen der Einfluss der Beobachtung anderer Menschen auf die Hirnaktivität systematisch untersucht wurde. Es scheint noch recht wenig gesicherte Kenntnisse über den Einfluss auf das Verhalten zu geben. Dennoch ist es nicht ausgeschlossen, dass Hirnforschung und Psychologie zukünftig zu Resultaten kommen werden, die in Personenstromsimulationen Berücksichtigung finden können. Für

das F.A.S.T.-Modell könnte dies beispielsweise bedeuten, dass der Reibungsparameter μ nicht mehr statisch und für alle Agenten gleich sondern veränderlich ist.

Von größerem Interesse für den Anwender als den Wissenschaftler ist die Berücksichtigung weiterer spezieller struktureller Elemente wie Aufzüge, Rolltreppen, verschiedene Arten von Türen, wie z.B. Drehtüren in das F.A.S.T.. Daneben können die Elemente, die bereits aufgenommen wurden ebenfalls weiter ausgearbeitet werden. Das Zusammenspiel von Treppen und Wänden ist hierfür ein Beispiel: Während beim Gehen in der Ebene eher Abstand von Wänden gehalten wird, rufen Handläufe auf Treppen genau das gegenteilige Verhalten hervor.

Experimente und Beobachtungen

Im Hinblick auf Treppen wäre die Verteilung von Pausenhäufigkeiten auf langen Treppen eine interessante Observable. Die Anzahl der Stufen, die freiwillig ohne Pause aufwärts gelaufen werden und die Dauer der Pausen dazwischen könnten einen Hinweis auf eine sinnvolle Begrenzung einer Treppenlänge nach oben hin geben, um im Evakuierungsfall keine zusätzlichen Schwierigkeiten durch die Treppenlänge zu bekommen. Weiterhin wären interessante Messgrößen a) ein vollständiges Fundamentaldiagramm bei gegebener Länge einer Treppe und b) die Abhängigkeit der Laufgeschwindigkeit von der Treppenlänge. Zusätzlich könnte man - ähnlich wie in der Ebene - nach der Abhängigkeit der Geschwindigkeit oder des Flusses von der Treppenbreite fragen.

Die große Zahl von Einflüssen auf den Ausgang eines Fußgängerexperimentes oder eine solche Beobachtung, lässt eine große Zahl Wiederholungen von identischen bzw. ähnlichen Experimenten wünschenswert erscheinen. Nur auf diese Weise wird es möglich sein die Einflüsse der unterschiedlichen Faktoren (Alter, Temperatur, Tageszeit, etc.) auf elementare Größen wie die freie Geschwindigkeit oder auch weniger gut fassbare Einflüsse, wie z.B. die Tendenz zur Aggression oder Kooperation, voneinander zu trennen.

Bei den in dieser Arbeit präsentierten Experimenten wäre eine Wiederholung mit deutlich älteren Teilnehmern und/oder einer heterogeneren Gruppe sicher ein nahe liegender erster Schritt. Was würde sich ändern, wenn die Teilnehmer Gepäckstücke bei sich trügen?

Beim Gegenstromexperiment wäre eine Variation der Breite nicht nur in Bezug auf den Fluss, sondern auch auf die Zahl der auftretenden Spuren, interessant. Weiterhin wäre es interessant ein ähnliches Experiment mit zyklischen Randbedingungen (Ring) und konstanter globaler Dichte durchzuführen. Mehr Resultate zur Rechts-Links-Asymmetrie und ein Vergleich mit Resultaten in Ländern mit Linksverkehr, könnte das Interesse auch von anderen als Fußgängerforschern auf sich ziehen.

Im Engstellenexperiment ist die Tiefe der Engstelle von Interesse. Würde sie über 40 cm erhöht, käme man in den Bereich eines Korridorexperimentes, würde sie reduziert, wäre man im Bereich typischer Türrahmentiefen.

Den maximal möglichen Fluss durch eine Engstelle könnte man in einem Experiment messen, bei dem die Teilnehmer auf zwei gleich große Gruppen verteilt werden und der Lohn für die Experimentteilnehmer für die schnellere Gruppe größer ist.

List of Figures

2.1	Rule table for CA-184 - The state of three cells determines the state of the center cell for the next round in the given way.	6
2.2	Compacted rule table for CA-184. Cells where the state does not matter (logical OR) are split diagonally.	6
2.3	Cell-oriented formulation of the deterministic $v_{max} = 2$ version of the Nagel-Schreckenberg model. A white cell does not contain a car. The different speeds are represented by red ($v = 0$), yellow ($v = 1$) and green ($v = 2$)	8
2.4	Color table for black and white copies of this work.	8
2.5	Cell-oriented formulation of the $v_{max} = 1$ version of the Nagel-Schreckenberg model. The brackets enclose alternatives of which one is chosen probabilistically. In cases where dawdling is possible, the state of two cells is fixed for the next round.	8
2.6	Cell-oriented formulation of the probabilistic $v_{max} = 2$ version of the Nagel-Schreckenberg model. Of the elements in the lower line, the left version is chosen with probability p and the right with $1 - p$	9
3.1	Structure of one round.	12
3.2	von Neumann- and Moore-neighborhood ($v_{max} = 1$).	13
3.3	Example: Complete neighborhoods for $v_{max} = 2$	14
3.4	Example: Complete neighborhoods for $v_{max} = 3$	14
3.5	Example for calculating $v(\phi)$ for one of the $v_{max} = 3$ neighborhoods. The gray number within the black discs is the index i	16
3.6	Example for the $v(\phi)$ dependence. ($v_{max} = 2$; neighborhoods 4, 5 and 8 as shown in figure 3.3.)	17
3.7	A forbidden neighborhood and its five possible smoothed versions	22
3.8	Node generating neighborhoods. The state of split cells does not matter.	23
3.9	Static floor field calculated with Dijkstra's algorithm. The brighter a cell is, the larger is its distance toward the exit. The exit is in the center of the right edge	23
3.10	Example for calculating inertia.	26
3.11	Situations after 200 rounds starting in a 100x100 cells room with 500 agents and $k_P = 0$ (left) respectively $k_P = 1$ (right)	27
3.12	Variant 0 of cell blocking rules: Only the used cell gets blocked.	29
3.13	Variant 1 of cell blocking rules: The used cell and the next nearest neighbors orthogonal to the direction of motion get blocked.	29

3.14	Variant 2 of cell blocking rules: The used cell, the next nearest and the next-to-next nearest neighbors orthogonal to the direction of motion get blocked.	29
3.15	Variant 3 of cell blocking rules: All cells around the new position get blocked.	29
3.16	An agent's undisturbed path to his destination.	30
3.17	Three agents with destination cells and a possible sequence of steps in the full shuffle update scheme.	31
3.18	The specific fundamental diagram for $v_{max} = 1$, $v_{max} = 3$ and $v_{max} = 5$	33
3.19	Influence of the direction of motion on the average speed.	35
3.20	Comparison of two simulations with a crowd (black) moving to the center of a circle. The left image shows agents with $v_{max} = 1$ after 180, the right one agents with $v_{max} = 5$ after 36 rounds. In both cases there has been $k_S = 10.0$ and $k_P = 5$	35
3.21	Two routes: Route A contains horizontal and vertical, route B diagonal parts.	36
3.22	For horizontal motion there are three possibilities to move from A to D in two steps within a Moore neighborhood, and in the case of an integer-valued static floor field these paths often have an identical probability to be chosen. Yet for a diagonal path there is only one possibility.	37
3.23	On the left: Situation with an integer-valued static floor field. On the right: situation with real-valued static floor field. Both snapshots show the situation after 180 seconds. Initially the agents ($v_{max} = 1$) were spread randomly over a circle area.	38
3.24	On the left: Occupancy with an integer-valued static floor field. On the right: Occupancy with a real-valued static floor field. Initially the agents ($v_{max} = 1$) were spread randomly over a circle area. The darker the pixel, the more often the cell was occupied by an agent in 1200 runs of the simulation.	38
3.25	Single steps versus one large leap.	39
3.26	Comparison of average speeds for leap and for steps strategy.	41
3.27	Probability to move v cells forward for $v_{max} = 5$	42
3.28	The specific fundamental diagram for $k_S = 0.3$, $k_S = 1.0$ and $k_S = 3.0$	43
3.29	Directions and the dynamic floor field.	43
3.30	The specific fundamental diagram for $k_D = 0.0$ and $k_D = 0.8$, for which a significantly larger flux can be achieved.	44
3.31	A group of 82 agents moving around a corner. From left to right: $k_I = k_W = 0$; $k_I = 1$ $k_W = 0$; $k_I = 0$ $k_W = 1$; with $k_S = 1$ and $v_{max} = 5$ for all three simulations	46
3.32	The specific fundamental diagrams for $k_I = 0.0$ and $k_I = 0.8$	47
3.33	The specific fundamental diagrams for $k_W = 0.0$ and $k_W = 0.8$	48
3.34	The specific fundamental diagrams without and with inter-agent repulsion	48
3.35	Floor plan with intersecting paths.	49

3.36	The time the crossing process takes decreases dramatically with increasing k_P at small k_P	50
3.37	The specific fundamental diagram for $\mu = 0.0$ and $\mu = 0.6$. Friction reduces the flux for a broad range of densities.	51
3.38	Exit designs: The number of the floor plan is the sum of numbers of cells which are blocked by a wall.	51
3.39	Exit design 34 - Transitions at exit together with the transition probabilities. The left and central branches show how the initial configuration reappears as one agent leaves the scenario after some rounds dawdling more or less, while the right branch shows how the configuration goes back to its initial state because an agent moves back on his initial position, implying that no agent leaves the scenario. Please note that the arrows that lead back to the initial state do not imply a progression of one round in time, while the other arrows do so.	54
3.40	The specific fundamental diagram for the four cell blocking variants, as defined in figures 3.12 to 3.15	58
3.41	Comparison of two fundamental diagrams from simulations with the fundamental diagram that was fitted to a bunch of empirical data sets in [104]. All parameters that are not given explicitly are zero as in the standard set. The relative deviations are shown in figure 3.42.	59
3.42	Relative deviations (simulation results) / (fit to empirical data) of the fundamental diagrams of figure 3.41.	60
3.43	The “normal exit strategy” with only one row of exit cells at the true point of the exit leads to the smallest maximal outflow.	61
3.44	The “deep exit strategy” with up to $max(v_{max})$ (maximum of all agents) rows of exit cells at the true point of the exit leads to a slightly increased outflow.	62
3.45	The “attractor exit strategy” with up to $max(v_{max})$ rows of exit cells in front of an attractor that the agents head for increases the outflow even more.	62
3.46	The “extra floor exit strategy” leads to the largest outflow. Here an agent is counted as having escaped if he is on a cell with a static floor field value of five or less.	62
3.47	Evacuation times (averages and standard deviations of 1000 simulations for each scenario) from a corridor with a length of 125 cells (50 m) and a width of 5 cells (2 m). Note that the calculation is done to higher densities than in [76]. For comparison with the results of scenario 2 in [76] it is helpful to know that 4.0 persons per square meter is equivalent to 0.64 agents per cell.	63
3.48	Initial positions of the agents in the scenario. (schematic view)	64
3.49	Relative difference of the numerically calculated standard deviation for the number of steps into a certain direction for $n = 100$ steps against the theoretical thermodynamic limit ($n \rightarrow \infty$) of the same standard deviation in dependence of the probability p to continue motion in the same direction.	67

3.50	One of twelve possible situations after an agent has passed.	68
3.51	Average z -value for different α at $\delta = 0.03$	70
3.52	Average evacuation times for different α at $\delta = 0.03$	71
3.53	σ_A for different α at $\delta = 0.03$	71
3.54	Correlation coefficients for different α and event distance at $v_{max} = 1$. . .	72
3.55	Correlation coefficients for different α and event distance at $v_{max} = 3$. . .	72
3.56	Correlation coefficients for different α and event distance at $v_{max} = 5$. . .	73
3.57	Fundamental diagrams at $k_S = 1.0$ and $k_D = 0$	76
3.58	Fundamental diagrams at $k_S = 1.0$ and $k_D = 0.8$	77
3.59	Comparison of computation time and predicted evacuation times in dependence of the number of agents and at constant initial density.	78
3.60	A space plot. Red agents stand still, green move with maximal velocity. .	83
3.61	The dynamic floor field.	84
3.62	Local density (left) and intermediate range density averaged over $v_{max} = 5$ neighborhoods (right).	85
3.63	Absolute and relative occupancy.	85
3.64	Absolute and relative significant congestions. A significant congestion is given for red values larger 51 (of a maximum of 255) in the absolute significant congestion plot.	86
3.65	Absolute and relative frustration.	87
3.66	Absolute and relative blockage.	88
3.67	Evacuationgraph.	89
3.68	Distribution of evacuation times.	89
3.69	Average speed during the evacuation process. The averaging is done over the agents as well as over the simulation runs.	90
3.70	Average global flux during the evacuation process. The averaging is done over the agents as well as over the simulation runs.	91
3.71	Statistics of exit-group usage behavior	92
3.72	Statistics of exit usage behavior	93
3.73	A space plot which shows the incapacitation state in presence of fire and smoke and the color table of reasons for incapacitation. Agents that do not suffer incapacitation are colored white.	93
3.74	Risk of suffering incapacity if a person stands on a certain starting position due to $CO + HCN$ (left), CO_2 (center) and heat (right).	94
3.75	Development of the number of incapacitated agents with time.	94
3.76	Positions where persons pass the threshold to incapacitation.	95
4.1	Floor plan without furniture. The approximate camera perspectives are drawn in red, the number of persons as counted on the day of the exercise in each class room in blue.	98

4.2	Evacuation graphs of both runs. The pupils were counted, when they left the second floor and moved down the first step of the stairway between second and first floor. In the first run (without the music class) the pupils on the second floor except the music class had left the second floor some time before the pupils of the third floor arrived. In the second run the pupils from the third floor arrived before all pupils of the second floor had left the second floor, but there was some dawdling of two pupils without apparent reason, leading again to an - in this case smaller - plateau in the evacuation graph.	99
4.3	Comparison of empirical and simulation results. The simulations were done after the exercise, so this is not a prediction but a calibration of the simulation.	100
4.4	Comparison of empirical and simulation results for the second exercise. . .	101
4.5	Comparison of empirical and simulations results for the second building. In the second exercise there was one person more in the building.	102
4.6	The walking times were measured at the part of the 18 stairs at the right to the triangle-shaped door (platform to platform). The whole stairway had this design of an alternation of stairs and platforms.	104
4.7	Histogram of the horizontal speeds for category A.	107
4.8	Histogram of the horizontal speeds for category B.	107
4.9	Histogram of the horizontal speeds for category C.	108
4.10	The floor plan. The participants initially stood within the “Starting Area”, without further advises how they should arrange there. The positions of the cameras are marked with “CAM L”, “CAM C”, and “CAM R”, of which the latter one filmed from above and the other ones from the side. The distance between the cameras is 5 meter, the height of the cornice 0.98 meter and the width (without the extra space above the cornice) is 1.98 meter.	111
4.11	A snapshot from the experiment.	112
4.12	Passing times (part <i>i</i>). The first thing one observes in this and figure 4.13 is that the results vary significantly more in the presence of counterflow. Naturally this effect is most distinctive when the group is very small and the selection of the group members (e.g. due to varying body height) becomes important. It is a priori not obvious that for a counterflow situation the passing time increases linearly with the group size, as is in the case of no counterflow. Yet the results of the 50% counterflow situations (compare figure 4.13) justify this assumption and thus table 4.5.	113
4.13	Passing times (part <i>ii</i>).	114

-
- 4.14 Comparison of passing times of a majority group with approximately constant group size. Since the size of the majority group varied slightly, the times were scaled accordingly. This figure demonstrates the significant influence some counterflow has on the passing time. However, the influence is not that big as one might assume at first: imagining the group to occupy a rectangle with the width of the corridor in the case of no counterflow and half of the width of the corridor in the case of 0.5 counterflow, one might guess, that the passing time at a spot behind the central meeting point of the two groups doubles. In fact it only increases by roughly 43%. Compare figure 4.15. 116
- 4.15 Comparison of total times: The total time is the time between the passing of the starting line by the first person until the time of the passing of the finishing line by the last person. The first figure shows the total times of the majority group. The second figure exhibits an influence of the counterflow on the total time, which with an increase of approximately 34% from no to 0.5 counterflow is slightly smaller than the influence on the passing time (compare figure 4.14). The absolute value of the slope of the regressionline, however, is bigger than in the case of the passing times. The reason for this is, that there is a minimum time larger than zero for the total time, while the passing time can get very close to zero for very small groups. 117
- 4.16 Walking speeds (part *i*). For no or only small counterflow there is only a small or even no influence of the group size on the walking times. 118
- 4.17 Walking speeds (part *ii*). The group size has an influence on the walking speed of the last person in the case of 0.5 counterflow and in terms of the variation of results as well on the speed of the first person. 119
- 4.18 Walking speed factors (part *i*). This is the ratio of the time the first person needs to move from the starting to the finishing line by the same time the last person needs. Note that the last and first person may have changed on the way in some cases. For the majority group this ratio is if any then unrecognizably affected at 0.1 counterflow compared to no counterflow situations. For the minority group there is an effect denoting that some people (first of the minority group) may do better when walking against a flow than others (last of the minority group). 120
- 4.19 Walking speed factors (part *ii*). The walking speed factors outline, what has been foreshadowed in the walking speeds: the relative difference in the speed of the first and the last person is most distinctive for large groups and 0.5 counterflow. The figure for 0.34 counterflow shows, that the minority group in both cases is more affected than the majority group. 121
- 4.20 Specific fluxes (part *i*): Number of persons / (1.98 m · passing time). . . . 123
-

4.21	Specific fluxes (part <i>ii</i>): Number of persons / (1.98 m · passing time). As with the passing and total times, it also holds for the specific flux, that compared to no counterflow (compare figure 4.20) the performance in the 0.5 counterflow case is not reduced by a factor of two, but only by approximately a factor of 1.5 (slightly depending on the measurements taken for comparison).	124
4.22	Comparison of specific fluxes. All results and selections. The third figure shows the results of the largest majority groups that could be formed and significantly less dispersed results than the rest of the data set. At the finishing line the specific flux was found to reduce from approximately 1.2 (no counterflow) to 0.9 persons per meter and second (0.5 counterflow).	125
4.23	Comparison of the sum of specific fluxes. The sum of fluxes in counterflow situations is always larger than the flux in the no counterflow situations.	126
4.24	Histogram of the number of lanes. Only those runs were counted, where the number of lanes could be verified to be the same at CAM C and CAM R (compare figure 4.10).	127
4.25	Two, three and four lanes.	128
4.26	A snapshot from the recordings at a bottleneck width of 40 cm.	130
4.27	The original time gaps data (black “+”s) and from that data two smoothed functions (green and blue curves) and a regression following $\bar{T}_G(t) = a \exp(-bt) + c$ for the widths 40 and 120 cm. The numerical values for a , b , and c can be found in table 4.7. The smoothing of the blue and green curve has been done using a Gaussian weight dependent on the time distance between the considered point in time and the time of the time gap (see equation (4.2)).	133
4.28	Running averages with a sample size of five. The upper diagram includes data of just one run, while for the lower one at first an average of the i -th time gaps of all runs of a certain bottleneck width has been done. A data point at position (i/\bar{T}_G) therefore has the meaning, that the average of the time gaps $i - 4$ to i was \bar{T}_G	135
4.29	Total times for all runs.	136
4.30	Total times for bottleneck widths between 40 and 100 cm.	137
4.31	Fluxes for all runs.	137
4.32	Fluxes for bottleneck widths between 40 and 100 cm.	138
4.33	Specific fluxes for all runs.	139
4.34	Specific fluxes for bottleneck widths between 40 and 100 cm.	139
4.35	Average of specific fluxes.	140
4.36	Specific fluxes (from the “80 persons data”) for the six runs with a bottleneck width of 100 cm in the chronological order of the runs.	140
4.37	Two participants dawdling in front of a 70 cm bottleneck.	141
4.38	Distribution of time gaps: small bottleneck widths. The partitioning of the time gap categories is done such that each category contains two frames.	143
4.39	Distribution of time gaps: large bottleneck widths. The partitioning of the time gap categories is done such that each category contains two frames.	144

5.1	Plan of the Rochusclub area with numbers of exits (1-7) and names of grandstands (A-ZF). Higher floors are moved to the right. Black pixels mark free cells, white and dark green walls. Exits are marked light green. Floor exits are drawn cyan and floor entrances magenta.	150
5.2	Situation after 960 rounds. On the left with the current configuration, on the right with the optimized configuration	153
5.3	Two grandstands. Walkways are colored black	153
5.4	Occupancy: The corner in front the exit is not used efficiently.	155
5.5	A free corridor, four configurations of a corridor with an obstacle and a corridor which is narrowed on the full length.	155
5.6	Outer area of a large stadium. 12.145 spectators leave the grandstands by two corridors. They then can choose to leave the whole area by one of two exits: on the lower left and on the bottom right corner. Both images are snapshots from ten minutes after the beginning of the evacuation process. In the left simulation all agents were sent to the left exit, which is closer to all of the agents' starting positions within on the grandstands. In the right simulation the agents distributed equally on the two exits, increasing the average path length but also the used capacity. Note: The interior of the stadium was explicitly not subject to the study and intentionally kept as simple as possible.	156
5.7	The passengers initially were spread randomly over the black area (cabin). The gray area marks free cells, which are not allowed as starting positions.	158
5.8	Each color marks a different fire sector. Black areas are assumed to be free of combustion products. The burning cabin is marked red.	158
5.9	The conditions in the burning cabin do not allow survival shortly after the flash over. Based on data by [164].	159
5.10	Incapacitation only occurred 22 seconds after the flash over and only in the burning cabin.	159
5.11	Expectation values for the number of incapacitated persons in dependence of the awakening probability p for different cabin occupation numbers n . .	160
B.1	Schematic view of (some of) the factors that influence the behavior during emergency situations. Note that other factors of which some are stated above as for example the degree of relatedness (kin selection) of the whole or parts of the group have an influence as well.	183
C.1	Participant statistics.	188
C.2	Results of the participant poll.	189
D.1	Participants' statistics.	191
D.2	Participant poll.	192

List of Tables

3.1	Names and squared maximal distances of the neighborhoods.	15
3.2	Average speeds and relative deviations (by angle) for all complete neighborhoods up to $v=10$	19
3.3	Selected neighborhoods.	20
3.4	One quarter of the assignment “Neighboring cell \rightarrow maximum speed”. (An agent with maximum speed v_{max} can reach all cells with a number $\leq v_{max}$.)	20
3.5	Speed \rightarrow Stair speed assignment.	31
3.6	Scenarios and results.	34
3.7	Walking times in dependence of v_{max} and the chosen path.	36
3.8	Comparison of average speeds between many steps and one leap strategy for different k_S . See also figure 3.26.	41
3.9	Simulation parameters for guided and non-guided evacuations.	45
3.10	Simulation results for guided and non-guided evacuations.	45
3.11	Average evacuation times (100 runs) for a small and a large group moving around a corner. The distance to walk has been about four times longer for the large group. All evacuation times differ mutually by more than the sums of their standard deviations.	46
3.12	Evacuation times in dependence of friction and exit design.	52
3.13	Results of simulations without dynamic floor field.	69
3.14	Results of simulations with dynamic floor field and $v_{max} = 1$	69
3.15	Results of simulations with dynamic floor field and $v_{max} = 3$	70
3.16	Results of simulations with dynamic floor field and $v_{max} = 5$	70
3.17	Computation times and predicted evacuation time. Compare figure 3.59.	77
4.1	Empirical results of the exercise.	98
4.2	Overview of comparisons.	103
4.3	Basic Results. All speeds and standard deviations in m/s respectively stairs/s.	106
4.4	Horizontal walking speeds on a short stair.	106
4.5	Results of linear regressions for the dependence between passing time at the finishing line and group size, with and without forced inclusion of the offspring. n : number of persons. Note that a counterflow fraction of 0.90 denotes the minority group of an experiment with 10% counterflow. Compare figures 4.12 and 4.13.	115
4.6	The sequence of runs.	131

4.7	Results of a regression following equation (4.1) for the temporal evolution of the time gaps.	132
4.8	Averages, standard deviations, skewnesses, and kurtoses (defined such that the kurtosis of the normal distribution equals zero) of the time gaps.	145
5.1	Comparison of Current and Optimized Configuration.	151
5.2	Total evacuation times.	152
5.3	Single egress times.	152
5.4	Evacuation times.	154
5.5	Average individual egress times.	154
5.6	Averages of measured fluxes (in persons per second; minimum number of people in a measurement: 10) through two types of grandstand exits. Type of average 1): Sum of people of all measurements divided by sum of times of all measurements; Average type 2); Average of all fluxes, regardless of the number of people; Average type 3): Average of fluxes weighted by number of people.	154
5.7	Results	156
5.8	Results of 100 simulation runs (each).	157
A.1	Historical record of crowd disasters.	166
A.1	Historical record of crowd disasters (continued).	167
A.1	Historical record of crowd disasters (continued).	168
A.1	Historical record of crowd disasters (continued).	169
C.1	The sequence of runs.	190

Danksagung (Acknowledgments)

Ich danke an dieser Stelle zahlreichen Personen, die in allgemeiner oder auch spezieller Weise zum Gelingen dieser Arbeit beigetragen haben.

Der erste Dank gebührt Prof. Dr. Michael Schreckenbergr für die Bereitstellung des Themas, die Betreuung der Arbeit und die Leitung der Arbeitsgruppe „Physik von Transport und Verkehr“ in einer Weise, die ideale Arbeitsbedingungen garantiert.

Mein großer Dank gilt auch Dr. Hubert Klüpfel von der TraffGo HT GmbH und Prof. Dr. Andreas Schadschneider von der Universität zu Köln, mit denen ich während der gesamten Dauer der Arbeit immer wieder freundschaftliche und inspirierende Diskussionen geführt habe.

Auch die Diskussionen und Besprechungen mit den beiden anderen Mitglieder des „Ped-Nets“ - Christian Rogsch von der Bergischen Universität Wuppertal und Dr. Armin Seyfried vom Forschungszentrum Jülich - waren des immer wieder sehr hilfreich.

Im Rahmen des PeSOS-Projektes sei Rolf Nagel und Katharina Wortberg von der Flensburger Schiffbau Gesellschaft, Dr. Karsten Loer und Dr. Daniel Povel vom Germanischen Lloyd, Tim Meyer-König von der TraffGo HT, Gijs Streppel und Thomas Weigend von der Jos. L. Meyer Werft und Dr. Ralf Fiedler vom Projektträger Jülich für die gute Zusammenarbeit gedankt.

Ein herzliches Dankeschön geht an meine Kollegen - die aktuellen und ehemaligen Mitarbeiterinnen und Mitarbeiter, Doktoranden, Diplomandinnen, Praktikanten und Praktikantinnen und Studentinnen und Studenten der AG „Physik von Transport und Verkehr“ - gleichermaßen für die fachliche Zusammenarbeit wie für die freundschaftliche und humorvoll-gelöste Atmosphäre: Robert Barlović, Alexander Bernhart, Johannes Brüggmann, Thorsten Chmura, Roland Chrobok, Birgit Dahm-Courths, Christian Ehling, Anna Grünebohm, Lars-Christian Habel, Sigurdur Hafstein, Torsten Huisinga, Maike Kaufman, Frank Königstein, Sabine Knoche, Florian Mazur, Stephan Nies, Andreas Pottmeier, Mareike Quessel, Daniel Weber, Michael Wiedemann, Marko Wölki und Thomas Zaksek.

Jedem aufmerksamen Leser dieser Arbeit dürfte nicht verborgen geblieben sein, dass viele Teile der Arbeit nur mit tatkräftiger und informationeller Unterstützung vieler anderer Personen erstellt werden konnten. Da vieles davon keineswegs selbstverständlich war und Klarheit über alle Anteile anderer Personen an dieser Arbeit bestehen soll, ist es mir ein Bedürfnis und auch meine Pflicht folgende Personen in einem speziellen Bezug zu nennen:

- Bei der Auswertung der beiden Experimente war Anna Grünebohm eine große und sehr effektive Hilfe. Ohne Florian Mazurs Engagement bei der Planung und Durchführung des Experimentes in der Sportschule Wedau, wäre dieses nicht

möglich gewesen. Die Auswertung zur Spurbildung wurde von Maike Kaufman gemacht und ist auch Teil ihrer Diplomarbeit. In diesem Zusammenhang danke ich weiterhin besonders Mareike Quessel und Hubert Klüpfel. Mareike Quessel hat den Grundriss 4.10 erstellt und Hubert Klüpfel hat die Experimente fotografisch dokumentiert. Von ihm stammt das Bild 4.11. Weiterer Helfer dank bei den beiden Experimenten geht an Birgit Dahm-Courths, Christian Ehling, Lars-Christian Habel, Frank Königstein und Thomas Zaksek.

- Prof. Dr. Joachim Bauer (Universitätsklinikum Freiburg) danke ich für seine schnelle und freundliche Antwort auf meine Nachfrage zu seinem Buch.
 - Klaus Becker (Betreuender Architekt des niederländischen Pavillons der Expo 2000) danke ich für den freundlichen Kontakt und die Bereitstellung der Maße der Treppe.
 - Johannes Brüggemann möchte ich besonders für einen halben Tag des Ausharrens zwischen Taubenüberresten im Obergeschoss des Kölner Hauptbahnhofes danken, auch wenn sich diese Filmaufnahmen (noch) nicht verwerten ließen. Das war mit Abstand die größte Zumutung, die ich jemandem im Verlauf dieser Arbeiten angetan habe. In diesem Zusammenhang sei auch Herrn Geratewohl von der DB AG für die Drehgenehmigung und die unkomplizierte Zusammenarbeit gedankt.
 - Frau Dommers, Leiterin der Grundschule „Am Knappert“ in Duisburg-Rahm, und ihren Kolleginnen sowie dem Hausmeister Herrn te Paß danke ich für die gute und unkomplizierte Zusammenarbeit bei der in Sektion 4.1 beschriebenen Untersuchung der Feueralarmübung in der Grundschule „Am Knappert“. Bei der Dokumentation dieser Übung haben Frank Königstein, Florian Mazur und Mareike Quessel assistiert.
 - Alexander Jelen (Turnier-Direktor 2004) und Andreas Kühnel (betreuender Architekt) des ATP Turniers am Rochusclub danke ich für die gute Zusammenarbeit und Ermöglichung in Sektion 5.1 dargestellten Untersuchung und Ergebnisse. An den Filmaufnahmen waren Torsten Huisinga, Sabine Knoche, Frank Königstein, Florian Mazur, Andreas Pottmeier, Daniel Weber und Michael Wiedemann beteiligt.
 - Meinem Vater Georg Kretz danke ich für die sprachliche Durchsicht dieser Arbeit und allgemeine Hinweise zur englischen Sprache.
 - Michael Larisch (ASZ GmbH, Ahlen) danke ich für Hinweise auf den aktuellen Stand der Literatur zum Verhalten im Brandfall.
 - Dem „Feuerwehrmann“ und Freund aus Kindergarten Tagen Christoph Slaby danke ich für mehrere Hinweise zu den aktuellen Diskussionen in den Brandschutzfachkreisen.
 - Matthias Wolf (Berliner Zeitung) danke ich für die freundliche Bereitstellung von Informationen, die über seinen BZ-Artikel hinausgingen.
-

Zu guter letzt geht der größte Dank an meine Eltern Georg und Rita, sowie meine beiden Brüder Dominik und Sebastian. Wie es der Zufall will, nimmt Dominik in den Tagen der Fertigstellung dieser Arbeit sein Physikstudium auf. Ich wünsche ihm hierzu alles Gute.

Lebenslauf (Curriculum Vitae)

Persönliche Daten

Name: Tobias Kretz
Geboren am: 18. April 1978
Geboren in: 74821 Mosbach

Schulbildung

08/1988 – 06/1997 Schüler am Nicolaus-Kistner-Gymnasium in Mosbach. Abitur mit den Leistungskursen Mathematik und Physik.

Zivildienst

08/1997 – 08/1998 Zivildienst

Hochschulbildung

10/1998 – 10/2000 Grundstudium der Physik an der Universität Karlsruhe (TH). Vordiplom mit dem Nebenfach „Physikalische Chemie“.

05/2000 – 07/2003 Stipendiat des Cusanuswerkes.

10/2000 – 07/2003 Hauptstudium der Physik an der Universität Karlsruhe (TH) mit den Nebenfächern „Partielle Differentialgleichungen“ und „Allgemeine Relativitätstheorie“.

02/2001 – 11/2006 Stipendiat von e-fellows.net.

04/2002 – 07/2003 Anfertigung der Diplomarbeit mit dem Titel „Schwache Zerfälle schwerer Mesonen“ am „Institut für Theoretische Teilchenphysik“ (Prof. Dr. Kühn).

10/2003 – 10/2006 Anfertigung der vorliegenden Dissertation in der Arbeitsgruppe „Physik von Transport und Verkehr“ (Prof. Dr. Schreckenberg) an der Universität Duisburg-Essen.

Duisburg, den 26. Februar 2007

Teilpublikationen (Pre-Publications)

T. Kretz, M. Wölki, and M. Schreckenberg. Characterizing correlations of flow oscillations at bottlenecks. *J. Stat. Mech.*, **P02005**, February 2006. DOI:10.1088/1742-5468/2006/02/P02005

T. Kretz and M. Schreckenberg. F.A.S.T. - Floor field- and Agent-based Simulation Tool. In *Proceedings of the International Symposium of Transport Simulation 2006 (ISTS06)*, Lausanne, Switzerland, September 2006. Electronic publication OAI:arXiv.org:physics/0609097.

T. Kretz and M. Schreckenberg. The F.A.S.T.-Model. Pages 712–715 in S. El Yacoubi, B. Chopard, and S. Bandini, editors. *Cellular Automata - 7th International Conference on Cellular Automata for Research and Industry, ACRI 2006*, Perpignan, France, September 2006. Springer-Verlag Berlin Heidelberg. DOI:10.1007/11861201_85.

T. Kretz, A. Grünebohm, M. Kaufman, F. Mazur, and M. Schreckenberg. Experimental study of pedestrian counterflow in a corridor. *J. Stat. Mech.*, **P10001**, October 2006. DOI:10.1088/1742-5468/2006/10/P10001.

T. Kretz, A. Grünebohm, and M. Schreckenberg. Experimental study of pedestrian flow through a bottleneck. *J. Stat. Mech.*, **P10014**, October 2006. DOI:10.1088/1742-5468/2006/10/P10014.

T. Kretz and M. Schreckenberg. Moore and more and symmetry. Pages 297–308 in N. Waldau, P. Gattermann, H. Knoflacher, and M. Schreckenberg, editors. *Pedestrian and Evacuation Dynamics '05*, Vienna, Austria. December 2006. Springer Berlin Heidelberg New York.

T. Kretz, A. Grünebohm, A. Kessel, H. Klüpfel, T. Meyer-König, and M. Schreckenberg. Upstairs Walking Speed Distributions on a Long Stairway. *Safety Science (in press)* (2007) DOI:10.1016/j.ssci.2006.10.001

Erklärung (Declaration)

Ich versichere, dass ich die von mir vorgelegte Dissertation selbständig angefertigt, die benutzten Quellen und Hilfsmittel vollständig angegeben und die Stellen der Arbeit einschließlich der Abbildungen, die anderen Werken im Wortlaut oder dem Sinn nach entnommen sind, in jedem Einzelfall als Entlehnung kenntlich gemacht habe; dass diese Dissertation noch keiner anderen Fakultät oder Universität zur Prüfung vorgelegen hat; dass sie abgesehen von den angegebenen Teilpublikationen noch nicht veröffentlicht worden ist, sowie, dass ich eine solche Veröffentlichung vor Abschluss des Promotionsverfahrens nicht vornehmen werde. Die Bestimmungen dieser Promotionsordnung sind mir bekannt. Die von mir vorgelegte Dissertation ist von Herrn Professor Dr. Michael Schreckenberg betreut worden.

Duisburg, den 10. Oktober 2006
